Report No. XX

OPERATIONAL QUANTITIES FOR EXTERNAL RADIATION EXPOSURE

Joint report of

THE INTERNATIONAL COMMISSION ON RADIATION UNITS AND MEASUREMENTS

and

THE INTERNATIONAL COMMISSION ON RADIOLOGICAL PROTECTION

MONTH 2017

Journal of the ICRU Volume XX No X 2017
ISBN XXXXXXXXXX
Published by Oxford University Press

OPERATIONAL QUANTITIES FOR EXTERNAL RADIATION EXPOSURE

Report Committee

N.E.Hertel (Co-Chair), Georgia Institute of Technology, USA.

D.T. Bartlett (Co-Chair), Abingdon, UK

R.Behrens, Physikalisch-Technische Bundesanstalt, Braunschweig, Germany

J-M.Bordy, CEA, LIST, Laboratoire National Henri Becquerel (LNE-LNHB), 91191 Gif-sur-Yvette, France

G..Dietze†, Braunschweig, Germany

A. Endo, Japan Atomic Energy Agency, Japan

G.Gualdrini, Ente per le Nuove Tecnologie, L'Energia e L'Ambiente, Bologna, Italy (until 2015)

T. Otto, European Organization for Nuclear Research (CERN), Geneva, Switzerland

M.Pelliccioni, Istituto Nazionale di Fisica Nucleare, Frascati, Italy

Consultants to the Report Committee

P. Ambrosi, Physikalisch-Technische Bundesanstalt, Braunschweig, Germany (until 2014)

M.B.Bellamy, Center for Radiation Protection Knowledge, Oak Ridge National Laboratory, Oak Ridge, USA

J-F. Bottollier-Depois, Institut de Radioprotection et de Sûreté Nucléaire,

Fontenay-aux-Roses, France

J. Daures, CEA, LIST, Laboratoire National Henri Becquerel (LNE-LNHB), 91191 Gif-sur-Yvette, France

K.F.Eckerman, Oak Ridge, USA

P. Ferrari, Ente per le Nuove Tecnologie, L'Energia e L'Ambiente, Bologna, Italy

B.R.L. Siebert, Braunschweig, Germany

K.G. Veinot, Y-12 National Security Complex, Oak Ridge, USA

ICRU Sponsors

D.T. Burns, Bureau International des Poids et Mesures, Sèvres, France

E. Fantuzzi, Ente per le Nuove Tecnologie, L'Energia e L'Ambiente, Bologna, Italy

H-G. Menzel, Heidelberg, Germany

†Deceased. Dr Dietze played an important role in the development of the recommendations of this Report. The Commission wishes to acknowledge the loss resulting from his untimely death on 25th January 2015 .

Dedication to Günther Dietze

Dr. Günther Dietze died on the 25th of January, 2015.

Günther was a member of the International Commission on Radiation Units and Measurements (ICRU) Fundamental Quantities and Units Committee, which recently published Report 85a *Fundamental Quantities and Units for Ionizing Radiation*, and was on the ICRU Committees that prepared Report 47 *Measurement of Dose from External Photon and Electron Radiations*, and Report 57 *Conversion Coefficients for use in Radiological Protection Against External Radiation*. He contributed strongly to the preparation of this Report.

At the Physikalisch-Technische Bundesanstalt (PTB), Braunschweig, he was Head of the Ionizing Radiation Division, with responsibility for radioactivity, dose measurements for medical applications, radiation protection dosimetry, and neutron metrology. He had a strong interest in neutron dosimetry, publishing many papers on detectors and spectrometers. He was a member of, and later led the German Radiation Protection Commission, and was a member of the Group of Experts established under Article 31 of the EURATOM treaty. He was one of the first Council Members of EURADOS, and was Chairman from 1991 to 2001.

Günther served on many national and international committees, and was a member of the International Commission on Radiological Protection Committee 2, contributing significantly to Task Groups, and to the Committees that prepared several publications including Publication 103, *The 2007 Recommendations of the International Commission on Radiological Protection*, and was Chairman of the Committee that prepared Publication 123, *Assessment of Radiation Exposure of Astronauts in Space*. He was a Consultant Editor of the journal Radiation Protection Dosimetry.

Günther's death is a significant loss to the dosimetry community.

Operational Quantities for External Radiation Exposure

Preface

Abstract

Executive Summary

1 Introduction

2 Concepts and Terms

2.1 Particle Energy

2.2 Charged Particle Equilibrium

2.3 ICRU 4-Element (soft) Tissue

2.4 ICRU Sphere

2.5 ICRP and ICRU Adult Anthropomorphic Reference Computational Phantoms

2.6 Conversion Coefficients

3 Definitions of Quantities

3.1 Radiometric Quantities

3.1.1 Fluence

3.1.2 Fluence Rate

3.1.3 Particle Radiance

3.2 Dosimetric Quantities

3.2.1 Kerma

3.2.2 Absorbed Dose

3.3 Protection Quantities

3.3.1 Mean Absorbed Dose in an Organ or Tissue

3.3.2 Effective Dose

3.4 Operational Quantities for External Exposure

3.4.1 Ambient Dose

3.4.2 Ambient Dose Rate

3.4.3 Directional Absorbed Dose in the Lens of the Eye

3.4.4 Directional Absorbed Dose in the Lens of the Eye Rate

3.4.5 Directional Absorbed Dose in Local Skin

3.4.6 Directional Absorbed Dose in Local Skin Rate

3.4.7 Personal Dose

3.4.8 Personal Absorbed Dose in the Lens of the Eye

3.4.9 Personal Absorbed Dose in Local Skin

4 Conversion Coefficients

4.1Conversion Coefficients for the Operational Quantities

4.2 Comparison of Quantities of Values Recommended and Previous Conversion Coefficients

4.2.1General Remarks

4.2.2 Ambient and Personal Dose

4.2.3 Directional and Personal Absorbed Dose in the Lens of the Eye

4.2.4 Directional and Personal Absorbed Dose in Local Skin

5 Applications of Operational Quantities

5.1 Operational Quantities and their Application in Occupational Radiation Protection

5.2 Operational Quantities and their Application in Environmental Monitoring

6 Calibration of Area Monitoring Instruments and Personal Dosimeters

6.1 General

6.2 Calibration Phantoms for Personal Dosimeters

7 Conclusions

Appendix A Values of Conversion Coefficients

A.1 Ambient Dose

A.2 Personal Dose

A.3 Directional and Personal Absorbed Dose in the Lens of the Eye

A.4 Directional and Personal Absorbed Dose in Local Skin

A.5 Operational Quantities for Photons for Energies up to 50MeV Calculated with the Kerma-Approximation Method

A.6 Air Kerma

Appendix B Descriptions of Codes

B.1 PHITS

B.2 FLUKA

B.3 MCNP

B.4 EGSnrc

B.5 Revised Stopping Powers

Appendix C Informative: Alternative Conversion Coefficients for the Absorbed Dose in the Lens of the Eye

C.1 Directional and Personal Absorbed Dose in the Lens of the Eye, Maximum of Sensitive cells or Complete Lens

C.2 Photons for Energies up to 50MeV Calculated with the Kerma-Approximation Method

References

Preface

The International Commission on Radiological Protection, (ICRP), recommends protection quantities for dose limits of occupationally exposed persons and members of the public, and for the optimization of radiation protection (ICRP, 2007). The quantities are not point quantities, and are not appropriate for the calibration of instruments for area and individual dose measurements. A second class of quantities, operational dose quantities, has been defined by ICRU for this purpose. These are point quantities. In principle, determinations by instruments of the operational quantities, to which quantities instruments are calibrated and type tested, will provide estimates of the protection quantities for particular radiation exposures.

Absorbed dose index and dose equivalent index were recommended in ICRU Report 19 (ICRU, 1971) as the operational quantities for exposure to external radiation. In ICRU Report 20 (ICRU, 1971) there is consideration of the use of MADE (maximum dose equivalent in an irradiated body). Further development of the operational quantities was made in Report 39 (ICRU, 1985) and Report 43 (ICRU, 1988). These Reports defined ambient dose equivalent, directional dose equivalent, and individual dose equivalent, as operational quantities that were then partly modified in ICRU Report 51 (ICRU, 1993). Information on the application of these quantities was given for photons and electrons in ICRU Report 47 (ICRU, 1992) and for neutrons in Report 66 (ICRU, 2001). Sets of values of conversion coefficients from radiometric and dosimetric quantities were given in ICRU Report 57 (ICRU, 1998), published jointly with ICRP in Publication 74 (ICRP, 1996).

The operational quantities previously recommended were based on dose equivalent at a point in the ICRU sphere and on dose equivalent at a point in the body. The quantities recommended in this Report are defined as radiometric and dosimetric quantities at a point multiplied by conversion coefficients; the conversion coefficients are based on values of the protection quantities effective dose, absorbed dose in the lens of the eye, and absorbed dose in local skin.

Abstract

The Commission defines a set of operational dose quantities for the determination of the exposure of external radiation by measurement or calculation. These assessments serve as estimates of values of the protection quantities defined by the International Commission on Radiological Protection (ICRP) that are generally not measurable. The set of ICRU operational dose quantities in current use was defined 30 years ago.

The rationale for operational quantities has been examined taking into account the recent changes in the definitions of the protection quantities (ICRP, 2010); the changes in the fields of application of the operational quantities and protection quantities in medicine, scientific research, and natural sources of radiation; and the extension of types of particles and range of energies contributing to doses to workers and members of the public. The previous operational quantities were based on the dose equivalent that would be produced at a depth in the hypothetical ICRU 4-element sphere, and on dose equivalent in soft tissue at a point in the body. The investigations which have been carried out that have led to the recommendations given in this Report have included the study the values of weighted absorbed doses at different depths in tissue-equivalent phantoms and the combination of different depths. The operational quantities recommended in this Report are defined in terms of radiometric and dosimetric quantities at a point in space multiplied by values of conversion coefficients to the protection quantities, effective dose, absorbed dose in the lens of the eye, and absorbed dose in local skin, calculated for broad parallel beams incident on the body. The relationship of the recommended operational quantities to the protection quantities has been investigated. The impact of changes on routine measurement practice, including instrument design and calibration has been considered.

Executive Summary

This Report considers in Section 1 the background of the use of protection quantities and operational quantities for the quantification of the exposure of the human body to ionizing radiation. The protection quantities have been revised, owing partly to the changes in application and partly to the changes in the particle types and range of energies involved. The operational quantities require revision for these reasons, but also for the limitations of the previous quantities. The concepts and terms used in this Report are explained in Section 2, and the definitions of the relevant radiometric and dosimetric quantities, the protection and the operational quantities for radiation protection of external exposure are given in Section 3. The recommended operational quantities for area monitoring are ambient dose, directional absorbed dose to the lens of the eye and directional absorbed dose to local skin; for individual monitoring personal dose, personal absorbed dose to the lens of the eye and personal absorbed dose to local skin. In Section 4, information is given on the method of computation of the recommended quantities is given. Comparisons are made between the recommended and previous values of the conversion coefficients. These comparisons show the limitations of the previous quantities. Section 5 considers the areas of application of the operational quantities in occupational radiation protection and in environmental monitoring. The calibration of area monitoring instruments and personal dosimeters are considered in Section 6 with information on calibration procedures and the calibration phantoms. Section 7 gives the general conclusions on the improvements of the recommended operational quantities that overcome the limitations of the previous quantities and provide a solution to the protection problems in radiation fields of higher-energy photons, electrons and neutrons, and for other particle types.

Appendix A gives values of the conversion coefficients to ambient dose, personal dose, directional absorbed dose in the lens of the eye, directional absorbed dose in local skin, personal absorbed dose in the lens of the eye, and personal absorbed dose in local skin from particle fluence.

For photons, two additional data sets of conversion coefficients are given: to the operational quantities from air kerma; and to the operational quantities from fluence or air kerma calculated using the kerma-approximation method to approach charged-particle equilibrium. In Appendix B there are brief descriptions of the computer codes used for the calculation of these values. Informative tables and figures are given in Appendix C to the maximum value of the absorbed dose in the lens of the eye to the sensitive cells or the complete lens from particle fluence, and for photons from air kerma.

1 Introduction

Radiological protection requires the quantification of the extent of exposure of the human body to ionizing radiation. To this end, the International Commission on Radiological Protection (ICRP) developed the protection quantities, mean absorbed dose in an organ or tissue, equivalent dose in an organ or tissue, and effective dose (ICRP, 1977, 1991, 2007). The protection quantities are used for the implementation of dose limits and for guiding quantitatively the optimization principles. The latest data set of conversion coefficients from particle fluence to the protection quantities was recommended in ICRP Publication 116 (ICRP, 2010), which was jointly published with the International Commission on Radiation Units and Measurements (ICRU). The conversion coefficients of ICRP Publication 116 are calculated based on the definition of the protection quantities in the 2007 Recommendations of the ICRP (ICRP, 2007). ICRP Publication 116 extends radiation type and energy range of conversion coefficients in comparison with ICRP Publication 74 (ICRP, 1996) and ICRU Report 57 (ICRU, 1998) and supersedes the conversion coefficients for the protection quantities in these Reports. Human-body-related protection quantities are defined in organs and tissues and are not measurable in practice; therefore, they cannot be used directly as quantities in radiation monitoring. The ICRU has developed a set of operational quantities to be used in radiation measurements for external exposure to estimate the protection quantities. The current operational quantities in use were defined in the 1980s (ICRU, 1985, 1988) and have been applied in many countries under radiological protection directives and regulations over the past 30 years. The previous system of operational quantities has some limitations (Bartlett and Dietze, 2010; Bartlett *et al.*, 2013) and needs further improvements to consider changes in the fields of application, including the extension of radiation type and energy range (ICRP, 2007, 2010, 2016; ICRU, 2010). The determination of an operational quantity should give a value that is a close estimate of the value of the protection quantity.

This Report recommends a redefinition of the operational quantities as the products of radiometric or dosimetric quantities at a point in space or on the surface of the body and conversion coefficients related to values of protection quantities (Endo, 2016a). Consideration on this approach has been given previously (see, for example, Sidwell *et al*., 1969; ICRP Publication 15 (ICRP, 1969); NCRP Report 38 (NCRP,1971); Burlin and Wheatley, 1971; Commission of the European Communities (CEC, 1983); ICRP Publication 21 (ICRP, 1973); Burlin, Davies, and Wheatley, 1979; Burlin, 1981; Jahr *et al*., 1981; Siebert and Bartlett, 1995). The practical application of such a quantity can be made if conversion coefficients to an internationally agreed phantom exist. ICRP and ICRU have now defined ICRP/ICRU adult reference phantoms in ICRP Publication 110 (ICRP, 2009) that are widely accepted. These phantoms are used to define reference values of conversion coefficients to the protection quantities and can be used to define the operational quantities. The recommended operational quantities simplify the systems of protection and operational quantities, and assists in the comprehension of radiological protection quantities by users.

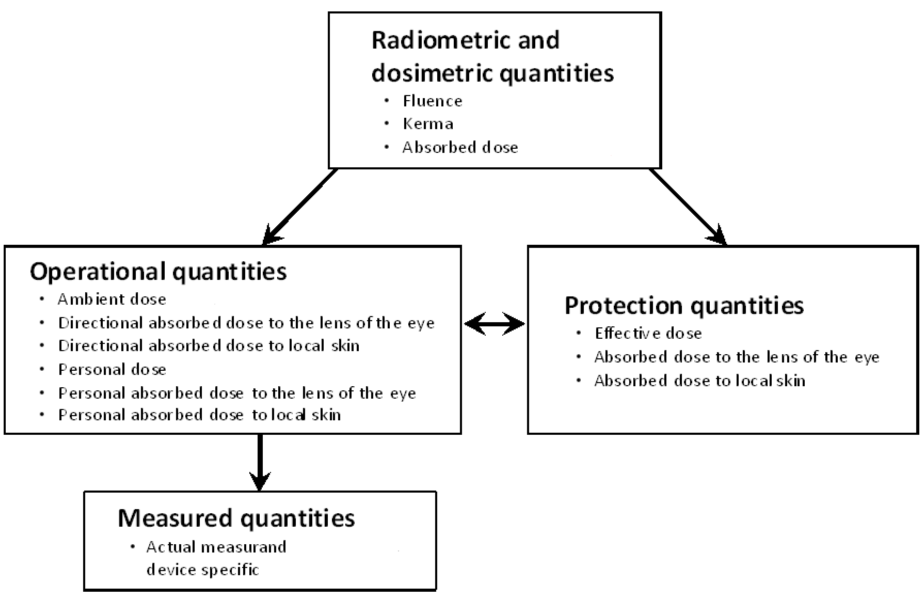

Figure1: Scheme of relationships of quantities

The ICRP protection quantity effective dose is considered to provide a single risk-related quantity for stochastic radiation effects, valid for all adult persons exposed under the same conditions, independent of sex, age, size, and other individual properties of the person exposed. Internal exposure from the intake of radionuclides can also be considered using this effective-dose concept. The quantity effective dose is for consideration of stochastic effects at doses below 100 mSv for setting exposure limits and for optimization. At higher values of dose, tissue reactions (deterministic effects) are of concern, and absorbed doses are to be evaluated (Harrison *et al*, 2016). For evaluating tissue reactions, mean absorbed dose in the organ or tissue is assessed, weighted for high-LET radiation by a specific RBE. The RBE values will depend on the radiation type and energy, and can differ for different biological endpoints and different organs or tissues (ICRP, 2007).

For doses below dose constraints or investigation levels, in common practice, the protection quantities are assessed in terms of the operational quantities. There is the possibility of significant sources of uncertainty in the assessment of the protection quantities from the operational quantities [“Determination of protection quantities based on different knowledge of external exposure” German booklet need reference]. To assess a more precise value and its uncertainty as doses approach the constraints or investigation levels, information will be needed on the types of radiation involved, the uniformity of the radiation field and of its energy and direction distributions, the position of the instrument or dosimeter and its response characteristics, and whether the exposure is partial or whole-body. In some instances, additional information can be obtained by computer simulation of the exposure situation.

This Report provides a set of conversion coefficients from fluence to the operational quantities for the particles photons, neutrons, electrons, positrons, protons, negative and positive muons, negative and positive pions, and helium ions, for energies up to 200 GeV, and also from air kerma for photons to 50 MeV. Conversion coefficients to the protection quantities for a few field geometries are provided in ICRP Publication 116 (ICRP, 2010). However, more data for additional incident angles of incidence that are not provided by ICRP Publication 116 are given to characterize the operational quantities for directional and individual monitoring. These data sets are also required for the calibration and type testing of area monitoring instruments and personal dosimeters. The consistency of numerical values of conversion coefficients to effective dose between ICRP Publication 116 and the calculations in this Report to ambient dose and personal dose was studied and validated (Endo, 2017). The numerical values of conversion coefficients to directional and personal absorbed dose to the lens of the eye and local skin were carried out using one computer code but were validated by two other codes at a number of discrete energies and angles. The statistical uncertainties in the calculations are around 1 % or less.

Although the conversion coefficients from fluence or air kerma are to values of protection quantities that are not point quantities but are averaged over an organ or tissue, or the sum of these averages, the operational quantities that are recommended are point quantities.

2 Concepts and Terms

2.1 Particle Energy

In this Report, the quantity particle kinetic energy and photon energy, is given the symbol E_{p}, to distinguish the quantity from the quantity effective dose, symbol E.

2.2 Charged-Particle Equilibrium

Charged-particle equilibrium exists at a point if the distribution of charged-particle radiance (Section 3.1.3) with respect to particle energy is constant within distances equal to the charged-particle range. Under condition of charged-particle equilibrium the numerical value of collision kerma (Section 3.2.1) at a point of interest approaches the value of absorbed dose (Section 3.2.2).

2.3 ICRU 4-Element (soft) Tissue

ICRU 4-element soft tissue (ICRU, 1980) has a density of 1 g cm^{-3}, and a composition by mass of 76.2 % oxygen, 11.1 % carbon, 10.1 % hydrogen, and 2.6 % nitrogen, with no further specification of other properties of that material.

2.4 ICRU Sphere

The ICRU sphere (ICRU, 1980) is a 30 cm diameter sphere of ICRU 4-element tissue. The ICRU sphere is no longer used in the recommended definitions of the operational quantities.

2.5 ICRP and ICRU Adult Anthropomorphic Reference Computational Phantoms

The anthropomorphic reference computational phantoms of ICRP and ICRU are models of the human body presented and described in ICRP Publication 110 (ICRP, 2009), with the anatomical and physiological characteristics defined in ICRP Publication 89 (ICRP, 2002). The models are represented by arrays of cuboid voxels based on medical tomographic images in which the anatomy is described by small three-dimensional volume elements. The collections of these voxels, of a number of compositions and densities (ICRP, 2009), are used to specify the organs and tissues of the human body. Two reference phantoms have been defined for adults, a male and female one. These generalized body phantoms do not represent any individual human body.

2.6 Conversion Coefficients

Conversion coefficients relate a protection or operational quantity to a radiometric or dosimetric quantity. This term is used in external exposure situations, while in internal dosimetry the ratios of dose quantities and activity quantities are called dose coefficients. For external exposure, conversion coefficients are given to the operational quantities from the radiometric and dosimetric quantities fluence or air kerma.

An internationally agreed set of conversion coefficients for protection quantities is available for general use in radiological protection practice for occupational exposures (ICRP, 2010). They are calculated for whole-body irradiation of the phantoms in vacuum exposed to broad parallel beams assumed to represent occupational exposure for the field geometries: antero-posterior, (AP), postero-anterior, (PA), left lateral, (LLAT), right lateral, (RLAT), rotational, (ROT), isotropic, (ISO), superior hemisphere semi-isotropic (SS-ISO), inferior hemisphere semi-isotropic (IS-ISO). They are available for these ideal exposure geometries only.

Conversion coefficients from particle fluence and air kerma to the previously recommended operational quantities in well specified exposure conditions were published by ICRU and ICRP (ICRU, 1998; ICRP, 1996). Such data have often been applied for calibration of area monitoring instruments and personal dosimeters used in radiation protection by the ICRU (ICRU, 2001) and the International Organization for Standardization, (ISO), (ISO, 1998; 1999; 2006; 2008): these data are replaced by those given in this Report.

3 Definitions of Quantities

3.1 Radiometric Quantities

3.1.1 Fluence

The *fluence*, Φ, (ICRU, 2011) is the quotient of dN by da, where dN is the number of particles incident on a sphere of cross-sectional area da, thus:

$$\Phi = \frac{\mathrm{d}N}{\mathrm{d}a}. \tag{3.1}$$

The unit of fluence is m^{-2}.

In dosimetric calculations, fluence is frequently expressed in terms of the lengths of the particle trajectories. It can be shown (Weinberg and Wigner, 1958) that the fluence, Φ, is given by

$$\Phi = \mathrm{d}l/\mathrm{d}V, \tag{3.2}$$

where dl is the sum of the lengths of particle trajectories in the volume dV.

For a radiation field that does not vary over the time interval, t, and is composed of particles with velocity v, the fluence, Φ, is given by:

$$\Phi = n\, v\, t, \tag{3.3}$$

where n is the *particle number density*, given by $n = \mathrm{d}N/\mathrm{d}V$, where d$N$ is the number of particles in the volume dV.

The distributions, Φ_{Ep} of the fluence with respect to energy are given by:

$$\Phi_{E\mathrm{p}} = \mathrm{d}\Phi/\mathrm{d}E_{\mathrm{p}}, \tag{3.4}$$

where dΦ is the fluence of particles of energy interval between E_{p} and E_{p} + dE_{p}. In certain circumstances quantities involving the differential solid angle, d$\boldsymbol{\Omega}$, are required. The complete representation of the double differential of fluence can be written $\Phi_{E\mathrm{p},\boldsymbol{\Omega}}(E_{\mathrm{p}}, \boldsymbol{\Omega})$.

3.1.2 Fluence Rate

The *fluence rate*, $\dot{\Phi}$, (ICRU, 2011) is the quotient of dΦ by dt, where dΦ is the increment of the fluence of particles in the time interval dt, thus:

$$\dot{\Phi} = \frac{\mathrm{d}\Phi}{\mathrm{d}t}. \tag{3.5}$$

The unit of fluence rate is m^{-2} s^{-1}.

3.1.3 Particle Radiance

The *particle radiance*, $\dot{\Phi}_{\Omega}$, (ICRU, 2011) is the quotient of $\mathrm{d}\dot{\Phi}$ by $\mathrm{d}\boldsymbol{\Omega}$, where $\mathrm{d}\dot{\Phi}$ is the fluence rate of particles propagating within a solid angle $\mathrm{d}\boldsymbol{\Omega}$ around a specified direction, thus:

$$\dot{\Phi}_{\Omega} = \frac{\mathrm{d}\dot{\Phi}}{\mathrm{d}\Omega}. \tag{3.6}$$

The unit of particle radiance is m^{-2} s^{-1} sr^{-1}. The distribution of particle radiance with respect to energy is given by:

$$\dot{\Phi}_{\Omega,E} = \frac{\mathrm{d}\dot{\Phi}_{\Omega}}{\mathrm{d}E_p}, \tag{3.7}$$

where $\mathrm{d}\dot{\Phi}_{\Omega}$ is the particle radiance for particles of energy between E_{p} and $E_{\mathrm{p}} + \mathrm{d}E_{\mathrm{p}}$. The quantity $\dot{\Phi}_{\Omega,Ep}$ is sometimes termed angular flux or phase flux in radiation-transport theory.

Apart from aspects that are of minor importance in the present context (*e.g.*, polarization), the field of any radiation of a given particle type is completely specified by the distribution of the particle radiance with respect to particle energy, $\dot{\Phi}_{\Omega,Ep}$, as this defines number, energy, local density, and arrival rate of particles propagating in a given direction. This quantity, as well as the distribution of the energy radiance with respect to energy, can be considered as basic in radiometry.

3.2 Dosimetric Quantities

3.2.1 Kerma

The *kerma*, K, (ICRU, 2011) for ionizing uncharged particles, is the quotient of $\mathrm{d}E_{\mathrm{ptr}}$ by $\mathrm{d}m$, where $\mathrm{d}E_{\mathrm{ptr}}$ is the mean sum of the initial kinetic energies of all the charged particles liberated in a mass $\mathrm{d}m$ of a material by the uncharged particles incident on $\mathrm{d}m$, thus:

$$K = \frac{\mathrm{d}E_{\mathrm{ptr}}}{\mathrm{d}m}. \tag{3.8}$$

The unit of kerma is J kg^{-1}. The special name for the unit of kerma is gray (Gy); 1 Gy = 1 J kg^{-1}.

Although kerma is a quantity that concerns the initial transfer of energy to matter, it is sometimes used as an approximation to absorbed dose. The numerical value of the kerma approaches that of the absorbed dose to the degree that *charged-particle equilibrium* exists, that radiative losses are negligible, and that the kinetic energy of the uncharged particles is large compared to the binding energy of the liberated charged particles.

A quantity related to the kerma, termed the *collision kerma*, has long been used as an approximation to absorbed dose (Attix, 1979a; 1979b) when radiative losses are not negligible. The collision kerma, K_{col}, excludes the radiative losses by the liberated charged particles, and for a fluence, Φ, of uncharged particles of energy E_{p} in a specified material is given by:

$$K_{\mathrm{col}} = \Phi E_{\mathrm{p}} \frac{\mu_{\mathrm{en}}}{\rho} = \Phi E_{\mathrm{p}} \frac{\mu_{\mathrm{tr}}}{\rho}\left(1-g\right) = K\left(1-g\right) \tag{3.9}$$

where μ_{en}/ρ is the mass energy-absorption coefficient and μ_{tr}/ρ is the mass energy-transfer coefficient of the material for uncharged particles of energy E_{p}**,** and g is the fraction of the total kinetic energy of liberated charged particles that would be lost in radiative processes in that material.

In dosimetric calculations, the collision kerma, K_{col}, can be expressed in terms of the distribution, $\Phi_{E\mathrm{p}}$, of the uncharged-particle fluence with respect to energy as:

$$K_{\mathrm{col}} = \int \Phi_{E\mathrm{p}} E_{\mathrm{p}} \frac{\mu_{\mathrm{en}}}{\rho}\,\mathrm{d}E_{\mathrm{p}} = \int \Phi_{E\mathrm{p}} E_{\mathrm{p}} \frac{\mu_{\mathrm{tr}}}{\rho}\left(1-g\right)\,\mathrm{d}E_{\mathrm{p}} = K\left(1-\bar{g}\right) \tag{3.10}$$

where $\bar{g}$ is the mean value of g averaged over the distribution of the kerma with respect to the electron energy.

The *kerma rate*, $\dot{K}$, is the quotient of dK by dt, where dK is the increment of the kerma in the time interval dt, thus:

$$\dot{K} = \frac{\mathrm{d}K}{\mathrm{d}t}. \tag{3.11}$$

The unit of kerma rate is J kg^{-1} s^{-1}. The special name for the unit of kerma rate is gray per second (Gy s^{-1}).

3.2.2 Absorbed Dose

The *absorbed dose*, D, (ICRU, 2011) is the quotient of $\mathrm{d}\bar{\varepsilon}$ by dm, where $\mathrm{d}\bar{\varepsilon}$ is the mean energy imparted by ionizing radiation to matter of mass dm, thus:

$$D = \frac{\mathrm{d}\bar{\varepsilon}}{\mathrm{d}m}. \tag{3.12}$$

The unit of absorbed dose is J kg^{-1}. The special name for the unit of absorbed dose is gray (Gy).

3.2.3 Absorbed Dose Rate

The *absorbed dose rate*, $\dot{D}$, (ICRU, 2011) is the quotient of dD by dt, where dD is the increment of the absorbed dose in the time interval dt, thus:

$$\dot{D} = \frac{\mathrm{d}D}{\mathrm{d}t}. \tag{3.13}$$

The unit of absorbed dose rate is J kg^{-1} s^{-1}. The special name for the unit of absorbed dose rate is gray per second (Gy s^{-1}).

3.3 Protection Quantities

3.3.1 Mean Absorbed Dose in an Organ or Tissue

The *mean absorbed dose in an organ or tissue* T is D_T, (ICRP, 2007) defined by:

$$D_T = 1/m_T \int D \,\mathrm{d}m \tag{3.14}$$

where m_T is the mass of the organ or tissue, and D is the absorbed dose in the mass element dm . The integration extends over the whole organ or tissue.

The unit of mean absorbed dose is joule per kilogram (J kg^{-1}), and its special name is gray (Gy).

Two organs or tissues with small or no contribution to effective dose (Section 3.3.3) merit attention: the control of the exposure of local skin and the lens of the eye to prevent deterministic tissue reactions that occur above a threshold dose.

The absorbed dose in local skin is defined as that averaged over 1 cm^2 of the skin between depths of 50 µm and 100 µm anywhere on the surface of the body. The composition of skin is given in ICRP Publication 89 (ICRP, 2002), of density 1.09 g cm^{-3} (ICRP, 2009). The specific annual dose limits recommended for the skin apply to the absorbed dose to local skin at the most highly irradiated area of the skin. There has also been increased concern of the effects of irradiation in the lens of the eye, which has led to a reduction in annual dose limits (ICRP, 2012).

3.3.2 Effective Dose

The weighted sum of absorbed doses in all specified organs and tissues of the body, E, (ICRP, 2007), given by the expression:

$$E = \sum_{\mathrm{T}} w_{\mathrm{T}} \sum_{\mathrm{R}} w_{\mathrm{R}} D_{\mathrm{T,R}} \quad (3.15)$$

where $D_{\mathrm{T,R}}$ is the mean absorbed dose in an organ or tissue T averaged over the male and female reference phantoms from radiation of type R, w_{R} is the radiation weighting factor for the radiation R incident on the body, and w_{T} is the sex-averaged tissue weighting factor. The sum is performed over organs and tissues considered to be sensitive to the induction of stochastic effects.

The unit of effective dose is J kg^{-1}. The special name for the unit of effective dose is sievert (Sv).

3.4 Operational Quantities for External Exposure

3.4.1 Ambient Dose

The *ambient dose*, H^*, at a point in a radiation field, is the product of the particle fluence at that point, Φ, and the conversion coefficient, $h^*_{E\mathrm{max}}$, relating particle fluence to the maximum value of effective dose, E_{max}.

For a given particle type i with kinetic energy E_p, the conversion coefficient $h^*_{E\max,i}(E_p) = E_{\max,i}(E_p)/\Phi_i(E_{p,})$ is calculated for exposure of the whole-body ICRP/ICRU adult reference phantoms (ICRP, 2009) for broad parallel beams of the radiation field incident in irradiation geometries AP, PA, LLAT, RLAT, ROT, ISO, SS-ISO, and IS-ISO fields for photons and neutrons; AP, PA, ISO, SS-ISO, and IS-ISO fields for electrons, positrons, muons and pions; and AP, PA, and ISO for He ions (ICRP, 2010).

For a distribution of particles of type i:

$$H^*_i = \int h^*_{E\max,i}(E_p)\,[\mathrm{d}\Phi_i(E_p)/\mathrm{d}E_p]\,\mathrm{d}E_p \qquad (3.16)$$

where $\mathrm{d}\Phi_i(E_p)/\mathrm{d}E_p$ is the fluence of particles with kinetic energies in the interval $\mathrm{d}E_p$ around E_p. The sum over all contributing particle types is:

$$H^* = \sum H^*_i \qquad (3.17)$$

The unit of ambient dose is J kg^{-1}. The special name for the unit of ambient dose is sievert (Sv).

3.4.2 Ambient Dose Rate

The *ambient dose rate* $\dot{H}^*$ is the quotient of $\mathrm{d}H^*$ by $\mathrm{d}t$, where $\mathrm{d}H^*$ is the increment of the ambient dose in the time interval $\mathrm{d}t$, thus:

$$\dot{H}^* = \frac{\mathrm{d}H^*}{\mathrm{d}t}. \qquad (3.18)$$

The unit of ambient dose rate is J kg^{-1} s^{-1}. The special name for the unit of ambient dose rate is sievert per second (Sv s^{-1}).

3.4.3 Directional Absorbed Dose in the Lens of the Eye

The *directional absorbed dose in the lens of the eye*, $D'_{\mathrm{lens}}(\Omega)$, at a point in a radiation field with a specified direction of incidence, Ω, is the product of the particle fluence at that point, $\Phi(\Omega)$, and the conversion coefficient, $d'_{\mathrm{lens}}(\Omega)$, relating particle fluence to the value of absorbed dose in the lens of the eye.

For a given particle type i with kinetic energy E_p, the conversion coefficient $d'_{\mathrm{lens},i}(E_p,\Omega) = D'_{\mathrm{lens},i}(E_p,\Omega)/\Phi_i(E_p,\Omega)$ is calculated for exposure of the whole-body of the stylized eye model (Behrens and Dietze, 2011) for broad parallel beams of the radiation field incident in the direction Ω**.** For a given Ω, the maximum value of absorbed dose in the lens of the right or left eye is taken.

For a distribution of particles of type i:

$$D'_{\mathrm{lens},i}(\Omega) = \int d'_{\mathrm{lens},i}(E_p,\Omega)\,[\mathrm{d}\Phi_i(E_p,\Omega)/\mathrm{d}E_p]\,\mathrm{d}E_p \qquad (3.19)$$

where $\mathrm{d}\Phi_i(E_p,\Omega)/\mathrm{d}E_p$ is the fluence of particles with direction of incidence Ω and with kinetic energies in the interval $\mathrm{d}E_p$ around E_p. The sum over all contributing particle types i with direction of incidence Ω is:

$$D'_{\mathrm{lens}}(\Omega) = \sum D'_{\mathrm{lens},i}(\Omega) \qquad (3.20)$$

The unit of directional absorbed dose in the lens of the eye is J kg^{-1}. The special name for the unit of directional absorbed dose in the lens of the eye is gray (Gy).

The specification of the incident direction, Ω, requires a reference system for coordinates in which the direction of incidence is expressed. This reference system for an area monitoring quantity can be related to the radiation field in which the operational quantity is to be determined. In the particular case of a unidirectional field, the direction can be related to the angle, α, between this direction and the direction of incidence, Ω_0, that is antero-posterior, AP, to the stylized eye model. When $\alpha = 0^{\mathrm{o}}$, the value of $D'_{\mathrm{lens}}(\Omega)$ at the point of interest for measurements using this specified direction shall be written D'_{lens}.

3.4.4 Directional Absorbed Dose Rate in the Lens of the Eye

The *directional absorbed dose rate in the lens of the eye,* $\dot{\boldsymbol{D}}'_{\mathrm{lens}}(\Omega)$, is the quotient of $\mathrm{d}D'_{\mathrm{lens}}(\Omega)$ by dt, where $\mathrm{d}D'_{\mathrm{lens}}(\Omega)$ is the increment of directional absorbed dose in the lens of the eye in the time interval dt, thus:

$$\dot{D}'_{\mathrm{lens}}(\Omega) = \frac{\mathrm{d}D'_{\mathrm{lens}}(\Omega)}{\mathrm{d}t}. \qquad (3.21)$$

The unit of directional absorbed dose rate in the lens of the eye is J kg^{-l} s^{-1}. The special name for the unit of directional absorbed dose rate in the lens of the eye is gray per second (Gy s^{-1}).

3.4.5 Directional Absorbed Dose in Local Skin

The *directional absorbed dose in local skin*, $D'_{\mathrm{local\ skin}}(\Omega)$, at a point in a radiation field with a specified direction of incidence, Ω, is the product of the particle fluence at that point, Φ_i, and the conversion coefficient, $d'_{\mathrm{local\ skin}}(\Omega)$, relating particle fluence to the value of absorbed dose in local skin.

For a given particle type i with kinetic energy E_{p}, the conversion coefficient $d'_{\mathrm{local\ skin},i}(E_{\mathrm{p}},\Omega) = D'_{\mathrm{local\ skin},i}(E_{\mathrm{p}},\Omega)/\Phi(E_{\mathrm{p}},\Omega)$ is calculated for exposure to broad parallel beams of the radiation field incident in the direction Ω. The conversion coefficient is calculated for exposure of a specified phantom, an ICRU 4-element tissue 300 mm x 300 mm x 150 mm slab (ρ=1.0 g cm^{-3}), in which the dose is averaged over the volume of a right circular cylinder between the depths of 50µm and 100 µm and a cross sectional area of 1 cm^2 below the center of the front surface. Inside the phantom there is an outer layer of 2 mm skin of density 1.09 g cm^{-3} (ICRP, 2009) of elemental composition given in ICRP Publication 89 (ICRP, 2002).

For a distribution of particles of type i:

$$D'_{\mathrm{local\ skin},i}(\Omega) = \int d'_{\mathrm{local\ skin},i}(E_{\mathrm{p}},\Omega)[\mathrm{d}\Phi_i(E_{\mathrm{p}},\Omega))/\mathrm{d}E_{\mathrm{p}}]\ \mathrm{d}E_{\mathrm{p}} \qquad (3.22)$$

where $\mathrm{d}\Phi_i(E_{\mathrm{p}},\Omega))/\mathrm{d}E_{\mathrm{p}}$ is the fluence of particles with direction of incidence Ω and with kinetic energies in the interval $\mathrm{d}E_{\mathrm{p}}$ around E_{p}. The sum over all contributing particle types with direction of incidence Ω is:

$$D'_{\mathrm{local\ skin}}(\Omega) = \sum D'_{\mathrm{local\ skin},i}(\Omega) \qquad (3.23)$$

The unit of directional absorbed dose in local skin is J kg^{-1}. The special name for the unit of directional absorbed dose in local skin is gray (Gy).

The specification of the direction of incidence, Ω, requires a reference system for coordinates in which the direction is expressed. This reference system for an area monitoring quantity can be related to the radiation field in which the operational quantity is to be determined. In the particular case of a unidirectional field, the direction can be related to the angle, α, between this direction, and the direction of incidence, Ω_0, that is normal to the front surface of the slab phantom. When $\alpha = 0°$, the value of $D'_{\mathrm{localskin}}(\Omega)$ at the point of interest for measurements using this specified direction shall be written $D'_{\mathrm{local\ skin}}$.

3.4.6 Directional Absorbed Dose Rate in Local Skin

The *directional absorbed dose rate in local skin*, $\dot{\boldsymbol{D}}'_{\mathrm{local\ skin}}(\Omega)$, is the quotient of $\mathrm{d}D'_{\mathrm{local\ skin}}(\Omega)$ by dt, where $\mathrm{d}D'_{\mathrm{local\ skin}}(\Omega)$ is the increment of the directional absorbed dose to local skin in the time interval dt, thus:

$$\dot{D}'_{\mathrm{local\ skin}}(\Omega) = \frac{\mathrm{d}D'_{\mathrm{local\ skin}}(\Omega)}{\mathrm{d}t}. \qquad (3.24)$$

The unit of directional absorbed dose rate in local skin is J kg^{-1} s^{-1}. The special name for the unit of directional absorbed dose rate in local skin is gray per second (Gy s^{-1}).

3.4.7 Personal Dose

The *personal dose*, H_{p}, at a point on the body is the product of the particle fluence incident at that point, Φ, and the conversion coefficient, h_{p}, relating particle fluence to the value of effective dose, E.

For a given particle type i with kinetic energy E_{p} and direction of incidence[1] Ω, the conversion coefficient $h_{\mathrm{p},i}(E_{\mathrm{p}},\Omega) = E(E_{\mathrm{p}},\Omega)/\Phi_i(E_{\mathrm{p}},\Omega)$ is calculated for broad parallel beams incident on the whole-body ICRP/ICRU adult reference phantoms (ICRP, 2009). For a given Ω, the maximum value of effective dose is taken for radiation incident from left or right.

For a distribution of particles of type i:

$$H_{\mathrm{p},i} = \iint h_{\mathrm{p},i}(E_{\mathrm{p}},\Omega)\ [\mathrm{d}\Phi_i(E_{\mathrm{p}},\Omega)/\mathrm{d}\,E_{\mathrm{p}}\mathrm{d}\Omega]\ \mathrm{d}E_{\mathrm{p}}\mathrm{d}\Omega \qquad (3.25)$$

---

[1]A right-handed orthogonal system for the bodyis adopted in which the X-axis is from right to left, the Y-axis from front to back and the Z-axis from toe to head. The irradiation directional angle Ω is defined in terms of the componentsθ and φ, with θbeing the angle with respect to the Z-axis (positive θpointing to the head) and φ being the projection on to the XY-plane (positive φpointing to the left).

where $d\Phi_i(E_p,\Omega)/dE_p d\Omega$ is the fluence of particles at that point, with kinetic energies in the interval dE_p around E_p, and directions of incidence in the interval $d\Omega$ around Ω. The sum over all contributing particle types is:

$$H_p = \sum H_{p,i} \tag{3.26}$$

The unit of personal dose is J kg^{-1}. The special name for the unit of personal dose is sievert (Sv).

3.4.8 Personal Absorbed Dose in the Lens of the Eye

The *personal absorbed dose in the lens of the eye*, $D_{p\ lens}$, at a point on the head or body is the product of the particle fluence incident at that point, Φ, and the conversion coefficient, $d_{p\ lens}$, relating particle fluence to the value of absorbed dose in the lens of the eye.

For a given particle type i with kinetic energy E_p and direction of incidence[2] Ω, the conversion coefficient $d_{plens,i}(E_p,\Omega) = D_{p\ lens,i}(E_p,\Omega)/\Phi_i(E_p,\Omega)$ is calculated for broad parallel beams incident on the whole-body stylized eye model (Behrens and Dietze, 2011). For a given Ω, the maximum value of the absorbed doses in the lens of the right or left eye is taken.

For a distribution of particles of type i:

$$D_{p\ lens,i} = \iint d_{p\ lens,i}(E_p,\Omega))\ [d\Phi_i(E_p,\Omega)/dE_p d\Omega)]\ dE_p d\Omega \tag{3.27}$$

where $d\Phi_i(E_p,\Omega)/dE_p d\Omega$ is the fluence of particles at that point with kinetic energies in the interval dE_p around E_p, and directions of incidence in the interval $d\Omega$ around Ω. The sum over all contributing particle types is:

$$D_{p\ lens} = \sum D_{plens,i} \tag{3.28}$$

The unit of personal absorbed dose in the lens of the eye is J kg^{-1}. The special name for the unit of personal absorbed dose in the lens of the eye is gray (Gy).

3.4.9 Personal Absorbed Dose in Local Skin

[2]A right-handed orthogonal system for the body is adopted in which the X-axis is from right to left, the Y-axis from front to back and the Z-axis from toe to head. The irradiation directional angle Ω is defined in terms of the componentsθ and φ, with θbeing the angle with respect to the Z-axis (positive θpointing to the head) and φ being the projection on to the XY-plane (positive φ pointing to the left).[This isthe same asforH_p, but different tothatforcalculationsforthe Behrens Dietze model in ICRP Publication 116]

The *personal absorbed dose in local skin*, $D_{\mathrm{p\ local\ skin}}$, is the product of the particle fluence incident on the body or extremities, Φ, and the conversion coefficient, $d_{\mathrm{p\ local\ skin}}$, relating particle fluence to the value of absorbed dose in local skin.

For a given particle type i with kinetic energy E_{p} and direction of incidence[3] Ω, the conversion coefficient $d_{\mathrm{p\ local\ skin},i}(E_{\mathrm{p}},\Omega) = D_{\mathrm{p\ local\ skin},i}(E_{\mathrm{p}},\Omega)/\Phi_i(E_{\mathrm{p}},\Omega)$ is calculated for exposure of the specified phantoms to broad parallel beams:

- for the trunk, a slab of ICRU 4-element tissue (ρ=1.0 g cm^{-3}) with dimensions 300 mm x 300 mm x 150 mm, in which the dose is averaged over the volume of a right circular cylinder between the depths of 50 µm and 100 µm and a cross sectional area of 1 cm² below the center of the front surface;
- for the extremities a pillar of ICRU 4-element tissue (ρ=1.11 g cm^{-3}) with dimensions 73 mm diameter and 300 mm length, in which the dose is averaged over the volume between the radii 36.4 mm and 36.45 mm with a circle of area 1 cm² projected onto the upper and lower cylindrical surfaces perpendicular to and at the center of the pillar;
- for the finger a rod of ICRU 4-element tissue (ρ=1.11 g cm^{-3}) with dimensions 19 mm diameter and 300 mm length, in which the dose is averaged over the volume between the radii 9.4 mm and 9.45 mm with a circle of area 1 cm² projected onto the upper and lower cylindrical surfaces perpendicular to and at the center of the pillar.

Inside each phantom there is an outer layer of 2 mm skin of density 1.09 g cm^{-3} (ICRP. 2009) with the elemental composition given in ICRP Publication 89 (2002).

For a distribution of particles of type i:

$$D_{\mathrm{p\ local\ skin},i}= \iint d_{\mathrm{p\ local\ skin},i}(E_{\mathrm{p}},\Omega)\ [\mathrm{d}\Phi_i(E_{\mathrm{p}},\Omega)/\mathrm{d}E_{\mathrm{p}}\mathrm{d}\Omega]\ \mathrm{d}E_{\mathrm{p}}\mathrm{d}\Omega \qquad (3.29)$$

[3]The angle Ω is defined such that the angle θ is the angle of irradiation direction with the axis of the cylinderfor the pillar and rod; and the angle θ+ π/2 is the angle of irradiation direction with the normal of the incident radiation surface for the slab; and φ being the angle of irradiation direction projected onto the plane perpendicular to the cylindrical axis for the pillar and rod;and the normal of the incident radiation surface for the slab; with arbitrary direction in this plane for the pillar and rod, as both are cylindrical symmetric;and with one of the main axis in this planefor the slab.

where $d\Phi_i(E_p,\Omega)/dE_p d\Omega$ is the fluence of particles with kinetic energies in the interval dE_p around E_p, and directions of incidence in the interval $d\Omega$ around Ω. The sum over all contributing particle types is:

$$D_{\text{p local skin}} = \sum D_{\text{p local skin},i} \tag{3.30}$$

The unit of personal absorbed dose in local skin is J kg^{-1}. The special name for the unit of personal absorbed dose in local skin is gray (Gy).

4 Conversion Coefficients

4.1 Conversion Coefficients for the Operational Quantities

The conversion coefficients are calculated for irradiation of the whole-body ICRP/ICRU adult reference phantoms (ICRP, 2009) and the phantoms for absorbed dose in the lens of the eye and local skin for broad parallel beams of the radiation field phantoms exposed *in vacuo*. The specification of the incident direction, Ω, requires a reference system for coordinates in which Ω is expressed. For the responses of area monitoring instruments to determine directional absorbed dose, this reference system can be related to the radiation field. For personal dosimeters to determine personal dose and absorbed dose in the lens of the eye and in local skin, this reference system is related to the body, head and eye, and extremity. In the particular case of a unidirectional field orthogonal to the axis of the whole-body ICRP/ICRU adult reference phantoms from toe to head, or the Z-axis (slab phantom), or the cylinder axis (cylindrical phantoms),the direction of incidence between the direction of the radiation field, Ω, and the direction, Ω_0, that is antero-posterior to the phantom, is α.

In Appendix A, Tables A.1.1a to A.1.10 and Figures A.1.1a to A.1.10 give the numerical values of conversion coefficients of ambient dose, H^*, (see Section 3.4.1) from fluence for photons, neutrons, electrons, positrons, protons, negative muons, and positive muons, for energies up to 10 GeV; for negative pions and positive pions for energies up to 200 GeV; and for He ions up to 100 GeV u^{-1}. Table A.1b and Figure A.1b give the numerical values from air kerma for photons up to 50 MeV.

Tables A.2.1a to A.2.10, and Figures A.2.1a to A.2.10 give the numerical values of the conversion coefficients from fluence to personal dose, H_p (see Section 3.4.7) for photons, neutrons, electrons, positrons, protons, negative muons, positive muons, negative pions and positive pions for energies up to 1GeV; and for He ions up to 1GeV u^{-1}; and in Table A.2.1b and Figure A.2.1b from air kerma for photons up to 50 MeV. The upper energies selected are considered appropriate for personal monitoring measurements. Other than for AP, PA, cranial, and caudal incidence, the value of effective dose will depend on the angle of incidence, and the conversion coefficients for irradiations in the horizontal plane the maximum value of right and left incidences of irradiation is taken. The conversion coefficients are given from 0° (A-P) to 90° in 15°, 180°, and for the irradiation geometries rotational (ROT), isotropic (ISO), superior hemisphere semi-isotropic (SS-ISO), and inferior hemisphere semi-isotropic (IS-ISO).

The numerical values of the conversion coefficients from particle fluence to directional absorbed dose in the lens of the eye, $D'_{\mathrm{lens}}(\Omega)$, (see Section 3.4.3) and personal absorbed dose in the lens of the eye, $D_{\mathrm{p\ lens}}$, (see Section 3.4.8), are the same for the same fluence, particle type, energy, and direction or angle of incidence. Tables A.3.1a to A.3.5 and Figures A.3.1a to A.3.5 give the values for photons, neutrons, electrons, positrons, and protons, from fluence, and Table A.3b and Figure A.3b for photons from air kerma for energies up to 50 MeV. The conversion coefficients are given from 0° (A-P) to 90° in 15° steps and for a rotational field (ROT).

The numerical values of the conversion coefficients of directional absorbed dose in local skin, $D'_{\mathrm{local\ skin}}(\Omega)$, (see Section 3.4.5), and personal absorbed dose in local skin, $D_{\mathrm{p\ local\ skin}}$, (see Section 3.4.9), are the same for the 300 mm x 300 mm x 150 mm slab phantom, for the same fluence, particle type, energy, and direction or angle of incidence. Tables A.4.1.1a to A.4.5 and Figures A.4.1.1a to A.4.5 give the values from fluence for photons, neutrons, electrons, positrons, and protons, for energies up to 50 MeV; and for alpha particles up to 10 MeV, and table A.4.1b and Figure A.4.1b from air kerma for photons. For directional and personal absorbed dose in local skin for the body, the conversion coefficients are given from 0° (A-P) to 75° in 15° steps; for exposure of the extremity and finger for angles from 0° to 180° in 15° steps and for a rotational field (ROT).

The calibration of area monitoring instruments and personal dosimeters to measure photons for ambient dose, personal dose, directional and personal absorbed dose in the lens of the eye and in local skin, are performed routinely in air with sufficient material in front of the instrument to provide full charged-particle equilibrium. The calibration is in terms of air kerma (ISO 29661:2012 (ISO, 2012)).

Appendix A.5 gives values of conversion coefficients of the operational quantities in terms of photon fluence and air kerma for this procedure for energies up to 50 MeV, using the kerma-approximation method in the calculation to approximate charged-particle equilibrium.

Appendix B describes the computer codes to calculate the conversion coefficients.

Appendix C for information gives conversion coefficients to the operational quantity absorbed dose to the maximum value of the absorbed dose in the complete lens or in the sensitive cells.

When a precise interpolation among the values of the conversion coefficients presented in this Report is required, it is recommended that a procedure similar to that used in ICRP Publication 116 (ICRP, 2010) should be followed. For interpolations of the operational quantities per fluence, a four-point (cubic) Lagrangian interpolation formula is recommended, and a log–log graph scale is appropriate. For interpolations of the operational quantities per air kerma, a linear-log graph scale is more appropriate.

4.2 Comparison of Values of Recommended and Previous Operational Quantities

4.2.1 General Remarks

In ICRP Publication 116 (ICRP, 2010), the values of the conversion coefficients from fluence to the protection quantities for all particles are calculated using full transport of the radiation field. The values of the conversion coefficients of the operational quantity ambient dose equivalent included in the figures in ICRP Publication 116 are also calculated using full transport of secondary particles. In ICRU Report 57 (ICRU, 1998) and ICRP Publication 74 (ICRP, 1996), the values of conversion coefficients for $H'(10)$ and $H_p(10)$, $H'(0.07)$ and $H_p(0.07)$ for photons were calculated using the kerma- approximation method; ICRU and ICRP note that care must be taken in using these values. The respective ranges of electrons in tissue are 10 mm, 3mm, and 0.07 mm for energies of 2 MeV, 740 keV, and 65 keV, Above these energies, conditions for charged-particle equilibrium are not met for calculations of $H'(10)$ and $H_p(10)$, $H'(3)$ and $H_p(3)$, $H'(0.07)$ and $H_p(0.07)$ for irradiation of the

ICRU sphere or the body *in vacuo* (Dimbylow and Francis, 1983, 1984; Ferrari and Pelliccioni, 1994, 1995; Daure *et al.*, 2011).

In some cases conversion coefficients for the current quantities are not available and therefore no comparisons are given. For the comparison of conversion coefficients for absorbed dose in the lens of the eye, values of $H_p(3)$ in a cylindrical phantom are used.

The symbols used in these figures are as follows: h^* for the fluence to ambient dose conversion coefficient ($=H^*/\Phi$), and $h^*(10)$ for the value of the previous ambient dose equivalent conversion coefficient ($=H^*(10)/\Phi$); h_p for the fluence to personal dose conversion coefficient ($= H_p/\Phi$) and $h_p(10)$ for the value of the previous personal dose equivalent conversion coefficient ($= H_p(10)/\Phi$); h'_{lens} and $h_{p\ lens}$ for the fluence to directional and personal absorbed dose in the lens of the eye conversion coefficient ($=D'_{lens}/\Phi$ and $=D_{p\ lens}/\Phi$), and $h'(3)$ and $h_p(3)$ for the previous fluence to directional and personal dose equivalent conversion coefficient ($=H'(3)/\Phi$ and $=H_p(3)$; $h'_{local\ skin}$ and $h_{p\ local\ skin}$ for the fluence to directional and personal absorbed dose in local skin conversion coefficient ($=D'_{local\ skin}/\Phi$ and $=D_{p\ local\ skin}/\Phi$), and $h'(0.07)$ and $h_p(0.07)$ for the previous fluence to directional and personal dose equivalent conversion coefficient ($=H'(0.07)/\Phi$ and $=H_p(0.07/\Phi)$).

4.2.2 Ambient Dose and Personal Dose

In the following figures, comparisons are given of the numerical values of conversion coefficients of the previous definitions with the recommended values, from particle fluence as a function of energy of ambient dose for photons, neutrons, electrons, positrons, protons, negative muons, positive muons, negative pions, positive pions, and He ions/α particles, and of personal dose for photons, neutrons, and electrons.

For higher-energy charged nuclei, $Z > 1$, the dose equivalent at 10 mm can be an inadequate estimation of effective dose (see ICRP Publication 123 (ICRP, 2013)).

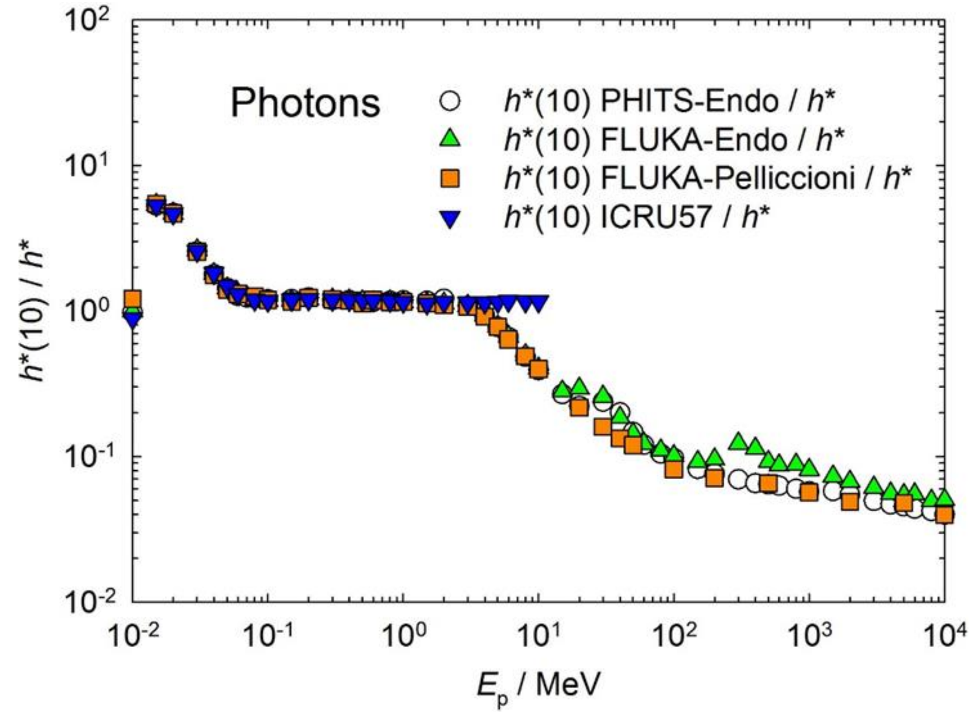

Figure 4.1: Comparisons of conversion coefficients for photons of $h^*(10)$ PHITS-Endo and $h^*(10)$ FLUKA-Endo (Endo, 2016b), $h^*(10)$ FLUKA-Pellicciони (Pellicciони, 2000), and $h^*(10)$ (ICRU, 1998) with kerma approximation; with those for h^*.

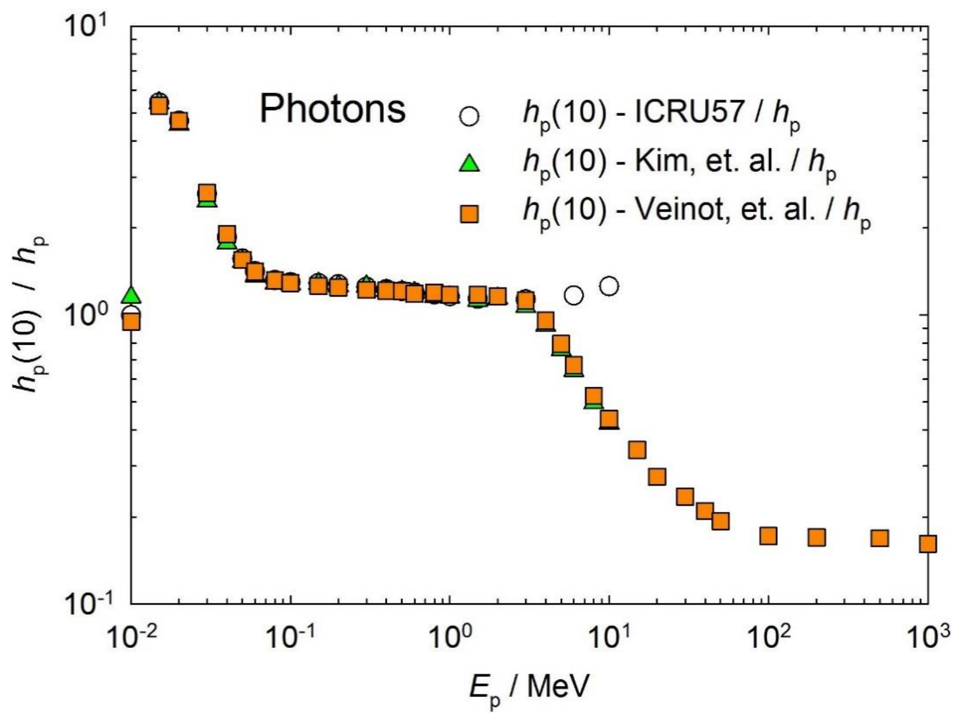

Figure 4.2: Comparison of conversion coefficients for photons of $h_p(10)$ (Kim and Kim, 1999; Veinot and Hertel, 2011), and $h_p(10)$ (ICRU, 1998) using the kerma approximation, with those for h_p.

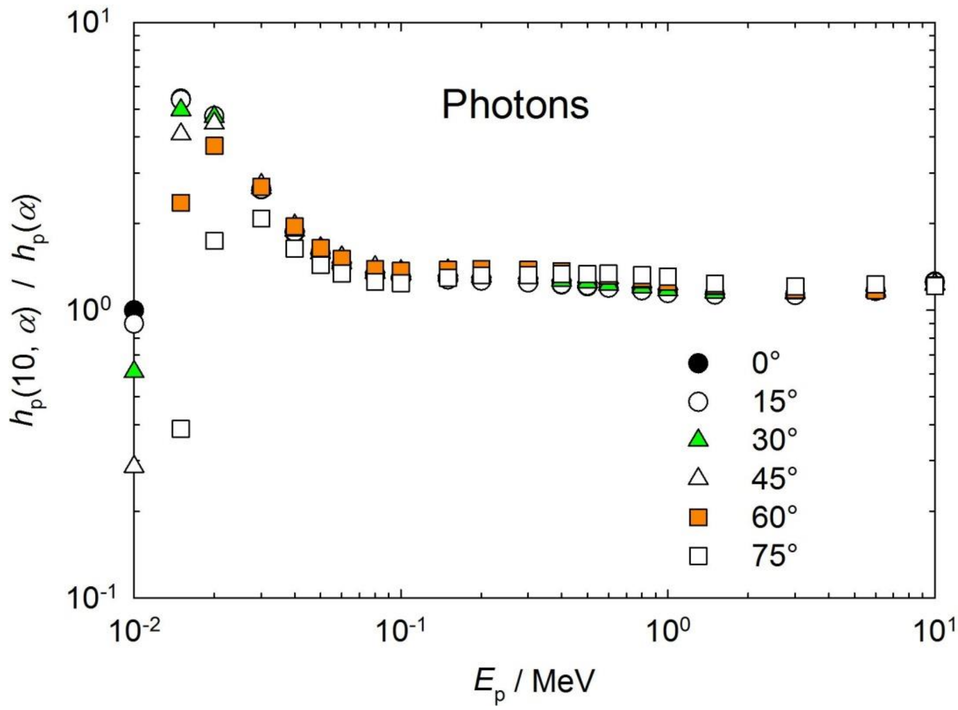

Figure 4.3: Comparison of conversion coefficients for photons $h_p(10,\alpha)$ (ICRU, 1998) using the kerma approximation, with those for $h_p(\alpha)$ (Endo, 2017).

The significant overestimate of effective dose for photons by the previous value of ambient dose equivalent and personal dose equivalent below 100 keV by up to a factor of 5 is because numerical values of dose equivalent at a depth of 10 mm in tissue do not reflect effective dose but were derived to approximately reproduce the maximum dose equivalent in the body, with the exception for a small energy region between 20 keV and 100 keV for dose equivalent to endosteal cells. There is a progressive underestimation of effective dose by $H^*(10)$ and $H_p(10)$ for photons of energies above 10 MeV (Pelliccioni, 1998, 2000). The use of the kerma-approximation method in the calculation of conversion coefficients in ICRP Publication 74 (ICRP, 1996) and ICRU Report 57 (ICRU, 1998) allows an agreement of the numerical values of the previous published values of ambient and personal dose equivalent in this energy region, with effective dose.

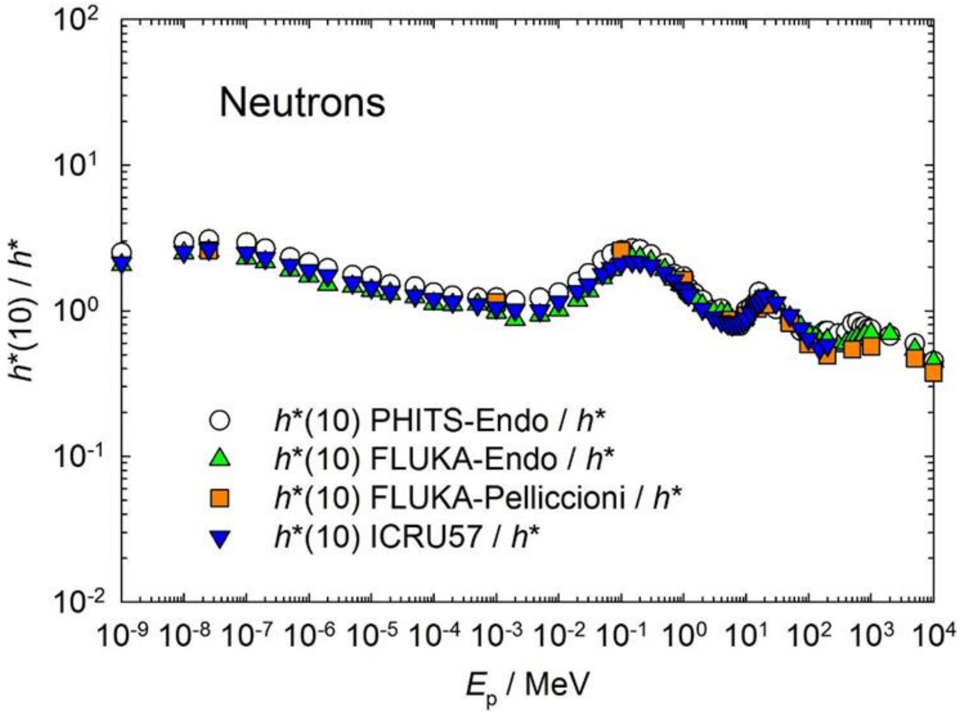

Figure 4.4: Comparisons of conversion coefficients for neutrons of $h^*(10)$ PHITS-Endo and $h^*(10)$ FLUKA-Endo (Endo, 2016b), $h^*(10)$ FLUKA-Pelliccioni (Pelliccioni, 2000), and $h^*(10)$ ICRU Report57 (ICRU, 1998); with those for h^*.

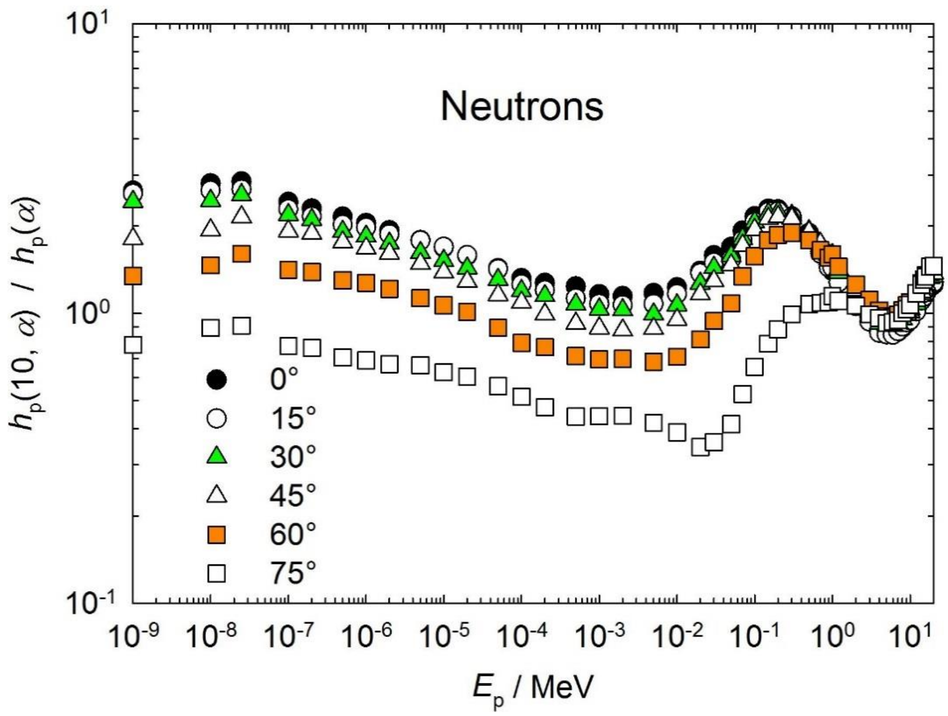

Figure 4.5: Comparisons of conversion coefficients for neutrons of $h_p(10, \alpha)$ (ICRU, 1998) with those for $h_p(\alpha)$ (Endo, 2017).

The depth of 10 mm in the sphere, or in the body is not the most appropriate to estimate effective dose for neutrons (ICRU, 1985).There are also changes to the ratio from a quantity using quality factor, $H^*(10)$ to conversion coefficients based on effective dose that uses radiation weighting factor. There is a progressive underestimation of effective dose by the previous quantity, $H^*(10)$, for neutrons of energies above 10 MeV.

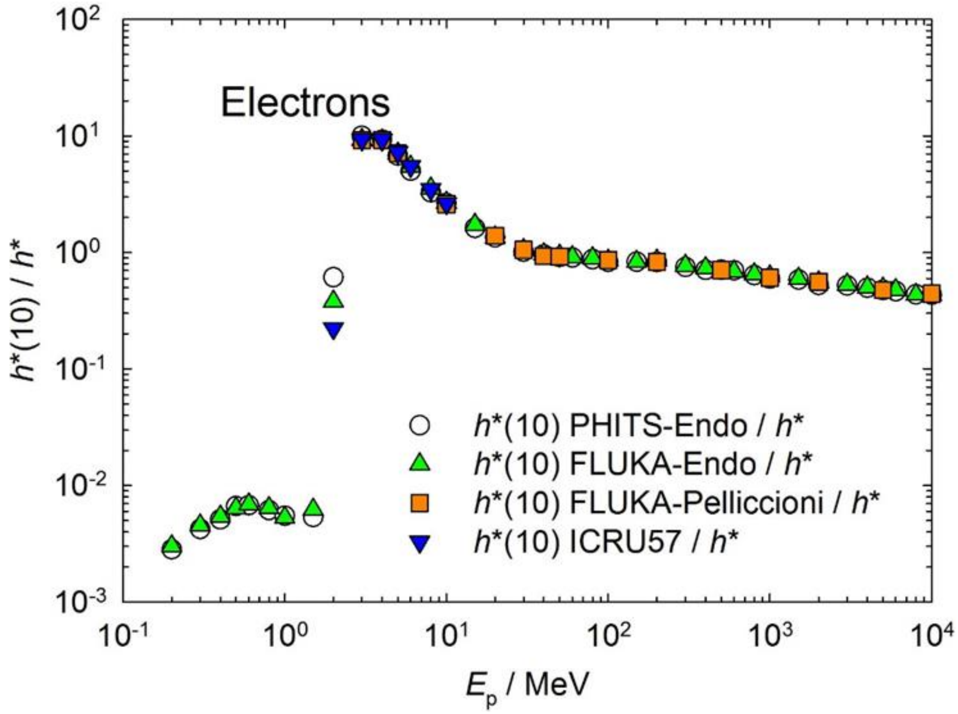

Figure 4.6: Comparisons of conversion coefficients for electrons of $h^*(10)$ PHITS-Endo and $h^*(10)$ FLUKA-Endo (Endo, 2016b), $h^*(10)$ FLUKA-Pelliccioni (Pelliccioni, 2000), and $h^*(10)$ ICRU Report 57 (ICRU, 1998); with those for h^*.

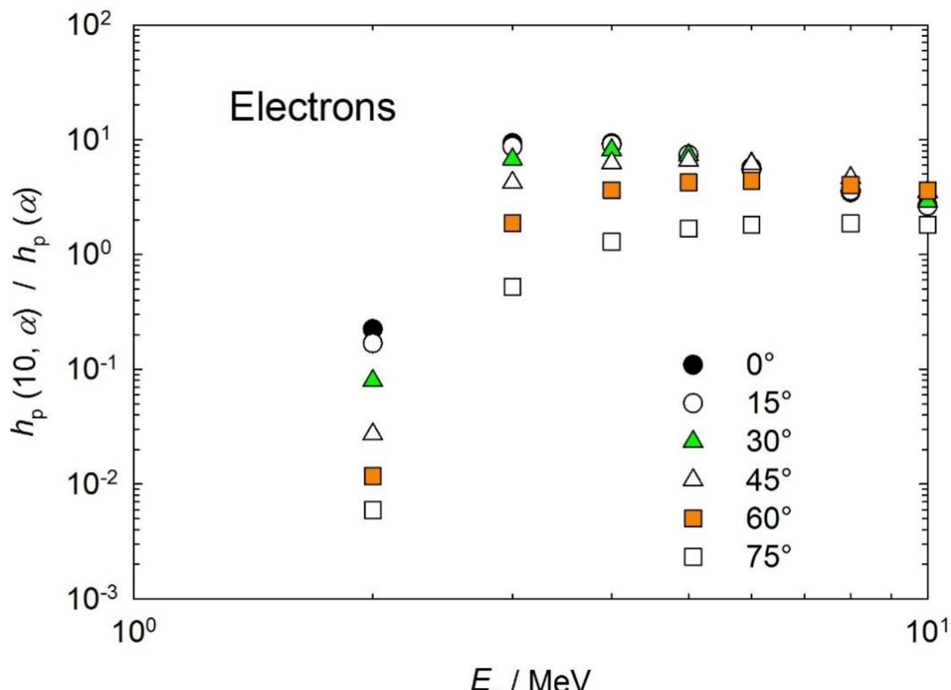

Figure 4.7: Comparison of conversion coefficients for electrons for $h_p(10, \alpha)$ (ICRU, 1998; Grosswendt and Chartier, 1994) with those for $h_p(\alpha)$ (Endo, 2017).

For electrons, the previous quantities, $H^*(10)$ and $H_p(10)$, overestimated the recommended quantities between 1 and 10 MeV.

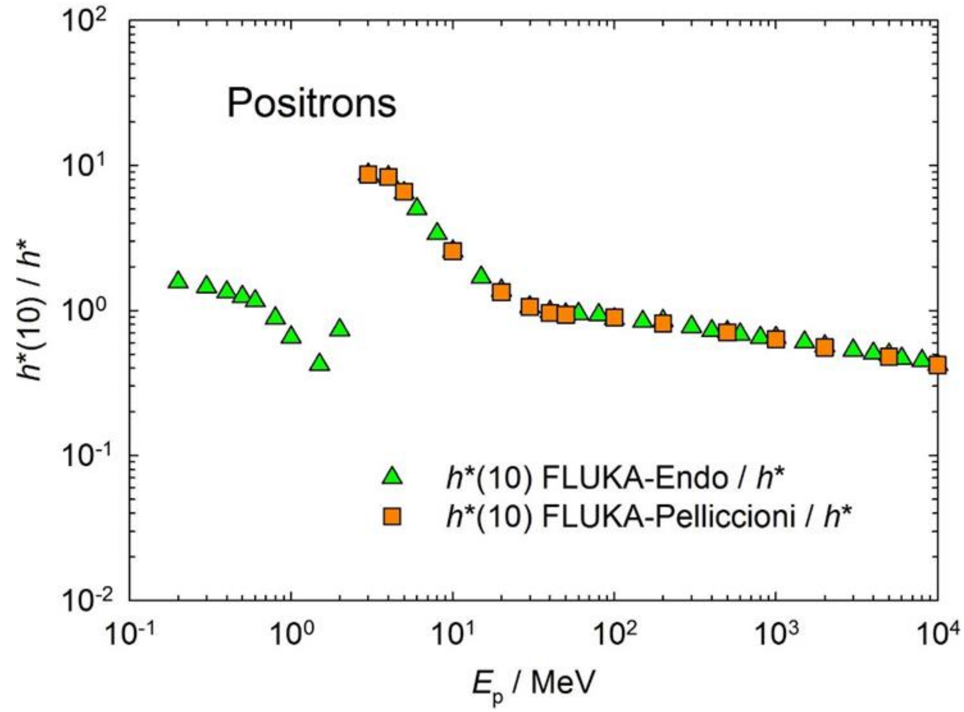

Figure 4.8: Comparisons of conversion coefficients for positrons of *h**(10) FLUKA-Endo (Endo, 2016b) and *h**(10) FLUKA-Pelliccioni (Pelliccioni, 2000); with those for *h**.

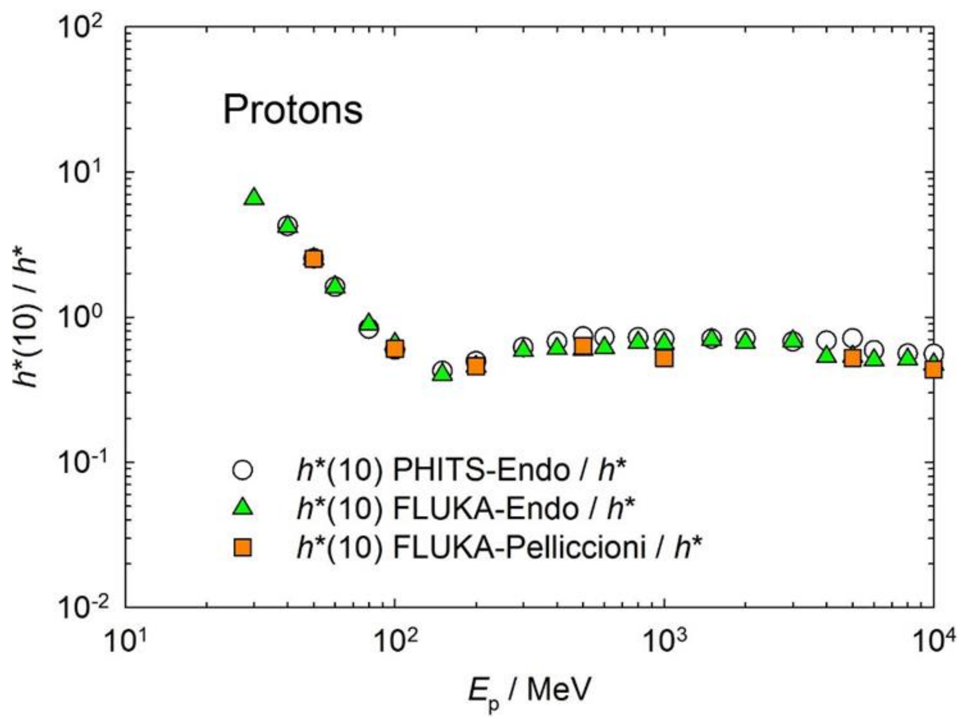

Figure 4.9: Comparisons of conversion coefficients for protons of *h**(10) PHITS-Endo and *h**(10) FLUKA-Endo (Endo, 2016b), and *h**(10) FLUKA-Pelliccioni (Pelliccioni, 2000); with those for *h**.

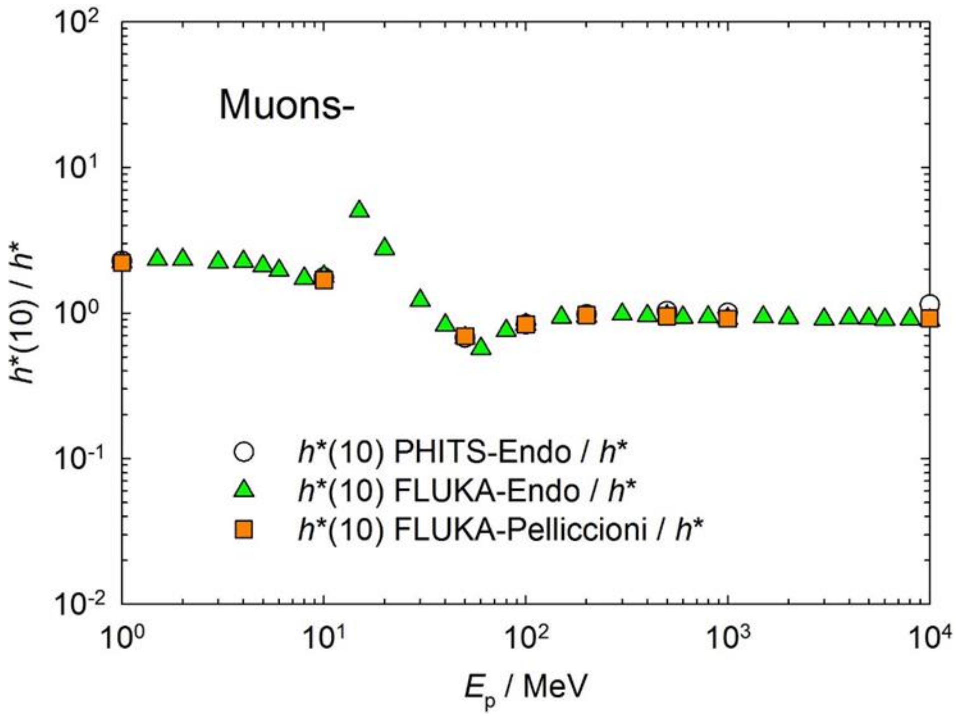

Figure 4.10: Comparisons of conversion coefficients for negative muons of $h^*(10)$ PHITS-Endo and $h^*(10)$ FLUKA-Endo (Endo, 2016b), and $h^*(10)$ FLUKA-Pelliccioni (Pelliccioni, 2000); with those for h^*.

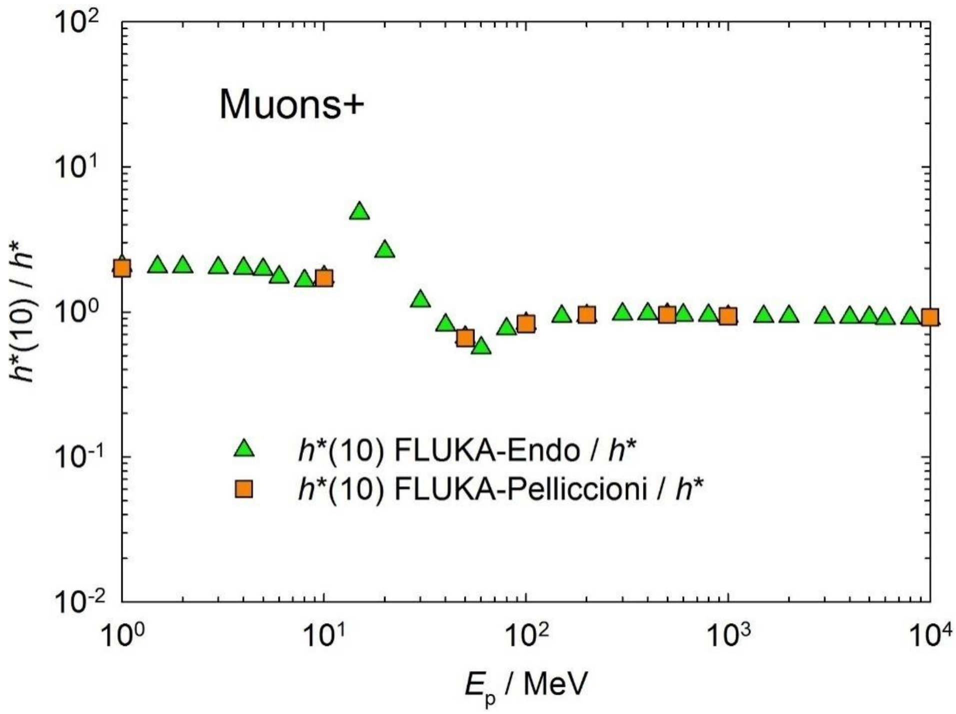

Figure 4.11: Comparisons of conversion coefficients for positive muons of $h^*(10)$ FLUKA-Endo (Endo, 2016b) and $h^*(10)$ FLUKA-Pelliccioni (Pelliccioni, 2000); with those for h^*.

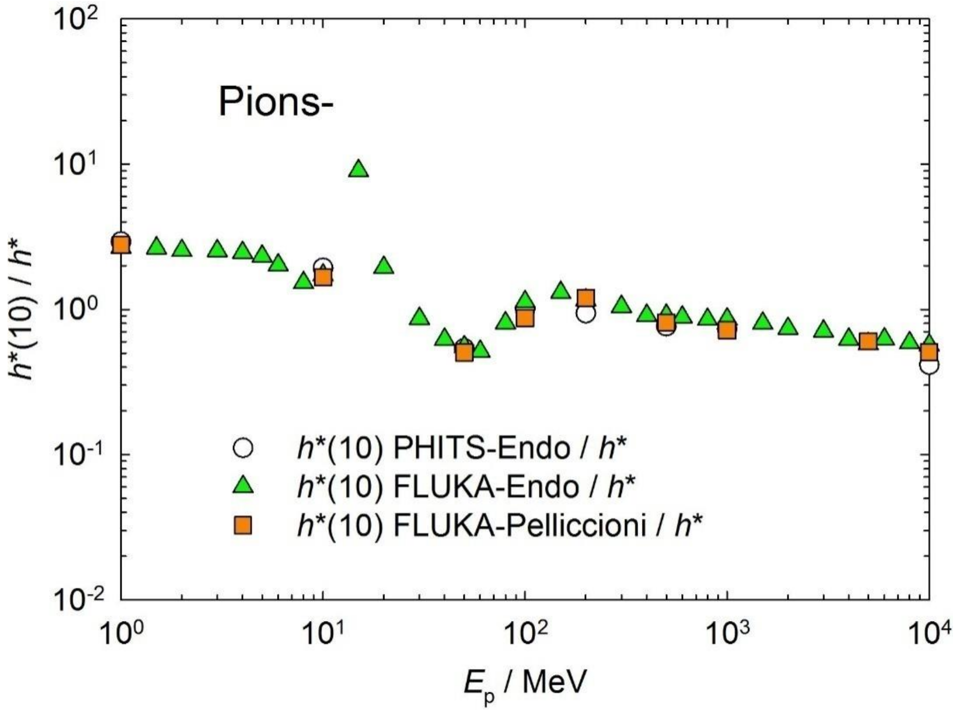

Figure 4.12: Comparisons of conversion coefficients for negative pions of *h**(10) PHITS-Endo, *h**(10) FLUKA-Endo (Endo, 2016b), and *h**(10) FLUKA-Pellicconi (Pelliccioni, 2000); with those for *h**.

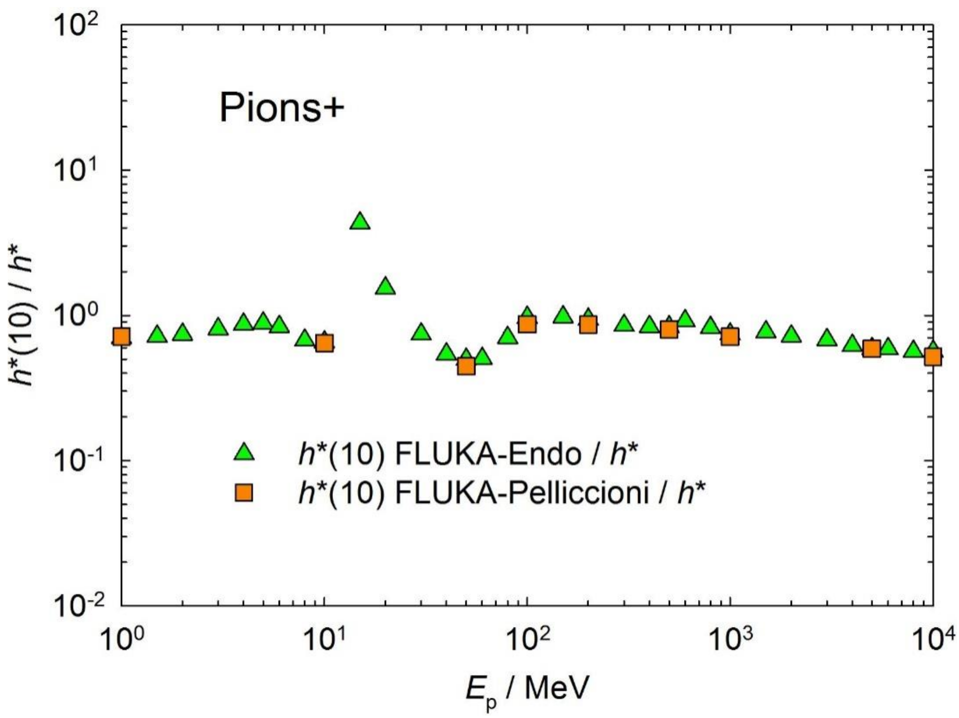

Figure 4.13: Comparisons of conversion coefficients for positive pions of *h**(10) FLUKA-Endo (Endo, 2016b) and *h**(10) FLUKA-Pellicconi (Pelliccioni, 2000); with those for *h**

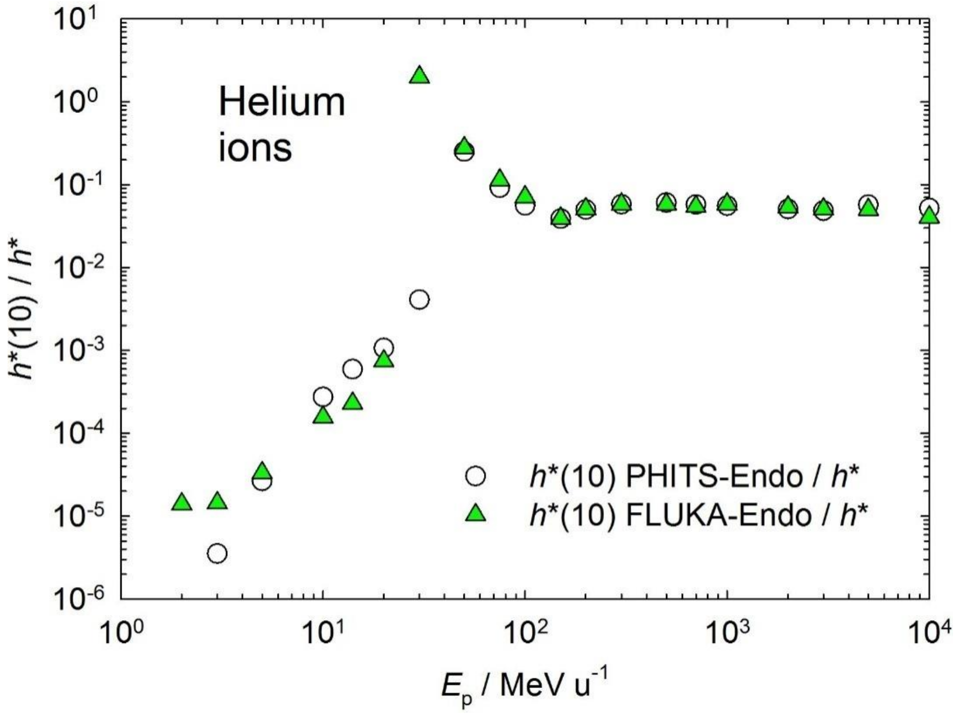

Figure 4.14: Comparisons of conversion coefficients for helium ions of $h^*(10)$ PHITS-Endo and $h^*(10)$ FLUKA-Endo (Endo, 2016b); with those for h^*.

4.2.3 Directional and Personal Absorbed Dose in the Lens of the Eye

For the same fluence, particle type, energy, and direction of incidence, the numerical values of conversion coefficients from particle fluence to directional and personal absorbed dose in the lens of the eye are the same. In the following figures, comparisons are given of the numerical values of conversion coefficients of the previous definitions, $H'(0.07)$ or $H_p(0.07)$, with the recommended values of the conversion coefficients, $d'(\alpha)_{lens}$ and $d(\alpha)_{p\ lens}$, from particle fluence as a function of energy for photons and electrons.

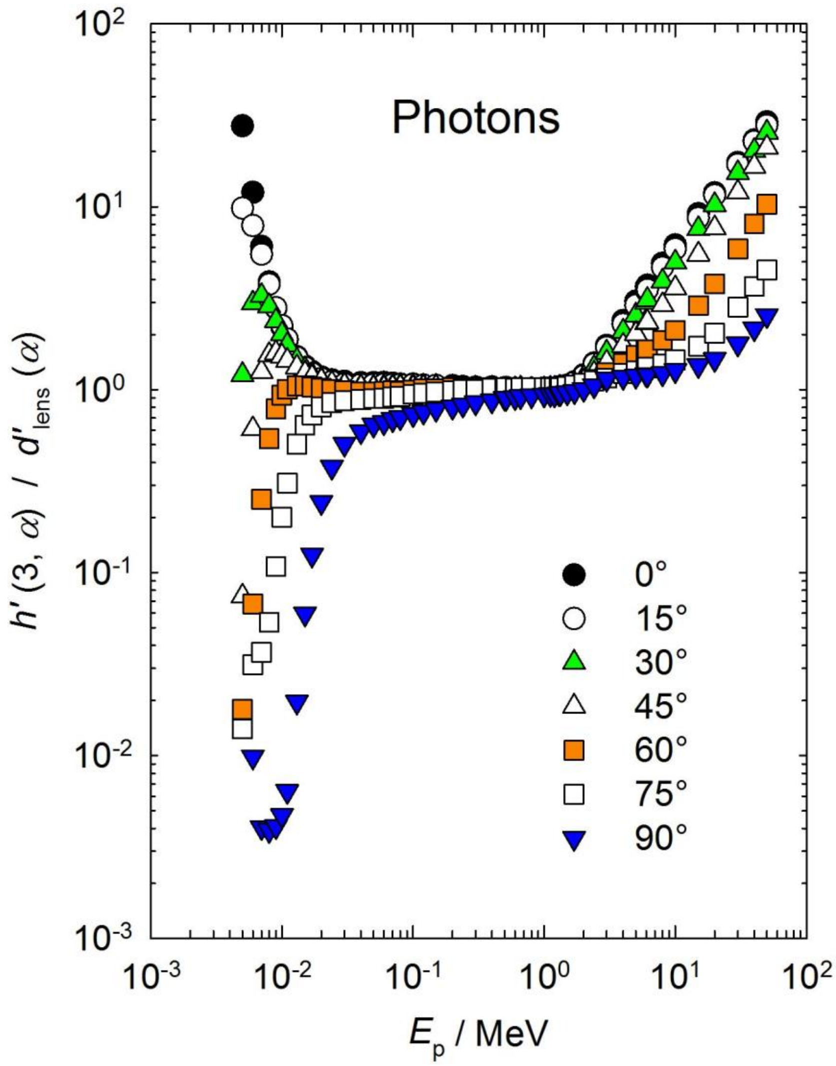

Figure 4.15: Comparison of conversion coefficients for photons for $h'(3,\alpha)$ (Behrens, 2017b), with kerma approximation, with those for $d'(\alpha)_{\mathrm{lens}}$ (Behrens, 2017a).

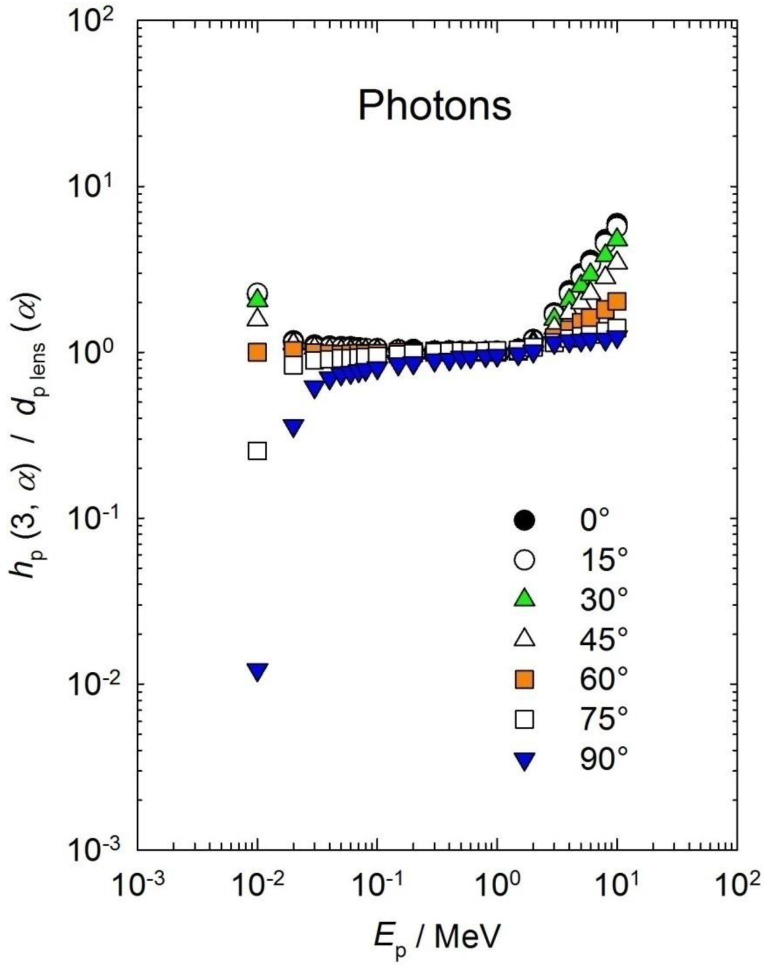

Figure 4.16 Comparison of conversion coefficients for photons for $h_p(3,\alpha)$ (Gualdrini *et al*. 2011; Daures *et al*., 2011), made with kerma approximation, with those for $d(\alpha)_{p\ lens}$ (Behrens, 2017a) . Data for $h_p(3,\alpha)$ are only available from 10keV to 10 MeV.

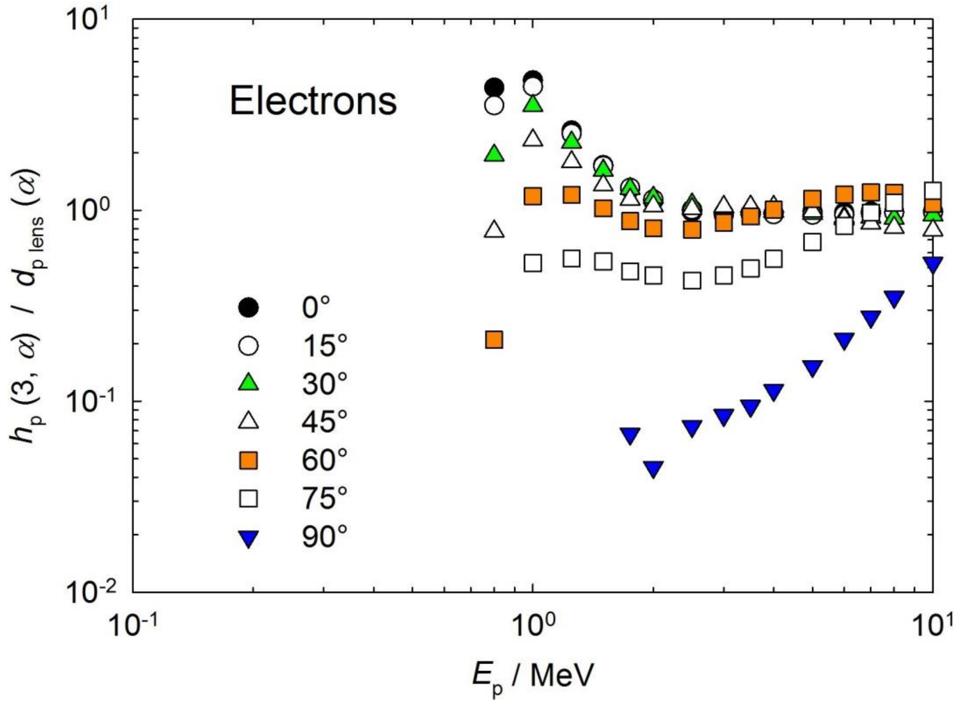

Figure 4.17 Comparison of conversion coefficients of electrons for $h_p(3, \alpha)$ (Ferrari and Gualdrini, 2012) with those for $d_{p\ lens}(\alpha)$, maximum for complete lens of both lenses (Behrens, 2017a).

The Figures show that the numerical values of directional dose equivalent and personal dose equivalent at a depth of 3mm for photons and electrons at certain energies and angles of incidence do not give a good indication of absorbed dose in the lens of the eye. There is concern in nuclear medicine utilizing beta radiation for the accurate assessment of absorbed dose to the lens of the eye.

4.2.4 Directional and Personal Absorbed Dose in Local Skin

For the same fluence, particle type, energy, direction, and specific phantom, the numerical values of conversion coefficients from particle fluence to directional and personal absorbed dose in local skin are the same. In the following figures, comparisons are given of the of the numerical values of previous definitions for $H'(0.07)$ or $H_p(0.07)$, with the recommended values of the conversion coefficients, $d'_{\text{local skin slab}}(\alpha)$ and $d'_{\text{local skin slab}}(\alpha)$, from particle fluence as a function of energy for photons and electrons.

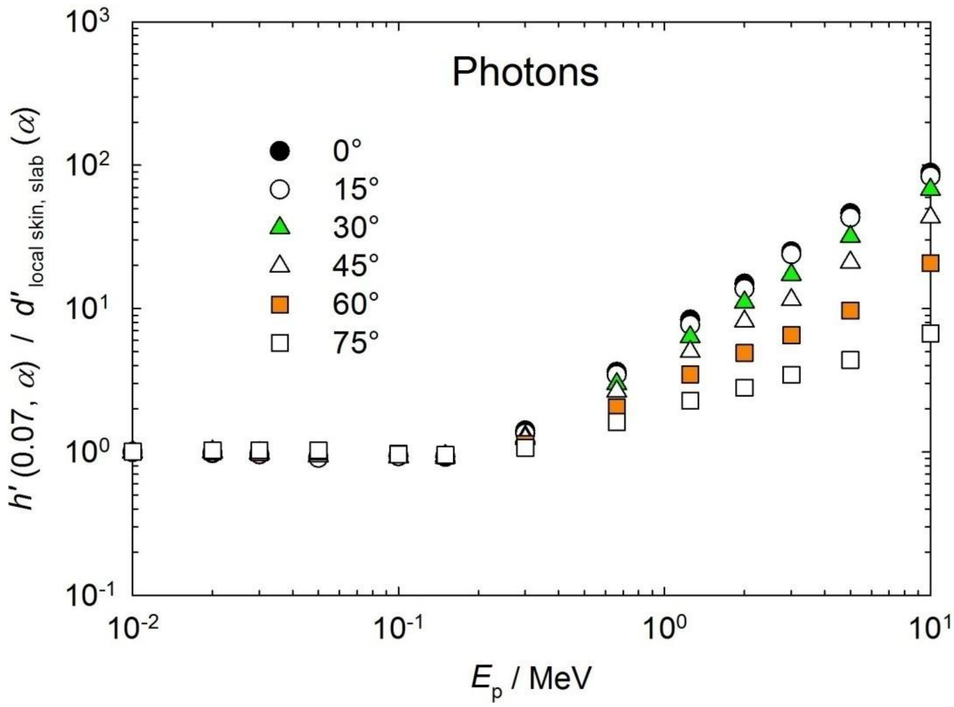

Figure 4.18: Comparison of conversion coefficients for photons for $h'(0.07, \alpha)$ using the kerma approximation (ICRU, 1998) with those for $d'_{\text{local skin slab}}(\alpha)$ (Daures et al., 2017).

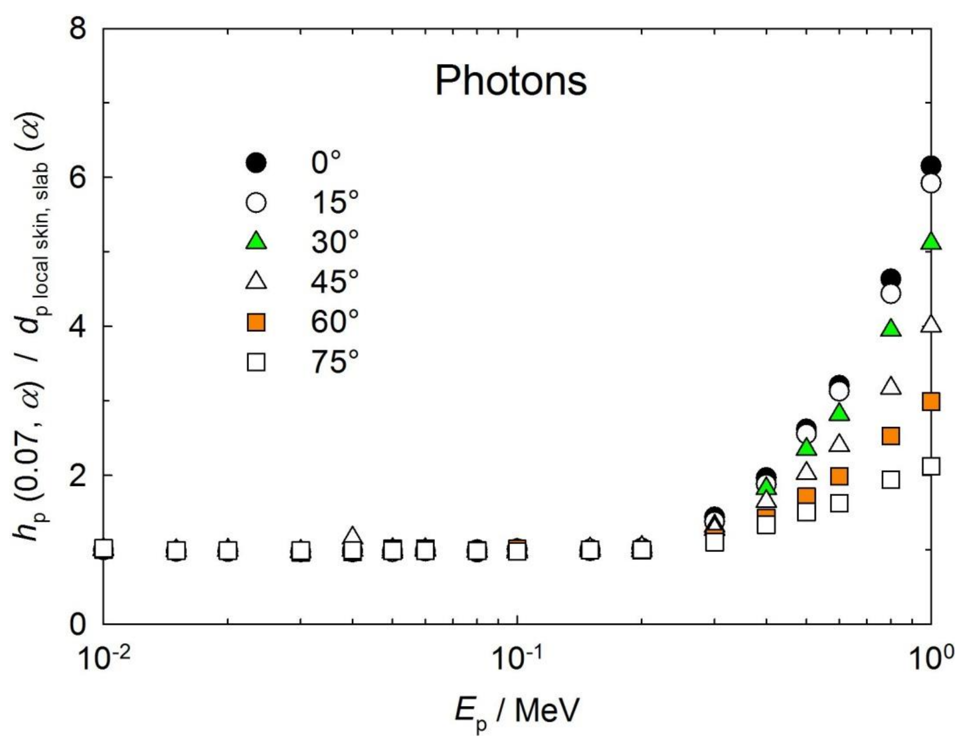

Figure 4.19: Comparison of conversion coefficients for photons for $h_{\text{p}}(0.07, \alpha)$ using the kerma approximation (ICRU, 1998) with those for $d_{\text{plocal skin slab}}(\alpha)$ (Daures et al., 2017).

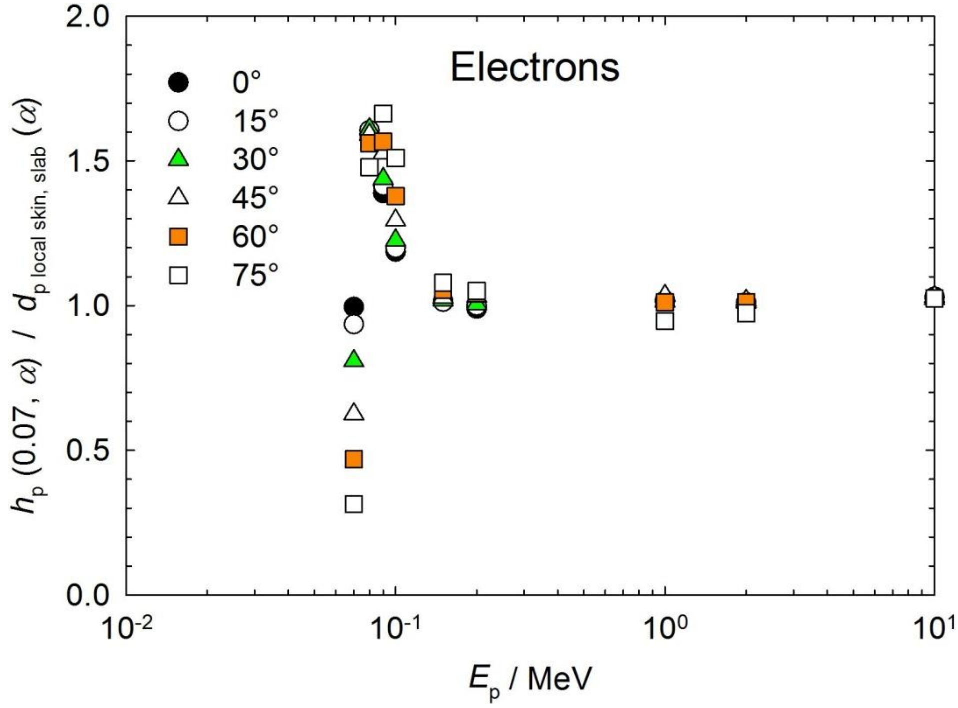

Figure 4.20: Comparison of conversion coefficients for electrons for $h_p(0.07, \alpha)$ (ICRU, 1998) with those for $d_{plocal\ skin\ slab}(\alpha)$ (Daures et al., 2017).

The numerical values of the conversion coefficients given in ICRU Report 57 (ICRU, 1998) and ICRP Publication 74 (ICRP, 1996) for $H'(0.07)$ and $H_p(0.07)$ for photons above 65 keV using the kerma-approximation method give an overestimation of absorbed dose in local skin, increasing to a factor of 90 for 10 MeV photons (Veinot and Hertel; 2011).

5 Applications of the Operational Quantities

5.1 Operational Quantities and their Application in Occupational Radiation Protection

The role of the operational quantities is to provide an adequate estimate of the protection quantities in order to assess compliance with the limits and for optimization (see Table 5.1). The range of particle types and energies given for the protection quantities in ICRP Publication 116 (ICRP 2010) are as follows: photons, neutrons, electrons, positrons, protons, negative muons, and positive muons up to 10 GeV; negative pions and positive pions up to 200 GeV; and He ions up to 100 GeV u^{-1}.

Table 5.1: Scheme of operational quantities for dose monitoring in external radiation fields.

Task	Operational quantities for	
	area monitoring	**individual monitoring**
Control of effective dose	ambient dose, H^*	personal dose , H_p
Control of doses in the the lens of the eye	directional absorbed dose in the lens of the eye, $D'_{lens}(\Omega)$	personal absorbed dose in the lens of the eye, $D_{p\ lens}$
Control of doses in local skin, the hands, and feet	directional absorbed dose in local skin, $D'_{local\ skin}(\Omega)$	personal absorbed dose in local skin , $D_{p\ local\ skin}$

In principle, the operational quantities should be defined for all particles and energies for which the protection quantities are provided. Up to now, an internationally agreed data set of conversion coefficients for operational quantities for monitoring external exposure has been given for photons, neutrons, and electrons in a restricted energy range. This has been sufficient for the large majority of applications in radiation protection, but more attention is being given to higher energies, and for other types of particles.

The areas of application of operational quantities have increased. The particle types and range of particle energies of the radiation fields used in medical diagnostics and therapy, and scientific research, has been extended. There is the inclusion of natural sources of radiation in ICRP recommendations: aircraft crews are one of the most highly exposed occupational groups, and the radiation field at flight altitudes includes a large component of high-energy particles from cosmic radiation (ICRU, 2010; ICRP, 2016).

The quantities personal dose, personal absorbed dose in the lens in the eye, and personal absorbed dose in local skin, are used for retrospective recording in order to show compliance with regulations in respect of limits, and for optimization.

Operational quantities are measurable. This means that the calibration coefficients of an area monitoring instrument and personal dosimeter can be determined in terms of an operational quantity in a reference field under reference conditions, where the value of the operational quantity at the point of test is well specified. The calibration coefficients of an area monitoring instrument and personal dosimeter are based on using a reference value of a radiometric or dosimetric quantity, which can be well realized by a standard field quantity at the point of test, and applying a reference conversion coefficient relating this radiometric or dosimetric quantity to an operational quantity. The value of the radiometric or dosimetric quantity shall be traceable to a national or international standard. The conversion coefficients for the operational quantities are an integral part of the metrological chain of traceability. In high-energy and complex radiation fields, there are no traceable reference fields to characterize and calibrate instruments.

An area monitoring instrument or a personal dosimeter could be designed for a limited range of particle types, energies and angles of incidence, and this will influence the calibration procedures, including type-testing, and the routine radiation protection measurement at the workplace.

5.2 Operational Quantities and their Application in Environmental Monitoring

Operational quantities were originally developed for the protection of occupationally exposed workers. The use of the quantities has been extended to monitoring of radiation exposure of the public from natural and artificial environmental sources of radiation. Applications are radiation monitoring at the fence of nuclear, medical and other facilities with ambient dosimeters and in contaminated environments by radionuclides released from such facilities. Radionuclides released into the environment deposit on the ground surface, and then migrate into the soil. The migration behavior of radionuclides in the soil depends on soil types, climate conditions, time after the deposition, and so on. The distribution of radionuclides in the soil influences the radiation field, energy distribution and angular distribution, above the ground (ICRU, 1994). Operational quantities play an important role to assess doses for the public under these complex radiation fields.

After the Fukushima Daiichi nuclear power plant accident, a large-scale national environmental monitoring program has been carried out, and comprehensive data including ambient dose equivalent rates at 1 m height above the ground surface and radioactivity in the soil have been collected (NRA, 2012). Though several kinds of radionuclides were detected by gamma-ray spectrometry of the soil samples, ^{137}Cs and ^{134}Cs were the significant radionuclides contributing most to the ambient dose equivalent rates. It is important to clarify the relation among radioactivity in the soil, relating the measurement of an area monitoring quantity in air and effective dose for the protection of the public (Saito *et al*., 2012, 2014; Petoussi-Henss *et al*., 2012).

6Calibration of Area Monitoring Instruments and Personal Dosimeters

6.1 General

The operational quantities for ambient dose, directional absorbed dose in the lens of the eye, and directional absorbed dose in local skin, are for all components of the radiation field in particle energy and direction at the point of interest, and for personal dose, personal absorbed dose in the lens of the eye, and personal absorbed dose in local skin, for all components of the radiation field in particle energy and angle of incidence on the body. This can include multiple scattering and nuclear reactions between the radiation source and the body. Area monitoring instruments and personal dosimeters normally will be specified to determine the contributions for a range of particle energies and directions and angles of incidence on the body and calibrated for these parameters.

The individual monitoring operational quantity is determined at a point on the body, head, or extremity, for the fluence or air kerma at that point and a conversion coefficient for broad parallel fields for this fluence or air kerma incident on the whole-body ICRP/ICRU adult reference phantoms (ICRP, 2009) or the phantoms for absorbed dose in the lens of the eye and local skin. Calibration procedures can be made to include angles of incidence of fluence or air kerma that are not directly incident at this point on the body, head, or extremity, using the incident fluence or air kerma at this point: the calibration procedure can be such as to simulate exposure of a person in rotational or isotropic exposure.

In routine procedures for the calibrations of area monitoring instruments and personal dosimeters in photon fields, conditions approximating full charged-particle equilibrium are used, and an additional set of conversion coefficients for photons calculated using the kerma-approximation method is provided (see Appendix A.5) for photon energies up to 50 MeV.

The measurement of H^*, generally requires that the radiation field be uniform over the dimensions of the instrument and that the instrument has an isotropic response. The measurement of

$D'_{lens}(\Omega)$ and $D'_{local\ skin}(\Omega)$, also requires that the radiation field be uniform over the dimensions of the instrument and that the instrument has the appropriate response as a function of direction.

No changes are needed in the radiation characteristics, production, and dosimetry of the standard reference fields of ISO, IEC, and BIPM, or in the calibration procedures, but a change to the recommended conversion coefficients for these fields will be required.

6.2 Calibration Phantoms for Personal Dosimeters

The recommended phantoms for the calibration of personal dosimeters for the different quantities are:

- for personal dose: a polymethyl methacrylate (PMMA) 300 mm x 300 mm x 150mm water filled slab (front wall 2.5 mm thick, other walls 10 mm thick) (ISO, 1999);
- for personal absorbed dose in the lens of the eye: a PMMA 200 mm diameter 200 mm length water filled cylinder (cylinder walls and end faces 5 mm thick) (Gualdrini *et al*. 2011; Daures *et al*., 2011; Vanhavere *et al*., 2012));
- for personal absorbed dose in local skin: for the trunk, a PMMA 300 mm x 300 mm x 150mm water filled slab (ISO, 1999); for the extremity, a PMMA 73 mm diameter 300 mm length water filled pillar (cylinder walls 2.5 mm thick, end faces 10 mm thick) (ISO, 1999); for the finger, a PMMA 19 mm diameter 300 mm length rod (ISO, 1999).

7 Conclusions

The use of operational quantities based on a value of a radiometric or dosimetric quantity at a point and a conversion coefficient to a protection quantity has been investigated previously. This approach is now considered acceptable as the ICRP and ICRU have defined adult reference computational phantoms for the protection quantities that are widely recognized, and have published conversion coefficients from particle fluence to these quantities. The use of operational quantities that are related directly to the values of the protection quantities simplifies the systems of protection and operational quantities, and assists in the comprehension and consistency of radiation protection quantities by users.

The recommendations of operational quantities in terms of conversion coefficients to ambient dose, directional absorbed dose in the lens of the eye, directional absorbed dose in local skin, personal dose, personal absorbed dose to the lens of the eye, and personal absorbed dose to local skin, are a clean break from the existing recommendations for operational quantities that are based on dose equivalent in the ICRU 4-element sphere and at a depth in the body, and will give a better estimate of the protection quantities.

There has been concern that ICRP might make significant changes to the tissue weighting factors and/or the radiation weighting factors, and this would require revisions of the values of the conversion coefficients for effective dose. In this were to take place, case, which is expected to be infrequent, changes to the conversion quantities to the operational quantities might then be considered, but would not be automatic.

The numerical values of conversion coefficients for ambient dose and personal dose for photons of energies from 70 keV to 2 MeV are very close to those given in the current definitions. The values of these quantities from 2 MeV to 10 MeV, in conditions with full charged-particle equilibrium when including the contributions to the quantities from the electron conversion coefficients, are very close to those given in ICRU Report 57 (ICRU, 1998) and ICRP Publication 74 (1996) calculated with the kerma-approximation method. The only changes required for this photon energy range for the calibration of area monitors and personal dosimeters, are a small change to the instrument constant. The calibration of photon area monitoring instruments and personal dosimeters are routinely performed under condition of charged particle equilibrium, and conversion coefficients are given calculated using the kerma-approximation method.

For neutrons, the recommended quantities for ambient dose and personal dose are a considerable improvement on the current values for the determination of the protection quantities. However, for area monitoring instruments based on the moderation of the neutron fluence, no changes are required initially for workplace fields.

Modifications of existing instrumentation might be required where this is considered to be necessary:

- for photon energies below 70 keV, to correct for the large overestimation of effective dose by current area monitors and personal dosimeters;
- to improve the estimation for photons and electrons of absorbed dose in the lens of the eye;
- to determine for photons with energies between 2 MeV and 10 MeV for ambient and personal dose, if charged-particle equilibrium is not present, but this will depend on the detector system;
- to improve the performance of area monitoring instruments and dosimeters for neutron energies from thermal to 2 MeV in order to correct for the lower value of the conversion coefficients from particle fluence to H^* and H_p compared to $H^*(10)$ and $H_p(10)$, and to improve the response above neutrons of energy of 50 MeV in order to correct for the higher value.

The recommended operational quantities will provide a solution to the protection problems in radiation fields of higher-energy photons, electrons and neutrons, and for other particle types.

Report No. XX

OPERATIONAL QUANTITIES FOR EXTERNAL RADIATION EXPOSURE

THE INTERNATIONAL COMMISSION ON RADIATION UNITS AND MEASUREMENTS
and
THE INTERNATIONAL COMMISSION ON RADIOLOGICAL PROTECTION

MONTH 2017

Journal of the ICRU Volume XX No X 2017
ISBN XXXXXXXXXX
Published by Oxford University Press

OPERATIONAL QUANTITIES FOR EXTERNAL RADIATION EXPOSURE

Report Committee

N.E.Hertel (Co-Chair), Georgia Institute of Technology, USA.

D.T. Bartlett (Co-Chair), Abingdon, UK

R.Behrens, Physikalisch-Technische Bundesanstalt, Braunschweig, Germany

J-M.Bordy, CEA, LIST, Laboratoire National Henri Becquerel (LNE-LNHB), 91191 Gif-sur-Yvette, France

G..Dietze†, Braunschweig, Germany

A. Endo, Japan Atomic Energy Agency, Japan

G.Gualdrini, Ente per le Nuove Tecnologie, L'Energia e L'Ambiente, Bologna, Italy (until 2015)

T. Otto, European Organization for Nuclear Research (CERN), Geneva, Switzerland

M.Pelliccioni, Istituto Nazionale di Fisica Nucleare, Frascati, Italy

Consultants to the Report Committee

P. Ambrosi, Physikalisch-Technische Bundesanstalt, Braunschweig, Germany (until 2014)

M.B.Bellamy, Center for Radiation Protection Knowledge, Oak Ridge National Laboratory, Oak Ridge, USA

J-F. Bottollier-Depois, Institut de Radioprotection et de Sûreté Nucléaire, Fontenay-aux-Roses, France

J. Daures, CEA, LIST, Laboratoire National Henri Becquerel (LNE-LNHB), 91191 Gif-sur-Yvette, France

K.F. Eckerman, Oak Ridge,USA

P. Ferrari, Ente per le Nuove Tecnologie, L'Energia e L'Ambiente, Bologna, Italy

B.R.L. Siebert, Braunschweig, Germany

K.G. Veinot, Y-12 National Security Complex, Oak Ridge, Tennessee, USA

ICRU Sponsors

D.T. Burns, Bureau International des Poids et Mesures, Sèvres, France

E. Fantuzzi, Ente per le Nuove Tecnologie, L'Energia e L'Ambiente, Bologna, Italy

H-G. Menzel, Heidelberg, Germany

†Deceased. Dr Dietze played an important role in the develepment of the recommendations of this Report. The Commission wishes to acknowledge the loss resulting from his untimely death on 25th January 2015 .

Appendix A

Values of conversion coefficients

A.1 Ambient Dose

Tables A.1.1a to A.1.10 and Figures A.1.1a to A.1.10 give the values of conversion coefficients, $h^{*}_{E\mathrm{max}}$, from particle fluence to ambient dose for photons, neutrons, electrons, positrons, protons, negative muons, and positive muons for energies up to 10 GeV; for negative pions and positive pions for energies up to 200 GeV; and for He ions up to 100 GeV u^{-1}. The conversion coefficients relate the particle fluence to the maximum value of the effective dose, E_{max}, calculated for whole-body exposure of the ICRP/ICRU adult reference phantoms (ICRP, 2009) for broad parallel beams incident in irradiation geometries AP, PA, LLAT, RLAT, ROT, ISO, SS-ISO, and IS-ISO fields for photons and neutrons; AP, PA, ISO, SS-ISO, and IS-ISO fields for electrons, positrons, muons and pions; and AP, PA, and ISO for He ions (ICRP, 2010). For photons of energy up to 50 MeV, Table A.1.1b and Figure A.1.1b give conversion coefficients from air kerma.

Table A.1.1a Conversion coefficients from photon fluence to ambient dose (ICRP, 2010; Endo 2016b).

E_p / MeV	h^*_{Emax} / (pSv cm^2)	E_p / MeV	h^*_{Emax} / (pSv cm^2)
5.000E-03	1.34E-02	2.000E+00	7.48E+00
6.000E-03	1.66E-02	3.000E+00	9.75E+00
7.000E-03	2.25E-02	4.000E+00	1.17E+01
8.000E-03	3.35E-02	5.000E+00	1.34E+01
9.000E-03	4.90E-02	6.000E+00	1.50E+01
1.000E-02	6.85E-02	6.129E+00	1.52E+01
1.200E-02	1.05E-01	8.000E+00	1.86E+01
1.300E-02	1.22E-01	1.000E+01	2.21E+01
1.500E-02	1.56E-01	1.500E+01	3.04E+01
1.700E-02	1.81E-01	2.000E+01	3.82E+01
2.000E-02	2.25E-01	3.000E+01	5.13E+01
2.500E-02	2.75E-01	4.000E+01	6.18E+01
3.000E-02	3.12E-01	5.000E+01	7.23E+01
4.000E-02	3.50E-01	6.000E+01	8.21E+01
5.000E-02	3.69E-01	8.000E+01	9.81E+01
6.000E-02	3.89E-01	1.000E+02	1.10E+02
7.000E-02	4.11E-01	1.500E+02	1.30E+02
8.000E-02	4.43E-01	2.000E+02	1.44E+02
1.000E-01	5.18E-01	3.000E+02	1.61E+02
1.500E-01	7.47E-01	4.000E+02	1.73E+02
2.000E-01	1.00E+00	5.000E+02	1.81E+02
3.000E-01	1.51E+00	6.000E+02	1.87E+02
4.000E-01	2.00E+00	8.000E+02	1.96E+02
5.000E-01	2.47E+00	1.000E+03	2.06E+02
5.110E-01	2.52E+00	1.500E+03	2.13E+02
6.000E-01	2.91E+00	2.000E+03	2.36E+02
6.620E-01	3.17E+00	3.000E+03	2.53E+02
8.000E-01	3.73E+00	4.000E+03	2.67E+02
1.000E+00	4.49E+00	5.000E+03	2.77E+02
1.117E+00	4.90E+00	6.000E+03	2.85E+02
1.330E+00	5.60E+00	8.000E+03	2.99E+02
1.500E+00	6.12E+00	1.000E+04	3.07E+02

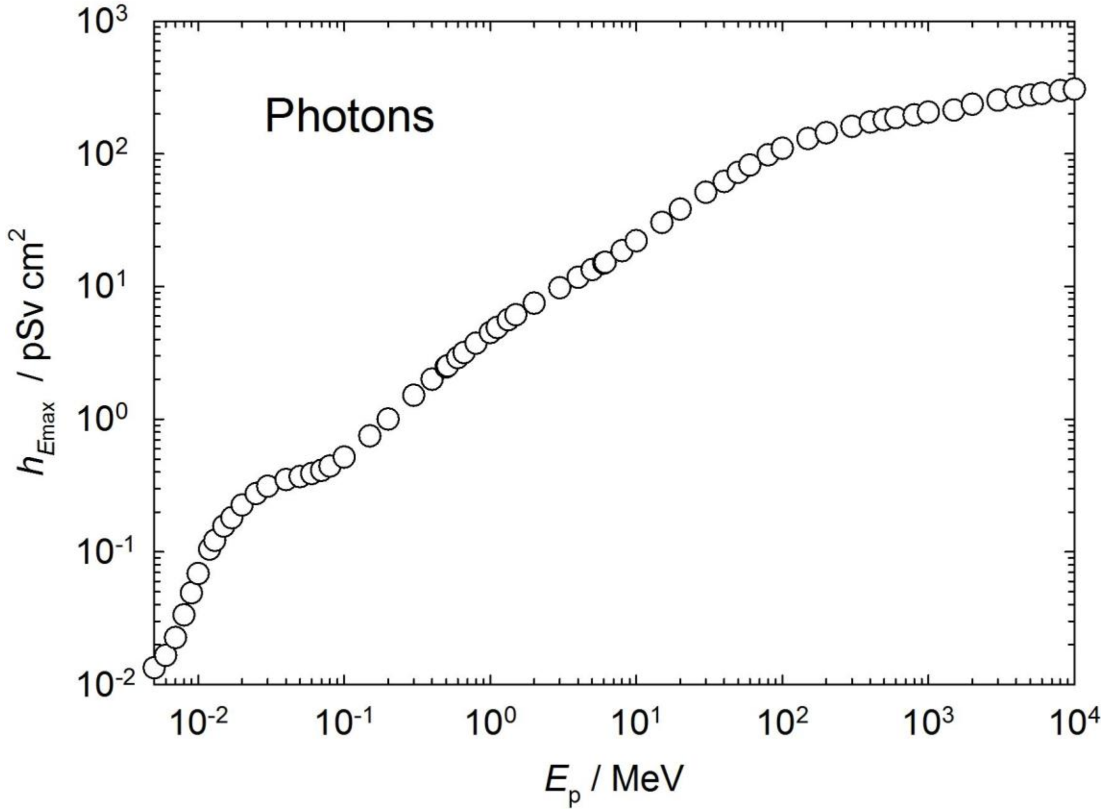

Figure A.1.1a Conversion coefficients from photon fluence to ambient dose (ICRP, 2010; Endo 2016b).

Table A.1.1b Conversion coefficients from photon air kerma to ambient dose (ICRP, 2010; Endo 2016b).

E_p / MeV	h^*_{Emax} / (Sv Gy^{-1})	E_p / MeV	h^*_{Emax} / (Sv Gy^{-1})
5.000E-03	4.37E-04	5.000E-01	1.04E+00
6.000E-03	7.81E-04	5.110E-01	1.04E+00
7.000E-03	1.45E-03	6.000E-01	1.02E+00
8.000E-03	2.84E-03	6.620E-01	1.02E+00
9.000E-03	5.31E-03	8.000E-01	1.01E+00
1.000E-02	9.26E-03	1.000E+00	1.00E+00
1.200E-02	2.09E-02	1.117E+00	1.00E+00
1.300E-02	2.88E-02	1.330E+00	1.00E+00
1.500E-02	4.99E-02	1.500E+00	9.96E-01
1.700E-02	7.58E-02	2.000E+00	9.90E-01
2.000E-02	1.34E-01	3.000E+00	9.77E-01
2.500E-02	2.60E-01	4.000E+00	9.64E-01
3.000E-02	4.32E-01	5.000E+00	9.45E-01
4.000E-02	8.16E-01	6.000E+00	9.28E-01
5.000E-02	1.14E+00	6.129E+00	9.25E-01
6.000E-02	1.35E+00	8.000E+00	9.24E-01
7.000E-02	1.43E+00	1.000E+01	9.16E-01
8.000E-02	1.44E+00	1.500E+01	8.82E-01
1.000E-01	1.39E+00	2.000E+01	8.42E-01
1.500E-01	1.25E+00	3.000E+01	7.48E-01
2.000E-01	1.17E+00	4.000E+01	6.62E-01
3.000E-01	1.09E+00	5.000E+01	6.07E-01
4.000E-01	1.06E+00		

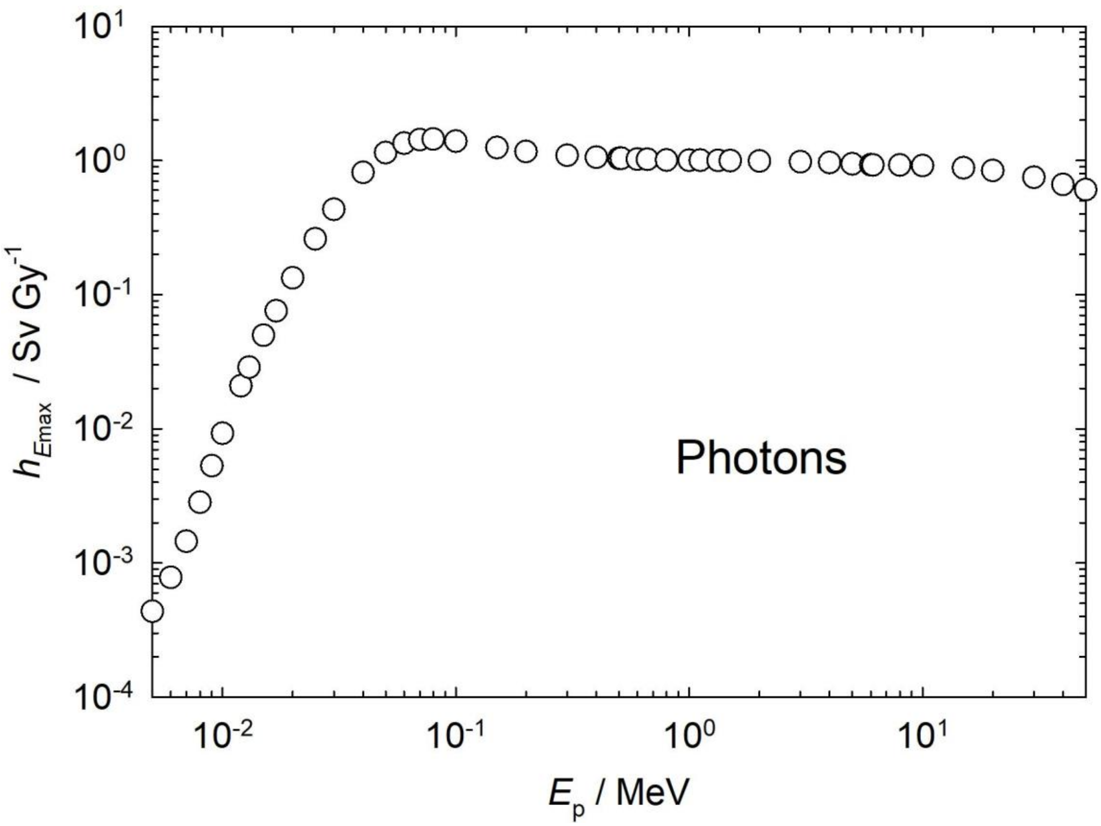

Figure A.1.1b Conversion coefficients from photon air kerma to ambient dose (ICRP, 2010; Endo 2016b).

Table A.1.2 Conversion coefficients from neutron fluence to ambient dose (ICRP, 2010).

E_p / MeV	h^*_{Emax} / (pSv cm^2)	E_p / MeV	h^*_{Emax} / (pSv cm^2)
1.00E-09	3.09E+00	3.00E+00	4.58E+02
1.00E-08	3.55E+00	4.00E+00	4.83E+02
2.50E-08	4.00E+00	5.00E+00	4.94E+02
1.00E-07	5.20E+00	6.00E+00	4.98E+02
2.00E-07	5.87E+00	7.00E+00	4.99E+02
5.00E-07	6.59E+00	8.00E+00	4.99E+02
1.00E-06	7.03E+00	9.00E+00	5.00E+02
2.00E-06	7.39E+00	1.00E+01	5.00E+02
5.00E-06	7.71E+00	1.20E+01	4.99E+02
1.00E-05	7.82E+00	1.40E+01	4.95E+02
2.00E-05	7.84E+00	1.50E+01	4.93E+02
5.00E-05	7.82E+00	1.60E+01	4.90E+02
1.00E-04	7.79E+00	1.80E+01	4.84E+02
2.00E-04	7.73E+00	2.00E+01	4.77E+02
5.00E-04	7.54E+00	2.10E+01	4.74E+02
1.00E-03	7.54E+00	3.00E+01	4.53E+02
2.00E-03	7.61E+00	5.00E+01	4.33E+02
5.00E-03	7.97E+00	7.50E+01	4.39E+02
1.00E-02	9.11E+00	1.00E+02	4.44E+02
2.00E-02	1.22E+01	1.30E+02	4.46E+02
3.00E-02	1.57E+01	1.50E+02	4.46E+02
5.00E-02	2.30E+01	1.80E+02	4.47E+02
7.00E-02	3.06E+01	2.00E+02	4.48E+02
1.00E-01	4.19E+01	3.00E+02	4.73E+02
1.50E-01	6.06E+01	4.00E+02	5.15E+02
2.00E-01	7.88E+01	5.00E+02	5.33E+02
3.00E-01	1.14E+02	6.00E+02	5.69E+02
5.00E-01	1.77E+02	7.00E+02	6.25E+02
7.00E-01	2.32E+02	8.00E+02	6.38E+02
9.00E-01	2.79E+02	9.00E+02	6.45E+02
1.00E+00	3.01E+02	1.00E+03	6.63E+02
1.20E+00	3.30E+02	2.00E+03	7.69E+02
1.50E+00	3.65E+02	5.00E+03	1.04E+03
2.00E+00	4.07E+02	1.00E+04	1.39E+03

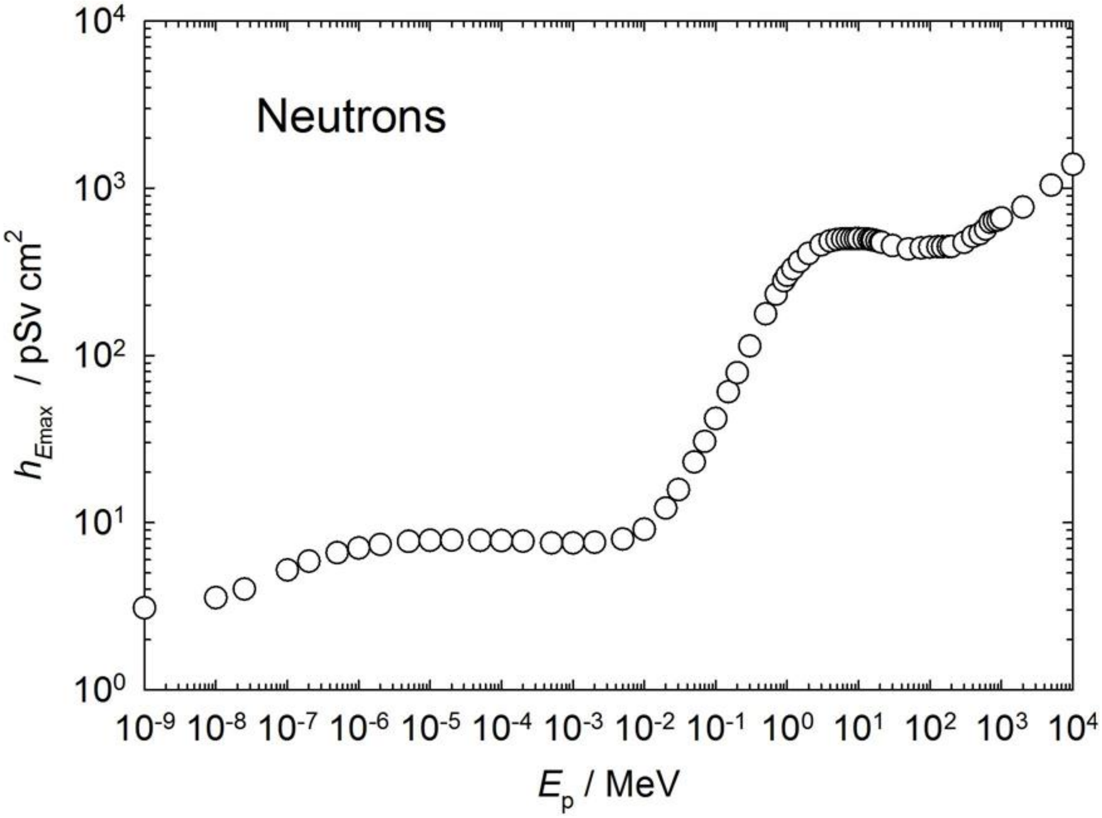

Figure A.1.2 Conversion coefficients from neutron fluence to ambient dose (ICRP, 2010).

Table A.1.3 Conversion coefficients from electron fluence to ambient dose (ICRP, 2010).

E_p / MeV	h^*_{Emax} / (pSv cm^2)	E_p / MeV	h^*_{Emax} / (pSv cm^2)
1.00E-02	2.69E-02	1.50E+01	1.88E+02
1.50E-02	4.04E-02	2.00E+01	2.36E+02
2.00E-02	5.39E-02	3.00E+01	3.02E+02
3.00E-02	8.10E-02	4.00E+01	3.29E+02
4.00E-02	1.08E-01	5.00E+01	3.37E+02
5.00E-02	1.35E-01	6.00E+01	3.44E+02
6.00E-02	1.63E-01	8.00E+01	3.58E+02
8.00E-02	2.18E-01	1.00E+02	3.66E+02
1.00E-01	2.75E-01	1.50E+02	3.79E+02
1.50E-01	4.18E-01	2.00E+02	3.88E+02
2.00E-01	5.69E-01	3.00E+02	4.11E+02
3.00E-01	8.89E-01	4.00E+02	4.35E+02
4.00E-01	1.24E+00	5.00E+02	4.49E+02
5.00E-01	1.63E+00	6.00E+02	4.64E+02
6.00E-01	2.05E+00	8.00E+02	4.88E+02
8.00E-01	4.04E+00	1.00E+03	5.08E+02
1.00E+00	7.10E+00	1.50E+03	5.25E+02
1.50E+00	1.50E+01	2.00E+03	5.68E+02
2.00E+00	2.24E+01	3.00E+03	6.08E+02
3.00E+00	3.61E+01	4.00E+03	6.38E+02
4.00E+00	4.82E+01	5.00E+03	6.61E+02
5.00E+00	5.93E+01	6.00E+03	6.83E+02
6.00E+00	7.06E+01	8.00E+03	7.16E+02
8.00E+00	9.79E+01	1.00E+04	7.42E+02
1.00E+01	1.25E+02		

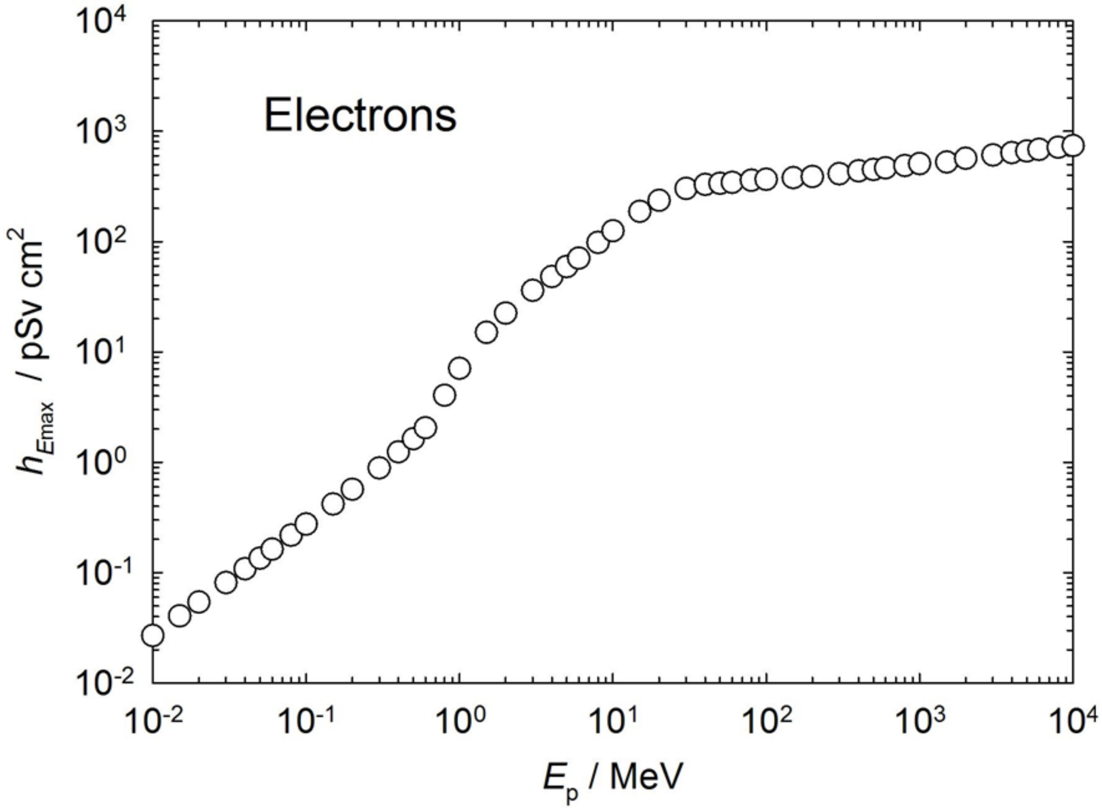

Figure A.1.3 Conversion coefficients from electron fluence to ambient dose (ICRP, 2010).

Table A.1.4 Conversion coefficients from positron fluence to ambient dose (ICRP, 2010).

E_p / MeV	h^*_{Emax} / (pSv cm^2)	E_p / MeV	h^*_{Emax} / (pSv cm^2)
1.00E-02	3.28E+00	1.50E+01	1.84E+02
1.50E-02	3.29E+00	2.00E+01	2.29E+02
2.00E-02	3.30E+00	3.00E+01	2.94E+02
3.00E-02	3.33E+00	4.00E+01	3.20E+02
4.00E-02	3.36E+00	5.00E+01	3.27E+02
5.00E-02	3.39E+00	6.00E+01	3.34E+02
6.00E-02	3.42E+00	8.00E+01	3.49E+02
8.00E-02	3.47E+00	1.00E+02	3.57E+02
1.00E-01	3.53E+00	1.50E+02	3.71E+02
1.50E-01	3.67E+00	2.00E+02	3.83E+02
2.00E-01	3.84E+00	3.00E+02	4.12E+02
3.00E-01	4.16E+00	4.00E+02	4.35E+02
4.00E-01	4.52E+00	5.00E+02	4.49E+02
5.00E-01	4.90E+00	6.00E+02	4.62E+02
6.00E-01	5.36E+00	8.00E+02	4.85E+02
8.00E-01	7.41E+00	1.00E+03	5.05E+02
1.00E+00	1.05E+01	1.50E+03	5.22E+02
1.50E+00	1.83E+01	2.00E+03	5.66E+02
2.00E+00	2.57E+01	3.00E+03	6.04E+02
3.00E+00	3.91E+01	4.00E+03	6.33E+02
4.00E+00	5.10E+01	5.00E+03	6.59E+02
5.00E+00	6.17E+01	6.00E+03	6.83E+02
6.00E+00	7.29E+01	8.00E+03	7.16E+02
8.00E+00	9.90E+01	1.00E+04	7.46E+02
1.00E+01	1.26E+02		

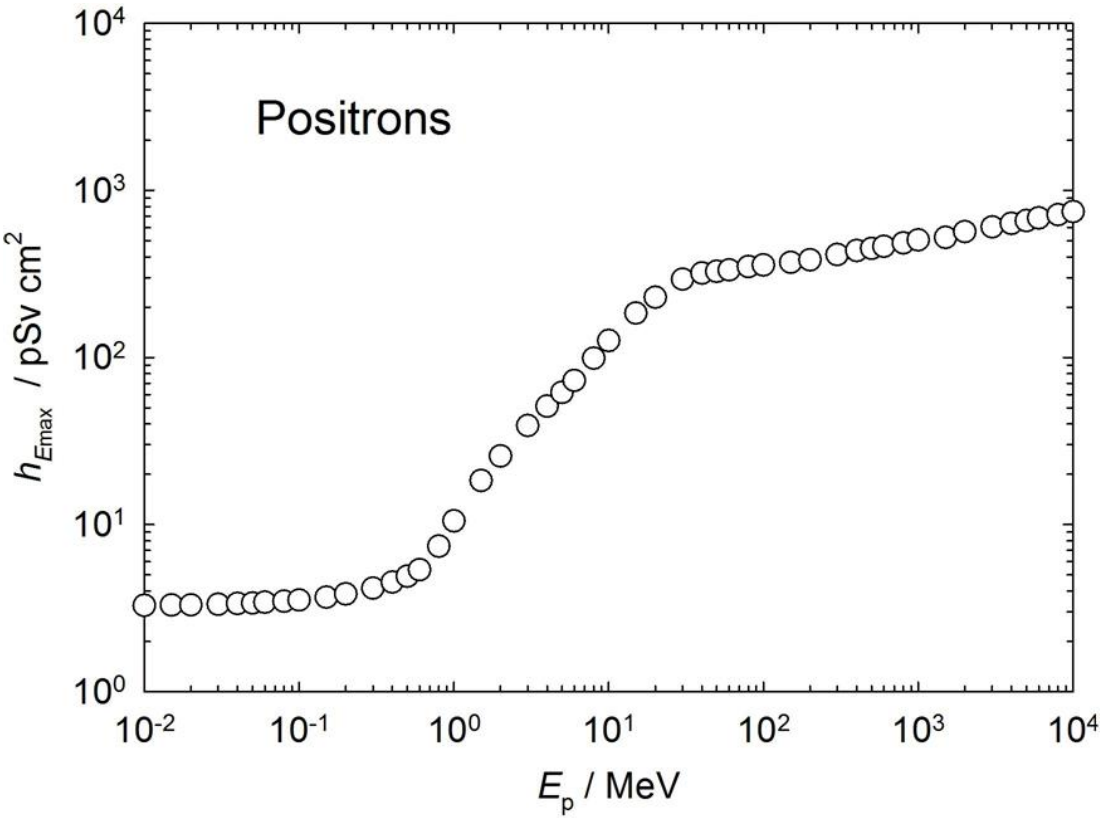

Figure A.1.4 Conversion coefficients from positron fluence to ambient dose (ICRP, 2010).

Table A.1.5 Conversion coefficients from proton fluence to ambient dose (ICRP, 2010).

E_p / MeV	h^*_{Emax} / (pSv cm^2)
1.00E+00	5.47E+00
1.50E+00	8.21E+00
2.00E+00	1.09E+01
3.00E+00	1.64E+01
4.00E+00	2.19E+01
5.00E+00	2.73E+01
6.00E+00	3.28E+01
8.00E+00	4.37E+01
1.00E+01	5.49E+01
1.50E+01	1.89E+02
2.00E+01	4.28E+02
3.00E+01	7.50E+02
4.00E+01	1.02E+03
5.00E+01	1.18E+03
6.00E+01	1.48E+03
8.00E+01	2.16E+03
1.00E+02	2.51E+03
1.50E+02	2.82E+03
2.00E+02	2.18E+03
3.00E+02	1.45E+03
4.00E+02	1.30E+03
5.00E+02	1.24E+03
6.00E+02	1.23E+03
8.00E+02	1.23E+03
1.00E+03	1.23E+03
1.50E+03	1.25E+03
2.00E+03	1.28E+03
3.00E+03	1.35E+03
4.00E+03	1.48E+03
5.00E+03	1.46E+03
6.00E+03	1.71E+03
8.00E+03	1.88E+03
1.00E+04	1.93E+03

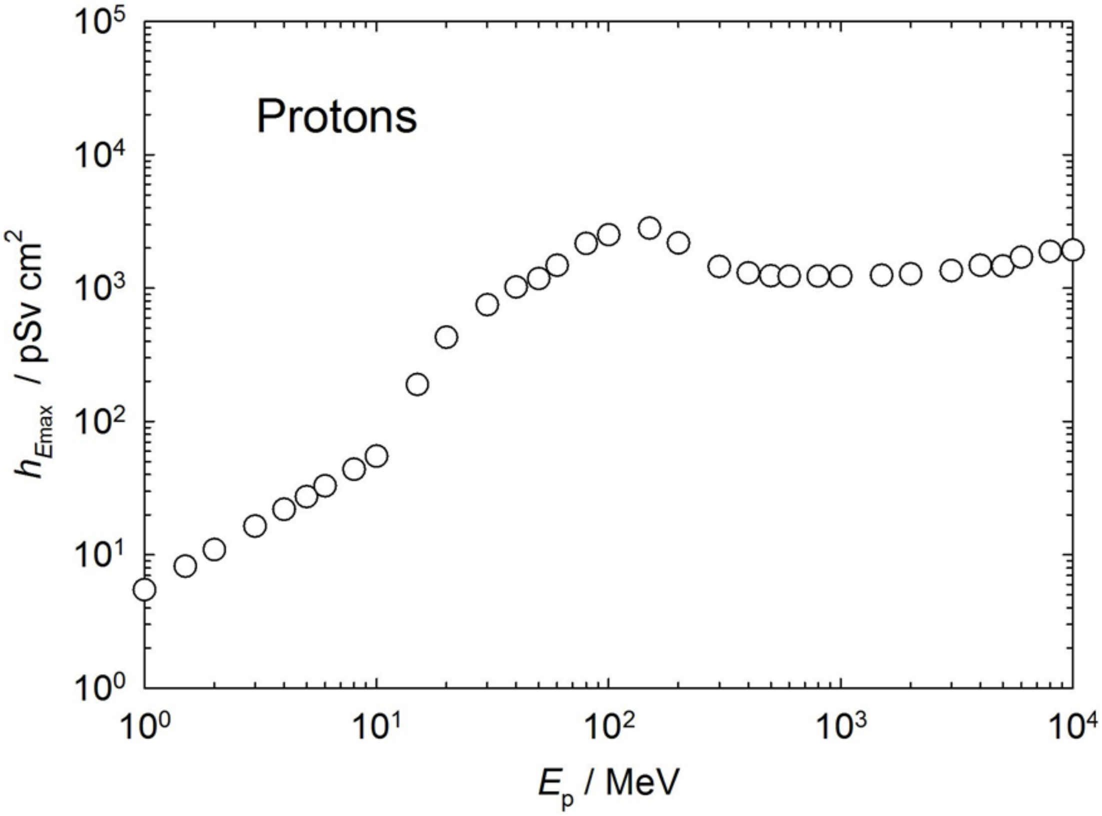

Figure A.1.5 Conversion coefficients from proton fluence to ambient dose (ICRP, 2010).

Table A.1.6 Conversion coefficients from negative muon fluence to ambient dose (ICRP, 2010).

E_p / MeV	$h^*_{E\mathrm{max}}$ / (pSv cm^2)
1.00E+00	1.80E+02
1.50E+00	1.80E+02
2.00E+00	1.84E+02
3.00E+00	1.88E+02
4.00E+00	1.93E+02
5.00E+00	2.05E+02
6.00E+00	2.42E+02
8.00E+00	2.93E+02
1.00E+01	3.32E+02
1.50E+01	4.14E+02
2.00E+01	4.65E+02
3.00E+01	6.57E+02
4.00E+01	7.35E+02
5.00E+01	7.55E+02
6.00E+01	7.75E+02
8.00E+01	5.05E+02
1.00E+02	4.35E+02
1.50E+02	3.55E+02
2.00E+02	3.33E+02
3.00E+02	3.22E+02
4.00E+02	3.22E+02
5.00E+02	3.24E+02
6.00E+02	3.28E+02
8.00E+02	3.33E+02
1.00E+03	3.42E+02
1.50E+03	3.38E+02
2.00E+03	3.41E+02
3.00E+03	3.44E+02
4.00E+03	3.47E+02
5.00E+03	3.48E+02
6.00E+03	3.47E+02
8.00E+03	3.49E+02
1.00E+04	3.49E+02

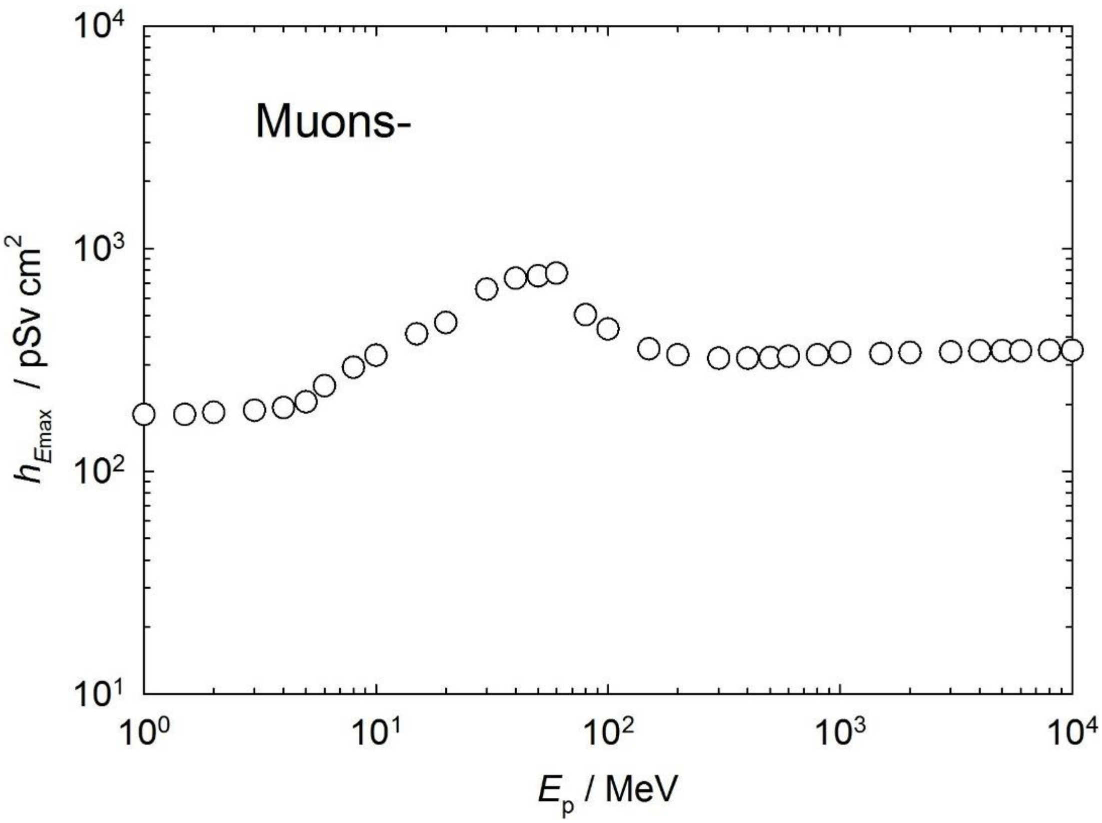

Figure A.1.6 Conversion coefficients from negative muon fluence to ambient dose (ICRP, 2010).

273 Table A.1.7 Conversion coefficients from positive muon fluence to ambient dose (ICRP, 2010).

274

E_p / MeV	$h^*_{E\max}$ / (pSv cm^2)
1.00E+00	1.94E+02
1.50E+00	1.96E+02
2.00E+00	1.98E+02
3.00E+00	2.02E+02
4.00E+00	2.07E+02
5.00E+00	2.16E+02
6.00E+00	2.51E+02
8.00E+00	3.00E+02
1.00E+01	3.40E+02
1.50E+01	4.25E+02
2.00E+01	4.81E+02
3.00E+01	6.74E+02
4.00E+01	7.51E+02
5.00E+01	7.68E+02
6.00E+01	7.87E+02
8.00E+01	5.10E+02
1.00E+02	4.37E+02
1.50E+02	3.54E+02
2.00E+02	3.33E+02
3.00E+02	3.20E+02
4.00E+02	3.21E+02
5.00E+02	3.23E+02
6.00E+02	3.25E+02
8.00E+02	3.30E+02
1.00E+03	3.34E+02
1.50E+03	3.39E+02
2.00E+03	3.41E+02
3.00E+03	3.44E+02
4.00E+03	3.47E+02
5.00E+03	3.48E+02
6.00E+03	3.47E+02
8.00E+03	3.49E+02
1.00E+04	3.49E+02

275

276

277

278

279

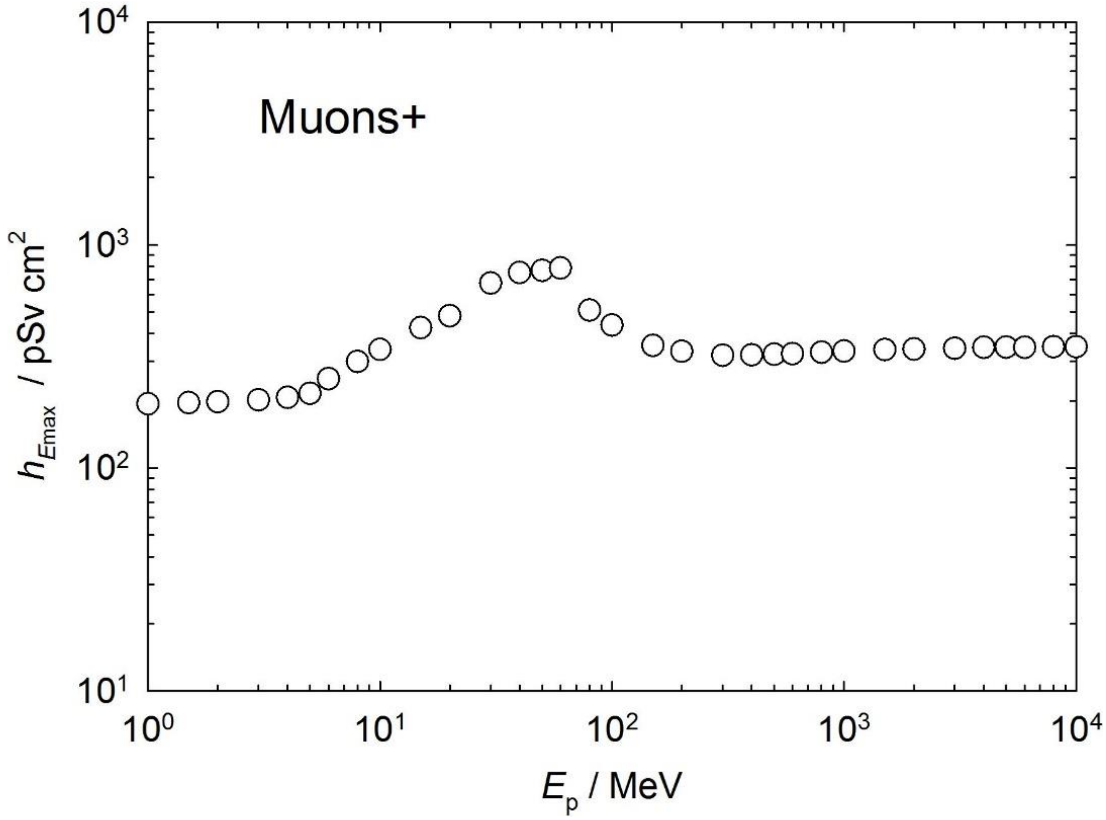

Figure A.1.7 Conversion coefficients from positive muon fluence to ambient dose (ICRP, 2010).

Table A.1.8 Conversion coefficients from negative pion fluence to ambient dose (ICRP, 2010).

E_p / MeV	h^*_{Emax} / (pSv cm^2)	E_p / MeV	h^*_{Emax} / (pSv cm^2)
1.00E+00	4.06E+02	6.00E+02	9.17E+02
1.50E+00	4.22E+02	8.00E+02	9.76E+02
2.00E+00	4.33E+02	1.00E+03	1.02E+03
3.00E+00	4.58E+02	1.50E+03	1.08E+03
4.00E+00	4.91E+02	2.00E+03	1.12E+03
5.00E+00	5.28E+02	3.00E+03	1.13E+03
6.00E+00	6.73E+02	4.00E+03	1.17E+03
8.00E+00	9.65E+02	5.00E+03	1.23E+03
1.00E+01	1.09E+03	6.00E+03	1.26E+03
1.50E+01	1.25E+03	8.00E+03	1.39E+03
2.00E+01	1.28E+03	1.00E+04	1.46E+03
3.00E+01	1.77E+03	1.50E+04	1.60E+03
4.00E+01	1.92E+03	2.00E+04	1.70E+03
5.00E+01	1.93E+03	3.00E+04	1.86E+03
6.00E+01	1.99E+03	4.00E+04	1.99E+03
8.00E+01	1.31E+03	5.00E+04	2.11E+03
1.00E+02	1.03E+03	6.00E+04	2.21E+03
1.50E+02	9.27E+02	8.00E+04	2.42E+03
2.00E+02	9.02E+02	1.00E+05	2.60E+03
3.00E+02	8.48E+02	1.50E+05	2.98E+03
4.00E+02	8.50E+02	2.00E+05	3.14E+03
5.00E+02	8.80E+02		

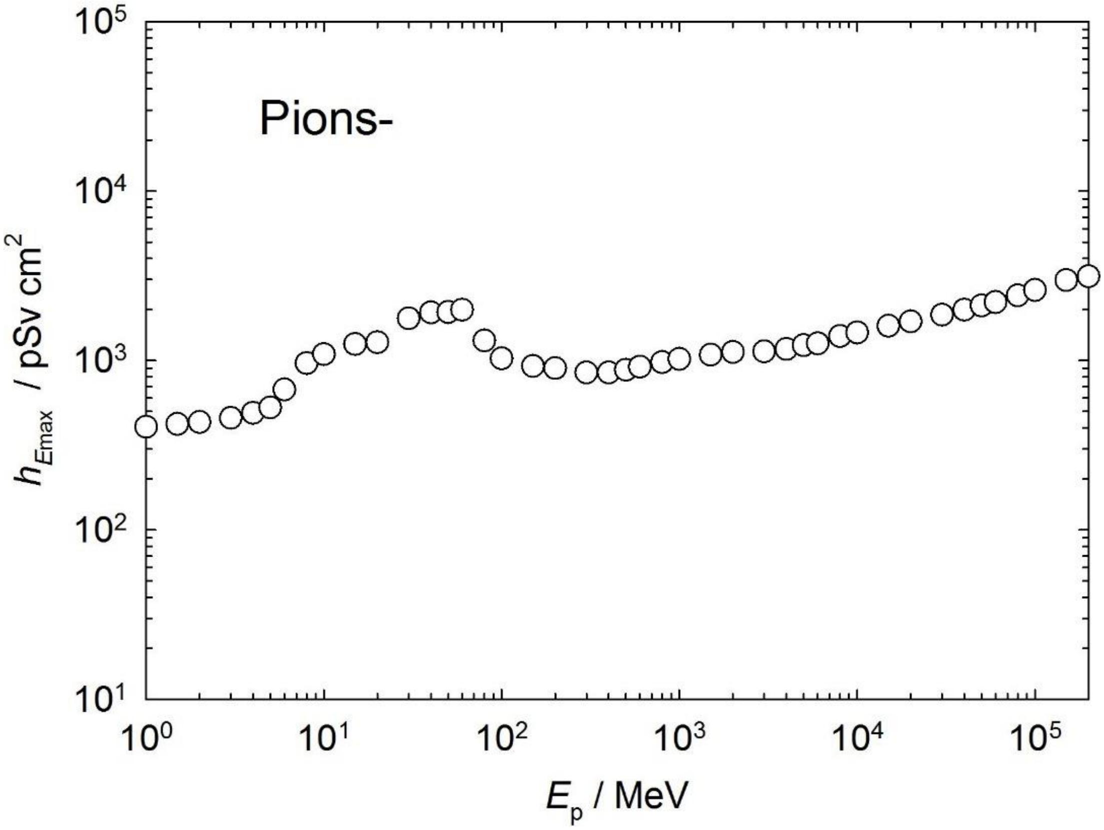

Figure A.1.8 Conversion coefficients from negative pion fluence to ambient dose (ICRP, 2010).

Table A.1.9 Conversion coefficients from positive pion fluence to ambient dose (ICRP, 2010).

E_p / MeV	$h^*_{E\max}$ / (pSv cm^2)	E_p / MeV	$h^*_{E\max}$ / (pSv cm^2)
1.00E+00	3.14E+02	6.00E+02	9.80E+02
1.50E+00	3.24E+02	8.00E+02	1.04E+03
2.00E+00	3.40E+02	1.00E+03	1.09E+03
3.00E+00	3.79E+02	1.50E+03	1.16E+03
4.00E+00	4.29E+02	2.00E+03	1.19E+03
5.00E+00	4.89E+02	3.00E+03	1.18E+03
6.00E+00	5.40E+02	4.00E+03	1.21E+03
8.00E+00	7.17E+02	5.00E+03	1.27E+03
1.00E+01	8.19E+02	6.00E+03	1.29E+03
1.50E+01	1.00E+03	8.00E+03	1.39E+03
2.00E+01	1.10E+03	1.00E+04	1.46E+03
3.00E+01	1.52E+03	1.50E+04	1.60E+03
4.00E+01	1.75E+03	2.00E+04	1.69E+03
5.00E+01	1.83E+03	3.00E+04	1.86E+03
6.00E+01	1.82E+03	4.00E+04	1.97E+03
8.00E+01	1.38E+03	5.00E+04	2.09E+03
1.00E+02	1.13E+03	6.00E+04	2.20E+03
1.50E+02	1.22E+03	8.00E+04	2.38E+03
2.00E+02	1.25E+03	1.00E+05	2.53E+03
3.00E+02	1.10E+03	1.50E+05	2.90E+03
4.00E+02	9.98E+02	2.00E+05	3.24E+03
5.00E+02	9.70E+02		

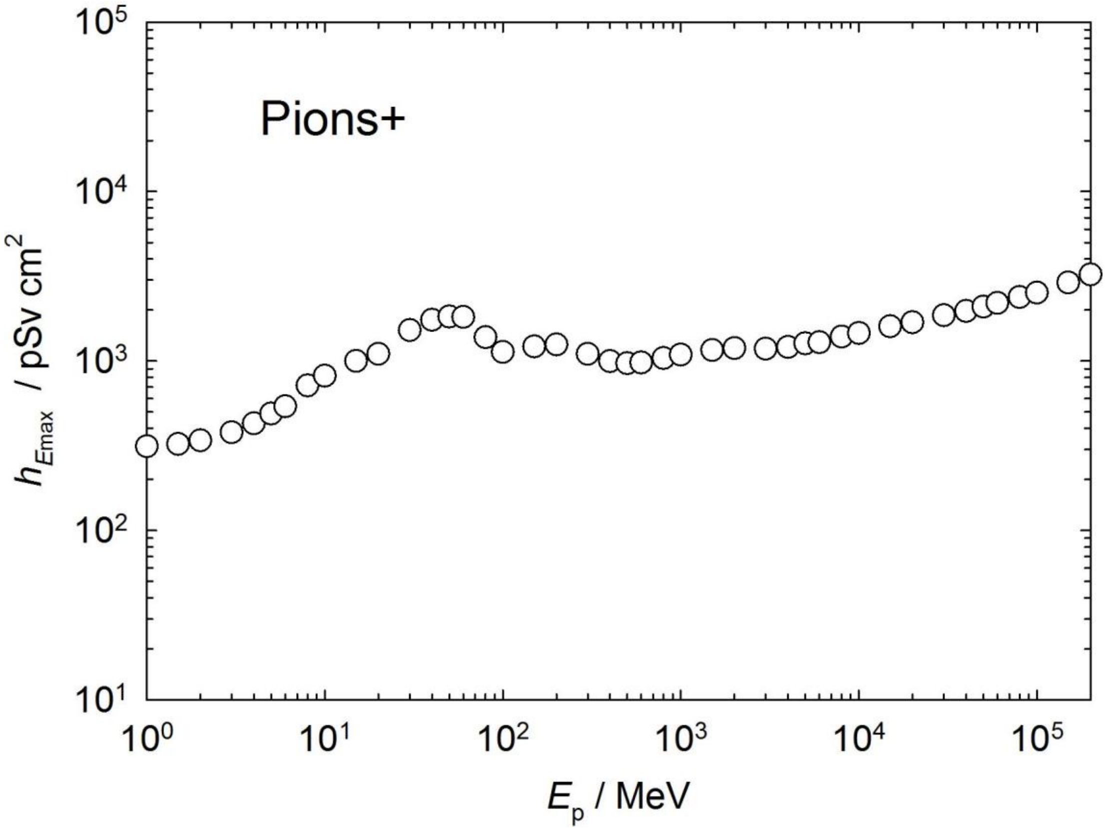

Figure A.1.9 Conversion coefficients from positive pion fluence to ambient dose (ICRP, 2010).

Table A.1.10 Conversion coefficients from He ion fluence to ambient dose (ICRP, 2010).

E_p / MeV u^{-1}	h^{*}_{Emax} / (pSv cm^2)
1.00E+00	2.19E+02
2.00E+00	4.38E+02
3.00E+00	6.57E+02
5.00E+00	1.09E+03
1.00E+01	2.19E+03
1.40E+01	4.61E+03
2.00E+01	1.72E+04
3.00E+01	3.01E+04
5.00E+01	4.75E+04
7.50E+01	8.05E+04
1.00E+02	1.01E+05
1.50E+02	1.10E+05
2.00E+02	7.29E+04
3.00E+02	5.33E+04
5.00E+02	4.49E+04
7.00E+02	4.60E+04
1.00E+03	4.47E+04
2.00E+03	4.80E+04
3.00E+03	5.01E+04
5.00E+03	5.17E+04
1.00E+04	6.26E+04
2.00E+04	7.10E+04
5.00E+04	9.67E+04
1.00E+05	1.24E+05

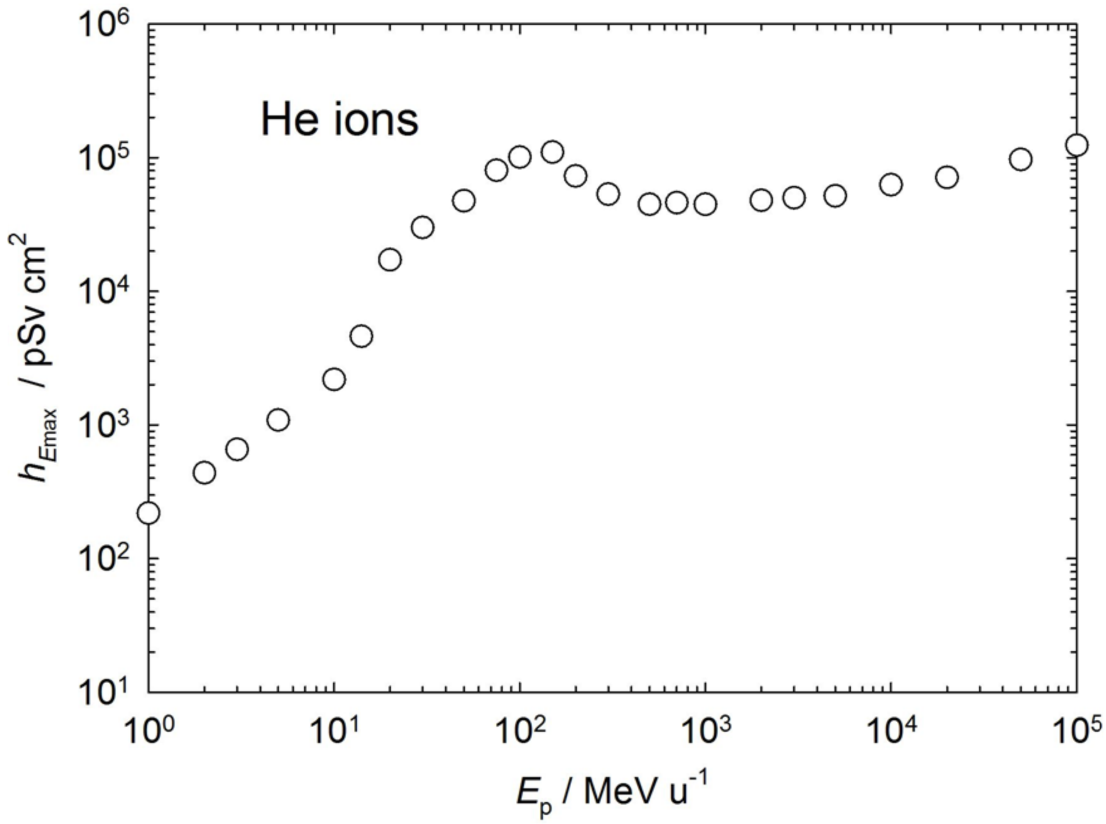

Figure A.1.10 Conversion coefficients from He ion fluence to ambient dose (ICRP, 2010).

A.2 Personal Dose

Tables A.2.1 to A.2.10 and Figures A.2.1 to A.2.10 give the values of conversion coefficients from particle fluence to personal dose for photons, neutrons, electrons, positrons, protons, negative muons, positive muons, negative pions and positive pions for energies up to 1GeV, and for He ions up to 1GeV u^{-1}. The conversion coefficients relate the particle fluence to effective dose, *E*, calculated for whole-body exposure of the ICRP/ICRU adult reference phantoms (ICRP, 2009) for broad parallel beams incident at angles of incidence from 0° (A-P) to 90° in 15° steps, the maximum value of right or left irradiations is taken, 180°, rotational, isotropic, superior hemisphere semi-isotropic, and inferior hemisphere semi-isotropic fields.

$$h_{\mathrm{p}}(\alpha) = \frac{E(\alpha)}{\Phi(\alpha)}$$

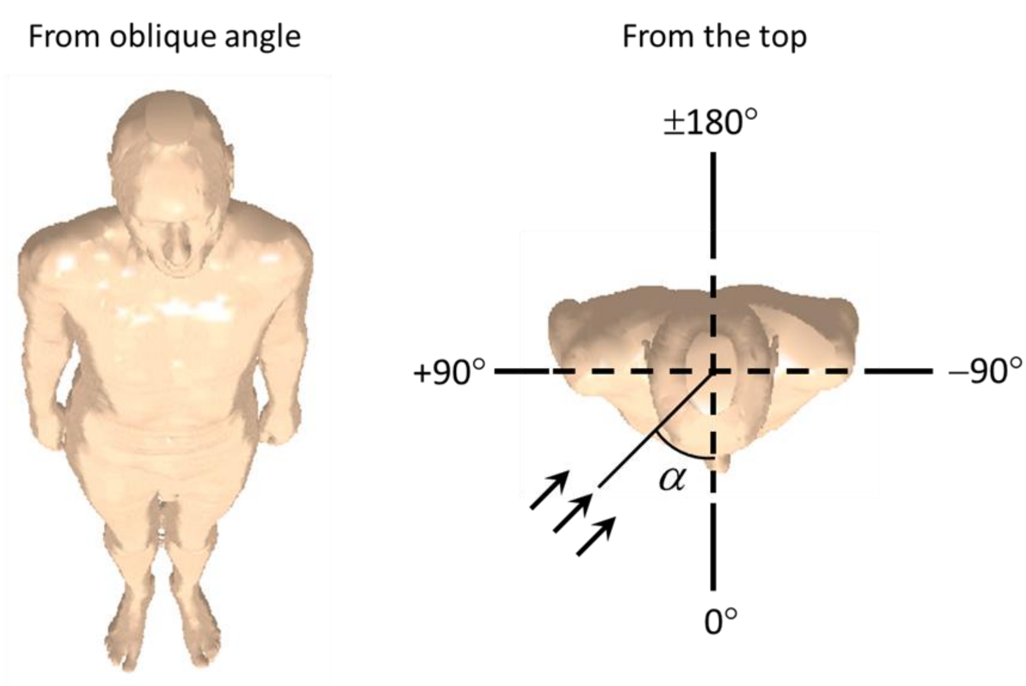

Definition of the incident angle α for parallel beam irradiation: the origin of the coordinate system is located at the center of the human body.

The conversion coefficients of Tables A.2.1a to A.2.10 and Figures A.2.1a to A.2.10 are compiled from those given in ICRP Publication 116 (ICRP, 2010) and from calculations by Endo (2016b, 2017). ICRP Publication 116 provides conversion coefficients for broad parallel and isotropic beams of the radiation field at that point incident in irradiation geometries AP, PA, LLAT, RLAT, ROT, ISO, SS-ISO, and IS-ISO fields for photons and neutrons; AP, PA, ISO, SS-ISO, and IS-ISO fields for electrons, positrons, muons and pions; and AP, PA, and ISO for He ions. For photons of energy up to 50 MeV, Table A.4.1b and Figure A.4.1b give conversion coefficients from air kerma.

The AP, PA, LLAT and RLAT corresponds to $\alpha = 0°$, 180°, -90° and +90°, respectively, of $h_{\mathrm{p}}(\alpha)$, and these conversion coefficients from ICRP Publication 116 are used in Tables A.2.1a/b A.2.10 and Figures A.2.1a/b to A.2.10. The conversion coefficients for incident geometries not available from ICRP Publication 116 are taken from the calculations by Endo (2016b, 2017). The consistency of numerical values between ICRP Publication 116 and the calculations by Endo was studied and validated (Endo, 2017).

Table A.2.1a Conversion coefficients from photon fluence to personal dose (ICRP, 2010; Endo, 2016b, 2017).

E_p / MeV	$h_p(\alpha)$ / (pSv cm^2)											
	0°	max(±15°)	max(±30°)	max(±45°)	max(±60°)	max(±75°)	max(±90°)	180°	ROT	ISO	SS-ISO	IS-ISO
5.0E-03	1.34E-02	1.41E-02	1.39E-02	1.31E-02	1.16E-02	9.41E-03	6.87E-03	1.33E-02	1.15E-02	1.04E-02	1.05E-02	1.02E-02
6.0E-03	1.66E-02	1.80E-02	1.82E-02	1.72E-02	1.53E-02	1.20E-02	8.29E-03	1.59E-02	1.41E-02	1.28E-02	1.31E-02	1.25E-02
7.0E-03	2.25E-02	2.45E-02	2.45E-02	2.28E-02	1.99E-02	1.51E-02	9.92E-03	1.78E-02	1.74E-02	1.58E-02	1.61E-02	1.53E-02
8.0E-03	3.35E-02	3.51E-02	3.41E-02	3.07E-02	2.60E-02	1.93E-02	1.21E-02	1.87E-02	2.16E-02	1.94E-02	2.00E-02	1.87E-02
9.0E-03	4.90E-02	5.01E-02	4.70E-02	4.09E-02	3.39E-02	2.46E-02	1.49E-02	1.86E-02	2.73E-02	2.36E-02	2.45E-02	2.26E-02
1.0E-02	6.85E-02	6.77E-02	6.23E-02	5.31E-02	4.29E-02	3.09E-02	1.89E-02	1.84E-02	3.37E-02	2.88E-02	3.01E-02	2.75E-02
1.2E-02	1.05E-01	1.04E-01	9.53E-02	8.00E-02	6.24E-02	4.50E-02	2.71E-02	1.62E-02	4.70E-02	3.95E-02	4.06E-02	3.75E-02
1.3E-02	1.22E-01	1.21E-01	1.11E-01	9.37E-02	7.27E-02	5.19E-02	3.15E-02	1.56E-02	5.32E-02	4.49E-02	4.58E-02	4.26E-02
1.5E-02	1.56E-01	1.52E-01	1.40E-01	1.19E-01	9.36E-02	6.56E-02	4.16E-02	1.55E-02	6.65E-02	5.60E-02	5.77E-02	5.43E-02
1.7E-02	1.81E-01	1.80E-01	1.68E-01	1.44E-01	1.16E-01	7.98E-02	4.97E-02	1.75E-02	7.83E-02	6.50E-02	6.54E-02	6.32E-02
2.0E-02	2.25E-01	2.19E-01	2.05E-01	1.81E-01	1.48E-01	1.01E-01	6.54E-02	2.61E-02	9.88E-02	8.13E-02	8.22E-02	8.02E-02
2.5E-02	2.75E-01	2.71E-01	2.57E-01	2.32E-01	1.93E-01	1.38E-01	8.55E-02	5.64E-02	1.30E-01	1.04E-01	1.05E-01	1.01E-01
3.0E-02	3.12E-01	3.07E-01	2.93E-01	2.62E-01	2.19E-01	1.62E-01	1.09E-01	9.46E-02	1.59E-01	1.27E-01	1.29E-01	1.25E-01
4.0E-02	3.50E-01	3.43E-01	3.31E-01	2.96E-01	2.54E-01	1.97E-01	1.38E-01	1.63E-01	1.99E-01	1.58E-01	1.62E-01	1.54E-01
5.0E-02	3.69E-01	3.62E-01	3.53E-01	3.14E-01	2.74E-01	2.12E-01	1.58E-01	2.09E-01	2.26E-01	1.80E-01	1.84E-01	1.76E-01
6.0E-02	3.89E-01	3.85E-01	3.67E-01	3.30E-01	2.91E-01	2.31E-01	1.74E-01	2.43E-01	2.48E-01	1.98E-01	2.04E-01	1.94E-01
7.0E-02	4.11E-01	4.12E-01	3.92E-01	3.53E-01	3.11E-01	2.52E-01	1.91E-01	2.73E-01	2.73E-01	2.18E-01	2.23E-01	2.09E-01
8.0E-02	4.43E-01	4.38E-01	4.21E-01	3.81E-01	3.41E-01	2.78E-01	2.11E-01	3.02E-01	2.97E-01	2.38E-01	2.46E-01	2.32E-01
1.0E-01	5.18E-01	5.15E-01	4.90E-01	4.56E-01	4.10E-01	3.32E-01	2.55E-01	3.63E-01	3.56E-01	2.86E-01	2.95E-01	2.79E-01
1.5E-01	7.47E-01	7.52E-01	7.18E-01	6.63E-01	6.07E-01	5.04E-01	3.91E-01	5.43E-01	5.29E-01	4.29E-01	4.45E-01	4.13E-01
2.0E-01	1.00E+00	1.00E+00	9.68E-01	9.01E-01	8.26E-01	7.00E-01	5.46E-01	7.45E-01	7.22E-01	5.89E-01	6.10E-01	5.68E-01
3.0E-01	1.51E+00	1.51E+00	1.46E+00	1.38E+00	1.27E+00	1.10E+00	8.80E-01	1.16E+00	1.12E+00	9.32E-01	9.64E-01	9.00E-01
4.0E-01	2.00E+00	2.00E+00	1.94E+00	1.84E+00	1.72E+00	1.50E+00	1.23E+00	1.58E+00	1.53E+00	1.28E+00	1.32E+00	1.24E+00
5.0E-01	2.47E+00	2.47E+00	2.40E+00	2.30E+00	2.17E+00	1.90E+00	1.57E+00	1.99E+00	1.92E+00	1.63E+00	1.67E+00	1.59E+00
6.0E-01	2.91E+00	2.93E+00	2.85E+00	2.70E+00	2.58E+00	2.26E+00	1.91E+00	2.39E+00	2.31E+00	1.97E+00	2.02E+00	1.92E+00
8.0E-01	3.73E+00	3.75E+00	3.66E+00	3.53E+00	3.37E+00	2.96E+00	2.57E+00	3.14E+00	3.04E+00	2.62E+00	2.70E+00	2.54E+00
1.0E+00	4.49E+00	4.55E+00	4.42E+00	4.27E+00	4.11E+00	3.62E+00	3.21E+00	3.84E+00	3.73E+00	3.25E+00	3.32E+00	3.18E+00
1.5E+00	6.12E+00	6.17E+00	6.06E+00	5.90E+00	5.70E+00	5.26E+00	4.66E+00	5.41E+00	5.24E+00	4.67E+00	4.74E+00	4.58E+00
2.0E+00	7.48E+00	7.53E+00	7.41E+00	7.24E+00	6.96E+00	6.55E+00	5.94E+00	6.77E+00	6.56E+00	5.91E+00	6.03E+00	5.77E+00
3.0E+00	9.75E+00	9.84E+00	9.66E+00	9.61E+00	9.36E+00	8.75E+00	8.18E+00	9.13E+00	8.85E+00	8.08E+00	8.22E+00	7.94E+00
4.0E+00	1.17E+01	1.17E+01	1.16E+01	1.16E+01	1.14E+01	1.06E+01	1.02E+01	1.12E+01	1.09E+01	1.00E+01	1.02E+01	9.80E+00
5.0E+00	1.34E+01	1.34E+01	1.33E+01	1.34E+01	1.34E+01	1.25E+01	1.20E+01	1.32E+01	1.27E+01	1.18E+01	1.20E+01	1.16E+01
6.0E+00	1.50E+01	1.51E+01	1.49E+01	1.50E+01	1.49E+01	1.42E+01	1.37E+01	1.50E+01	1.44E+01	1.35E+01	1.37E+01	1.33E+01
8.0E+00	1.78E+01	1.80E+01	1.81E+01	1.80E+01	1.80E+01	1.73E+01	1.69E+01	1.86E+01	1.76E+01	1.66E+01	1.69E+01	1.63E+01
1.0E+01	2.05E+01	2.06E+01	2.08E+01	2.08E+01	2.09E+01	2.05E+01	2.00E+01	2.21E+01	2.07E+01	1.97E+01	1.99E+01	1.93E+01
1.5E+01	2.61E+01	2.65E+01	2.65E+01	2.67E+01	2.75E+01	2.73E+01	2.73E+01	3.04E+01	2.77E+01	2.68E+01	2.68E+01	2.62E+01
2.0E+01	3.08E+01	3.10E+01	3.14E+01	3.21E+01	3.32E+01	3.41E+01	3.44E+01	3.82E+01	3.44E+01	3.38E+01	3.39E+01	3.37E+01
3.0E+01	3.79E+01	3.84E+01	3.87E+01	4.07E+01	4.34E+01	4.56E+01	4.80E+01	5.13E+01	4.60E+01	4.61E+01	4.61E+01	4.61E+01
4.0E+01	4.32E+01	4.36E+01	4.49E+01	4.73E+01	5.17E+01	5.64E+01	6.09E+01	6.18E+01	5.60E+01	5.69E+01	5.66E+01	5.72E+01
5.0E+01	4.71E+01	4.74E+01	4.89E+01	5.26E+01	5.84E+01	6.53E+01	7.23E+01	7.01E+01	6.43E+01	6.61E+01	6.58E+01	6.66E+01
6.0E+01	5.01E+01	5.15E+01	5.40E+01	5.86E+01	6.53E+01	7.44E+01	8.21E+01	7.65E+01	7.11E+01	7.41E+01	7.35E+01	7.47E+01
8.0E+01	5.45E+01	5.63E+01	5.87E+01	6.42E+01	7.35E+01	8.55E+01	9.81E+01	8.62E+01	8.18E+01	8.71E+01	8.55E+01	8.89E+01
1.0E+02	5.78E+01	5.97E+01	6.22E+01	6.89E+01	7.91E+01	9.32E+01	1.10E+02	9.27E+01	8.95E+01	9.75E+01	9.61E+01	9.89E+01
1.5E+02	6.32E+01	6.47E+01	6.80E+01	7.64E+01	8.88E+01	1.06E+02	1.30E+02	1.03E+02	1.02E+02	1.16E+02	1.15E+02	1.18E+02
2.0E+02	6.72E+01	6.86E+01	7.23E+01	8.10E+01	9.58E+01	1.15E+02	1.44E+02	1.10E+02	1.10E+02	1.29E+02	1.25E+02	1.35E+02
3.0E+02	7.23E+01	7.47E+01	7.79E+01	8.77E+01	1.04E+02	1.26E+02	1.61E+02	1.18E+02	1.21E+02	1.47E+02	1.40E+02	1.54E+02
4.0E+02	7.54E+01	7.88E+01	8.21E+01	9.23E+01	1.10E+02	1.34E+02	1.73E+02	1.23E+02	1.28E+02	1.59E+02	1.50E+02	1.68E+02
5.0E+02	7.74E+01	7.97E+01	8.37E+01	9.40E+01	1.13E+02	1.38E+02	1.81E+02	1.27E+02	1.32E+02	1.67E+02	1.58E+02	1.78E+02
6.0E+02	7.87E+01	8.11E+01	8.49E+01	9.58E+01	1.15E+02	1.43E+02	1.87E+02	1.30E+02	1.36E+02	1.74E+02	1.65E+02	1.83E+02
8.0E+02	8.04E+01	8.26E+01	8.74E+01	9.83E+01	1.19E+02	1.48E+02	1.95E+02	1.34E+02	1.41E+02	1.85E+02	1.74E+02	1.96E+02
1.0E+03	8.16E+01	8.40E+01	8.94E+01	1.01E+02	1.22E+02	1.52E+02	2.02E+02	1.37E+02	1.45E+02	1.93E+02	1.80E+02	2.06E+02

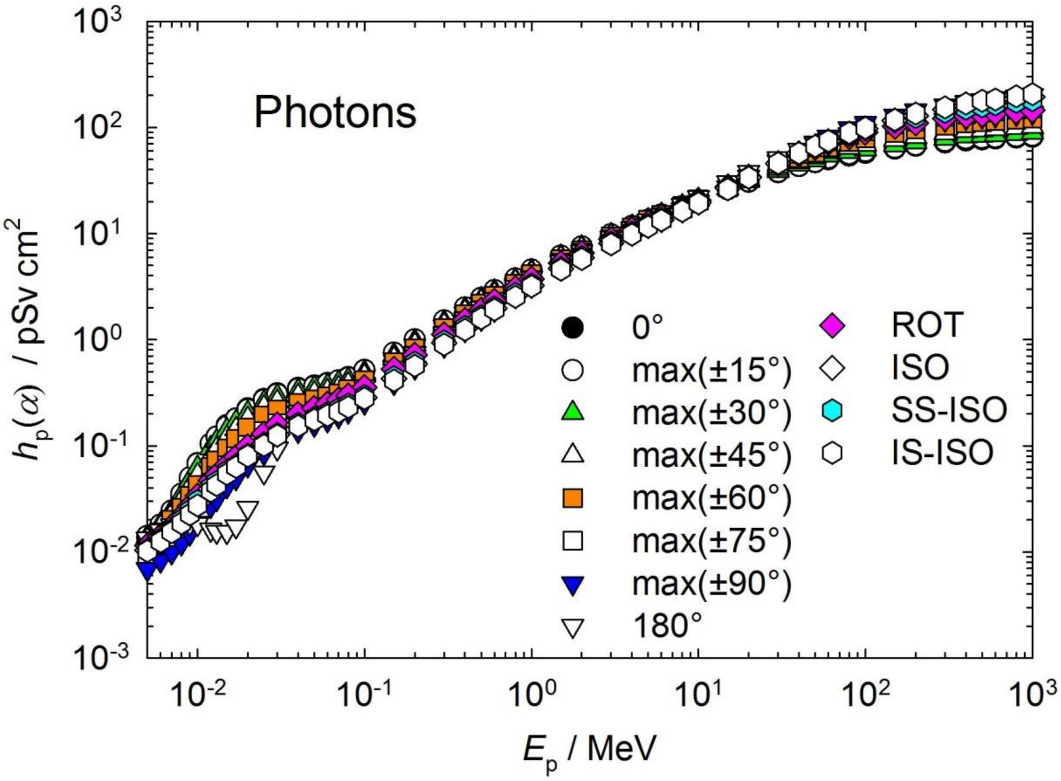

Figure A.2.1a Conversion coefficients from photon fluence to personal dose (ICRP, 2010; Endo, 2016b, 2017).

Table A.2.1b Conversion coefficients from photon air kerma to personal dose (ICRP, 2010; Endo, 2016b, 2017).

E_p / MeV	$h_p(\alpha)$ / (Sv Gy^{-1})											
	0°	max(±15°)	max(±30°)	max(±45°)	max(±60°)	max(±75°)	max(±90°)	180°	ROT	ISO	SS-ISO	IS-ISO
5.0E-03	4.36E-04	4.61E-04	4.55E-04	4.26E-04	3.79E-04	3.07E-04	2.24E-04	4.35E-04	3.74E-04	3.39E-04	3.42E-04	3.33E-04
6.0E-03	7.80E-04	8.47E-04	8.55E-04	8.12E-04	7.18E-04	5.64E-04	3.90E-04	7.47E-04	6.62E-04	6.05E-04	6.15E-04	5.90E-04
7.0E-03	1.45E-03	1.58E-03	1.58E-03	1.47E-03	1.29E-03	9.77E-04	6.40E-04	1.15E-03	1.12E-03	1.02E-03	1.04E-03	9.89E-04
8.0E-03	2.84E-03	2.98E-03	2.90E-03	2.60E-03	2.21E-03	1.64E-03	1.02E-03	1.59E-03	1.84E-03	1.64E-03	1.69E-03	1.58E-03
9.0E-03	5.31E-03	5.44E-03	5.10E-03	4.44E-03	3.67E-03	2.67E-03	1.62E-03	2.02E-03	2.96E-03	2.56E-03	2.66E-03	2.45E-03
1.0E-02	9.26E-03	9.15E-03	8.41E-03	7.17E-03	5.80E-03	4.18E-03	2.55E-03	2.49E-03	4.55E-03	3.89E-03	4.07E-03	3.72E-03
1.2E-02	2.09E-02	2.08E-02	1.90E-02	1.59E-02	1.24E-02	8.96E-03	5.39E-03	3.23E-03	9.36E-03	7.87E-03	8.09E-03	7.47E-03
1.3E-02	2.87E-02	2.86E-02	2.62E-02	2.21E-02	1.72E-02	1.22E-02	7.43E-03	3.67E-03	1.26E-02	1.06E-02	1.08E-02	1.01E-02
1.5E-02	4.99E-02	4.87E-02	4.49E-02	3.82E-02	3.00E-02	2.10E-02	1.33E-02	4.96E-03	2.13E-02	1.79E-02	1.85E-02	1.74E-02
1.7E-02	7.56E-02	7.54E-02	7.04E-02	6.04E-02	4.84E-02	3.34E-02	2.08E-02	7.31E-03	3.28E-02	2.72E-02	2.74E-02	2.64E-02
2.0E-02	1.34E-01	1.30E-01	1.22E-01	1.07E-01	8.76E-02	6.02E-02	3.88E-02	1.55E-02	5.87E-02	4.83E-02	4.88E-02	4.76E-02
2.5E-02	2.60E-01	2.56E-01	2.43E-01	2.19E-01	1.83E-01	1.31E-01	8.10E-02	5.34E-02	1.23E-01	9.81E-02	9.92E-02	9.57E-02
3.0E-02	4.32E-01	4.25E-01	4.06E-01	3.62E-01	3.04E-01	2.25E-01	1.51E-01	1.31E-01	2.20E-01	1.76E-01	1.79E-01	1.73E-01
4.0E-02	8.16E-01	8.00E-01	7.71E-01	6.91E-01	5.92E-01	4.59E-01	3.22E-01	3.80E-01	4.64E-01	3.68E-01	3.78E-01	3.59E-01
5.0E-02	1.14E+00	1.12E+00	1.09E+00	9.72E-01	8.50E-01	6.57E-01	4.89E-01	6.47E-01	7.00E-01	5.57E-01	5.70E-01	5.45E-01
6.0E-02	1.35E+00	1.33E+00	1.27E+00	1.14E+00	1.01E+00	8.01E-01	6.02E-01	8.41E-01	8.58E-01	6.85E-01	7.06E-01	6.72E-01
7.0E-02	1.43E+00	1.43E+00	1.36E+00	1.23E+00	1.08E+00	8.74E-01	6.64E-01	9.49E-01	9.49E-01	7.57E-01	7.74E-01	7.27E-01
8.0E-02	1.44E+00	1.43E+00	1.37E+00	1.24E+00	1.11E+00	9.05E-01	6.88E-01	9.85E-01	9.68E-01	7.76E-01	8.02E-01	7.56E-01
1.0E-01	1.39E+00	1.39E+00	1.32E+00	1.23E+00	1.11E+00	8.94E-01	6.87E-01	9.77E-01	9.59E-01	7.70E-01	7.94E-01	7.51E-01
1.5E-01	1.25E+00	1.26E+00	1.20E+00	1.11E+00	1.01E+00	8.41E-01	6.52E-01	9.06E-01	8.83E-01	7.16E-01	7.42E-01	6.89E-01
2.0E-01	1.17E+00	1.17E+00	1.13E+00	1.05E+00	9.64E-01	8.17E-01	6.37E-01	8.70E-01	8.43E-01	6.88E-01	7.12E-01	6.63E-01
3.0E-01	1.09E+00	1.10E+00	1.05E+00	9.98E-01	9.20E-01	7.96E-01	6.36E-01	8.39E-01	8.10E-01	6.74E-01	6.97E-01	6.51E-01
4.0E-01	1.06E+00	1.06E+00	1.03E+00	9.74E-01	9.08E-01	7.91E-01	6.50E-01	8.35E-01	8.09E-01	6.77E-01	6.98E-01	6.55E-01
5.0E-01	1.04E+00	1.04E+00	1.01E+00	9.65E-01	9.13E-01	7.97E-01	6.60E-01	8.36E-01	8.07E-01	6.85E-01	7.02E-01	6.68E-01
6.0E-01	1.02E+00	1.03E+00	1.00E+00	9.50E-01	9.08E-01	7.93E-01	6.72E-01	8.40E-01	8.12E-01	6.93E-01	7.10E-01	6.75E-01
8.0E-01	1.01E+00	1.01E+00	9.89E-01	9.54E-01	9.09E-01	7.99E-01	6.94E-01	8.48E-01	8.21E-01	7.08E-01	7.29E-01	6.86E-01
1.0E+00	1.00E+00	1.02E+00	9.87E-01	9.52E-01	9.17E-01	8.09E-01	7.16E-01	8.57E-01	8.32E-01	7.25E-01	7.41E-01	7.10E-01
1.5E+00	9.96E-01	1.00E+00	9.86E-01	9.60E-01	9.28E-01	8.55E-01	7.58E-01	8.80E-01	8.52E-01	7.60E-01	7.71E-01	7.46E-01
2.0E+00	9.90E-01	9.97E-01	9.81E-01	9.59E-01	9.21E-01	8.67E-01	7.86E-01	8.96E-01	8.68E-01	7.82E-01	7.98E-01	7.64E-01
3.0E+00	9.77E-01	9.86E-01	9.68E-01	9.63E-01	9.38E-01	8.77E-01	8.20E-01	9.15E-01	8.87E-01	8.10E-01	8.24E-01	7.96E-01
4.0E+00	9.64E-01	9.67E-01	9.59E-01	9.56E-01	9.38E-01	8.76E-01	8.40E-01	9.23E-01	8.98E-01	8.24E-01	8.40E-01	8.07E-01
5.0E+00	9.45E-01	9.44E-01	9.40E-01	9.45E-01	9.42E-01	8.81E-01	8.46E-01	9.31E-01	8.96E-01	8.32E-01	8.46E-01	8.18E-01
6.0E+00	9.28E-01	9.32E-01	9.23E-01	9.25E-01	9.21E-01	8.77E-01	8.47E-01	9.28E-01	8.91E-01	8.35E-01	8.47E-01	8.23E-01
8.0E+00	8.84E-01	8.94E-01	8.99E-01	8.95E-01	8.96E-01	8.61E-01	8.40E-01	9.24E-01	8.74E-01	8.25E-01	8.40E-01	8.10E-01
1.0E+01	8.50E-01	8.54E-01	8.61E-01	8.61E-01	8.68E-01	8.50E-01	8.29E-01	9.16E-01	8.58E-01	8.16E-01	8.25E-01	8.00E-01
1.5E+01	7.57E-01	7.68E-01	7.70E-01	7.75E-01	7.97E-01	7.94E-01	7.92E-01	8.82E-01	8.04E-01	7.78E-01	7.77E-01	7.59E-01
2.0E+01	6.79E-01	6.84E-01	6.93E-01	7.08E-01	7.31E-01	7.51E-01	7.58E-01	8.42E-01	7.58E-01	7.45E-01	7.47E-01	7.43E-01
3.0E+01	5.53E-01	5.60E-01	5.64E-01	5.93E-01	6.32E-01	6.65E-01	7.00E-01	7.48E-01	6.71E-01	6.72E-01	6.72E-01	6.72E-01
4.0E+01	4.63E-01	4.67E-01	4.81E-01	5.07E-01	5.54E-01	6.05E-01	6.53E-01	6.62E-01	6.00E-01	6.10E-01	6.07E-01	6.13E-01
5.0E+01	3.95E-01	3.98E-01	4.11E-01	4.41E-01	4.90E-01	5.48E-01	6.07E-01	5.88E-01	5.39E-01	5.55E-01	5.52E-01	5.59E-01

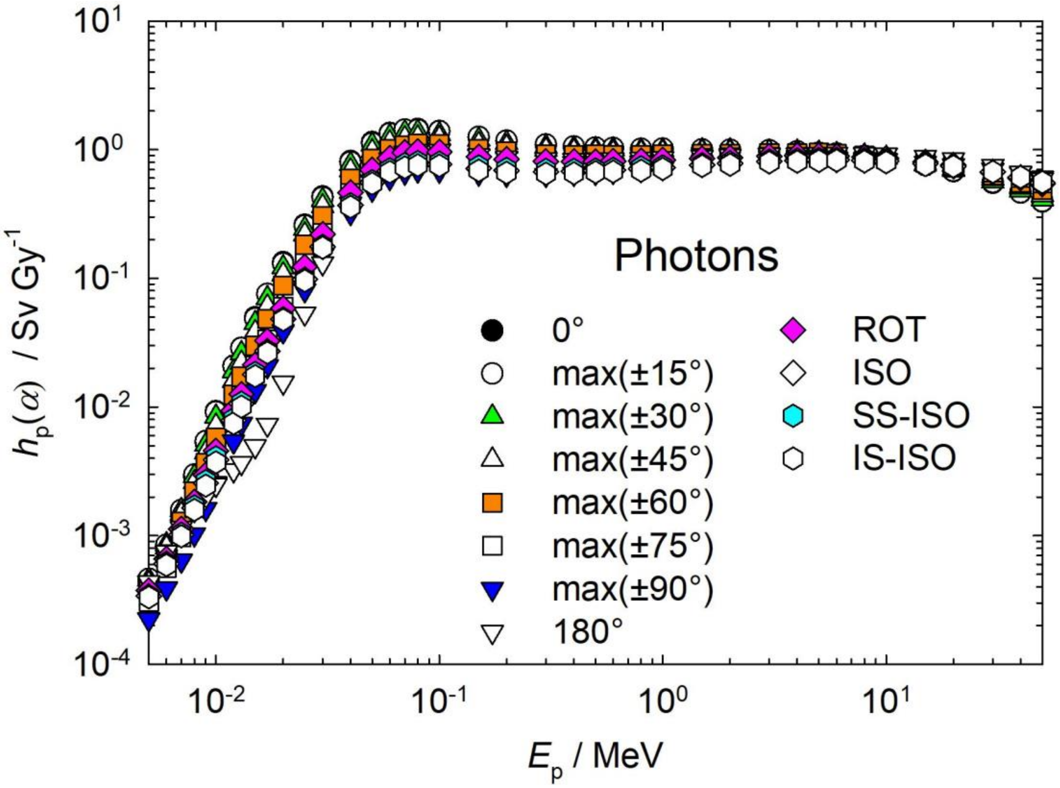

Figure A.2.1b Conversion coefficients from photon air kerma to personal dose (ICRP, 2010; Endo, 2016b, 2017).

Table A.2.2 Conversion coefficients from neutron fluence to personal dose (ICRP, 2010; Endo, 2017).

E_p / MeV	$h_p(\alpha)$ / (pSv cm^2)											
	0°	max(±15°)	max(±30°)	max(±45°)	max(±60°)	max(±75°)	max(±90°)	180°	ROT	ISO	SS-ISO	IS-ISO
1.0E-09	3.09E+00	2.95E+00	2.70E+00	2.34E+00	1.94E+00	1.45E+00	1.04E+00	1.85E+00	1.70E+00	1.29E+00	1.35E+00	1.23E+00
1.0E-08	3.55E+00	3.52E+00	3.23E+00	2.77E+00	2.30E+00	1.68E+00	1.15E+00	2.11E+00	2.03E+00	1.56E+00	1.58E+00	1.54E+00
2.5E-08	4.00E+00	3.96E+00	3.55E+00	3.07E+00	2.52E+00	1.91E+00	1.32E+00	2.44E+00	2.31E+00	1.76E+00	1.76E+00	1.76E+00
1.0E-07	5.20E+00	5.11E+00	4.71E+00	4.08E+00	3.32E+00	2.51E+00	1.70E+00	3.25E+00	2.98E+00	2.26E+00	2.33E+00	2.19E+00
2.0E-07	5.87E+00	5.83E+00	5.27E+00	4.62E+00	3.76E+00	2.79E+00	1.94E+00	3.72E+00	3.36E+00	2.54E+00	2.61E+00	2.47E+00
5.0E-07	6.59E+00	6.67E+00	6.16E+00	5.34E+00	4.34E+00	3.28E+00	2.21E+00	4.33E+00	3.86E+00	2.92E+00	2.99E+00	2.85E+00
1.0E-06	7.03E+00	7.03E+00	6.51E+00	5.70E+00	4.57E+00	3.49E+00	2.40E+00	4.73E+00	4.17E+00	3.15E+00	3.25E+00	3.05E+00
2.0E-06	7.39E+00	7.46E+00	6.83E+00	5.90E+00	4.82E+00	3.69E+00	2.52E+00	5.02E+00	4.40E+00	3.32E+00	3.37E+00	3.27E+00
5.0E-06	7.71E+00	7.80E+00	7.11E+00	6.13E+00	5.06E+00	3.74E+00	2.64E+00	5.30E+00	4.59E+00	3.47E+00	3.56E+00	3.38E+00
1.0E-05	7.82E+00	7.89E+00	7.24E+00	6.24E+00	5.13E+00	3.89E+00	2.65E+00	5.44E+00	4.68E+00	3.52E+00	3.62E+00	3.42E+00
2.0E-05	7.84E+00	7.93E+00	7.26E+00	6.28E+00	5.07E+00	3.89E+00	2.68E+00	5.51E+00	4.72E+00	3.54E+00	3.60E+00	3.48E+00
5.0E-05	7.82E+00	7.88E+00	7.21E+00	6.32E+00	5.12E+00	3.85E+00	2.66E+00	5.55E+00	4.73E+00	3.55E+00	3.65E+00	3.45E+00
1.0E-04	7.79E+00	7.82E+00	7.22E+00	6.18E+00	5.18E+00	3.85E+00	2.65E+00	5.57E+00	4.72E+00	3.54E+00	3.64E+00	3.44E+00
2.0E-04	7.73E+00	7.83E+00	7.15E+00	6.26E+00	5.11E+00	3.86E+00	2.66E+00	5.59E+00	4.67E+00	3.52E+00	3.64E+00	3.40E+00
5.0E-04	7.54E+00	7.68E+00	7.12E+00	6.15E+00	5.03E+00	3.82E+00	2.62E+00	5.60E+00	4.60E+00	3.47E+00	3.67E+00	3.27E+00
1.0E-03	7.54E+00	7.59E+00	7.06E+00	6.10E+00	4.99E+00	3.76E+00	2.61E+00	5.60E+00	4.58E+00	3.46E+00	3.64E+00	3.28E+00
2.0E-03	7.61E+00	7.69E+00	7.08E+00	6.21E+00	4.97E+00	3.76E+00	2.60E+00	5.62E+00	4.61E+00	3.48E+00	3.64E+00	3.32E+00
5.0E-03	7.97E+00	8.15E+00	7.51E+00	6.44E+00	5.28E+00	4.03E+00	2.74E+00	5.95E+00	4.86E+00	3.66E+00	3.88E+00	3.44E+00
1.0E-02	9.11E+00	9.26E+00	8.61E+00	7.45E+00	6.10E+00	4.55E+00	3.13E+00	6.81E+00	5.57E+00	4.19E+00	4.38E+00	4.00E+00
2.0E-02	1.22E+01	1.24E+01	1.15E+01	9.95E+00	8.16E+00	6.11E+00	4.21E+00	8.93E+00	7.41E+00	5.61E+00	5.80E+00	5.42E+00
3.0E-02	1.57E+01	1.61E+01	1.48E+01	1.29E+01	1.04E+01	7.93E+00	5.40E+00	1.12E+01	9.46E+00	7.18E+00	7.66E+00	6.70E+00
5.0E-02	2.30E+01	2.34E+01	2.18E+01	1.87E+01	1.54E+01	1.15E+01	7.91E+00	1.57E+01	1.37E+01	1.04E+01	1.10E+01	9.80E+00
7.0E-02	3.06E+01	3.12E+01	2.91E+01	2.50E+01	2.03E+01	1.54E+01	1.05E+01	2.00E+01	1.80E+01	1.37E+01	1.47E+01	1.27E+01
1.0E-01	4.19E+01	4.25E+01	3.94E+01	3.45E+01	2.83E+01	2.10E+01	1.44E+01	2.59E+01	2.43E+01	1.86E+01	1.94E+01	1.78E+01
1.5E-01	6.06E+01	6.11E+01	5.71E+01	5.00E+01	4.10E+01	3.08E+01	2.08E+01	3.49E+01	3.47E+01	2.66E+01	2.77E+01	2.55E+01
2.0E-01	7.88E+01	7.96E+01	7.43E+01	6.55E+01	5.37E+01	4.03E+01	2.72E+01	4.31E+01	4.47E+01	3.44E+01	3.57E+01	3.31E+01
3.0E-01	1.14E+02	1.14E+02	1.07E+02	9.45E+01	7.85E+01	5.89E+01	3.97E+01	5.81E+01	6.38E+01	4.94E+01	5.11E+01	4.77E+01
5.0E-01	1.77E+02	1.80E+02	1.70E+02	1.52E+02	1.26E+02	9.47E+01	6.37E+01	8.59E+01	9.91E+01	7.71E+01	7.97E+01	7.45E+01
7.0E-01	2.32E+02	2.35E+02	2.23E+02	2.00E+02	1.69E+02	1.28E+02	8.55E+01	1.12E+02	1.31E+02	1.02E+02	1.08E+02	9.60E+01
9.0E-01	2.79E+02	2.83E+02	2.70E+02	2.41E+02	2.03E+02	1.56E+02	1.05E+02	1.36E+02	1.60E+02	1.26E+02	1.30E+02	1.22E+02
1.0E+00	3.01E+02	2.89E+02	2.76E+02	2.48E+02	2.08E+02	1.57E+02	1.15E+02	1.48E+02	1.74E+02	1.37E+02	1.31E+02	1.43E+02
1.2E+00	3.30E+02	3.34E+02	3.18E+02	2.90E+02	2.45E+02	1.90E+02	1.30E+02	1.67E+02	1.93E+02	1.53E+02	1.57E+02	1.49E+02
1.5E+00	3.65E+02	3.71E+02	3.56E+02	3.25E+02	2.79E+02	2.20E+02	1.50E+02	1.95E+02	2.19E+02	1.74E+02	1.83E+02	1.65E+02
2.0E+00	4.07E+02	4.12E+02	3.96E+02	3.65E+02	3.19E+02	2.57E+02	1.79E+02	2.35E+02	2.54E+02	2.03E+02	2.13E+02	1.93E+02
3.0E+00	4.58E+02	4.58E+02	4.42E+02	4.14E+02	3.70E+02	3.08E+02	2.21E+02	2.92E+02	3.01E+02	2.44E+02	2.58E+02	2.30E+02
4.0E+00	4.83E+02	4.91E+02	4.78E+02	4.46E+02	3.99E+02	3.32E+02	2.49E+02	3.30E+02	3.31E+02	2.71E+02	2.81E+02	2.61E+02
5.0E+00	4.94E+02	4.93E+02	4.79E+02	4.59E+02	4.19E+02	3.57E+02	2.69E+02	3.54E+02	3.51E+02	2.90E+02	3.05E+02	2.75E+02
6.0E+00	4.98E+02	5.00E+02	4.86E+02	4.66E+02	4.27E+02	3.69E+02	2.84E+02	3.71E+02	3.65E+02	3.03E+02	3.15E+02	2.91E+02
7.0E+00	4.99E+02	4.97E+02	4.83E+02	4.63E+02	4.29E+02	3.81E+02	2.95E+02	3.83E+02	3.74E+02	3.13E+02	3.28E+02	2.98E+02
8.0E+00	4.99E+02	4.94E+02	4.83E+02	4.60E+02	4.29E+02	3.78E+02	3.03E+02	3.92E+02	3.81E+02	3.21E+02	3.29E+02	3.13E+02
9.0E+00	5.00E+02	4.95E+02	4.82E+02	4.65E+02	4.30E+02	3.86E+02	3.10E+02	3.98E+02	3.86E+02	3.27E+02	3.32E+02	3.22E+02
1.0E+01	5.00E+02	5.07E+02	4.92E+02	4.76E+02	4.39E+02	3.93E+02	3.16E+02	4.04E+02	3.90E+02	3.32E+02	3.40E+02	3.24E+02
1.2E+01	4.99E+02	5.10E+02	4.96E+02	4.77E+02	4.46E+02	3.96E+02	3.25E+02	4.12E+02	3.95E+02	3.39E+02	3.49E+02	3.29E+02
1.4E+01	4.95E+02	4.98E+02	4.89E+02	4.72E+02	4.42E+02	4.00E+02	3.33E+02	4.17E+02	3.98E+02	3.44E+02	3.56E+02	3.32E+02
1.5E+01	4.93E+02	4.95E+02	4.86E+02	4.70E+02	4.42E+02	3.99E+02	3.36E+02	4.19E+02	3.98E+02	3.46E+02	3.59E+02	3.33E+02
1.6E+01	4.90E+02	4.89E+02	4.80E+02	4.67E+02	4.38E+02	4.00E+02	3.38E+02	4.20E+02	3.99E+02	3.47E+02	3.62E+02	3.32E+02
1.8E+01	4.84E+02	4.67E+02	4.65E+02	4.46E+02	4.24E+02	3.88E+02	3.43E+02	4.22E+02	3.99E+02	3.50E+02	3.65E+02	3.35E+02
2.0E+01	4.77E+02	4.65E+02	4.62E+02	4.47E+02	4.26E+02	3.91E+02	3.47E+02	4.23E+02	3.98E+02	3.52E+02	3.73E+02	3.31E+02
2.1E+01	4.74E+02	4.10E+02	4.04E+02	3.98E+02	3.89E+02	3.62E+02	3.48E+02	4.23E+02	3.98E+02	3.53E+02	3.35E+02	3.71E+02
3.0E+01	4.53E+02	4.29E+02	4.24E+02	4.19E+02	4.05E+02	3.91E+02	3.60E+02	4.22E+02	3.95E+02	3.58E+02	3.66E+02	3.50E+02
5.0E+01	4.33E+02	4.01E+02	4.00E+02	4.01E+02	3.94E+02	3.87E+02	3.80E+02	4.28E+02	3.95E+02	3.71E+02	3.46E+02	3.96E+02
7.5E+01	4.20E+02	4.12E+02	4.14E+02	4.10E+02	4.09E+02	4.05E+02	3.99E+02	4.39E+02	4.02E+02	3.87E+02	3.53E+02	4.21E+02
1.0E+02	4.02E+02	4.14E+02	4.19E+02	4.21E+02	4.26E+02	4.26E+02	4.09E+02	4.44E+02	4.06E+02	3.97E+02	3.73E+02	4.21E+02
1.3E+02	3.82E+02	4.24E+02	4.32E+02	4.41E+02	4.49E+02	4.50E+02	4.16E+02	4.46E+02	4.11E+02	4.07E+02	4.12E+02	4.02E+02
1.5E+02	3.73E+02	4.20E+02	4.25E+02	4.41E+02	4.47E+02	4.58E+02	4.20E+02	4.46E+02	4.14E+02	4.12E+02	4.09E+02	4.15E+02
1.8E+02	3.63E+02	4.08E+02	4.12E+02	4.35E+02	4.52E+02	4.59E+02	4.25E+02	4.47E+02	4.18E+02	4.21E+02	4.22E+02	4.20E+02
2.0E+02	3.59E+02	4.08E+02	4.13E+02	4.35E+02	4.58E+02	4.72E+02	4.29E+02	4.48E+02	4.22E+02	4.26E+02	4.33E+02	4.19E+02
3.0E+02	3.63E+02	3.84E+02	3.92E+02	4.08E+02	4.35E+02	4.53E+02	4.51E+02	4.64E+02	4.43E+02	4.55E+02	4.37E+02	4.73E+02
4.0E+02	3.89E+02	4.03E+02	4.13E+02	4.28E+02	4.47E+02	4.68E+02	4.83E+02	4.96E+02	4.72E+02	4.88E+02	4.61E+02	5.15E+02
5.0E+02	4.22E+02	4.39E+02	4.54E+02	4.70E+02	4.92E+02	5.15E+02	5.23E+02	5.33E+02	5.03E+02	5.21E+02	5.09E+02	5.33E+02
6.0E+02	4.57E+02	4.76E+02	4.88E+02	5.09E+02	5.31E+02	5.54E+02	5.63E+02	5.69E+02	5.32E+02	5.53E+02	5.66E+02	5.40E+02
7.0E+02	4.86E+02	4.97E+02	5.10E+02	5.26E+02	5.51E+02	5.76E+02	5.97E+02	5.99E+02	5.58E+02	5.80E+02	6.25E+02	5.35E+02
8.0E+02	5.08E+02	5.12E+02	5.27E+02	5.48E+02	5.74E+02	6.00E+02	6.20E+02	6.23E+02	5.80E+02	6.04E+02	6.38E+02	5.70E+02
9.0E+02	5.24E+02	5.25E+02	5.40E+02	5.59E+02	5.83E+02	6.09E+02	6.38E+02	6.40E+02	5.98E+02	6.24E+02	6.45E+02	6.03E+02
1.0E+03	5.37E+02	5.35E+02	5.45E+02	5.70E+02	5.94E+02	6.22E+02	6.51E+02	6.54E+02	6.14E+02	6.42E+02	6.63E+02	6.21E+02

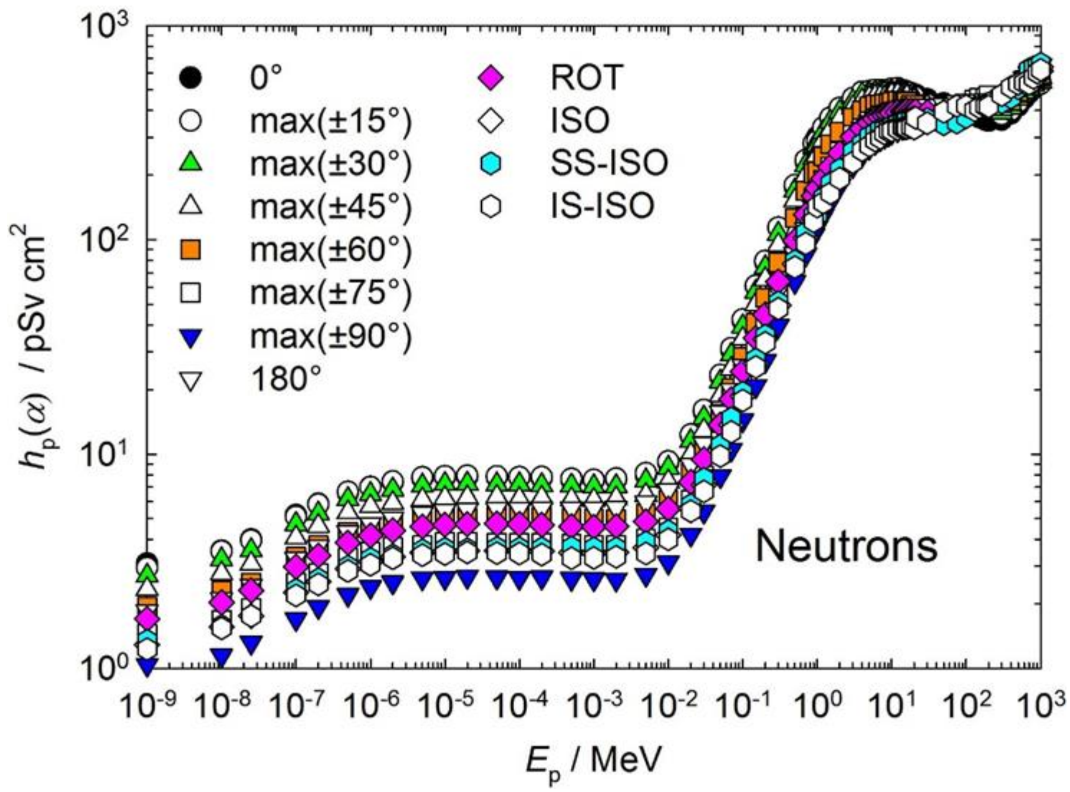

Figure A.2.2 Conversion coefficients from neutron fluence to personal dose (ICRP, 2010; Endo, 2017).

Table A.2.3 Conversion coefficients from electron fluence to personal dose (ICRP, 2010; Endo, 2017).

E_p / MeV	$h_p(\alpha)$ / (pSv cm^2)											
	0°	max(±15°)	max(±30°)	max(±45°)	max(±60°)	max(±75°)	max(±90°)	180°	ROT	ISO	SS-ISO	IS-ISO
1.0E-02	2.69E-02	2.60E-02	2.44E-02	2.21E-02	1.98E-02	1.67E-02	1.35E-02	2.68E-02	2.13E-02	1.88E-02	1.89E-02	1.87E-02
1.5E-02	4.04E-02	3.89E-02	3.65E-02	3.29E-02	2.95E-02	2.50E-02	2.02E-02	4.02E-02	3.17E-02	2.83E-02	2.84E-02	2.82E-02
2.0E-02	5.39E-02	5.17E-02	4.86E-02	4.38E-02	3.92E-02	3.32E-02	2.70E-02	5.35E-02	4.22E-02	3.77E-02	3.78E-02	3.76E-02
3.0E-02	8.10E-02	7.76E-02	7.29E-02	6.58E-02	5.89E-02	4.99E-02	4.05E-02	8.01E-02	6.34E-02	5.67E-02	5.70E-02	5.64E-02
4.0E-02	1.08E-01	1.04E-01	9.77E-02	8.81E-02	7.89E-02	6.68E-02	5.41E-02	1.07E-01	8.48E-02	7.58E-02	7.59E-02	7.57E-02
5.0E-02	1.35E-01	1.30E-01	1.22E-01	1.10E-01	9.88E-02	8.37E-02	6.77E-02	1.33E-01	1.06E-01	9.48E-02	9.50E-02	9.46E-02
6.0E-02	1.63E-01	1.56E-01	1.47E-01	1.33E-01	1.19E-01	1.01E-01	8.13E-02	1.60E-01	1.27E-01	1.14E-01	1.15E-01	1.13E-01
8.0E-02	2.18E-01	2.10E-01	1.98E-01	1.79E-01	1.60E-01	1.35E-01	1.09E-01	2.13E-01	1.70E-01	1.52E-01	1.54E-01	1.50E-01
1.0E-01	2.75E-01	2.64E-01	2.50E-01	2.26E-01	2.02E-01	1.70E-01	1.36E-01	2.67E-01	2.13E-01	1.91E-01	1.92E-01	1.90E-01
1.5E-01	4.18E-01	4.03E-01	3.86E-01	3.51E-01	3.13E-01	2.61E-01	2.06E-01	3.99E-01	3.23E-01	2.91E-01	2.94E-01	2.88E-01
2.0E-01	5.69E-01	5.49E-01	5.30E-01	4.86E-01	4.34E-01	3.59E-01	2.78E-01	5.30E-01	4.37E-01	3.93E-01	3.96E-01	3.90E-01
3.0E-01	8.89E-01	8.68E-01	8.55E-01	7.96E-01	7.04E-01	5.66E-01	4.27E-01	7.87E-01	6.73E-01	6.06E-01	6.16E-01	5.96E-01
4.0E-01	1.24E+00	1.22E+00	1.23E+00	1.16E+00	1.02E+00	8.00E-01	5.83E-01	1.04E+00	9.21E-01	8.32E-01	8.51E-01	8.13E-01
5.0E-01	1.63E+00	1.61E+00	1.66E+00	1.58E+00	1.38E+00	1.07E+00	7.50E-01	1.28E+00	1.19E+00	1.08E+00	1.09E+00	1.07E+00
6.0E-01	2.05E+00	2.07E+00	2.16E+00	2.06E+00	1.79E+00	1.35E+00	9.23E-01	1.50E+00	1.48E+00	1.35E+00	1.38E+00	1.32E+00
8.0E-01	4.04E+00	3.82E+00	3.75E+00	3.41E+00	2.86E+00	2.06E+00	1.33E+00	1.68E+00	2.23E+00	1.97E+00	2.03E+00	1.91E+00
1.0E+00	7.10E+00	6.62E+00	6.16E+00	5.33E+00	4.24E+00	2.96E+00	1.82E+00	1.68E+00	3.23E+00	2.76E+00	2.86E+00	2.66E+00
1.5E+00	1.50E+01	1.41E+01	1.28E+01	1.07E+01	8.19E+00	5.58E+00	3.22E+00	1.62E+00	5.93E+00	4.96E+00		
2.0E+00	2.24E+01	2.14E+01	1.94E+01	1.62E+01	1.24E+01	8.41E+00	4.87E+00	1.62E+00	8.73E+00	7.24E+00	7.59E+00	6.89E+00
3.0E+00	3.61E+01	3.47E+01	3.17E+01	2.66E+01	2.06E+01	1.42E+01	8.62E+00	1.95E+00	1.42E+01	1.19E+01	1.25E+01	1.13E+01
4.0E+00	4.82E+01	4.73E+01	4.35E+01	3.68E+01	2.86E+01	2.01E+01	1.26E+01	2.62E+00	1.96E+01	1.64E+01	1.72E+01	1.56E+01
5.0E+00	5.93E+01	5.90E+01	5.50E+01	4.70E+01	3.68E+01	2.58E+01	1.66E+01	3.63E+00	2.50E+01	2.10E+01	2.18E+01	2.02E+01
6.0E+00	7.06E+01	7.02E+01	6.63E+01	5.69E+01	4.54E+01	3.24E+01	2.09E+01	5.04E+00	3.07E+01	2.55E+01	2.62E+01	2.48E+01
8.0E+00	9.79E+01	9.72E+01	9.40E+01	8.37E+01	6.74E+01	4.68E+01	3.08E+01	9.46E+00	4.43E+01	3.55E+01	3.59E+01	3.51E+01
1.0E+01	1.25E+02	1.27E+02	1.23E+02	1.14E+02	9.21E+01	6.55E+01	4.26E+01	1.83E+01	5.87E+01	4.67E+01	4.74E+01	4.60E+01
1.5E+01	1.88E+02	1.88E+02	1.82E+02	1.70E+02	1.43E+02	1.08E+02	7.02E+01	5.31E+01	9.63E+01	7.69E+01		
2.0E+01	2.36E+02	2.36E+02	2.27E+02	2.11E+02	1.85E+02	1.42E+02	9.47E+01	1.04E+02	1.34E+02	1.06E+02	1.10E+02	1.02E+02
3.0E+01	3.02E+02	3.05E+02	2.91E+02	2.75E+02	2.45E+02	2.02E+02	1.38E+02	2.20E+02	2.03E+02	1.64E+02	1.71E+02	1.57E+02
4.0E+01	3.29E+02	3.34E+02	3.26E+02	3.11E+02	2.90E+02	2.56E+02	1.89E+02	2.97E+02	2.56E+02	2.12E+02	2.21E+02	2.01E+02
5.0E+01	3.37E+02	3.41E+02	3.39E+02	3.34E+02	3.18E+02	2.97E+02	2.44E+02	3.31E+02	2.90E+02	2.49E+02	2.57E+02	2.41E+02
6.0E+01	3.41E+02	3.46E+02	3.43E+02	3.41E+02	3.33E+02	3.22E+02	2.79E+02	3.44E+02	3.12E+02	2.75E+02	2.82E+02	2.68E+02
8.0E+01	3.46E+02	3.51E+02	3.50E+02	3.51E+02	3.51E+02	3.47E+02	3.21E+02	3.58E+02	3.37E+02	3.09E+02	3.16E+02	3.02E+02
1.0E+02	3.49E+02	3.52E+02	3.54E+02	3.55E+02	3.57E+02	3.58E+02	3.43E+02	3.66E+02	3.51E+02	3.31E+02	3.37E+02	3.25E+02
1.5E+02	3.55E+02	3.58E+02	3.60E+02	3.66E+02	3.72E+02	3.76E+02	3.72E+02	3.79E+02	3.70E+02	3.63E+02		
2.0E+02	3.59E+02	3.61E+02	3.64E+02	3.67E+02	3.78E+02	3.87E+02	3.93E+02	3.88E+02	3.84E+02	3.83E+02	3.84E+02	3.82E+02
3.0E+02	3.65E+02	3.68E+02	3.69E+02	3.76E+02	3.90E+02	4.05E+02	4.24E+02	3.99E+02	3.98E+02	4.10E+02	4.09E+02	4.11E+02
4.0E+02	3.69E+02	3.70E+02	3.74E+02	3.83E+02	3.97E+02	4.17E+02	4.42E+02	4.08E+02	4.08E+02	4.30E+02	4.25E+02	4.35E+02
5.0E+02	3.72E+02	3.74E+02	3.76E+02	3.86E+02	4.04E+02	4.24E+02	4.55E+02	4.14E+02	4.16E+02	4.45E+02	4.41E+02	4.49E+02
6.0E+02	3.75E+02	3.78E+02	3.79E+02	3.91E+02	4.10E+02	4.31E+02	4.66E+02	4.19E+02	4.24E+02	4.57E+02	4.50E+02	4.64E+02
8.0E+02	3.79E+02	3.79E+02	3.86E+02	3.96E+02	4.14E+02	4.43E+02	4.89E+02	4.28E+02	4.37E+02	4.78E+02	4.68E+02	4.88E+02
1.0E+03	3.82E+02	3.83E+02	3.88E+02	4.02E+02	4.25E+02	4.51E+02	5.04E+02	4.34E+02	4.47E+02	4.95E+02	4.82E+02	5.08E+02

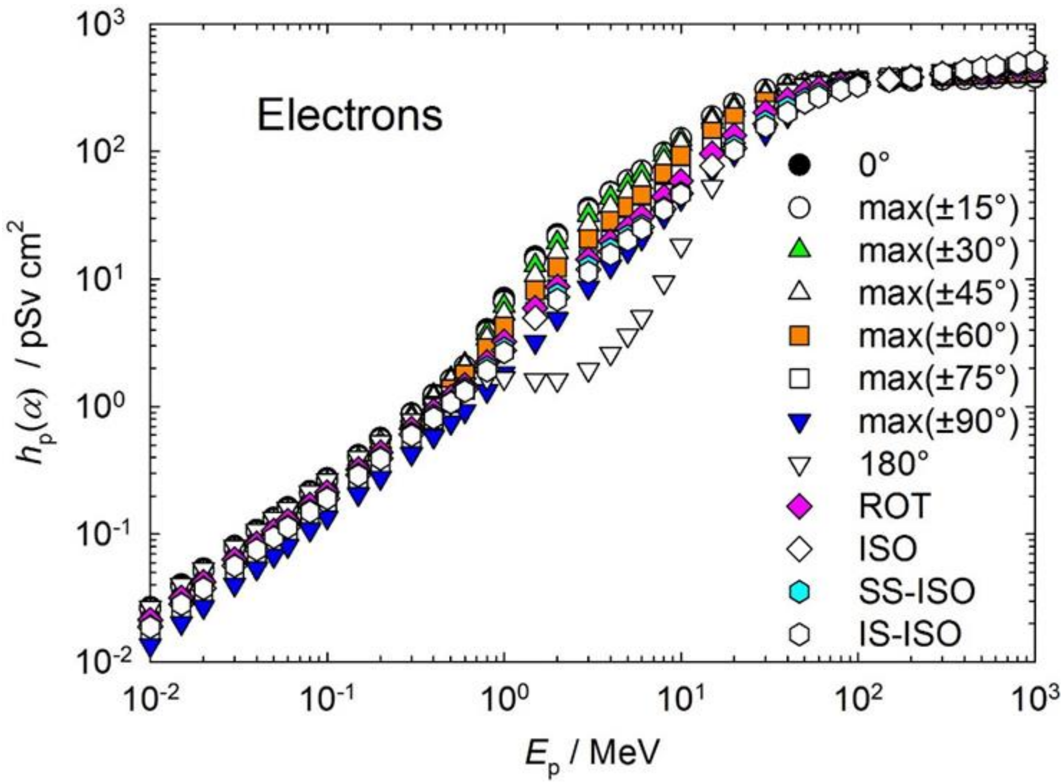

Figure A.2. 3 Conversion coefficients from electron fluence to personal dose (ICRP, 2010; Endo, 2017)

Table A.2.4 Conversion coefficients from positron fluence to personal dose (ICRP, 2010; Endo, 2017).

E_p / MeV	$h_p(\alpha)$ / (pSv cm^2)										
	0°	max(±15°)	max(±30°)	max(±45°)	max(±60°)	max(±75°)	max(±90°)	180°	ROT	ISO	SS-ISO	IS-ISO
1.0E-02	3.28E+00	3.14E+00	2.86E+00	2.44E+00	1.99E+00	1.50E+00	1.07E+00	1.62E+00	1.77E+00	1.39E+00	1.45E+00	1.33E+00
1.5E-02	3.29E+00	3.04E+00	2.74E+00	2.34E+00	1.91E+00	1.45E+00	1.03E+00	1.64E+00	1.71E+00	1.40E+00	1.47E+00	1.33E+00
2.0E-02	3.30E+00	2.99E+00	2.72E+00	2.30E+00	1.88E+00	1.44E+00	1.03E+00	1.65E+00	1.70E+00	1.41E+00	1.46E+00	1.36E+00
3.0E-02	3.33E+00	3.01E+00	2.70E+00	2.30E+00	1.88E+00	1.44E+00	1.04E+00	1.68E+00	1.70E+00	1.43E+00	1.49E+00	1.37E+00
4.0E-02	3.36E+00	3.09E+00	2.79E+00	2.38E+00	1.94E+00	1.49E+00	1.07E+00	1.71E+00	1.75E+00	1.45E+00	1.50E+00	1.40E+00
5.0E-02	3.39E+00	3.10E+00	2.81E+00	2.39E+00	1.94E+00	1.48E+00	1.08E+00	1.73E+00	1.77E+00	1.47E+00	1.52E+00	1.42E+00
6.0E-02	3.42E+00	3.12E+00	2.83E+00	2.40E+00	1.95E+00	1.50E+00	1.09E+00	1.76E+00	1.78E+00	1.49E+00	1.57E+00	1.41E+00
8.0E-02	3.47E+00	3.14E+00	2.85E+00	2.43E+00	2.00E+00	1.54E+00	1.11E+00	1.82E+00	1.82E+00	1.53E+00	1.60E+00	1.46E+00
1.0E-01	3.53E+00	3.20E+00	2.90E+00	2.46E+00	2.03E+00	1.58E+00	1.14E+00	1.87E+00	1.86E+00	1.57E+00	1.63E+00	1.51E+00
1.5E-01	3.67E+00	3.35E+00	3.04E+00	2.59E+00	2.15E+00	1.66E+00	1.20E+00	2.01E+00	1.97E+00	1.67E+00	1.72E+00	1.62E+00
2.0E-01	3.84E+00	3.48E+00	3.18E+00	2.73E+00	2.26E+00	1.75E+00	1.27E+00	2.14E+00	2.07E+00	1.77E+00	1.81E+00	1.73E+00
3.0E-01	4.16E+00	3.81E+00	3.52E+00	3.04E+00	2.54E+00	1.96E+00	1.42E+00	2.40E+00	2.32E+00	1.98E+00	2.05E+00	1.91E+00
4.0E-01	4.52E+00	4.16E+00	3.88E+00	3.42E+00	2.84E+00	2.20E+00	1.56E+00	2.65E+00	2.57E+00	2.21E+00	2.28E+00	2.14E+00
5.0E-01	4.90E+00	4.55E+00	4.32E+00	3.84E+00	3.22E+00	2.45E+00	1.72E+00	2.90E+00	2.84E+00	2.45E+00	2.54E+00	2.36E+00
6.0E-01	5.36E+00	5.01E+00	4.79E+00	4.31E+00	3.63E+00	2.76E+00	1.90E+00	3.12E+00	3.13E+00	2.72E+00	2.82E+00	2.62E+00
8.0E-01	7.41E+00	6.81E+00	6.42E+00	5.67E+00	4.71E+00	3.49E+00	2.32E+00	3.32E+00	3.90E+00	3.38E+00	3.51E+00	3.25E+00
1.0E+00	1.05E+01	9.64E+00	8.87E+00	7.59E+00	6.10E+00	4.44E+00	2.82E+00	3.37E+00	4.94E+00	4.20E+00	4.39E+00	4.01E+00
1.5E+00	1.83E+01	1.71E+01	1.55E+01	1.30E+01	1.01E+01	7.08E+00	4.28E+00	3.44E+00	7.66E+00	6.42E+00		
2.0E+00	2.57E+01	2.43E+01	2.20E+01	1.85E+01	1.43E+01	9.99E+00	5.95E+00	3.59E+00	1.05E+01	8.70E+00	9.13E+00	8.27E+00
3.0E+00	3.91E+01	3.74E+01	3.40E+01	2.85E+01	2.24E+01	1.59E+01	9.69E+00	4.19E+00	1.59E+01	1.33E+01	1.39E+01	1.27E+01
4.0E+00	5.10E+01	4.95E+01	4.56E+01	3.86E+01	3.03E+01	2.17E+01	1.36E+01	5.11E+00	2.13E+01	1.80E+01	1.88E+01	1.72E+01
5.0E+00	6.17E+01	6.08E+01	5.67E+01	4.83E+01	3.82E+01	2.73E+01	1.75E+01	6.31E+00	2.66E+01	2.24E+01	2.33E+01	2.15E+01
6.0E+00	7.29E+01	7.19E+01	6.79E+01	5.85E+01	4.70E+01	3.37E+01	2.19E+01	8.03E+00	3.23E+01	2.69E+01	2.77E+01	2.61E+01
8.0E+00	9.90E+01	9.75E+01	9.41E+01	8.45E+01	6.82E+01	4.77E+01	3.14E+01	1.40E+01	4.61E+01	3.67E+01	3.77E+01	3.57E+01
1.0E+01	1.26E+02	1.25E+02	1.21E+02	1.11E+02	9.09E+01	6.53E+01	4.25E+01	2.36E+01	5.95E+01	4.76E+01	4.89E+01	4.63E+01
1.5E+01	1.84E+02	1.83E+02	1.77E+02	1.65E+02	1.41E+02	1.05E+02	7.07E+01	5.90E+01	9.55E+01	7.55E+01		
2.0E+01	2.29E+02	2.26E+02	2.17E+02	2.03E+02	1.78E+02	1.38E+02	9.26E+01	1.11E+02	1.30E+02	1.04E+02	1.08E+02	1.00E+02
3.0E+01	2.94E+02	2.91E+02	2.79E+02	2.60E+02	2.33E+02	1.93E+02	1.35E+02	2.21E+02	1.95E+02	1.62E+02	1.65E+02	1.59E+02
4.0E+01	3.20E+02	3.14E+02	3.10E+02	2.96E+02	2.75E+02	2.47E+02	1.83E+02	2.91E+02	2.42E+02	2.09E+02	2.10E+02	2.08E+02
5.0E+01	3.27E+02	3.22E+02	3.20E+02	3.13E+02	3.00E+02	2.82E+02	2.28E+02	3.21E+02	2.76E+02	2.43E+02	2.44E+02	2.42E+02
6.0E+01	3.33E+02	3.27E+02	3.28E+02	3.23E+02	3.17E+02	3.05E+02	2.63E+02	3.34E+02	2.96E+02	2.68E+02	2.67E+02	2.69E+02
8.0E+01	3.39E+02	3.36E+02	3.36E+02	3.34E+02	3.33E+02	3.28E+02	3.02E+02	3.49E+02	3.20E+02	3.02E+02	3.00E+02	3.04E+02
1.0E+02	3.42E+02	3.39E+02	3.40E+02	3.39E+02	3.41E+02	3.41E+02	3.26E+02	3.57E+02	3.34E+02	3.23E+02	3.19E+02	3.27E+02
1.5E+02	3.49E+02	3.48E+02	3.48E+02	3.51E+02	3.57E+02	3.61E+02	3.61E+02	3.71E+02	3.55E+02	3.56E+02		
2.0E+02	3.54E+02	3.54E+02	3.54E+02	3.58E+02	3.66E+02	3.74E+02	3.80E+02	3.81E+02	3.68E+02	3.77E+02	3.71E+02	3.83E+02
3.0E+02	3.62E+02	3.60E+02	3.61E+02	3.69E+02	3.82E+02	3.92E+02	4.09E+02	3.93E+02	3.85E+02	4.05E+02	3.98E+02	4.12E+02
4.0E+02	3.66E+02	3.64E+02	3.66E+02	3.75E+02	3.90E+02	4.06E+02	4.33E+02	4.02E+02	3.99E+02	4.25E+02	4.15E+02	4.35E+02
5.0E+02	3.69E+02	3.69E+02	3.72E+02	3.81E+02	3.97E+02	4.17E+02	4.44E+02	4.09E+02	4.08E+02	4.40E+02	4.31E+02	4.49E+02
6.0E+02	3.72E+02	3.71E+02	3.76E+02	3.85E+02	4.02E+02	4.26E+02	4.60E+02	4.15E+02	4.18E+02	4.53E+02	4.44E+02	4.62E+02
8.0E+02	3.76E+02	3.76E+02	3.80E+02	3.92E+02	4.14E+02	4.35E+02	4.79E+02	4.24E+02	4.32E+02	4.74E+02	4.63E+02	4.85E+02
1.0E+03	3.79E+02	3.81E+02	3.83E+02	3.96E+02	4.20E+02	4.48E+02	4.98E+02	4.30E+02	4.36E+02	4.91E+02	4.77E+02	5.05E+02

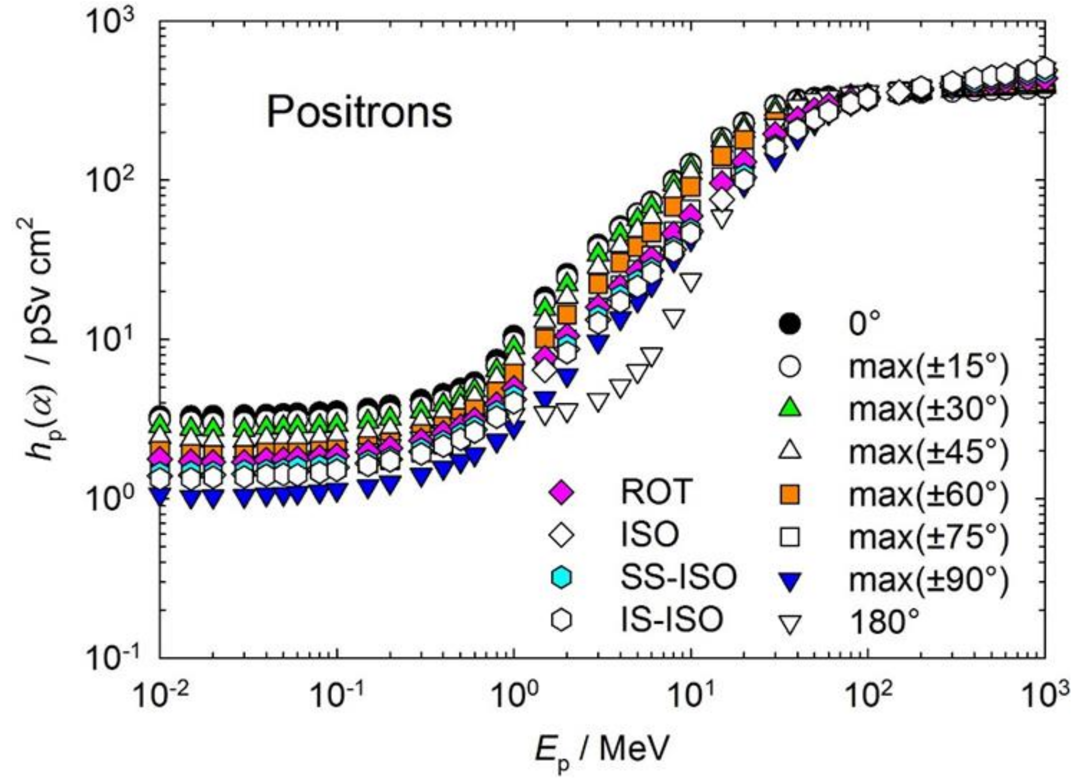

Figure A.2.4 Conversion coefficients from positron fluence to personal dose (ICRP, 2010; Endo, 2017).

Table A.2.5 Conversion coefficients from proton fluence to personal dose (ICRP, 2010; Endo, 2017).

E_p / MeV	$h_p(\alpha)$ / (pSv cm^2)											
	0°	max(±15°)	max(±30°)	max(±45°)	max(±60°)	max(±75°)	max(±90°)	180°	ROT	ISO	SS-ISO	IS-ISO
1.0E+00	5.46E+00	5.30E+00	5.01E+00	4.53E+00	4.07E+00	3.44E+00	2.81E+00	5.47E+00	4.50E+00	3.52E+00	3.44E+00	3.51E+00
1.5E+00	8.20E+00	7.94E+00	7.50E+00	6.78E+00	6.09E+00	5.16E+00	4.21E+00	8.21E+00	6.75E+00	5.28E+00	5.16E+00	5.26E+00
2.0E+00	1.09E+01	1.06E+01	9.98E+00	9.02E+00	8.10E+00	6.87E+00	5.62E+00	1.09E+01	8.98E+00	7.02E+00	6.86E+00	7.00E+00
3.0E+00	1.64E+01	1.58E+01	1.49E+01	1.34E+01	1.21E+01	1.03E+01	8.43E+00	1.64E+01	1.34E+01	1.05E+01	1.03E+01	1.05E+01
4.0E+00	2.19E+01	2.10E+01	1.97E+01	1.78E+01	1.60E+01	1.36E+01	1.12E+01	2.19E+01	1.78E+01	1.39E+01	1.36E+01	1.39E+01
5.0E+00	2.73E+01	2.61E+01	2.44E+01	2.20E+01	1.98E+01	1.69E+01	1.40E+01	2.73E+01	2.21E+01	1.73E+01	1.69E+01	1.72E+01
6.0E+00	3.28E+01	3.12E+01	2.90E+01	2.60E+01	2.34E+01	2.01E+01	1.68E+01	3.28E+01	2.63E+01	2.05E+01	2.01E+01	2.05E+01
8.0E+00	4.37E+01	4.09E+01	3.77E+01	3.36E+01	3.03E+01	2.64E+01	2.24E+01	4.37E+01	3.45E+01	2.68E+01	2.62E+01	2.67E+01
1.0E+01	5.49E+01	6.37E+01	6.84E+01	6.62E+01	5.84E+01	4.40E+01	2.81E+01	5.46E+01	5.01E+01	4.58E+01	4.66E+01	4.50E+01
1.5E+01	1.89E+02	1.87E+02	1.52E+02	1.33E+02	1.17E+02	8.64E+01	5.07E+01	5.61E+01	9.37E+01	8.01E+01	8.31E+01	7.71E+01
2.0E+01	4.28E+02	4.08E+02	3.59E+02	2.95E+02	2.09E+02	1.47E+02	8.28E+01	4.36E+01	1.65E+02	1.36E+02	1.45E+02	1.27E+02
3.0E+01	7.50E+02	7.31E+02	6.73E+02	5.63E+02	4.30E+02	2.98E+02	1.80E+02	3.61E+01	2.96E+02	2.49E+02	2.66E+02	2.32E+02
4.0E+01	1.02E+03	1.01E+03	9.32E+02	7.81E+02	6.23E+02	4.45E+02	2.90E+02	4.55E+01	4.22E+02	3.58E+02	3.81E+02	3.35E+02
5.0E+01	1.18E+03	1.20E+03	1.18E+03	1.04E+03	8.06E+02	5.54E+02	3.79E+02	7.15E+01	5.32E+02	4.51E+02	4.62E+02	4.40E+02
6.0E+01	1.48E+03	1.47E+03	1.44E+03	1.34E+03	1.10E+03	7.52E+02	5.00E+02	1.56E+02	6.87E+02	5.51E+02	5.47E+02	5.55E+02
8.0E+01	2.16E+03	2.18E+03	2.12E+03	1.95E+03	1.72E+03	1.32E+03	7.99E+02	5.60E+02	1.09E+03	8.37E+02	8.71E+02	8.03E+02
1.0E+02	2.51E+03	2.50E+03	2.37E+03	2.21E+03	1.97E+03	1.58E+03	9.94E+02	1.19E+03	1.44E+03	1.13E+03	1.18E+03	1.08E+03
1.5E+02	2.38E+03	2.40E+03	2.41E+03	2.46E+03	2.31E+03	2.11E+03	1.64E+03	2.82E+03	2.16E+03	1.79E+03	1.85E+03	1.73E+03
2.0E+02	1.77E+03	1.79E+03	1.81E+03	1.84E+03	1.93E+03	2.03E+03	2.18E+03	1.93E+03	1.96E+03	1.84E+03	1.90E+03	1.78E+03
3.0E+02	1.38E+03	1.40E+03	1.40E+03	1.41E+03	1.43E+03	1.44E+03	1.45E+03	1.45E+03	1.44E+03	1.42E+03	1.45E+03	1.39E+03
4.0E+02	1.23E+03	1.25E+03	1.25E+03	1.26E+03	1.28E+03	1.28E+03	1.28E+03	1.30E+03	1.28E+03	1.25E+03	1.28E+03	1.22E+03
5.0E+02	1.15E+03	1.19E+03	1.19E+03	1.21E+03	1.22E+03	1.22E+03	1.21E+03	1.24E+03	1.22E+03	1.18E+03	1.21E+03	1.15E+03
6.0E+02	1.16E+03	1.16E+03	1.18E+03	1.18E+03	1.20E+03	1.20E+03	1.20E+03	1.23E+03	1.22E+03	1.17E+03	1.21E+03	1.13E+03
8.0E+02	1.11E+03	1.13E+03	1.14E+03	1.15E+03	1.18E+03	1.18E+03	1.20E+03	1.23E+03	1.20E+03	1.17E+03	1.18E+03	1.16E+03
1.0E+03	1.09E+03	1.11E+03	1.12E+03	1.14E+03	1.15E+03	1.16E+03	1.20E+03	1.23E+03	1.19E+03	1.15E+03	1.18E+03	1.12E+03

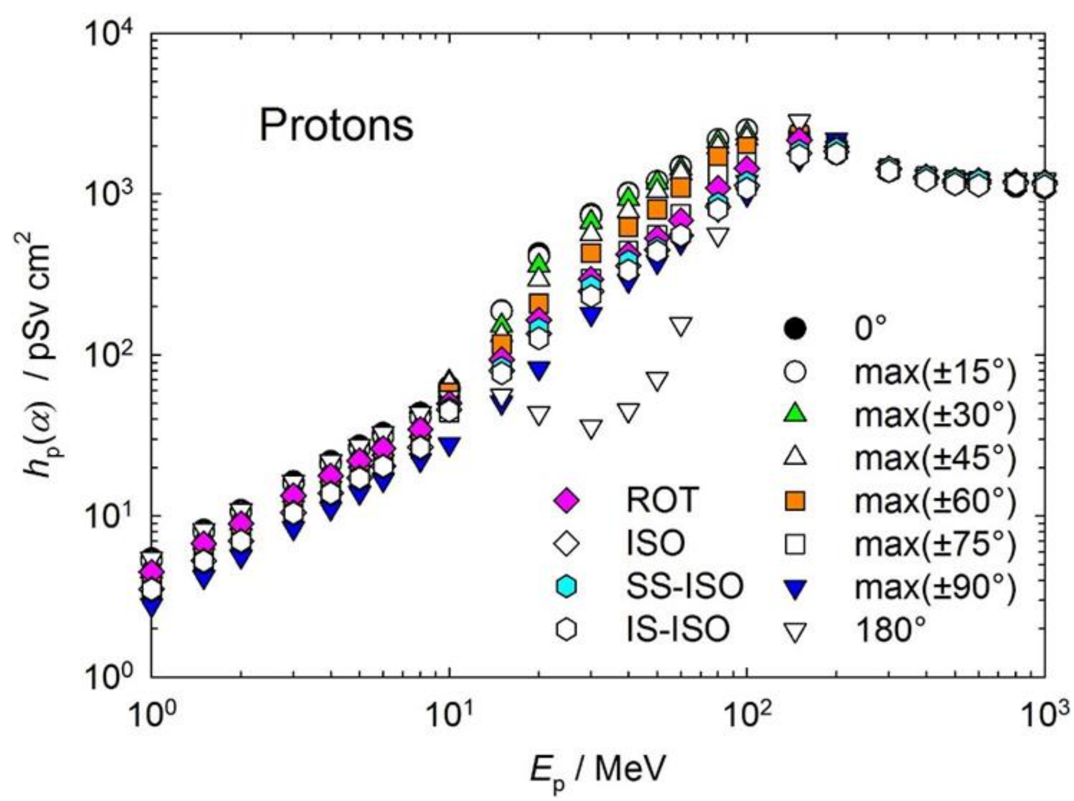

Figure A.2.5 Conversion coefficients from proton fluence to personal dose (ICRP, 2010; Endo, 2017).

Table A.2.6 Conversion coefficients from negative muon fluence to personal dose (ICRP, 2010; Endo, 2017).

E_p / MeV	$h_p(\alpha)$ / (pSv cm^2)											
	0°	max(±15°)	max(±30°)	max(±45°)	max(±60°)	max(±75°)	max(±90°)	180°	ROT	ISO	SS-ISO	IS-ISO
1.0E+00	1.80E+02	1.80E+02	1.65E+02	1.45E+02	1.18E+02	8.86E+01	5.72E+01	7.52E+01	9.75E+01	7.87E+01	8.18E+01	7.56E+01
1.5E+00	1.80E+02	1.82E+02	1.68E+02	1.45E+02	1.19E+02	8.89E+01	5.82E+01	7.68E+01	9.93E+01	7.95E+01	8.28E+01	7.62E+01
2.0E+00	1.84E+02	1.84E+02	1.72E+02	1.48E+02	1.21E+02	9.16E+01	5.86E+01	7.83E+01	1.00E+02	8.09E+01	8.39E+01	7.79E+01
3.0E+00	1.88E+02	1.89E+02	1.75E+02	1.53E+02	1.25E+02	9.38E+01	6.11E+01	8.14E+01	1.04E+02	8.37E+01	8.70E+01	8.04E+01
4.0E+00	1.93E+02	1.95E+02	1.81E+02	1.59E+02	1.29E+02	9.78E+01	6.30E+01	8.48E+01	1.07E+02	8.71E+01	9.06E+01	8.36E+01
5.0E+00	2.05E+02	2.06E+02	1.89E+02	1.69E+02	1.38E+02	1.03E+02	6.59E+01	8.77E+01	1.12E+02	9.15E+01	9.51E+01	8.79E+01
6.0E+00	2.42E+02	2.37E+02	2.12E+02	1.81E+02	1.47E+02	1.10E+02	7.09E+01	8.67E+01	1.22E+02	9.81E+01	1.03E+02	9.32E+01
8.0E+00	2.93E+02	2.83E+02	2.59E+02	2.20E+02	1.73E+02	1.27E+02	7.93E+01	8.68E+01	1.41E+02	1.13E+02	1.18E+02	1.08E+02
1.0E+01	3.32E+02	3.23E+02	2.97E+02	2.52E+02	2.01E+02	1.46E+02	9.33E+01	8.86E+01	1.58E+02	1.27E+02	1.33E+02	1.21E+02
1.5E+01	4.14E+02	4.07E+02	3.76E+02	3.26E+02	2.64E+02	1.92E+02	1.27E+02	1.00E+02	2.00E+02	1.61E+02	1.68E+02	1.54E+02
2.0E+01	4.65E+02	4.68E+02	4.46E+02	4.07E+02	3.29E+02	2.35E+02	1.57E+02	1.22E+02	2.41E+02	1.91E+02	1.97E+02	1.85E+02
3.0E+01	6.57E+02	6.63E+02	6.40E+02	5.92E+02	5.19E+02	3.91E+02	2.51E+02	2.51E+02	3.57E+02	2.75E+02	2.83E+02	2.67E+02
4.0E+01	7.35E+02	7.32E+02	6.96E+02	6.49E+02	5.83E+02	4.71E+02	3.15E+02	4.57E+02	4.62E+02	3.63E+02	3.77E+02	3.49E+02
5.0E+01	7.55E+02	7.63E+02	7.11E+02	6.61E+02	5.99E+02	5.23E+02	3.69E+02	7.03E+02	5.56E+02	4.46E+02	4.64E+02	4.28E+02
6.0E+01	6.28E+02	6.41E+02	6.64E+02	6.73E+02	6.15E+02	5.87E+02	4.56E+02	7.75E+02	5.98E+02	4.96E+02	5.15E+02	4.77E+02
8.0E+01	4.31E+02	4.37E+02	4.50E+02	4.80E+02	5.33E+02	6.02E+02	6.30E+02	4.85E+02	5.29E+02	4.98E+02	5.05E+02	4.91E+02
1.0E+02	3.82E+02	3.90E+02	3.91E+02	3.99E+02	4.08E+02	4.30E+02	4.84E+02	4.02E+02	4.27E+02	4.32E+02	4.35E+02	4.29E+02
1.5E+02	3.40E+02	3.50E+02	3.48E+02	3.53E+02	3.51E+02	3.51E+02	3.64E+02	3.45E+02	3.52E+02	3.54E+02	3.53E+02	3.55E+02
2.0E+02	3.26E+02	3.39E+02	3.38E+02	3.43E+02	3.43E+02	3.42E+02	3.48E+02	3.29E+02	3.39E+02	3.32E+02	3.31E+02	3.33E+02
3.0E+02	3.19E+02	3.36E+02	3.35E+02	3.40E+02	3.38E+02	3.37E+02	3.41E+02	3.21E+02	3.33E+02	3.21E+02	3.20E+02	3.22E+02
4.0E+02	3.20E+02	3.39E+02	3.37E+02	3.42E+02	3.41E+02	3.40E+02	3.44E+02	3.21E+02	3.36E+02	3.21E+02	3.20E+02	3.22E+02
5.0E+02	3.21E+02	3.43E+02	3.41E+02	3.46E+02	3.46E+02	3.44E+02	3.49E+02	3.24E+02	3.41E+02	3.23E+02	3.22E+02	3.24E+02
6.0E+02	3.25E+02	3.46E+02	3.44E+02	3.49E+02	3.48E+02	3.46E+02	3.51E+02	3.26E+02	3.43E+02	3.26E+02	3.24E+02	3.28E+02
8.0E+02	3.27E+02	3.49E+02	3.47E+02	3.52E+02	3.51E+02	3.50E+02	3.55E+02	3.32E+02	3.47E+02	3.31E+02	3.29E+02	3.33E+02
1.0E+03	3.33E+02	3.53E+02	3.52E+02	3.57E+02	3.56E+02	3.54E+02	3.59E+02	3.37E+02	3.51E+02	3.37E+02	3.32E+02	3.42E+02

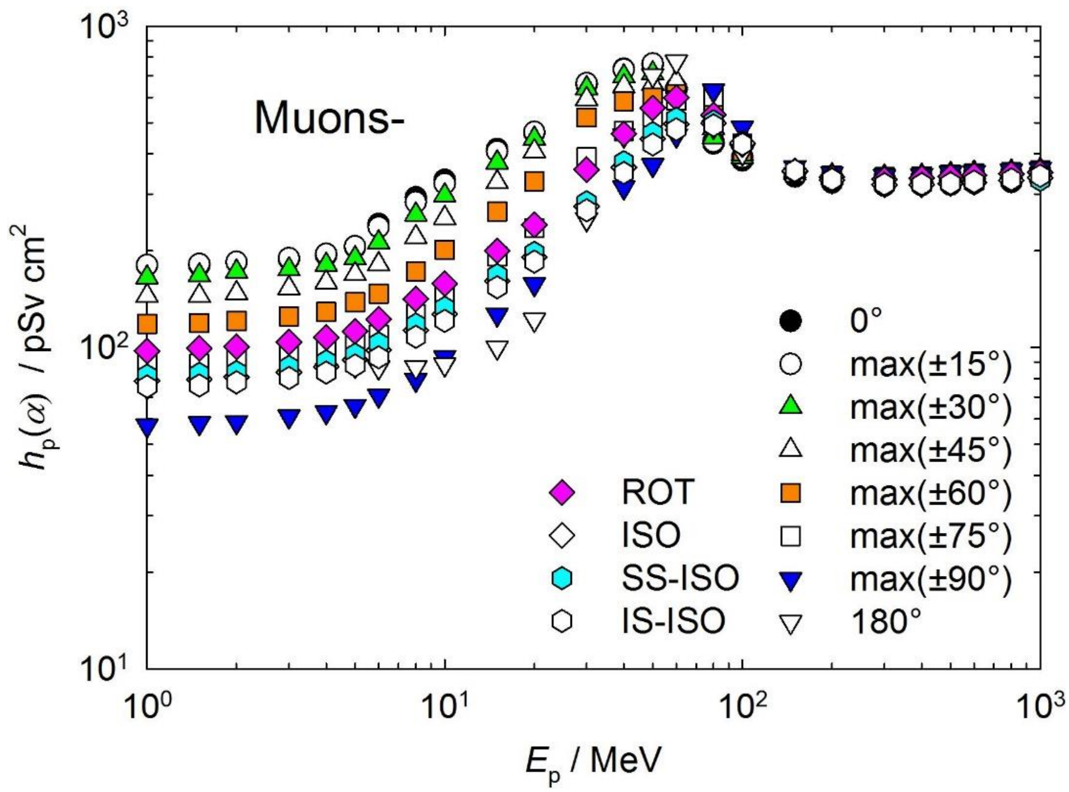

Figure A.2.6 Conversion coefficients from negative muon fluence to personal dose (ICRP, 2010; Endo, 2017)

Table A.2.7 Conversion coefficients from positive muon fluence to personal dose (ICRP, 2010; Endo, 2017).

E_p / MeV	$h_p(\alpha)$ / (pSv cm^2)											
	0°	max(±15°)	max(±30°)	max(±45°)	max(±60°)	max(±75°)	max(±90°)	180°	ROT	ISO	SS-ISO	IS-ISO
1.0E+00	1.94E+02	1.81E+02	1.68E+02	1.46E+02	1.20E+02	9.01E+01	5.91E+01	8.26E+01	1.00E+02	8.52E+01	8.89E+01	8.15E+01
1.5E+00	1.96E+02	1.84E+02	1.70E+02	1.48E+02	1.21E+02	9.01E+01	5.99E+01	8.41E+01	1.01E+02	8.62E+01	9.00E+01	8.24E+01
2.0E+00	1.98E+02	1.85E+02	1.72E+02	1.49E+02	1.23E+02	9.18E+01	6.05E+01	8.57E+01	1.02E+02	8.75E+01	9.12E+01	8.38E+01
3.0E+00	2.02E+02	1.91E+02	1.78E+02	1.54E+02	1.28E+02	9.39E+01	6.24E+01	8.89E+01	1.05E+02	9.03E+01	9.40E+01	8.66E+01
4.0E+00	2.07E+02	1.96E+02	1.84E+02	1.60E+02	1.31E+02	9.82E+01	6.43E+01	9.21E+01	1.09E+02	9.36E+01	9.74E+01	8.98E+01
5.0E+00	2.16E+02	2.07E+02	1.92E+02	1.70E+02	1.39E+02	1.04E+02	6.67E+01	9.43E+01	1.14E+02	9.77E+01	1.02E+02	9.34E+01
6.0E+00	2.51E+02	2.37E+02	2.13E+02	1.80E+02	1.48E+02	1.10E+02	7.03E+01	9.25E+01	1.22E+02	1.03E+02	1.08E+02	9.80E+01
8.0E+00	3.00E+02	2.85E+02	2.57E+02	2.19E+02	1.73E+02	1.27E+02	8.04E+01	9.28E+01	1.40E+02	1.17E+02	1.23E+02	1.11E+02
1.0E+01	3.40E+02	3.24E+02	2.95E+02	2.53E+02	2.01E+02	1.45E+02	9.38E+01	9.48E+01	1.58E+02	1.32E+02	1.38E+02	1.26E+02
1.5E+01	4.25E+02	4.08E+02	3.76E+02	3.26E+02	2.67E+02	1.96E+02	1.27E+02	1.08E+02	2.02E+02	1.67E+02	1.74E+02	1.60E+02
2.0E+01	4.81E+02	4.72E+02	4.48E+02	4.10E+02	3.33E+02	2.36E+02	1.60E+02	1.33E+02	2.43E+02	1.99E+02	2.05E+02	1.93E+02
3.0E+01	6.74E+02	6.70E+02	6.46E+02	5.96E+02	5.25E+02	3.94E+02	2.53E+02	2.65E+02	3.61E+02	2.84E+02	2.93E+02	2.75E+02
4.0E+01	7.51E+02	7.37E+02	7.01E+02	6.53E+02	5.88E+02	4.73E+02	3.18E+02	4.73E+02	4.67E+02	3.73E+02	3.89E+02	3.57E+02
5.0E+01	7.68E+02	7.68E+02	7.17E+02	6.65E+02	6.01E+02	5.23E+02	3.71E+02	7.21E+02	5.59E+02	4.56E+02	4.76E+02	4.36E+02
6.0E+01	6.35E+02	6.44E+02	6.66E+02	6.75E+02	6.19E+02	5.90E+02	4.59E+02	7.87E+02	5.99E+02	5.06E+02	5.25E+02	4.87E+02
8.0E+01	4.31E+02	4.37E+02	4.50E+02	4.80E+02	5.34E+02	6.05E+02	6.30E+02	4.83E+02	5.29E+02	5.02E+02	5.10E+02	4.94E+02
1.0E+02	3.81E+02	3.90E+02	3.91E+02	3.99E+02	4.08E+02	4.30E+02	4.83E+02	3.99E+02	4.27E+02	4.32E+02	4.37E+02	4.27E+02
1.5E+02	3.39E+02	3.50E+02	3.48E+02	3.53E+02	3.51E+02	3.51E+02	3.64E+02	3.45E+02	3.52E+02	3.54E+02	3.54E+02	3.54E+02
2.0E+02	3.26E+02	3.39E+02	3.38E+02	3.43E+02	3.42E+02	3.42E+02	3.48E+02	3.28E+02	3.39E+02	3.32E+02	3.31E+02	3.33E+02
3.0E+02	3.18E+02	3.36E+02	3.35E+02	3.39E+02	3.38E+02	3.37E+02	3.41E+02	3.20E+02	3.33E+02	3.20E+02	3.20E+02	3.20E+02
4.0E+02	3.19E+02	3.39E+02	3.37E+02	3.42E+02	3.41E+02	3.40E+02	3.44E+02	3.21E+02	3.36E+02	3.20E+02	3.20E+02	3.20E+02
5.0E+02	3.20E+02	3.43E+02	3.41E+02	3.46E+02	3.46E+02	3.44E+02	3.49E+02	3.23E+02	3.41E+02	3.22E+02	3.22E+02	3.22E+02
6.0E+02	3.22E+02	3.46E+02	3.44E+02	3.49E+02	3.48E+02	3.46E+02	3.51E+02	3.25E+02	3.43E+02	3.24E+02	3.24E+02	3.24E+02
8.0E+02	3.25E+02	3.49E+02	3.47E+02	3.52E+02	3.51E+02	3.50E+02	3.55E+02	3.30E+02	3.46E+02	3.29E+02	3.29E+02	3.29E+02
1.0E+03	3.27E+02	3.53E+02	3.52E+02	3.57E+02	3.56E+02	3.54E+02	3.59E+02	3.33E+02	3.51E+02	3.33E+02	3.32E+02	3.34E+02

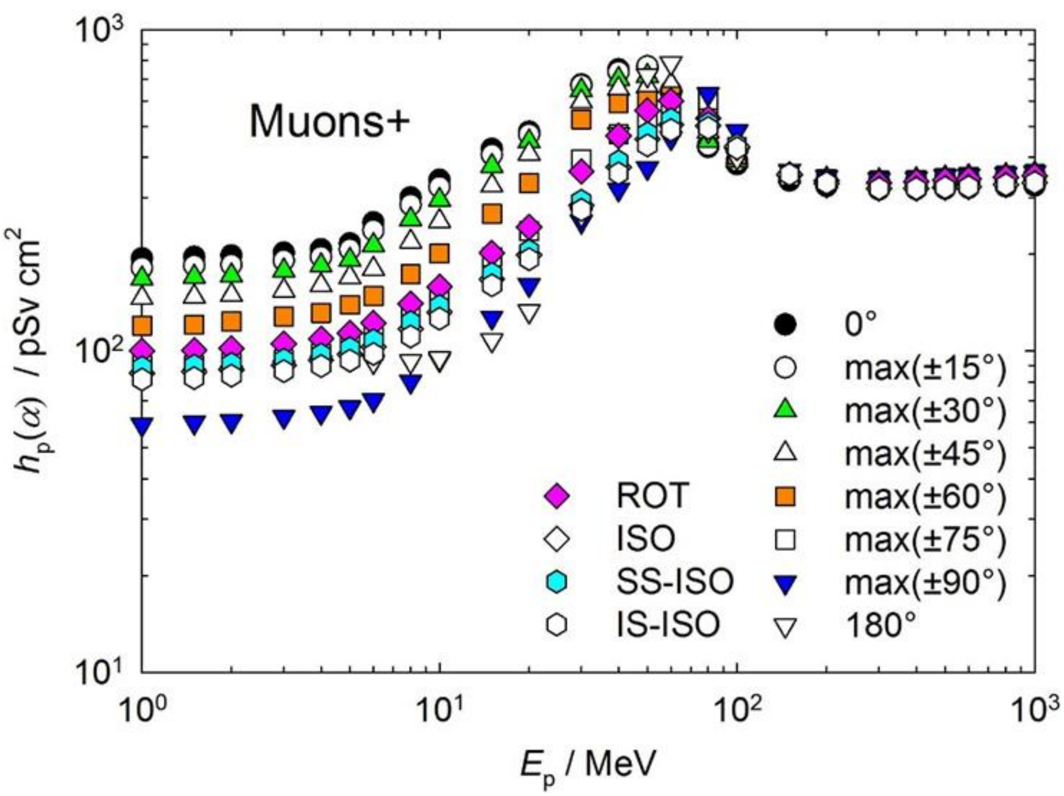

Figure A.2.7 Conversion coefficients from positive muon fluence to personal dose (ICRP, 2010; Endo, 2017).

Table A.2.8 Conversion coefficients from negative pion fluence to personal dose (ICRP, 2010; Endo, 2017).

E_p / MeV	$h_p(\alpha)$ / (pSv cm^2)											
	0°	max(±15°)	max(±30°)	max(±45°)	max(±60°)	max(±75°)	max(±90°)	180°	ROT	ISO	SS-ISO	IS-ISO
1.0E+00	4.06E+02	4.03E+02	3.75E+02	3.33E+02	2.88E+02	2.29E+02	1.76E+02	1.94E+02	2.45E+02	1.76E+02	1.91E+02	1.61E+02
1.5E+00	4.22E+02	4.24E+02	3.94E+02	3.46E+02	2.98E+02	2.36E+02	1.77E+02	2.01E+02	2.53E+02	1.89E+02	2.06E+02	1.72E+02
2.0E+00	4.33E+02	4.41E+02	4.11E+02	3.61E+02	3.09E+02	2.42E+02	1.79E+02	2.10E+02	2.61E+02	1.98E+02	2.17E+02	1.79E+02
3.0E+00	4.58E+02	4.73E+02	4.46E+02	3.93E+02	3.34E+02	2.58E+02	1.85E+02	2.25E+02	2.80E+02	2.15E+02	2.37E+02	1.93E+02
4.0E+00	4.91E+02	5.15E+02	4.85E+02	4.30E+02	3.64E+02	2.77E+02	1.93E+02	2.33E+02	3.00E+02	2.32E+02	2.55E+02	2.09E+02
5.0E+00	5.28E+02	5.67E+02	5.44E+02	4.82E+02	4.02E+02	3.01E+02	2.00E+02	2.37E+02	3.27E+02	2.51E+02	2.70E+02	2.32E+02
6.0E+00	6.73E+02	6.92E+02	6.29E+02	5.36E+02	4.45E+02	3.29E+02	2.12E+02	2.08E+02	3.59E+02	2.71E+02	3.02E+02	2.40E+02
8.0E+00	9.65E+02	9.84E+02	8.91E+02	7.28E+02	5.35E+02	4.03E+02	2.48E+02	1.81E+02	4.37E+02	3.17E+02	3.52E+02	2.82E+02
1.0E+01	1.09E+03	1.09E+03	1.00E+03	8.23E+02	6.54E+02	4.67E+02	2.89E+02	1.78E+02	4.88E+02	3.61E+02	3.96E+02	3.26E+02
1.5E+01	1.25E+03	1.25E+03	1.16E+03	9.87E+02	8.23E+02	6.03E+02	3.80E+02	1.97E+02	5.81E+02	4.39E+02	4.70E+02	4.08E+02
2.0E+01	1.28E+03	1.35E+03	1.32E+03	1.19E+03	9.40E+02	6.58E+02	4.71E+02	2.44E+02	6.62E+02	5.08E+02	5.31E+02	4.85E+02
3.0E+01	1.77E+03	1.87E+03	1.84E+03	1.69E+03	1.48E+03	1.03E+03	6.54E+02	5.47E+02	9.51E+02	6.76E+02	6.98E+02	6.54E+02
4.0E+01	1.92E+03	1.92E+03	1.85E+03	1.72E+03	1.53E+03	1.24E+03	8.17E+02	1.02E+03	1.18E+03	8.68E+02	9.01E+02	8.35E+02
5.0E+01	1.93E+03	1.93E+03	1.79E+03	1.63E+03	1.50E+03	1.32E+03	8.96E+02	1.70E+03	1.36E+03	1.02E+03	1.07E+03	9.70E+02
6.0E+01	1.68E+03	1.73E+03	1.81E+03	1.63E+03	1.50E+03	1.37E+03	1.01E+03	1.99E+03	1.47E+03	1.15E+03	1.21E+03	1.09E+03
8.0E+01	1.14E+03	1.18E+03	1.21E+03	1.27E+03	1.44E+03	1.47E+03	1.45E+03	1.31E+03	1.36E+03	1.15E+03	1.19E+03	1.11E+03
1.0E+02	9.95E+02	1.04E+03	1.04E+03	1.03E+03	1.05E+03	1.09E+03	1.22E+03	9.91E+02	1.08E+03	1.03E+03	1.03E+03	1.03E+03
1.5E+02	9.27E+02	9.52E+02	9.50E+02	9.48E+02	9.31E+02	9.13E+02	8.81E+02	8.89E+02	9.22E+02	8.57E+02	8.45E+02	8.69E+02
2.0E+02	9.02E+02	9.01E+02	9.04E+02	9.03E+02	8.89E+02	8.72E+02	8.43E+02	8.71E+02	8.71E+02	8.15E+02	8.28E+02	8.02E+02
3.0E+02	8.48E+02	8.66E+02	8.72E+02	8.76E+02	8.65E+02	8.61E+02	8.27E+02	8.43E+02	8.57E+02	7.94E+02	8.06E+02	7.82E+02
4.0E+02	8.44E+02	8.64E+02	8.63E+02	8.70E+02	8.54E+02	8.50E+02	8.33E+02	8.50E+02	8.43E+02	8.07E+02	8.02E+02	8.12E+02
5.0E+02	8.69E+02	8.90E+02	8.88E+02	8.87E+02	8.73E+02	8.71E+02	8.48E+02	8.80E+02	8.63E+02	8.38E+02	8.37E+02	8.39E+02
6.0E+02	9.01E+02	8.96E+02	8.84E+02	8.99E+02	8.94E+02	8.81E+02	8.68E+02	9.17E+02	8.83E+02	8.75E+02	8.90E+02	8.60E+02
8.0E+02	9.47E+02	9.33E+02	9.27E+02	9.42E+02	9.31E+02	9.36E+02	9.01E+02	9.76E+02	9.18E+02	9.35E+02	9.37E+02	9.33E+02
1.0E+03	9.77E+02	9.47E+02	9.40E+02	9.58E+02	9.53E+02	9.42E+02	9.22E+02	1.02E+03	9.38E+02	9.79E+02	9.78E+02	9.80E+02

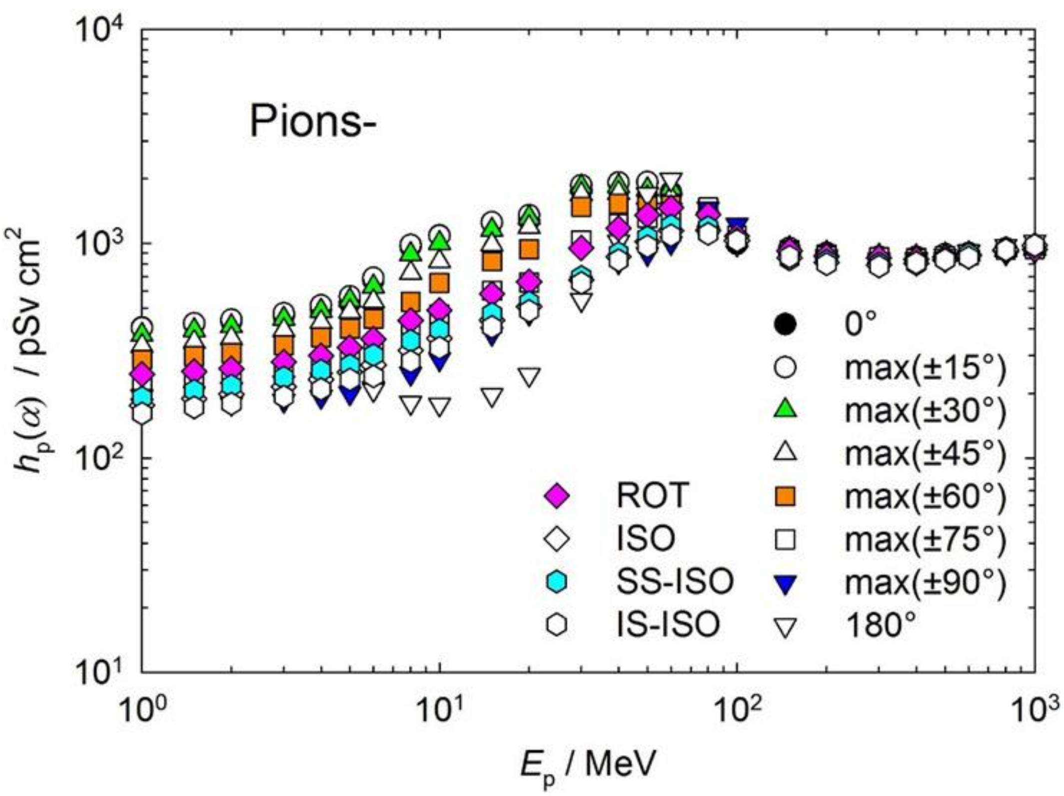

Figure A.2.8 Conversion coefficients from negative pion fluence to personal dose (ICRP, 2010; Endo, 2017).

Table A.2.9 Conversion coefficients from positive pion fluence to personal dose (ICRP, 2010; Endo, 2017).

E_p / MeV	$h_p(\alpha)$ / (pSv cm^2)											
	0°	max(±15°)	max(±30°)	max(±45°)	max(±60°)	max(±75°)	max(±90°)	180°	ROT	ISO	SS-ISO	IS-ISO
1.0E+00	3.14E+02	2.78E+02	2.57E+02	2.28E+02	1.98E+02	1.59E+02	1.21E+02	1.21E+02	1.65E+02	1.51E+02	1.70E+02	1.32E+02
1.5E+00	3.24E+02	2.90E+02	2.69E+02	2.36E+02	2.04E+02	1.63E+02	1.21E+02	1.25E+02	1.71E+02	1.60E+02	1.82E+02	1.38E+02
2.0E+00	3.40E+02	3.04E+02	2.81E+02	2.48E+02	2.12E+02	1.66E+02	1.22E+02	1.33E+02	1.76E+02	1.68E+02	1.84E+02	1.52E+02
3.0E+00	3.79E+02	3.36E+02	3.10E+02	2.73E+02	2.31E+02	1.80E+02	1.29E+02	1.51E+02	1.91E+02	1.83E+02	2.02E+02	1.64E+02
4.0E+00	4.29E+02	3.80E+02	3.52E+02	3.08E+02	2.57E+02	1.98E+02	1.38E+02	1.70E+02	2.16E+02	1.98E+02	2.20E+02	1.76E+02
5.0E+00	4.89E+02	4.38E+02	4.08E+02	3.54E+02	2.92E+02	2.22E+02	1.53E+02	1.83E+02	2.45E+02	2.16E+02	2.39E+02	1.93E+02
6.0E+00	5.40E+02	4.94E+02	4.53E+02	4.01E+02	3.25E+02	2.40E+02	1.58E+02	1.85E+02	2.64E+02	2.33E+02	2.57E+02	2.09E+02
8.0E+00	7.17E+02	6.51E+02	5.90E+02	4.90E+02	3.84E+02	2.83E+02	1.82E+02	1.77E+02	3.11E+02	2.65E+02	2.93E+02	2.37E+02
1.0E+01	8.19E+02	7.44E+02	6.75E+02	5.68E+02	4.55E+02	3.30E+02	2.12E+02	1.79E+02	3.52E+02	2.96E+02	3.28E+02	2.64E+02
1.5E+01	1.00E+03	9.15E+02	8.40E+02	7.26E+02	5.94E+02	4.31E+02	2.80E+02	2.01E+02	4.38E+02	3.67E+02	3.93E+02	3.41E+02
2.0E+01	1.10E+03	1.04E+03	9.95E+02	8.82E+02	7.06E+02	5.05E+02	3.50E+02	2.47E+02	5.17E+02	4.39E+02	4.66E+02	4.12E+02
3.0E+01	1.52E+03	1.47E+03	1.42E+03	1.30E+03	1.12E+03	7.90E+02	5.14E+02	4.94E+02	7.49E+02	6.02E+02	6.21E+02	5.83E+02
4.0E+01	1.75E+03	1.65E+03	1.58E+03	1.46E+03	1.30E+03	1.03E+03	6.84E+02	9.06E+02	9.77E+02	7.87E+02	8.20E+02	7.54E+02
5.0E+01	1.83E+03	1.71E+03	1.61E+03	1.48E+03	1.35E+03	1.15E+03	7.84E+02	1.48E+03	1.17E+03	9.53E+02	9.93E+02	9.13E+02
6.0E+01	1.66E+03	1.63E+03	1.65E+03	1.50E+03	1.38E+03	1.23E+03	8.99E+02	1.82E+03	1.30E+03	1.09E+03	1.15E+03	1.03E+03
8.0E+01	1.22E+03	1.21E+03	1.24E+03	1.29E+03	1.38E+03	1.37E+03	1.32E+03	1.38E+03	1.30E+03	1.16E+03	1.21E+03	1.11E+03
1.0E+02	1.13E+03	1.11E+03	1.11E+03	1.11E+03	1.11E+03	1.14E+03	1.21E+03	1.12E+03	1.12E+03	1.10E+03	1.10E+03	1.10E+03
1.5E+02	1.22E+03	1.19E+03	1.18E+03	1.17E+03	1.13E+03	1.08E+03	1.02E+03	1.15E+03	1.09E+03	1.05E+03	1.04E+03	1.06E+03
2.0E+02	1.25E+03	1.23E+03	1.23E+03	1.23E+03	1.20E+03	1.17E+03	1.10E+03	1.23E+03	1.18E+03	1.08E+03	1.12E+03	1.04E+03
3.0E+02	1.07E+03	1.08E+03	1.09E+03	1.10E+03	1.10E+03	1.10E+03	1.07E+03	1.10E+03	1.09E+03	1.02E+03	1.04E+03	1.00E+03
4.0E+02	9.69E+02	9.93E+02	9.99E+02	1.01E+03	1.01E+03	1.01E+03	9.92E+02	9.98E+02	1.00E+03	9.53E+02	9.36E+02	9.70E+02
5.0E+02	9.43E+02	9.75E+02	9.75E+02	9.87E+02	9.74E+02	9.73E+02	9.56E+02	9.70E+02	9.75E+02	9.30E+02	9.19E+02	9.41E+02
6.0E+02	9.52E+02	9.64E+02	9.63E+02	9.71E+02	9.66E+02	9.66E+02	9.56E+02	9.80E+02	9.62E+02	9.38E+02	9.44E+02	9.32E+02
8.0E+02	9.99E+02	1.01E+03	1.01E+03	1.03E+03	1.02E+03	1.02E+03	1.00E+03	1.04E+03	1.00E+03	9.93E+02	9.97E+02	9.89E+02
1.0E+03	1.04E+03	1.03E+03	1.03E+03	1.04E+03	1.04E+03	1.03E+03	1.02E+03	1.09E+03	1.03E+03	1.05E+03	1.05E+03	1.05E+03

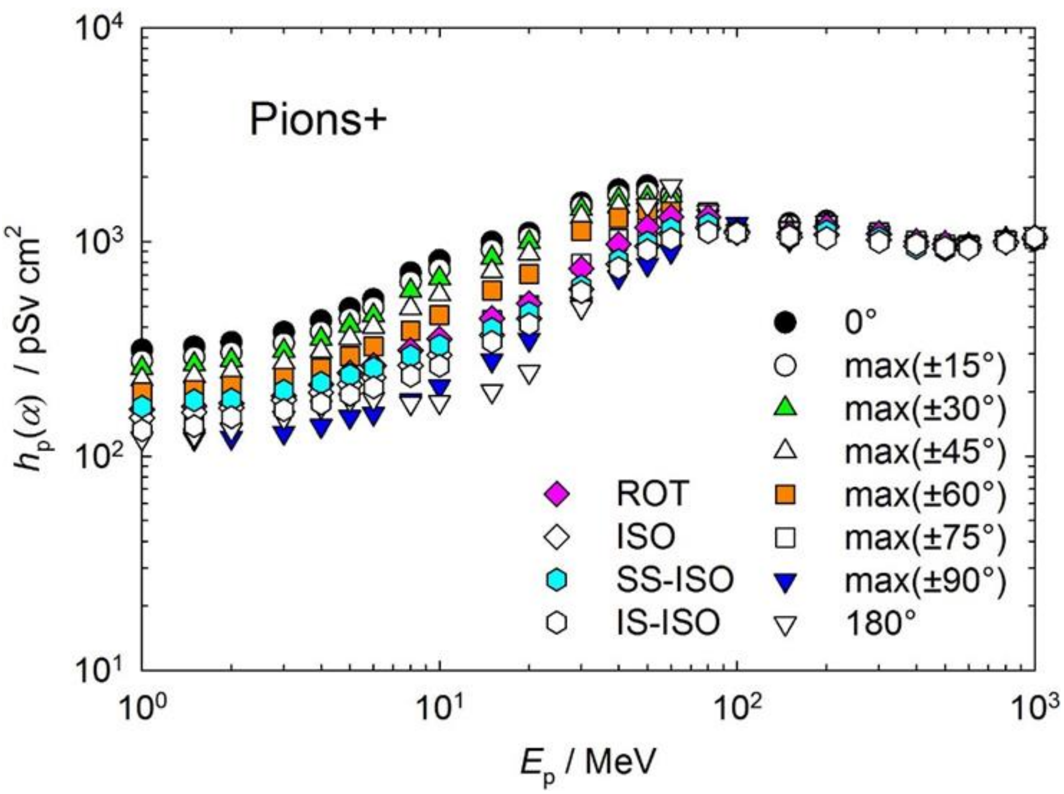

Figure A.2.9 Conversion coefficients from positive pion fluence to personal dose (ICRP, 2010; Endo, 2017).

Table A.2.10 Conversion coefficients from helium ion fluence to personal dose (ICRP, 2010; Endo, 2017).

E_p / MeV u^{-1}	$h_p(\alpha)$ / (pSv cm^2)											
	0°	max(±15°)	max(±30°)	max(±45°)	max(±60°)	max(±75°)	max(±90°)	180°	ROT	ISO	SS-ISO	IS-ISO
1.0E+00	2.19E+02	2.12E+02	2.00E+02	1.81E+02	1.63E+02	1.38E+02	1.10E+02	2.19E+02	1.76E+02	1.41E+02	1.38E+02	1.40E+02
2.0E+00	4.38E+02	4.23E+02	3.99E+02	3.61E+02	3.24E+02	2.75E+02	2.20E+02	4.38E+02	3.52E+02	2.81E+02	2.75E+02	2.80E+02
3.0E+00	6.56E+02	6.33E+02	5.95E+02	5.38E+02	4.83E+02	4.10E+02	3.30E+02	6.57E+02	5.26E+02	4.19E+02	4.10E+02	4.18E+02
5.0E+00	1.09E+03	1.04E+03	9.76E+02	8.79E+02	7.90E+02	6.76E+02	5.50E+02	1.09E+03	8.66E+02	6.89E+02	6.74E+02	6.87E+02
1.0E+01	2.19E+03	2.55E+03	2.73E+03	2.65E+03	2.34E+03	1.76E+03	1.10E+03	2.19E+03	1.97E+03	1.82E+03	1.86E+03	1.73E+03
1.4E+01	4.61E+03	5.04E+03	4.84E+03	4.67E+03	4.12E+03	2.94E+03	1.62E+03	2.56E+03	3.09E+03	2.81E+03	2.95E+03	2.64E+03
2.0E+01	1.72E+04	1.62E+04	1.43E+04	1.17E+04	8.33E+03	5.88E+03	3.27E+03	1.74E+03	6.56E+03	5.46E+03	5.73E+03	5.02E+03
3.0E+01	3.01E+04	2.91E+04	2.68E+04	2.24E+04	1.71E+04	1.19E+04	7.07E+03	1.44E+03	1.18E+04	9.86E+03	1.04E+04	9.15E+03
5.0E+01	4.75E+04	4.79E+04	4.68E+04	4.14E+04	3.21E+04	2.21E+04	1.51E+04	2.88E+03	2.15E+04	1.78E+04	1.86E+04	1.71E+04
7.5E+01	8.05E+04	8.04E+04	7.85E+04	7.34E+04	6.46E+04	4.68E+04	2.81E+04	1.75E+04	3.94E+04	3.00E+04	3.11E+04	2.91E+04
1.0E+02	1.01E+05	9.74E+04	9.26E+04	8.61E+04	7.70E+04	6.14E+04	3.88E+04	4.84E+04	5.64E+04	4.55E+04	4.62E+04	4.23E+04
1.5E+02	9.25E+04	9.17E+04	9.18E+04	9.32E+04	8.83E+04	8.04E+04	6.31E+04	1.10E+05	8.26E+04	6.95E+04	7.21E+04	6.61E+04
2.0E+02	6.74E+04	6.81E+04	6.86E+04	7.03E+04	7.32E+04	7.59E+04	8.26E+04	7.29E+04	7.36E+04	7.01E+04	7.20E+04	6.90E+04
3.0E+02	5.14E+04	5.16E+04	5.15E+04	5.21E+04	5.26E+04	5.23E+04	5.31E+04	5.33E+04	5.22E+04	5.25E+04	5.33E+04	5.22E+04
5.0E+02	4.27E+04	4.23E+04	4.23E+04	4.26E+04	4.29E+04	4.25E+04	4.25E+04	4.49E+04	4.23E+04	4.27E+04	4.27E+04	4.20E+04
7.0E+02	4.11E+04	4.00E+04	3.98E+04	4.04E+04	4.08E+04	4.07E+04	4.04E+04	4.60E+04	4.03E+04	4.19E+04	4.04E+04	4.03E+04
1.0E+03	4.00E+04	3.87E+04	3.84E+04	3.92E+04	3.96E+04	3.97E+04	3.91E+04	4.47E+04	3.92E+04	4.09E+04	3.89E+04	3.94E+04

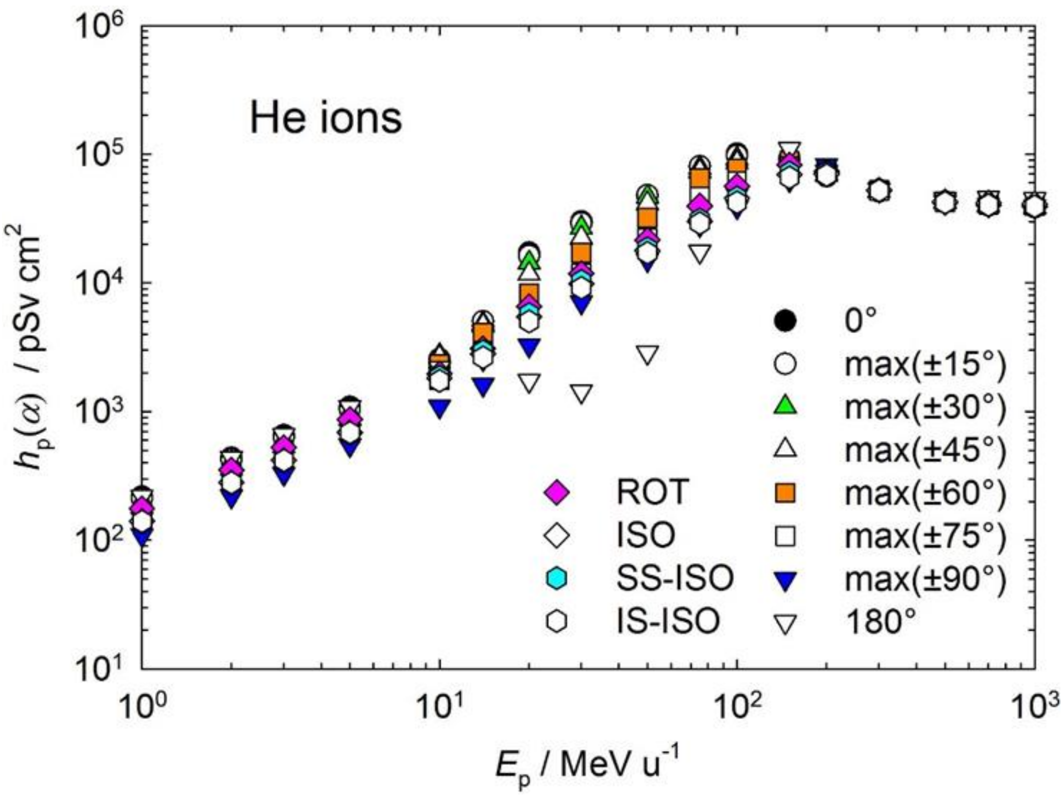

Figure A.2.10 Conversion coefficients from helium ion fluence to personal dose (ICRP, 2010; Endo, 2017).

A.3 Directional and Personal Absorbed Dose to the Lens of the Eye

The numerical values of conversion coefficients from particle fluence to directional absorbed dose in the lens of the eye d'_{lens} and from fluence to personal absorbed dose in the lens of the eye d_{plens} are the same and the symbol d_{lens}, is used in the following Tables. The conversion coefficients given here are to the value of the absorbed dose in the lens of the eye calculated for whole-body exposure of the stylized eye model (Behrens and Dietze, 2011) for broad parallel beams incident for angles, α, from 0° (A-P) to 90° in 15° steps. The maximum value of absorbed dose is taken for right or left irradiations; and for a rotational field.

Tables A.3.1a to A.3.4 and Figures A.3.1a to A.3.4 give the numerical values of the conversion coefficients for energies up to 50 MeV from particle fluence for photons, neutrons, electrons, and positrons; and Table A.3.1b and Figure A.3.1b for photons from air kerma.

Table A.3.1a Conversion coefficients from photon fluence to the maximum absorbed dose in the complete lens for left or right irradiations (Behrens, 2017a).

	$d_{\mathrm{lens}}(\alpha)$/ (pGy cm^2) for a radiation incidence at α							
E_{p} / MeV	0°	15°	30°	45°	60°	75°	90°	ROT
0.005	8.61E-06	1.63E-05	3.47E-05	3.29E-05	1.35E-05	1.66E-06	6.90E-08	8.85E-06
0.006	2.00E-03	2.44E-03	2.97E-03	2.85E-03	1.48E-03	4.08E-04	4.26E-05	8.75E-04
0.007	3.74E-02	3.56E-02	3.67E-02	3.38E-02	2.02E-02	7.75E-03	1.75E-03	1.24E-02
0.008	1.85E-01	1.72E-01	1.63E-01	1.50E-01	9.81E-02	4.70E-02	1.47E-02	5.81E-02
0.009	4.75E-01	4.41E-01	4.13E-01	3.77E-01	2.66E-01	1.50E-01	5.89E-02	1.50E-01
0.01	8.33E-01	7.78E-01	7.30E-01	6.72E-01	5.07E-01	3.20E-01	1.52E-01	2.74E-01
0.011	1.15E+00	1.10E+00	1.04E+00	9.66E-01	7.72E-01	5.35E-01	2.89E-01	3.98E-01
0.013	1.54E+00	1.52E+00	1.46E+00	1.35E+00	1.19E+00	9.32E-01	5.98E-01	5.80E-01
0.015	1.63E+00	1.63E+00	1.58E+00	1.49E+00	1.37E+00	1.16E+00	8.31E-01	6.57E-01
0.017	1.55E+00	1.57E+00	1.54E+00	1.46E+00	1.39E+00	1.23E+00	9.53E-01	6.66E-01
0.02	1.35E+00	1.37E+00	1.36E+00	1.30E+00	1.27E+00	1.16E+00	9.65E-01	6.19E-01
0.024	1.09E+00	1.11E+00	1.11E+00	1.07E+00	1.06E+00	9.98E-01	8.69E-01	5.35E-01
0.03	8.12E-01	8.35E-01	8.34E-01	8.13E-01	8.13E-01	7.80E-01	6.99E-01	4.34E-01
0.04	5.80E-01	5.93E-01	6.01E-01	5.89E-01	5.92E-01	5.69E-01	5.29E-01	3.36E-01
0.05	4.83E-01	4.94E-01	5.04E-01	4.96E-01	4.95E-01	4.76E-01	4.47E-01	2.95E-01
0.06	4.50E-01	4.59E-01	4.67E-01	4.64E-01	4.61E-01	4.50E-01	4.28E-01	2.85E-01
0.07	4.55E-01	4.63E-01	4.67E-01	4.63E-01	4.61E-01	4.53E-01	4.33E-01	2.94E-01
0.08	4.82E-01	4.83E-01	4.89E-01	4.85E-01	4.90E-01	4.79E-01	4.58E-01	3.15E-01
0.1	5.59E-01	5.62E-01	5.69E-01	5.71E-01	5.70E-01	5.57E-01	5.41E-01	3.76E-01
0.12	6.63E-01	6.66E-01	6.72E-01	6.73E-01	6.71E-01	6.63E-01	6.43E-01	4.52E-01
0.15	8.38E-01	8.40E-01	8.46E-01	8.45E-01	8.45E-01	8.36E-01	8.11E-01	5.80E-01
0.2	1.13E+00	1.15E+00	1.16E+00	1.17E+00	1.15E+00	1.14E+00	1.13E+00	8.10E-01
0.24	1.38E+00	1.38E+00	1.41E+00	1.42E+00	1.39E+00	1.38E+00	1.37E+00	1.00E+00
0.3	1.74E+00	1.75E+00	1.77E+00	1.80E+00	1.75E+00	1.75E+00	1.73E+00	1.28E+00
0.4	2.29E+00	2.32E+00	2.34E+00	2.38E+00	2.35E+00	2.31E+00	2.32E+00	1.75E+00
0.5	2.83E+00	2.84E+00	2.89E+00	2.93E+00	2.90E+00	2.84E+00	2.83E+00	2.22E+00
0.511	2.88E+00	2.88E+00	2.97E+00	3.01E+00	2.98E+00	2.89E+00	2.89E+00	2.26E+00
0.6	3.34E+00	3.36E+00	3.40E+00	3.46E+00	3.41E+00	3.36E+00	3.35E+00	2.64E+00
0.662	3.63E+00	3.65E+00	3.66E+00	3.77E+00	3.70E+00	3.65E+00	3.64E+00	2.90E+00
0.8	4.26E+00	4.28E+00	4.33E+00	4.39E+00	4.37E+00	4.28E+00	4.27E+00	3.46E+00
1	5.06E+00	5.09E+00	5.14E+00	5.27E+00	5.21E+00	5.08E+00	5.12E+00	4.20E+00
1.117	5.50E+00	5.55E+00	5.56E+00	5.65E+00	5.64E+00	5.56E+00	5.57E+00	4.63E+00
1.2	5.83E+00	5.84E+00	5.86E+00	5.98E+00	5.95E+00	5.82E+00	5.92E+00	4.87E+00
1.3	6.07E+00	6.14E+00	6.16E+00	6.35E+00	6.30E+00	6.15E+00	6.20E+00	5.18E+00
1.33	6.16E+00	6.26E+00	6.26E+00	6.40E+00	6.45E+00	6.29E+00	6.29E+00	5.25E+00
1.5	6.59E+00	6.63E+00	6.71E+00	6.88E+00	6.91E+00	6.74E+00	6.83E+00	5.76E+00
1.7	6.92E+00	6.93E+00	7.08E+00	7.25E+00	7.40E+00	7.23E+00	7.37E+00	6.20E+00
2	7.04E+00	7.16E+00	7.29E+00	7.66E+00	7.92E+00	7.88E+00	8.05E+00	6.75E+00
2.4	6.84E+00	6.93E+00	7.24E+00	7.84E+00	8.47E+00	8.64E+00	8.74E+00	7.32E+00
3	6.35E+00	6.49E+00	6.92E+00	7.87E+00	8.99E+00	9.61E+00	9.32E+00	7.86E+00
4	5.62E+00	5.85E+00	6.43E+00	7.67E+00	9.64E+00	1.09E+01	1.10E+01	8.63E+00
5	5.13E+00	5.35E+00	6.08E+00	7.68E+00	1.01E+01	1.22E+01	1.26E+01	9.35E+00
6	4.82E+00	5.05E+00	5.87E+00	7.60E+00	1.07E+01	1.34E+01	1.40E+01	9.99E+00
6.129	4.79E+00	5.06E+00	5.76E+00	7.62E+00	1.08E+01	1.34E+01	1.43E+01	1.01E+01
8	4.42E+00	4.67E+00	5.52E+00	7.47E+00	1.16E+01	1.56E+01	1.71E+01	1.14E+01
10	4.17E+00	4.38E+00	5.19E+00	7.16E+00	1.22E+01	1.76E+01	1.95E+01	1.27E+01
15	3.97E+00	4.16E+00	4.78E+00	6.58E+00	1.25E+01	2.08E+01	2.57E+01	1.58E+01
20	3.94E+00	4.08E+00	4.60E+00	6.15E+00	1.24E+01	2.29E+01	3.09E+01	1.89E+01
30	4.01E+00	4.12E+00	4.58E+00	5.84E+00	1.19E+01	2.46E+01	3.79E+01	2.45E+01
40	4.09E+00	4.18E+00	4.68E+00	5.69E+00	1.17E+01	2.55E+01	4.22E+01	2.95E+01
50	4.16E+00	4.32E+00	4.71E+00	5.70E+00	1.16E+01	2.64E+01	4.53E+01	3.36E+01

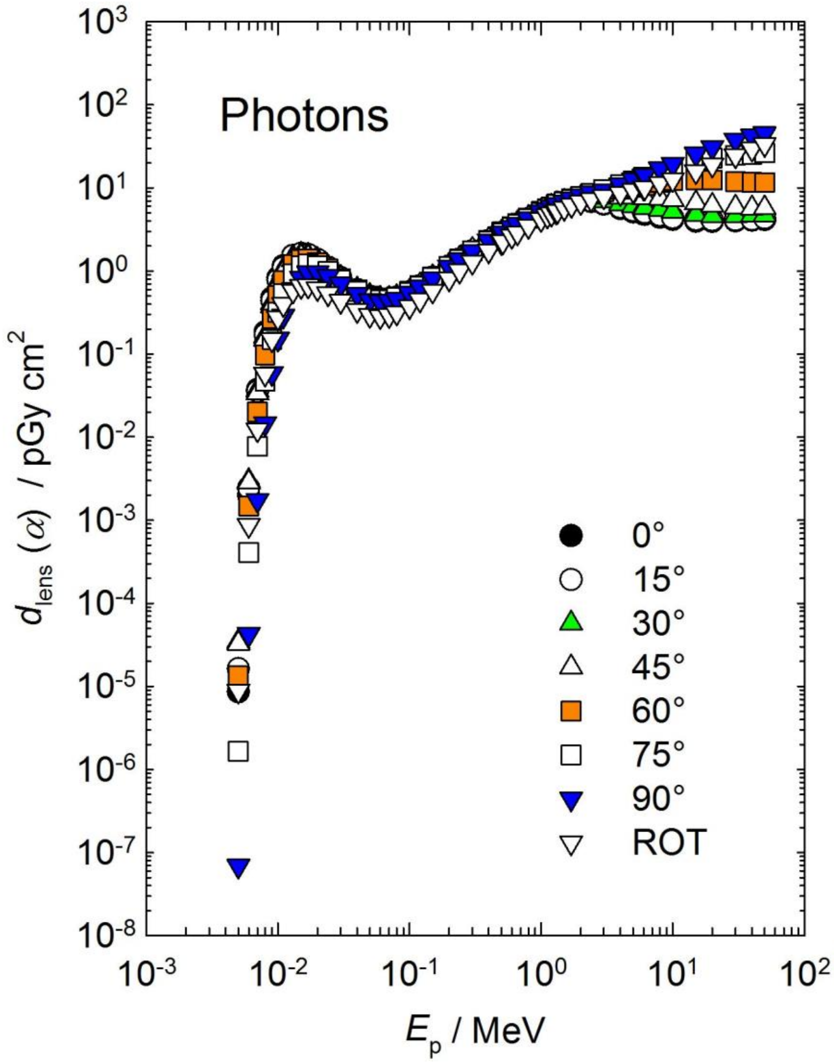

Figure A.3.1a Conversion coefficients from photon fluence to the maximum absorbed dose in the complete lens for left or right irradiations (Behrens, 2017a).

647 Table A.3.1b Conversion coefficients from photon air kerma to the maximum absorbed dose in the
648 complete lens for left or right irradiations (Behrens, 2017a).

E_p / MeV	$d_{lens}(\alpha)$/ (Gy Gy^{-1}) for a radiation incidence at α							
	0°	15°	30°	45°	60°	75°	90°	ROT
0.005	2.81E-07	5.30E-07	1.13E-06	1.07E-06	4.39E-07	5.42E-08	2.25E-09	2.89E-07
0.006	9.41E-05	1.15E-04	1.40E-04	1.34E-04	6.97E-05	1.92E-05	2.01E-06	4.12E-05
0.007	2.41E-03	2.29E-03	2.37E-03	2.18E-03	1.30E-03	5.00E-04	1.13E-04	7.99E-04
0.008	1.57E-02	1.46E-02	1.38E-02	1.27E-02	8.32E-03	3.98E-03	1.24E-03	4.92E-03
0.009	5.15E-02	4.78E-02	4.47E-02	4.09E-02	2.89E-02	1.63E-02	6.39E-03	1.63E-02
0.01	1.13E-01	1.05E-01	9.87E-02	9.09E-02	6.85E-02	4.33E-02	2.06E-02	3.70E-02
0.011	1.91E-01	1.82E-01	1.72E-01	1.60E-01	1.28E-01	8.86E-02	4.78E-02	6.59E-02
0.013	3.63E-01	3.59E-01	3.44E-01	3.20E-01	2.82E-01	2.20E-01	1.41E-01	1.37E-01
0.015	5.20E-01	5.21E-01	5.07E-01	4.76E-01	4.40E-01	3.72E-01	2.66E-01	2.10E-01
0.017	6.49E-01	6.58E-01	6.43E-01	6.11E-01	5.82E-01	5.15E-01	3.99E-01	2.79E-01
0.02	7.99E-01	8.15E-01	8.07E-01	7.71E-01	7.55E-01	6.91E-01	5.73E-01	3.68E-01
0.024	9.47E-01	9.64E-01	9.67E-01	9.29E-01	9.21E-01	8.67E-01	7.56E-01	4.66E-01
0.03	1.12E+00	1.16E+00	1.16E+00	1.13E+00	1.13E+00	1.08E+00	9.69E-01	6.02E-01
0.04	1.35E+00	1.38E+00	1.40E+00	1.37E+00	1.38E+00	1.33E+00	1.23E+00	7.85E-01
0.05	1.50E+00	1.53E+00	1.56E+00	1.54E+00	1.53E+00	1.48E+00	1.38E+00	9.12E-01
0.06	1.56E+00	1.59E+00	1.62E+00	1.61E+00	1.60E+00	1.56E+00	1.48E+00	9.86E-01
0.07	1.58E+00	1.61E+00	1.62E+00	1.61E+00	1.60E+00	1.58E+00	1.51E+00	1.02E+00
0.08	1.57E+00	1.58E+00	1.59E+00	1.58E+00	1.60E+00	1.56E+00	1.49E+00	1.03E+00
0.1	1.51E+00	1.51E+00	1.53E+00	1.54E+00	1.54E+00	1.50E+00	1.46E+00	1.01E+00
0.12	1.44E+00	1.45E+00	1.46E+00	1.46E+00	1.46E+00	1.44E+00	1.40E+00	9.81E-01
0.15	1.40E+00	1.40E+00	1.41E+00	1.41E+00	1.41E+00	1.39E+00	1.35E+00	9.67E-01
0.2	1.32E+00	1.34E+00	1.36E+00	1.37E+00	1.34E+00	1.33E+00	1.32E+00	9.45E-01
0.24	1.30E+00	1.30E+00	1.32E+00	1.33E+00	1.31E+00	1.30E+00	1.29E+00	9.44E-01
0.3	1.26E+00	1.26E+00	1.28E+00	1.31E+00	1.27E+00	1.26E+00	1.25E+00	9.28E-01
0.4	1.21E+00	1.23E+00	1.24E+00	1.26E+00	1.24E+00	1.22E+00	1.23E+00	9.27E-01
0.5	1.19E+00	1.19E+00	1.21E+00	1.23E+00	1.22E+00	1.19E+00	1.19E+00	9.31E-01
0.511	1.18E+00	1.18E+00	1.22E+00	1.24E+00	1.23E+00	1.19E+00	1.19E+00	9.28E-01
0.6	1.18E+00	1.18E+00	1.20E+00	1.22E+00	1.20E+00	1.18E+00	1.18E+00	9.28E-01
0.662	1.17E+00	1.17E+00	1.18E+00	1.21E+00	1.19E+00	1.17E+00	1.17E+00	9.31E-01
0.8	1.15E+00	1.16E+00	1.17E+00	1.19E+00	1.18E+00	1.15E+00	1.15E+00	9.35E-01
1	1.13E+00	1.13E+00	1.15E+00	1.18E+00	1.16E+00	1.13E+00	1.14E+00	9.36E-01
1.117	1.13E+00	1.14E+00	1.14E+00	1.16E+00	1.15E+00	1.14E+00	1.14E+00	9.48E-01
1.2	1.13E+00	1.13E+00	1.14E+00	1.16E+00	1.15E+00	1.13E+00	1.15E+00	9.42E-01
1.3	1.10E+00	1.12E+00	1.12E+00	1.16E+00	1.15E+00	1.12E+00	1.13E+00	9.43E-01
1.33	1.10E+00	1.12E+00	1.12E+00	1.14E+00	1.15E+00	1.12E+00	1.12E+00	9.39E-01
1.5	1.07E+00	1.08E+00	1.09E+00	1.12E+00	1.12E+00	1.10E+00	1.11E+00	9.37E-01
1.7	1.03E+00	1.03E+00	1.05E+00	1.08E+00	1.10E+00	1.08E+00	1.10E+00	9.22E-01
2	9.32E-01	9.48E-01	9.64E-01	1.01E+00	1.05E+00	1.04E+00	1.07E+00	8.93E-01
2.4	7.99E-01	8.10E-01	8.46E-01	9.16E-01	9.89E-01	1.01E+00	1.02E+00	8.54E-01
3	6.36E-01	6.51E-01	6.93E-01	7.89E-01	9.02E-01	9.63E-01	9.35E-01	7.88E-01
4	4.63E-01	4.82E-01	5.29E-01	6.32E-01	7.94E-01	9.01E-01	9.04E-01	7.11E-01
5	3.62E-01	3.77E-01	4.29E-01	5.41E-01	7.15E-01	8.61E-01	8.89E-01	6.60E-01
6	2.98E-01	3.12E-01	3.63E-01	4.70E-01	6.62E-01	8.30E-01	8.68E-01	6.18E-01
6.129	2.92E-01	3.08E-01	3.50E-01	4.63E-01	6.55E-01	8.13E-01	8.69E-01	6.15E-01
8	2.20E-01	2.32E-01	2.74E-01	3.71E-01	5.74E-01	7.73E-01	8.47E-01	5.67E-01
10	1.73E-01	1.81E-01	2.15E-01	2.97E-01	5.06E-01	7.28E-01	8.07E-01	5.26E-01
15	1.15E-01	1.21E-01	1.39E-01	1.91E-01	3.62E-01	6.04E-01	7.47E-01	4.59E-01
20	8.69E-02	9.00E-02	1.01E-01	1.35E-01	2.74E-01	5.04E-01	6.81E-01	4.17E-01
30	5.84E-02	6.00E-02	6.68E-02	8.51E-02	1.74E-01	3.59E-01	5.53E-01	3.57E-01
40	4.39E-02	4.48E-02	5.01E-02	6.10E-02	1.26E-01	2.73E-01	4.52E-01	3.16E-01
50	3.49E-02	3.62E-02	3.95E-02	4.79E-02	9.77E-02	2.21E-01	3.80E-01	2.82E-01

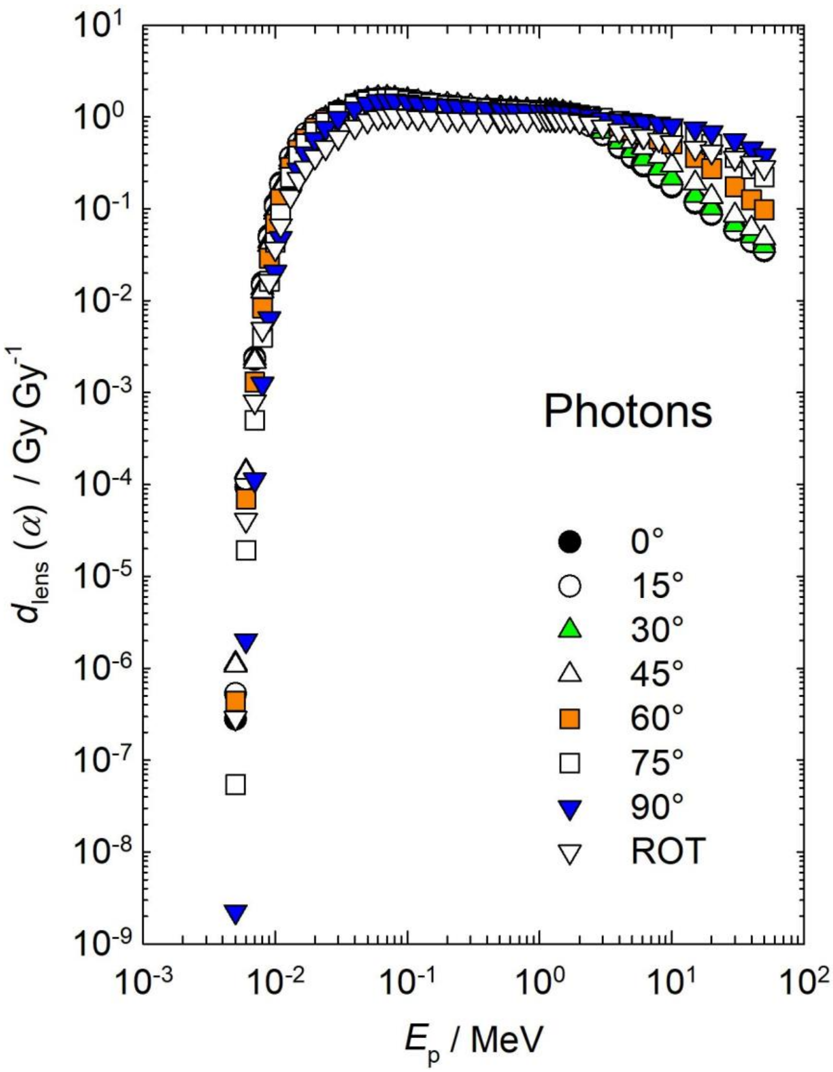

Figure A.3.1b Conversion coefficients from photon air kerma to the maximum absorbed dose in the complete lens for left or right irradiations (Behrens, 2017a).

Table A.3.2 and Figure A.3.2 Neutrons

Table A.3.3 Conversion coefficients from electron fluence to the maximum absorbed dose in the complete lens for left or right irradiations (Behrens, 2017a).

	$d_{\text{lens}}(\alpha)$ / (pGy cm^2) for a radiation incidence at α							
E_{p} / MeV	0°	15°	30°	45°	60°	75°	90°	ROT
0.01	6.50E-07	7.33E-07	6.46E-07	4.68E-07	3.82E-07	2.91E-07	1.67E-07	3.32E-07
0.015	1.55E-05	1.47E-05	1.37E-05	1.20E-05	1.10E-05	6.71E-06	3.99E-06	4.60E-06
0.02	5.26E-05	5.21E-05	4.29E-05	4.00E-05	3.07E-05	2.01E-05	1.56E-05	1.69E-05
0.03	1.62E-04	1.69E-04	1.52E-04	1.37E-04	9.59E-05	7.96E-05	4.59E-05	5.49E-05
0.04	3.16E-04	3.04E-04	3.07E-04	2.53E-04	1.99E-04	1.55E-04	8.87E-05	9.57E-05
0.05	4.90E-04	5.09E-04	4.76E-04	3.94E-04	3.45E-04	2.36E-04	1.44E-04	1.56E-04
0.06	6.27E-04	6.42E-04	6.12E-04	5.17E-04	4.43E-04	3.05E-04	1.93E-04	2.19E-04
0.08	1.03E-03	1.05E-03	9.82E-04	8.34E-04	7.25E-04	5.15E-04	3.28E-04	3.51E-04
0.1	1.43E-03	1.47E-03	1.34E-03	1.26E-03	1.01E-03	7.44E-04	4.96E-04	4.84E-04
0.15	2.60E-03	2.66E-03	2.48E-03	2.14E-03	1.79E-03	1.37E-03	9.10E-04	9.40E-04
0.2	3.87E-03	4.05E-03	3.76E-03	3.39E-03	2.81E-03	2.18E-03	1.43E-03	1.44E-03
0.3	7.36E-03	7.18E-03	6.86E-03	6.29E-03	5.15E-03	4.07E-03	2.84E-03	2.63E-03
0.4	1.14E-02	1.15E-02	1.08E-02	1.02E-02	8.49E-03	6.68E-03	4.73E-03	4.19E-03
0.5	1.65E-02	1.63E-02	1.56E-02	1.44E-02	1.22E-02	9.69E-03	6.87E-03	6.38E-03
0.6	4.71E-02	5.68E-02	6.98E-02	6.62E-02	4.51E-02	2.34E-02	1.16E-02	2.29E-02
0.7	1.46E+00	1.65E+00	1.88E+00	1.73E+00	1.17E+00	5.49E-01	1.73E-01	5.98E-01
0.8	1.00E+01	1.03E+01	1.04E+01	9.08E+00	6.28E+00	3.28E+00	1.18E+00	3.45E+00
1	6.95E+01	6.74E+01	6.02E+01	4.86E+01	3.36E+01	1.89E+01	7.80E+00	2.08E+01
1.25	1.92E+02	1.85E+02	1.64E+02	1.32E+02	9.15E+01	5.38E+01	2.43E+01	5.71E+01
1.5	3.08E+02	2.99E+02	2.69E+02	2.23E+02	1.61E+02	9.82E+01	4.72E+01	9.53E+01
1.75	3.85E+02	3.78E+02	3.50E+02	3.02E+02	2.28E+02	1.46E+02	7.39E+01	1.26E+02
2	4.16E+02	4.12E+02	3.95E+02	3.58E+02	2.83E+02	1.93E+02	1.03E+02	1.45E+02
2.5	4.08E+02	4.12E+02	4.13E+02	4.04E+02	3.52E+02	2.70E+02	1.62E+02	1.61E+02
3	3.78E+02	3.87E+02	3.99E+02	4.11E+02	3.82E+02	3.21E+02	2.11E+02	1.64E+02
3.5	3.54E+02	3.66E+02	3.82E+02	4.05E+02	3.91E+02	3.52E+02	2.54E+02	1.64E+02
4	3.39E+02	3.51E+02	3.69E+02	3.99E+02	3.87E+02	3.70E+02	2.86E+02	1.64E+02
5	3.23E+02	3.35E+02	3.54E+02	3.92E+02	3.68E+02	3.81E+02	3.33E+02	1.65E+02
6	3.15E+02	3.28E+02	3.49E+02	3.94E+02	3.49E+02	3.76E+02	3.61E+02	1.68E+02
7	3.10E+02	3.22E+02	3.46E+02	4.01E+02	3.37E+02	3.64E+02	3.75E+02	1.72E+02
8	3.07E+02	3.18E+02	3.41E+02	4.06E+02	3.28E+02	3.53E+02	3.76E+02	1.77E+02
10	3.04E+02	3.12E+02	3.30E+02	4.03E+02	3.44E+02	3.36E+02	3.61E+02	1.85E+02
15	3.01E+02	3.06E+02	3.09E+02	3.53E+02	4.15E+02	3.15E+02	3.25E+02	2.01E+02
20	3.01E+02	3.03E+02	3.05E+02	3.23E+02	4.03E+02	3.76E+02	3.12E+02	2.12E+02
30	3.03E+02	3.04E+02	3.06E+02	3.12E+02	3.67E+02	3.67E+02	3.09E+02	2.36E+02
40	3.03E+02	3.07E+02	3.03E+02	3.13E+02	3.47E+02	3.46E+02	3.13E+02	2.64E+02
50	3.00E+02	3.01E+02	3.06E+02	3.10E+02	3.41E+02	3.32E+02	3.13E+02	2.90E+02

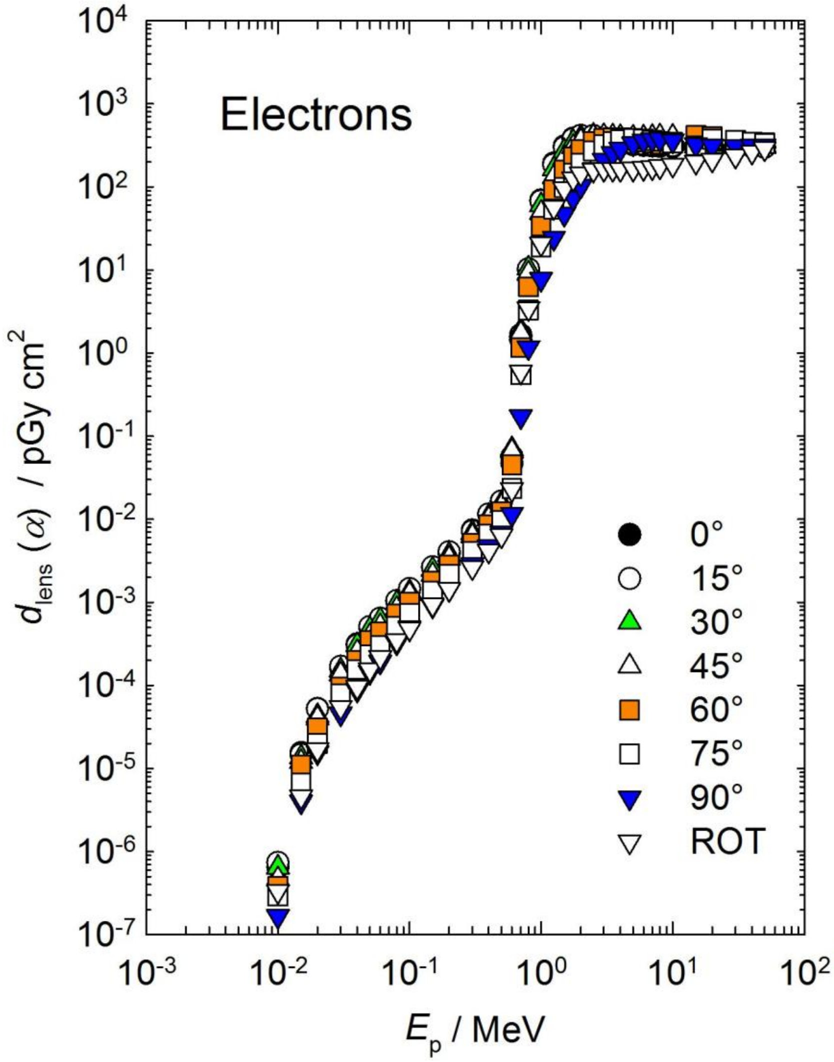

Figure A.3.3 Conversion coefficients from electrons fluence to the maximum absorbed dose in the complete lens for left or right irradiations (Behrens, 2017a).

Table A.3.4 Conversion coefficients from positron fluence to the maximum absorbed dose in the complete lens for left or right irradiations (Behrens, 2017a).

	$d_{\text{lens}}(\alpha)$ / (pGy cm^2) for a radiation incidence at α							
E_p / MeV	0°	15°	30°	45°	60°	75°	90°	ROT
0.001	6.79E+00	7.16E+00	7.32E+00	6.78E+00	5.84E+00	4.70E+00	3.40E+00	2.83E+00
0.002	6.47E+00	6.82E+00	6.92E+00	6.44E+00	5.51E+00	4.37E+00	3.11E+00	2.65E+00
0.003	6.32E+00	6.68E+00	6.79E+00	6.30E+00	5.38E+00	4.26E+00	3.01E+00	2.59E+00
0.004	6.29E+00	6.65E+00	6.78E+00	6.27E+00	5.37E+00	4.21E+00	2.95E+00	2.59E+00
0.005	6.30E+00	6.62E+00	6.75E+00	6.27E+00	5.33E+00	4.18E+00	2.94E+00	2.55E+00
0.006	6.26E+00	6.61E+00	6.71E+00	6.25E+00	5.24E+00	4.17E+00	2.88E+00	2.52E+00
0.007	6.27E+00	6.67E+00	6.70E+00	6.23E+00	5.28E+00	4.15E+00	2.91E+00	2.52E+00
0.008	6.26E+00	6.66E+00	6.65E+00	6.23E+00	5.31E+00	4.14E+00	2.93E+00	2.52E+00
0.009	6.25E+00	6.65E+00	6.71E+00	6.23E+00	5.30E+00	4.16E+00	2.89E+00	2.54E+00
0.01	6.26E+00	6.63E+00	6.71E+00	6.18E+00	5.33E+00	4.18E+00	2.86E+00	2.52E+00
0.013	6.25E+00	6.65E+00	6.67E+00	6.23E+00	5.26E+00	4.12E+00	2.89E+00	2.51E+00
0.015	6.24E+00	6.66E+00	6.65E+00	6.19E+00	5.31E+00	4.13E+00	2.89E+00	2.52E+00
0.017	6.23E+00	6.59E+00	6.71E+00	6.20E+00	5.30E+00	4.12E+00	2.91E+00	2.50E+00
0.02	6.23E+00	6.58E+00	6.69E+00	6.18E+00	5.28E+00	4.15E+00	2.92E+00	2.52E+00
0.024	6.27E+00	6.64E+00	6.70E+00	6.21E+00	5.30E+00	4.16E+00	2.88E+00	2.51E+00
0.03	6.26E+00	6.59E+00	6.66E+00	6.19E+00	5.26E+00	4.10E+00	2.88E+00	2.51E+00
0.04	6.26E+00	6.55E+00	6.73E+00	6.19E+00	5.28E+00	4.14E+00	2.85E+00	2.50E+00
0.05	6.29E+00	6.62E+00	6.66E+00	6.22E+00	5.31E+00	4.12E+00	2.89E+00	2.53E+00
0.06	6.26E+00	6.58E+00	6.68E+00	6.28E+00	5.28E+00	4.14E+00	2.88E+00	2.51E+00
0.07	6.29E+00	6.66E+00	6.75E+00	6.18E+00	5.31E+00	4.20E+00	2.91E+00	2.53E+00
0.08	6.26E+00	6.64E+00	6.73E+00	6.26E+00	5.31E+00	4.15E+00	2.91E+00	2.53E+00
0.1	6.30E+00	6.66E+00	6.70E+00	6.27E+00	5.36E+00	4.13E+00	2.90E+00	2.51E+00
0.15	6.36E+00	6.68E+00	6.79E+00	6.28E+00	5.35E+00	4.15E+00	2.93E+00	2.56E+00
0.2	6.43E+00	6.78E+00	6.85E+00	6.43E+00	5.46E+00	4.24E+00	2.94E+00	2.58E+00
0.3	6.56E+00	6.93E+00	7.02E+00	6.46E+00	5.48E+00	4.34E+00	2.98E+00	2.67E+00
0.4	6.76E+00	7.11E+00	7.16E+00	6.57E+00	5.62E+00	4.41E+00	3.07E+00	2.72E+00
0.5	6.98E+00	7.36E+00	7.42E+00	6.75E+00	5.82E+00	4.45E+00	3.16E+00	2.80E+00
0.6	7.31E+00	7.60E+00	7.67E+00	7.04E+00	5.95E+00	4.67E+00	3.25E+00	2.91E+00
0.7	9.18E+00	9.70E+00	9.91E+00	9.15E+00	7.40E+00	5.37E+00	3.51E+00	3.68E+00
0.8	1.89E+01	1.94E+01	1.96E+01	1.73E+01	1.31E+01	8.52E+00	4.68E+00	6.87E+00
1	8.22E+01	8.02E+01	7.23E+01	5.91E+01	4.20E+01	2.51E+01	1.20E+01	2.53E+01
1.25	2.05E+02	1.99E+02	1.76E+02	1.44E+02	1.03E+02	6.13E+01	2.90E+01	6.24E+01
1.5	3.17E+02	3.07E+02	2.78E+02	2.32E+02	1.70E+02	1.05E+02	5.25E+01	9.91E+01
1.75	3.84E+02	3.77E+02	3.51E+02	3.07E+02	2.35E+02	1.52E+02	7.86E+01	1.27E+02
2	4.06E+02	4.03E+02	3.87E+02	3.53E+02	2.88E+02	1.98E+02	1.08E+02	1.44E+02
2.5	3.88E+02	3.94E+02	3.97E+02	3.89E+02	3.49E+02	2.66E+02	1.65E+02	1.57E+02
3	3.59E+02	3.69E+02	3.78E+02	3.96E+02	3.69E+02	3.12E+02	2.12E+02	1.59E+02
3.5	3.38E+02	3.47E+02	3.65E+02	3.85E+02	3.73E+02	3.40E+02	2.48E+02	1.57E+02
4	3.22E+02	3.36E+02	3.53E+02	3.81E+02	3.68E+02	3.55E+02	2.78E+02	1.58E+02
5	3.10E+02	3.22E+02	3.42E+02	3.74E+02	3.49E+02	3.65E+02	3.23E+02	1.60E+02
6	3.05E+02	3.17E+02	3.38E+02	3.80E+02	3.36E+02	3.60E+02	3.48E+02	1.63E+02
7	3.00E+02	3.12E+02	3.34E+02	3.84E+02	3.25E+02	3.46E+02	3.59E+02	1.67E+02
8	2.99E+02	3.06E+02	3.32E+02	3.91E+02	3.16E+02	3.38E+02	3.61E+02	1.70E+02
10	2.96E+02	3.02E+02	3.23E+02	3.88E+02	3.33E+02	3.23E+02	3.44E+02	1.80E+02
15	2.97E+02	3.01E+02	3.06E+02	3.40E+02	3.94E+02	3.09E+02	3.17E+02	1.94E+02
20	2.98E+02	2.99E+02	3.01E+02	3.16E+02	3.86E+02	3.58E+02	3.05E+02	2.07E+02
30	2.99E+02	2.99E+02	3.00E+02	3.07E+02	3.53E+02	3.47E+02	3.03E+02	2.31E+02
40	2.99E+02	3.03E+02	3.03E+02	3.03E+02	3.40E+02	3.30E+02	3.01E+02	2.60E+02
50	3.02E+02	3.00E+02	3.03E+02	3.02E+02	3.31E+02	3.23E+02	3.03E+02	2.83E+02

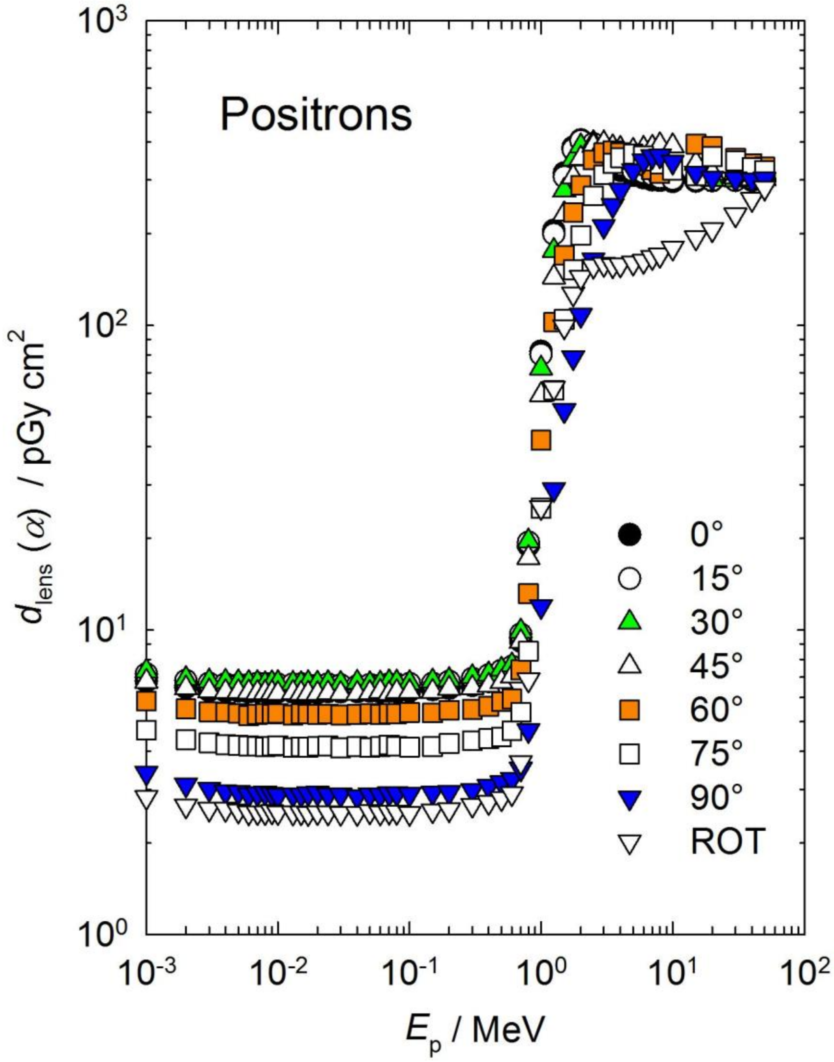

Figure A.3.4 Conversion coefficients from positron fluence to the maximum absorbed dose in the complete lens for left or right irradiations (Behrens, 2017a).

A.4 Directional and Personal Absorbed Dose to Local Skin

The numerical values of conversion coefficients from particle fluence to directional absorbed dose in local skin $d'_{\text{local skin}}$ and from particle fluence to personal absorbed dose in local skin $d_{\text{p local skin}}$ are the same for exposure of a specific phantom. The symbol $d_{\text{local skin}}$ is used in the following Tables for the slab phantom. Tables A.4.1.1a, A.4.1.2a, A.4.1.3a, A.4.4, A.4.5 and Figures A.4.1.1a, A.4.1.2a, A.4.1.3a, A.4.4, A.4.5 give the values of the conversion coefficients from particle fluence for photons, neutrons, electrons, and positrons, for energies up to 50 MeV, and for alpha particles up to 10 MeV; and in Tables A.4.1.1b, A.4.1.2b, A.4.1.3b, and Figures A.4.1.1b, A.4.1.2b, A.4.1.3b for photons from air kerma. The conversion coefficients relate the particle fluence to the value of the absorbed dose in local skin calculated for exposure of the specific phantoms for broad parallel beams incident in specific directions, and a rotational field. Conversion coefficients are calculated as follows:- for exposure of the trunk at the center of the front surface of a 300 mm x 300 mm x 150 mm slab phantom of ICRU 4-element tissue density 1.0 g cm^{-3}, for the volume of a right circular cylinder between depths of 50 and 100 µm and a cross sectional area of 1 cm^2 for angles, α, from 0° (A-P) to 75° in 15° steps; for exposure of the extremity at the center of the cylindrical surface of a 73 mm diameter 300 mm length pillar phantom of ICRU 4-element tissue of density 1.11 g cm^{-3}, for the volume between the radii 36.4 mm and 36.45 with a circle of area 1 cm^2 projected onto the upper and lower cylindrical surfaces perpendicular to the radii, for angles, α, from 0° to 180° in 15° steps, and a rotational field; for exposure of the finger at the center of the cylindrical surface of a 19 mm diameter 300 mm length rod of ICRU 4-element tissue density 1.11 g cm^{-3}, for the volume between the radii 9.4 mm and 9.45 of a circle of area 1 cm^2 projected onto the upper and lower cylindrical surfaces perpendicular to the radii, for angles, α, from 0° to 180° in 15° steps and a rotational field. Inside the phantoms there is an outer layer of 2 mm skin of elemental composition given in ICRP Publication 89 (2002) and of density of 1.09 g cm^{-3} (ICRP, 2009). The conversion coefficients for alpha particles given in Table A.4.5 and Figure A.4.5 have been calculated for the volume of a right circular cylinder between depths of 50 and 100 µm and a cross sectional area of 1 cm^2 at the center of the front surface of a 100 mm x 100 mm x 100 mm phantom of ICRU 4-element tissue density 1 g cm^{-3}, without the 2 mm skin layer (ICRP, 2010).

Table A.4.1.1a Conversion coefficients from photon fluence to directional and personal absorbed dose in local skin on the slab phantom (Daures *et al*., 2017).

E_p / MeV	$d_{local\ skin}$ / (pGy cm^2) for a radiation incidence at α					
	0°	15°	30°	45°	60°	75°
0.01	7.20E+00	7.17E+00	7.14E+00	7.04E+00	6.89E+00	6.38E+00
0.015	3.22E+00	3.20E+00	3.19E+00	3.17E+00	3.14E+00	3.04E+00
0.02	1.85E+00	1.83E+00	1.81E+00	1.80E+00	1.79E+00	1.73E+00
0.03	9.35E-01	9.24E-01	9.18E-01	9.05E-01	8.89E-01	8.24E-01
0.04	6.36E-01	6.47E-01	6.30E-01	5.26E-01	6.00E-01	5.45E-01
0.05	5.43E-01	5.46E-01	5.23E-01	5.26E-01	4.81E-01	4.49E-01
0.06	5.10E-01	5.06E-01	4.91E-01	4.85E-01	4.51E-01	4.25E-01
0.07	5.20E-01	5.14E-01	5.04E-01	4.87E-01	4.74E-01	4.48E-01
0.08	5.50E-01	5.31E-01	5.39E-01	5.24E-01	4.99E-01	4.63E-01
0.1	6.17E-01	6.09E-01	6.16E-01	6.21E-01	5.81E-01	5.63E-01
0.15	9.21E-01	9.04E-01	9.27E-01	8.95E-01	8.88E-01	8.66E-01
0.2	1.20E+00	1.21E+00	1.24E+00	1.19E+00	1.23E+00	1.20E+00
0.3	1.28E+00	1.34E+00	1.41E+00	1.46E+00	1.62E+00	1.69E+00
0.4	1.23E+00	1.29E+00	1.34E+00	1.49E+00	1.75E+00	1.87E+00
0.5	1.13E+00	1.16E+00	1.27E+00	1.49E+00	1.80E+00	2.07E+00
0.6	1.08E+00	1.11E+00	1.24E+00	1.47E+00	1.82E+00	2.25E+00
0.662	1.03E+00	1.08E+00	1.25E+00	1.41E+00	1.82E+00	2.26E+00
0.8	9.46E-01	9.89E-01	1.12E+00	1.41E+00	1.81E+00	2.40E+00
1	8.52E-01	8.87E-01	1.03E+00	1.33E+00	1.82E+00	2.62E+00
1.25	7.35E-01	7.98E-01	9.72E-01	1.23E+00	1.77E+00	2.65E+00
1.5	6.59E-01	7.06E-01	9.05E-01	1.23E+00	1.80E+00	2.78E+00
2	5.74E-01	6.23E-01	7.74E-01	1.05E+00	1.74E+00	2.98E+00
3	4.46E-01	4.66E-01	6.48E-01	9.71E-01	1.71E+00	3.17E+00
5	3.34E-01	3.57E-01	4.85E-01	7.33E-01	1.59E+00	3.44E+00
10	2.88E-01	3.05E-01	3.77E-01	5.88E-01	1.23E+00	3.72E+00
15	2.67E-01	2.80E-01	3.33E-01	5.02E-01	1.14E+00	3.78E+00
20	2.59E-01	2.58E-01	3.00E-01	4.96E-01	1.12E+00	3.93E+00
30	2.43E-01	2.38E-01	3.03E-01	4.16E-01	9.71E-01	4.14E+00
50	2.13E-01	2.01E-01	2.82E-01	3.86E-01	8.26E-01	3.78E+00

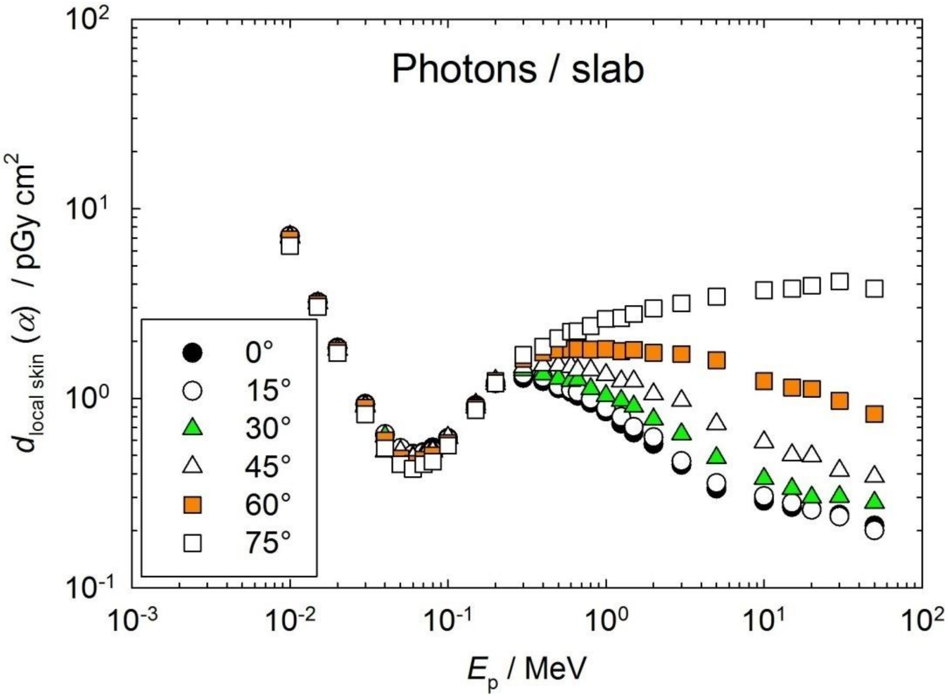

Figure A.4.1.1a Conversion coefficients from photon fluence to directional and personal absorbed dose in local skin on the slab phantom (Daures *et al*., 2017).

Table A.4.1.1b Conversion coefficients from photon air kerma to directional and personal absorbed dose in local skin on the slab phantom (Daures *et al*., 2017).

E_p / MeV	$d_{\text{local skin}}$ / (GyGy^{-1}) for a radiation incidence at α					
	0°	15°	30°	45°	60°	75°
0.01	9.73E-01	9.69E-01	9.65E-01	9.51E-01	9.31E-01	8.62E-01
0.015	1.03E+00	1.02E+00	1.02E+00	1.01E+00	1.00E+00	9.73E-01
0.02	1.10E+00	1.09E+00	1.07E+00	1.07E+00	1.06E+00	1.03E+00
0.03	1.30E+00	1.28E+00	1.27E+00	1.25E+00	1.23E+00	1.14E+00
0.04	1.48E+00	1.51E+00	1.47E+00	1.23E+00	1.40E+00	1.27E+00
0.05	1.68E+00	1.69E+00	1.62E+00	1.63E+00	1.49E+00	1.39E+00
0.06	1.77E+00	1.75E+00	1.70E+00	1.68E+00	1.56E+00	1.47E+00
0.07	1.81E+00	1.79E+00	1.75E+00	1.69E+00	1.65E+00	1.56E+00
0.08	1.79E+00	1.73E+00	1.76E+00	1.71E+00	1.63E+00	1.51E+00
0.1	1.66E+00	1.64E+00	1.66E+00	1.67E+00	1.56E+00	1.52E+00
0.15	1.54E+00	1.51E+00	1.55E+00	1.49E+00	1.48E+00	1.44E+00
0.2	1.40E+00	1.41E+00	1.45E+00	1.39E+00	1.44E+00	1.40E+00
0.3	9.26E-01	9.69E-01	1.02E+00	1.06E+00	1.17E+00	1.22E+00
0.4	6.50E-01	6.82E-01	7.08E-01	7.88E-01	9.25E-01	9.88E-01
0.5	4.75E-01	4.88E-01	5.34E-01	6.26E-01	7.57E-01	8.70E-01
0.6	3.80E-01	3.90E-01	4.36E-01	5.17E-01	6.40E-01	7.91E-01
0.662	3.31E-01	3.47E-01	4.02E-01	4.53E-01	5.85E-01	7.26E-01
0.8	2.56E-01	2.67E-01	3.03E-01	3.81E-01	4.89E-01	6.48E-01
1	1.90E-01	1.98E-01	2.30E-01	2.97E-01	4.06E-01	5.85E-01
1.25	1.38E-01	1.50E-01	1.82E-01	2.31E-01	3.32E-01	4.97E-01
1.5	1.07E-01	1.15E-01	1.47E-01	2.00E-01	2.93E-01	4.52E-01
2	7.60E-02	8.24E-02	1.02E-01	1.39E-01	2.30E-01	3.94E-01
3	4.47E-02	4.67E-02	6.49E-02	9.73E-02	1.71E-01	3.18E-01
5	2.36E-02	2.52E-02	3.42E-02	5.17E-02	1.12E-01	2.43E-01
10	1.19E-02	1.26E-02	1.56E-02	2.44E-02	5.10E-02	1.54E-01
15	7.75E-03	8.13E-03	9.66E-03	1.46E-02	3.31E-02	1.10E-01
20	5.71E-03	5.69E-03	6.61E-03	1.09E-02	2.47E-02	8.66E-02
30	3.54E-03	3.47E-03	4.42E-03	6.07E-03	1.42E-02	6.04E-02
50	1.79E-03	1.69E-03	2.37E-03	3.24E-03	6.93E-03	3.17E-02

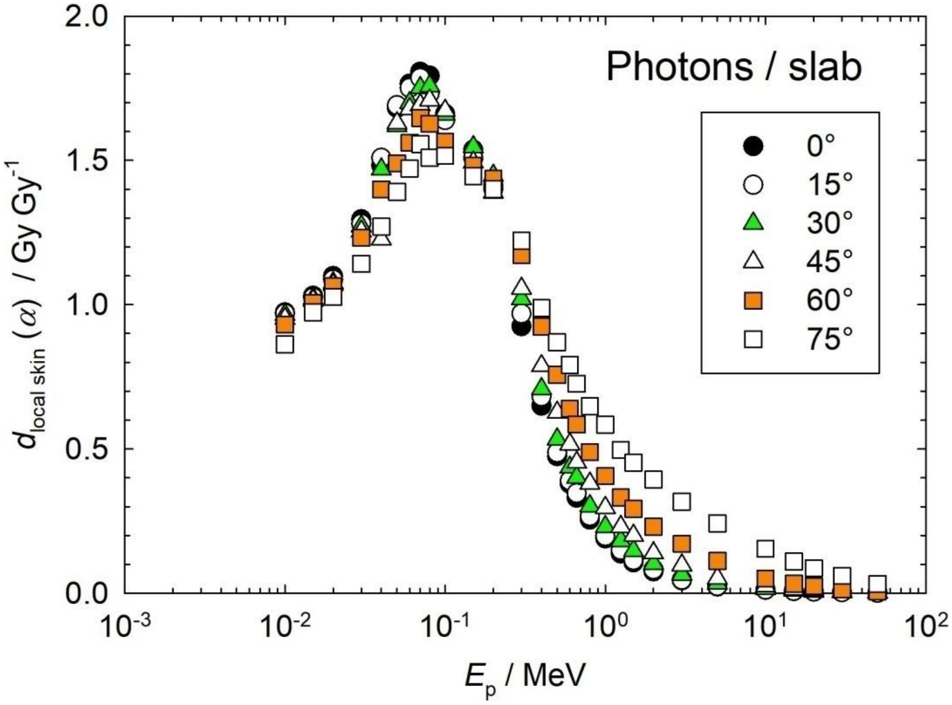

Figure A.4.1.1b Conversion coefficients from photon air kerma to directional and personal absorbed dose in local skin on the slab phantom (Daures *et al*., 2017).

Table A.4.1.2a. Conversion coefficients from photon fluence to personal absorbed dose in local skin on the pillar phantom (1/2) (Otto, 2017).

	$d_{\text{p local skin}}$ / (pGy cm^2) for a radiation incidence at α						
E_p / MeV	0°	15°	30°	45°	60°	75°	90°
0.002	2.94E+00	2.59E+00	1.67E+00	6.73E-01	1.10E-01	2.05E-03	3.28E-05
0.003	2.08E+01	1.98E+01	1.69E+01	1.20E+01	5.71E+00	8.73E-01	2.53E-03
0.004	2.62E+01	2.57E+01	2.38E+01	2.04E+01	1.43E+01	5.20E+00	9.54E-02
0.005	2.27E+01	2.24E+01	2.16E+01	1.99E+01	1.65E+01	9.14E+00	5.56E-01
0.007	1.40E+01	1.40E+01	1.37E+01	1.33E+01	1.24E+01	9.81E+00	1.83E+00
0.01	7.20E+00	7.22E+00	7.17E+00	7.14E+00	6.94E+00	6.37E+00	2.44E+00
0.015	3.22E+00	3.22E+00	3.22E+00	3.20E+00	3.18E+00	3.08E+00	2.00E+00
0.02	1.85E+00	1.84E+00	1.85E+00	1.83E+00	1.81E+00	1.77E+00	1.41E+00
0.03	8.97E-01	9.00E-01	9.04E-01	8.90E-01	8.86E-01	8.68E-01	7.72E-01
0.05	4.64E-01	4.67E-01	4.55E-01	4.63E-01	4.54E-01	4.50E-01	4.23E-01
0.07	4.19E-01	4.20E-01	4.17E-01	4.13E-01	4.13E-01	4.10E-01	3.90E-01
0.1	5.11E-01	5.11E-01	5.14E-01	5.09E-01	5.11E-01	5.13E-01	4.93E-01
0.15	7.77E-01	7.79E-01	7.73E-01	7.73E-01	7.83E-01	7.95E-01	7.74E-01
0.2	1.03E+00	1.04E+00	1.05E+00	1.06E+00	1.08E+00	1.11E+00	1.07E+00
0.3	1.11E+00	1.13E+00	1.19E+00	1.28E+00	1.42E+00	1.54E+00	1.58E+00
0.5	9.41E-01	9.72E-01	1.09E+00	1.28E+00	1.57E+00	1.90E+00	2.17E+00
0.662	8.19E-01	8.59E-01	9.85E-01	1.23E+00	1.58E+00	2.04E+00	2.47E+00
0.7	8.05E-01	8.37E-01	9.75E-01	1.21E+00	1.60E+00	2.08E+00	2.54E+00
1	6.63E-01	7.08E-01	8.32E-01	1.09E+00	1.60E+00	2.26E+00	2.98E+00
1.25	5.74E-01	6.08E-01	7.57E-01	1.10E+00	1.60E+00	2.35E+00	3.29E+00
1.5	5.33E-01	5.72E-01	7.29E-01	9.77E-01	1.56E+00	2.45E+00	3.53E+00
2	4.40E-01	4.63E-01	6.05E-01	9.11E-01	1.49E+00	2.57E+00	3.99E+00
3	3.24E-01	3.56E-01	4.96E-01	7.63E-01	1.37E+00	2.62E+00	4.69E+00
5	2.51E-01	2.76E-01	3.65E-01	5.63E-01	1.08E+00	2.48E+00	5.52E+00
7	2.03E-01	2.33E-01	2.92E-01	4.67E-01	8.95E-01	2.17E+00	6.06E+00
10	2.06E-01	1.94E-01	2.27E-01	3.74E-01	7.47E-01	1.81E+00	5.91E+00
15	1.81E-01	1.85E-01	2.11E-01	3.03E-01	5.35E-01	1.37E+00	5.44E+00
20	1.53E-01	1.54E-01	1.90E-01	2.47E-01	4.55E-01	1.15E+00	5.07E+00
30	1.49E-01	1.48E-01	1.58E-01	2.24E-01	3.73E-01	9.26E-01	4.67E+00
50	1.11E-01	1.11E-01	1.45E-01	1.76E-01	3.04E-01	7.51E-01	4.37E+00

Table A.4.1.2a Conversion coefficients from photon fluence to personal absorbed dose in local skin on the pillar phantom (2/2) (Otto, 2017).

	$d_{\mathrm{p\ local\ skin}}$ / (pGy cm^2) for a radiation incidence at α						
E_p / MeV	105°	120°	135°	150°	165°	180°	ROT
0.002	0.00E+00	0.00E+00	0.00E+00	0.00E+00	0.00E+00	0.00E+00	5.43E-01
0.003	0.00E+00	0.00E+00	0.00E+00	0.00E+00	0.00E+00	0.00E+00	5.48E+00
0.004	0.00E+00	0.00E+00	0.00E+00	0.00E+00	0.00E+00	0.00E+00	8.55E+00
0.005	0.00E+00	0.00E+00	0.00E+00	0.00E+00	0.00E+00	0.00E+00	8.45E+00
0.007	0.00E+00	0.00E+00	0.00E+00	0.00E+00	0.00E+00	0.00E+00	6.01E+00
0.01	4.14E-03	0.00E+00	0.00E+00	0.00E+00	0.00E+00	0.00E+00	3.41E+00
0.015	1.94E-01	1.07E-02	8.54E-04	1.52E-04	8.87E-05	3.80E-05	1.64E+00
0.02	4.41E-01	1.15E-01	3.88E-02	1.63E-02	1.05E-02	8.05E-03	1.01E+00
0.03	4.62E-01	2.65E-01	1.68E-01	1.24E-01	9.98E-02	9.86E-02	5.70E-01
0.05	3.24E-01	2.31E-01	1.86E-01	1.59E-01	1.43E-01	1.34E-01	3.38E-01
0.07	3.07E-01	2.40E-01	1.98E-01	1.67E-01	1.51E-01	1.49E-01	3.18E-01
0.1	3.99E-01	3.16E-01	2.63E-01	2.26E-01	2.17E-01	2.10E-01	4.03E-01
0.15	6.35E-01	5.25E-01	4.42E-01	3.99E-01	3.65E-01	3.56E-01	6.34E-01
0.2	9.12E-01	7.57E-01	6.46E-01	5.86E-01	5.39E-01	5.28E-01	8.87E-01
0.3	1.42E+00	1.21E+00	1.08E+00	9.82E-01	9.45E-01	9.33E-01	1.23E+00
0.5	2.12E+00	1.98E+00	1.85E+00	1.74E+00	1.68E+00	1.65E+00	1.64E+00
0.662	2.55E+00	2.48E+00	2.36E+00	2.28E+00	2.22E+00	2.18E+00	1.88E+00
0.7	2.66E+00	2.57E+00	2.46E+00	2.38E+00	2.32E+00	2.32E+00	1.93E+00
1	3.34E+00	3.36E+00	3.28E+00	3.24E+00	3.18E+00	3.19E+00	2.32E+00
1.25	3.75E+00	3.95E+00	3.93E+00	3.91E+00	3.92E+00	3.88E+00	2.62E+00
1.5	4.22E+00	4.48E+00	4.50E+00	4.47E+00	4.43E+00	4.49E+00	2.87E+00
2	4.97E+00	5.47E+00	5.63E+00	5.60E+00	5.62E+00	5.69E+00	3.37E+00
3	6.38E+00	7.19E+00	7.62E+00	7.67E+00	7.62E+00	7.67E+00	4.23E+00
5	8.92E+00	1.04E+01	1.11E+01	1.13E+01	1.14E+01	1.14E+01	5.77E+00
7	1.07E+01	1.33E+01	1.43E+01	1.47E+01	1.49E+01	1.49E+01	7.14E+00
10	1.28E+01	1.71E+01	1.90E+01	1.97E+01	2.00E+01	2.02E+01	9.01E+00
15	1.44E+01	2.18E+01	2.61E+01	2.79E+01	2.84E+01	2.86E+01	1.18E+01
20	1.50E+01	2.43E+01	3.06E+01	3.41E+01	3.57E+01	3.60E+01	1.38E+01
30	1.58E+01	2.71E+01	3.58E+01	4.13E+01	4.44E+01	4.53E+01	1.61E+01
50	1.70E+01	3.07E+01	4.16E+01	4.93E+01	5.37E+01	5.53E+01	1.88E+01

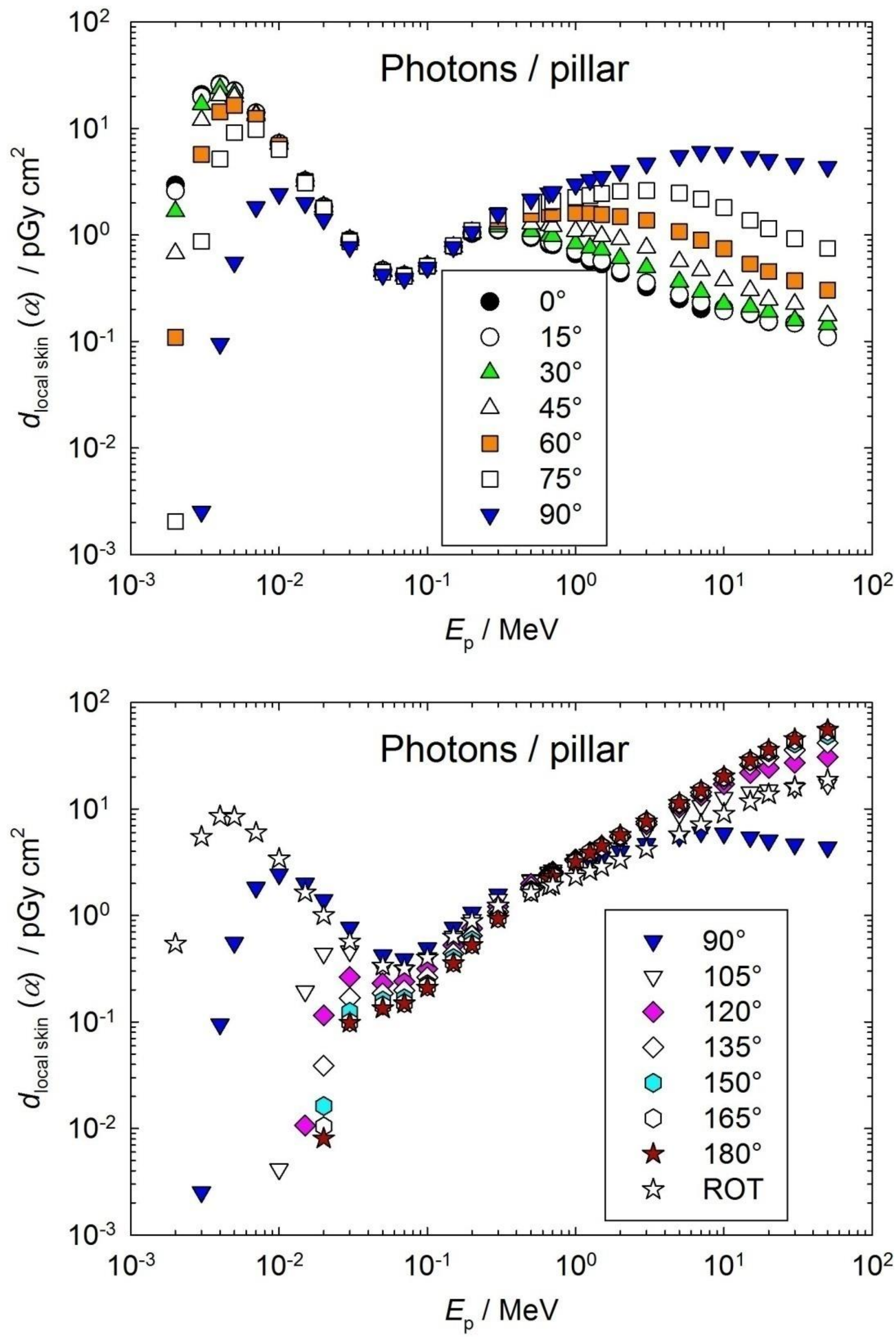

Figure A.4.1.2a Conversion coefficients from photon fluence to personal absorbed dose in local skin on the pillar phantom (Otto, 2017).

Table A.4.1.2b Conversion coefficients from photon air kerma to personal absorbed dose in local skin on the pillar phantom (1/2) (Otto, 2017).

E_p / MeV	$d_{p\,\text{local skin}}$ / (GyGy^{-1}) for a radiation incidence at α						
	0°	15°	30°	45°	60°	75°	90°
0.002	1.80E-02	1.58E-02	1.02E-02	4.11E-03	6.70E-04	1.25E-05	2.00E-07
0.003	2.76E-01	2.64E-01	2.24E-01	1.59E-01	7.59E-02	1.16E-02	3.36E-05
0.004	5.50E-01	5.39E-01	5.01E-01	4.28E-01	3.01E-01	1.09E-01	2.00E-03
0.005	7.40E-01	7.31E-01	7.04E-01	6.48E-01	5.38E-01	2.98E-01	1.81E-02
0.007	9.04E-01	9.01E-01	8.87E-01	8.60E-01	8.02E-01	6.33E-01	1.18E-01
0.01	9.74E-01	9.75E-01	9.69E-01	9.65E-01	9.38E-01	8.61E-01	3.30E-01
0.015	1.03E+00	1.03E+00	1.03E+00	1.02E+00	1.02E+00	9.86E-01	6.39E-01
0.02	1.10E+00	1.09E+00	1.10E+00	1.09E+00	1.07E+00	1.05E+00	8.35E-01
0.03	1.24E+00	1.25E+00	1.25E+00	1.23E+00	1.23E+00	1.20E+00	1.07E+00
0.05	1.44E+00	1.45E+00	1.41E+00	1.43E+00	1.41E+00	1.39E+00	1.31E+00
0.07	1.46E+00	1.46E+00	1.45E+00	1.43E+00	1.44E+00	1.43E+00	1.35E+00
0.1	1.37E+00	1.38E+00	1.38E+00	1.37E+00	1.37E+00	1.38E+00	1.33E+00
0.15	1.30E+00	1.30E+00	1.29E+00	1.29E+00	1.31E+00	1.33E+00	1.29E+00
0.2	1.20E+00	1.22E+00	1.23E+00	1.24E+00	1.26E+00	1.29E+00	1.25E+00
0.3	8.01E-01	8.14E-01	8.62E-01	9.27E-01	1.02E+00	1.11E+00	1.14E+00
0.5	3.96E-01	4.08E-01	4.57E-01	5.38E-01	6.58E-01	7.97E-01	9.11E-01
0.662	2.63E-01	2.76E-01	3.16E-01	3.97E-01	5.06E-01	6.56E-01	7.94E-01
0.7	2.46E-01	2.55E-01	2.98E-01	3.71E-01	4.88E-01	6.36E-01	7.75E-01
1	1.48E-01	1.58E-01	1.86E-01	2.43E-01	3.57E-01	5.04E-01	6.65E-01
1.25	1.08E-01	1.14E-01	1.42E-01	2.06E-01	3.00E-01	4.41E-01	6.17E-01
1.5	8.68E-02	9.30E-02	1.19E-01	1.59E-01	2.54E-01	3.99E-01	5.74E-01
2	5.82E-02	6.13E-02	8.01E-02	1.21E-01	1.97E-01	3.40E-01	5.28E-01
3	3.25E-02	3.57E-02	4.97E-02	7.65E-02	1.38E-01	2.62E-01	4.70E-01
5	1.77E-02	1.94E-02	2.57E-02	3.97E-02	7.60E-02	1.75E-01	3.90E-01
7	1.11E-02	1.28E-02	1.61E-02	2.57E-02	4.92E-02	1.20E-01	3.33E-01
10	8.54E-03	8.05E-03	9.39E-03	1.55E-02	3.09E-02	7.50E-02	2.45E-01
15	5.25E-03	5.36E-03	6.13E-03	8.80E-03	1.55E-02	3.98E-02	1.58E-01
20	3.37E-03	3.40E-03	4.20E-03	5.45E-03	1.00E-02	2.54E-02	1.12E-01
30	2.17E-03	2.16E-03	2.31E-03	3.27E-03	5.44E-03	1.35E-02	6.81E-02
50	9.33E-04	9.27E-04	1.22E-03	1.48E-03	2.55E-03	6.30E-03	3.67E-02

Table A.4.1.2b Conversion coefficients from photon air kerma to personal absorbed dose in local skin on the pillar phantom (2/2) (Otto, 2017).

	$d_{\mathrm{p\ local\ skin}}$ / (GyGy^{-1}) for a radiation incidence at α						
E_{p} / MeV	105°	120°	135°	150°	165°	180°	ROT
0.002	0.00E+00	0.00E+00	0.00E+00	0.00E+00	0.00E+00	0.00E+00	3.32E-03
0.003	0.00E+00	0.00E+00	0.00E+00	0.00E+00	0.00E+00	0.00E+00	7.27E-02
0.004	0.00E+00	0.00E+00	0.00E+00	0.00E+00	0.00E+00	0.00E+00	1.80E-01
0.005	0.00E+00	0.00E+00	0.00E+00	0.00E+00	0.00E+00	0.00E+00	2.76E-01
0.007	0.00E+00	0.00E+00	0.00E+00	0.00E+00	0.00E+00	0.00E+00	3.88E-01
0.01	5.60E-04	0.00E+00	0.00E+00	0.00E+00	0.00E+00	0.00E+00	4.61E-01
0.015	6.21E-02	3.41E-03	2.73E-04	4.87E-05	2.84E-05	1.22E-05	5.26E-01
0.02	2.62E-01	6.85E-02	2.31E-02	9.66E-03	6.24E-03	4.78E-03	5.97E-01
0.03	6.40E-01	3.67E-01	2.33E-01	1.72E-01	1.38E-01	1.37E-01	7.90E-01
0.05	1.00E+00	7.15E-01	5.75E-01	4.92E-01	4.44E-01	4.16E-01	1.05E+00
0.07	1.07E+00	8.36E-01	6.87E-01	5.79E-01	5.26E-01	5.19E-01	1.10E+00
0.1	1.07E+00	8.51E-01	7.08E-01	6.09E-01	5.85E-01	5.65E-01	1.08E+00
0.15	1.06E+00	8.75E-01	7.37E-01	6.65E-01	6.08E-01	5.93E-01	1.06E+00
0.2	1.07E+00	8.84E-01	7.54E-01	6.84E-01	6.29E-01	6.16E-01	1.04E+00
0.3	1.03E+00	8.76E-01	7.82E-01	7.10E-01	6.84E-01	6.75E-01	8.91E-01
0.5	8.92E-01	8.32E-01	7.77E-01	7.33E-01	7.06E-01	6.93E-01	6.88E-01
0.662	8.20E-01	7.95E-01	7.58E-01	7.34E-01	7.14E-01	7.02E-01	6.04E-01
0.7	8.13E-01	7.85E-01	7.52E-01	7.27E-01	7.10E-01	7.08E-01	5.91E-01
1	7.45E-01	7.50E-01	7.32E-01	7.23E-01	7.10E-01	7.12E-01	5.18E-01
1.25	7.03E-01	7.41E-01	7.37E-01	7.33E-01	7.35E-01	7.28E-01	4.91E-01
1.5	6.87E-01	7.28E-01	7.32E-01	7.27E-01	7.21E-01	7.31E-01	4.67E-01
2	6.58E-01	7.23E-01	7.45E-01	7.42E-01	7.44E-01	7.52E-01	4.45E-01
3	6.39E-01	7.21E-01	7.64E-01	7.69E-01	7.64E-01	7.69E-01	4.24E-01
5	6.29E-01	7.33E-01	7.80E-01	7.97E-01	8.03E-01	8.04E-01	4.07E-01
7	5.89E-01	7.33E-01	7.89E-01	8.08E-01	8.19E-01	8.21E-01	3.92E-01
10	5.30E-01	7.10E-01	7.88E-01	8.18E-01	8.30E-01	8.37E-01	3.74E-01
15	4.19E-01	6.33E-01	7.57E-01	8.10E-01	8.25E-01	8.29E-01	3.41E-01
20	3.31E-01	5.35E-01	6.75E-01	7.52E-01	7.87E-01	7.94E-01	3.03E-01
30	2.31E-01	3.95E-01	5.22E-01	6.02E-01	6.47E-01	6.61E-01	2.35E-01
50	1.43E-01	2.57E-01	3.49E-01	4.13E-01	4.51E-01	4.64E-01	1.58E-01

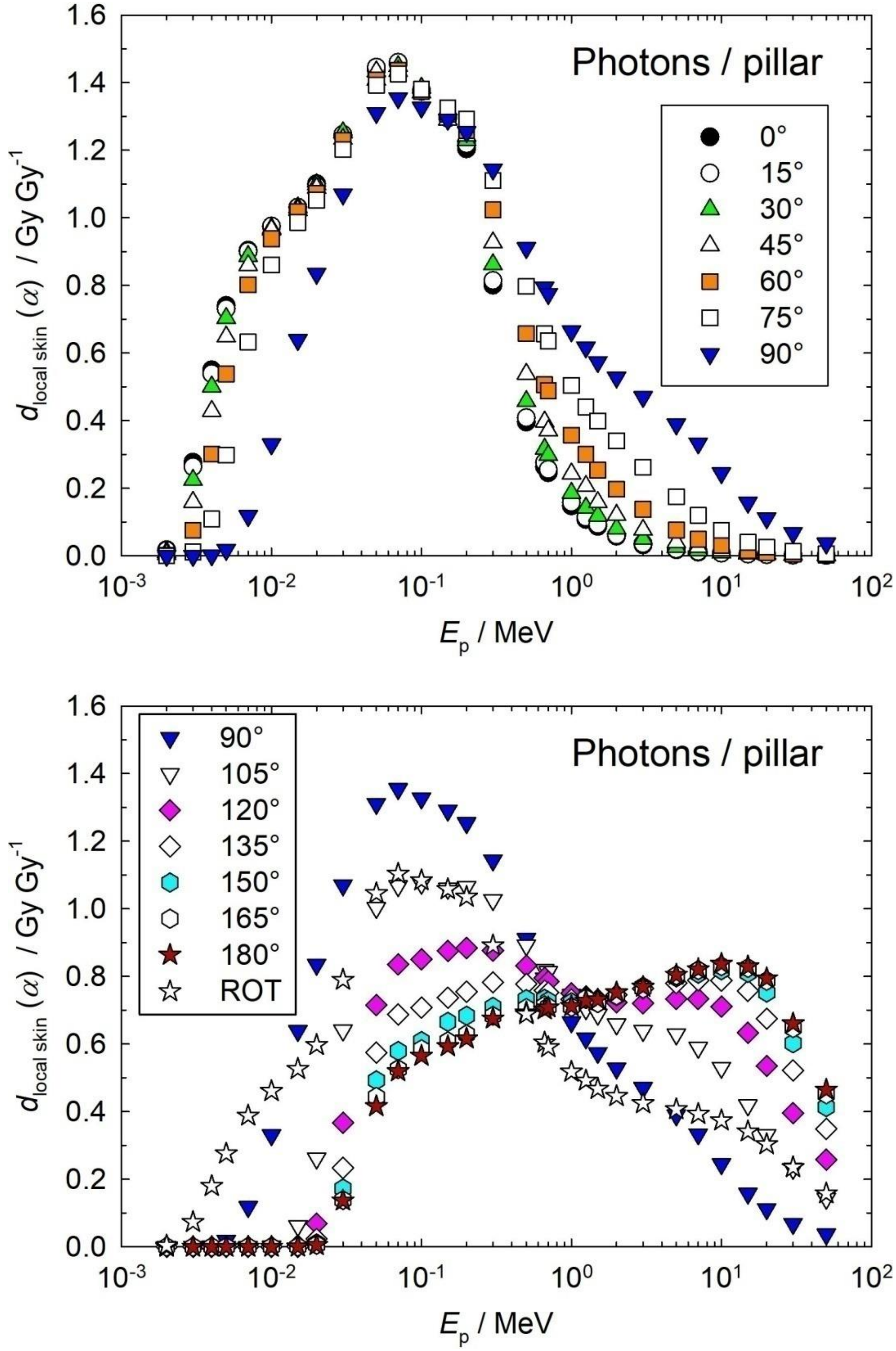

Figure A.4.1.2b Conversion coefficients from photon air kerma to personal absorbed dose in local skin on the pillar phantom (Otto, 2017).

Table A.4.1.3a Conversion coefficients from photon fluence to personal absorbed dose in local skin on the rod phantom (1/2) (Otto, 2017).

	$d_{\mathrm{p\ local\ skin}}$ / (pGy cm^2) for a radiation incidence at α						
E_p / MeV	0°	15°	30°	45°	60°	75°	90°
0.002	2.54E+00	2.28E+00	1.63E+00	9.08E-01	3.62E-01	8.54E-02	0.00E+00
0.003	1.97E+01	1.87E+01	1.58E+01	1.14E+01	6.66E+00	2.91E+00	7.39E-01
0.004	2.56E+01	2.49E+01	2.29E+01	1.90E+01	1.32E+01	7.36E+00	2.84E+00
0.005	2.24E+01	2.21E+01	2.10E+01	1.88E+01	1.45E+01	9.19E+00	4.35E+00
0.007	1.39E+01	1.38E+01	1.36E+01	1.30E+01	1.14E+01	8.19E+00	4.71E+00
0.01	7.22E+00	7.21E+00	7.17E+00	7.06E+00	6.68E+00	5.44E+00	3.65E+00
0.015	3.23E+00	3.22E+00	3.21E+00	3.18E+00	3.11E+00	2.83E+00	2.29E+00
0.02	1.80E+00	1.80E+00	1.80E+00	1.79E+00	1.77E+00	1.69E+00	1.50E+00
0.03	8.14E-01	8.14E-01	8.13E-01	8.09E-01	8.03E-01	7.84E-01	7.41E-01
0.05	3.83E-01	3.82E-01	3.81E-01	3.79E-01	3.77E-01	3.71E-01	3.58E-01
0.06	3.43E-01	3.43E-01	3.43E-01	3.42E-01	3.41E-01	3.37E-01	3.26E-01
0.07	3.44E-01	3.44E-01	3.44E-01	3.44E-01	3.43E-01	3.39E-01	3.29E-01
0.1	4.36E-01	4.36E-01	4.36E-01	4.36E-01	4.36E-01	4.33E-01	4.24E-01
0.15	6.93E-01	6.93E-01	6.94E-01	6.96E-01	6.97E-01	6.93E-01	6.79E-01
0.2	9.51E-01	9.53E-01	9.57E-01	9.64E-01	9.73E-01	9.74E-01	9.59E-01
0.3	1.02E+00	1.04E+00	1.10E+00	1.18E+00	1.28E+00	1.37E+00	1.42E+00
0.5	8.71E-01	9.05E-01	1.01E+00	1.19E+00	1.44E+00	1.70E+00	1.94E+00
0.662	7.67E-01	8.08E-01	9.36E-01	1.16E+00	1.48E+00	1.86E+00	2.22E+00
0.7	7.49E-01	7.90E-01	9.19E-01	1.15E+00	1.48E+00	1.88E+00	2.27E+00
1	6.19E-01	6.65E-01	8.10E-01	1.08E+00	1.51E+00	2.06E+00	2.65E+00
1.25	5.34E-01	5.79E-01	7.28E-01	1.02E+00	1.50E+00	2.16E+00	2.90E+00
1.5	4.72E-01	5.16E-01	6.63E-01	9.64E-01	1.48E+00	2.23E+00	3.09E+00
2	3.89E-01	4.28E-01	5.62E-01	8.55E-01	1.41E+00	2.29E+00	3.39E+00
3	2.92E-01	3.20E-01	4.27E-01	6.74E-01	1.21E+00	2.22E+00	3.65E+00
5	2.04E-01	2.23E-01	2.90E-01	4.56E-01	8.71E-01	1.82E+00	3.45E+00
10	1.33E-01	1.43E-01	1.79E-01	2.70E-01	5.29E-01	1.27E+00	2.75E+00
15	1.09E-01	1.17E-01	1.44E-01	2.13E-01	4.23E-01	1.10E+00	2.53E+00
20	9.85E-02	1.05E-01	1.28E-01	1.87E-01	3.73E-01	1.02E+00	2.45E+00
30	8.76E-02	9.32E-02	1.13E-01	1.62E-01	3.28E-01	9.65E-01	2.43E+00
50	8.12E-02	8.56E-02	1.02E-01	1.46E-01	3.00E-01	9.53E-01	2.51E+00

Table A.4.1.3a Conversion coefficients from photon fluence to personal absorbed dose in local skin on the rod phantom (2/2) (Otto, 2017).

	$d_{\mathrm{p\ local\ skin}}$ / (pGy cm^2) for a radiation incidence at α						
E_p / MeV	105°	120°	135°	150°	165°	180°	ROT
0.002	0.00E+00	0.00E+00	0.00E+00	0.00E+00	0.00E+00	0.00E+00	5.45E-01
0.003	4.71E-02	0.00E+00	0.00E+00	0.00E+00	0.00E+00	0.00E+00	5.51E+00
0.004	4.55E-01	0.00E+00	0.00E+00	0.00E+00	0.00E+00	0.00E+00	8.62E+00
0.005	1.08E+00	1.93E-02	0.00E+00	0.00E+00	0.00E+00	0.00E+00	8.52E+00
0.007	1.77E+00	1.70E-01	0.00E+00	0.00E+00	0.00E+00	0.00E+00	6.13E+00
0.01	1.85E+00	5.05E-01	5.54E-02	0.00E+00	0.00E+00	0.00E+00	3.60E+00
0.015	1.61E+00	9.41E-01	4.97E-01	2.91E-01	2.06E-01	1.84E-01	1.93E+00
0.02	1.24E+00	9.50E-01	7.16E-01	5.72E-01	4.97E-01	4.73E-01	1.29E+00
0.03	6.77E-01	6.02E-01	5.34E-01	4.86E-01	4.58E-01	4.49E-01	6.79E-01
0.05	3.39E-01	3.16E-01	2.95E-01	2.79E-01	2.69E-01	2.66E-01	3.39E-01
0.06	3.09E-01	2.89E-01	2.72E-01	2.59E-01	2.51E-01	2.48E-01	3.09E-01
0.07	3.14E-01	2.96E-01	2.78E-01	2.65E-01	2.57E-01	2.55E-01	3.13E-01
0.1	4.08E-01	3.89E-01	3.70E-01	3.56E-01	3.47E-01	3.44E-01	4.05E-01
0.15	6.57E-01	6.30E-01	6.05E-01	5.85E-01	5.71E-01	5.66E-01	6.53E-01
0.2	9.33E-01	8.95E-01	8.61E-01	8.39E-01	8.27E-01	8.25E-01	9.19E-01
0.3	1.44E+00	1.43E+00	1.40E+00	1.37E+00	1.35E+00	1.34E+00	1.30E+00
0.5	2.11E+00	2.20E+00	2.24E+00	2.25E+00	2.24E+00	2.24E+00	1.73E+00
0.662	2.50E+00	2.69E+00	2.79E+00	2.83E+00	2.85E+00	2.85E+00	1.99E+00
0.7	2.59E+00	2.79E+00	2.91E+00	2.96E+00	2.98E+00	2.99E+00	2.05E+00
1	3.17E+00	3.54E+00	3.77E+00	3.89E+00	3.95E+00	3.97E+00	2.45E+00
1.25	3.57E+00	4.08E+00	4.39E+00	4.57E+00	4.65E+00	4.68E+00	2.73E+00
1.5	3.92E+00	4.56E+00	4.97E+00	5.19E+00	5.30E+00	5.33E+00	2.98E+00
2	4.50E+00	5.41E+00	6.00E+00	6.33E+00	6.49E+00	6.53E+00	3.43E+00
3	5.27E+00	6.71E+00	7.73E+00	8.31E+00	8.59E+00	8.67E+00	4.13E+00
5	5.60E+00	7.86E+00	9.76E+00	1.11E+01	1.18E+01	1.20E+01	4.94E+00
10	4.93E+00	7.50E+00	9.93E+00	1.18E+01	1.30E+01	1.34E+01	4.92E+00
15	4.72E+00	7.37E+00	9.92E+00	1.19E+01	1.32E+01	1.36E+01	4.88E+00
20	4.68E+00	7.41E+00	1.01E+01	1.22E+01	1.35E+01	1.40E+01	4.93E+00
30	4.76E+00	7.67E+00	1.05E+01	1.28E+01	1.43E+01	1.48E+01	5.13E+00
50	5.02E+00	8.20E+00	1.14E+01	1.39E+01	1.55E+01	1.61E+01	5.51E+00

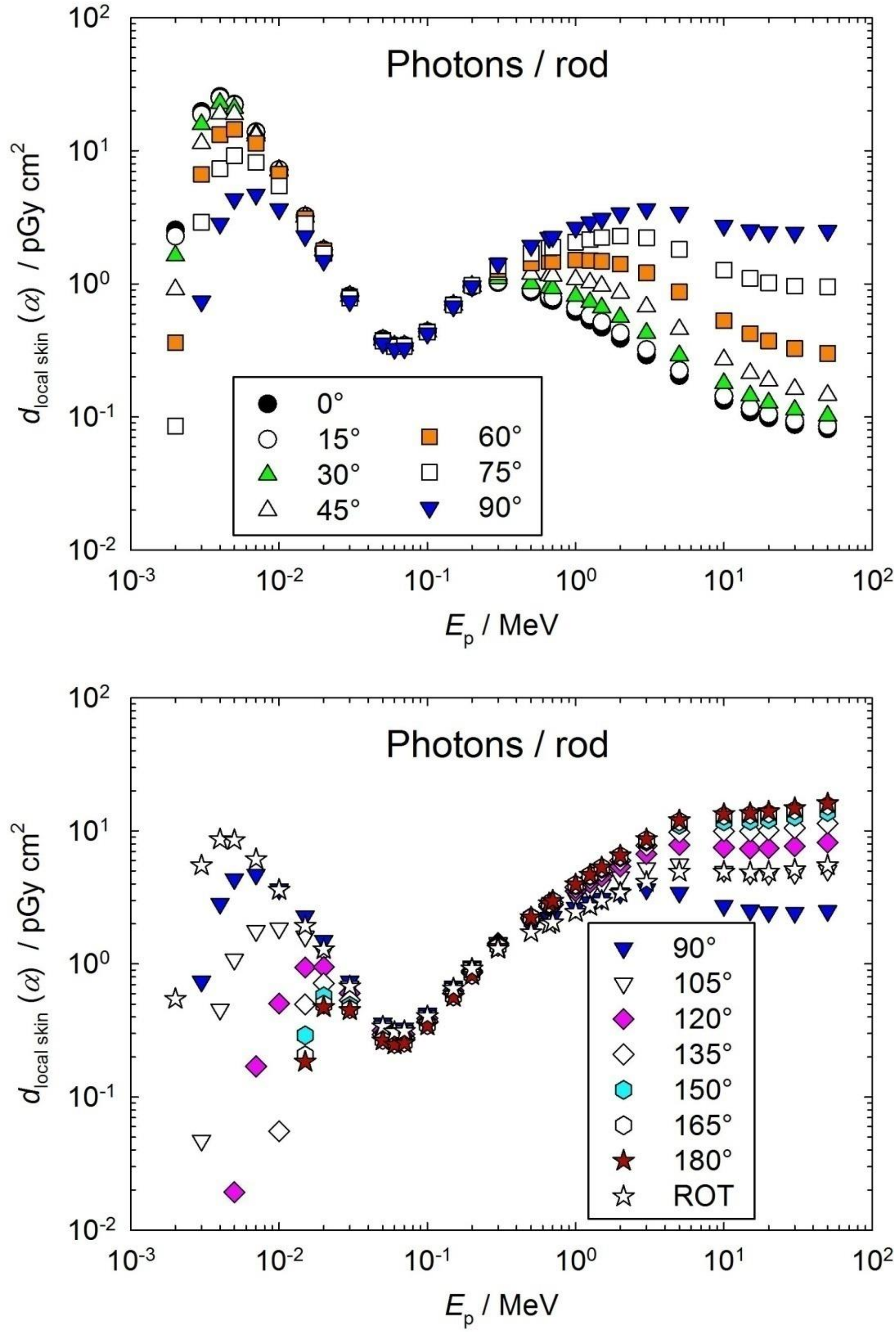

Figure A.4.1.3a Conversion coefficients from photon fluence to personal absorbed dose in local skin on the rod phantom (Otto, 2017).

Table A.4.1.3b Conversion coefficients from photon air kerma to personal absorbed dose in local skin on the rod phantom (1/2) (Otto, 2017).

	$d_{\mathrm{p\ local\ skin}}$ / (GyGy^{-1}) for a radiation incidence at α						
E_{p} / MeV	0°	15°	30°	45°	60°	75°	90°
0.002	1.55E-02	1.39E-02	9.96E-03	5.55E-03	2.21E-03	5.22E-04	0.00E+00
0.003	2.62E-01	2.48E-01	2.10E-01	1.51E-01	8.84E-02	3.86E-02	9.81E-03
0.004	5.38E-01	5.23E-01	4.81E-01	3.99E-01	2.77E-01	1.55E-01	5.96E-02
0.005	7.31E-01	7.21E-01	6.85E-01	6.13E-01	4.73E-01	3.00E-01	1.42E-01
0.007	8.97E-01	8.90E-01	8.77E-01	8.39E-01	7.35E-01	5.28E-01	3.04E-01
0.01	9.76E-01	9.74E-01	9.69E-01	9.54E-01	9.03E-01	7.35E-01	4.93E-01
0.015	1.03E+00	1.03E+00	1.03E+00	1.02E+00	9.95E-01	9.06E-01	7.33E-01
0.02	1.07E+00	1.07E+00	1.07E+00	1.06E+00	1.05E+00	1.00E+00	8.91E-01
0.03	1.13E+00	1.13E+00	1.13E+00	1.12E+00	1.11E+00	1.09E+00	1.03E+00
0.05	1.19E+00	1.18E+00	1.18E+00	1.17E+00	1.17E+00	1.15E+00	1.11E+00
0.06	1.19E+00	1.19E+00	1.19E+00	1.18E+00	1.18E+00	1.17E+00	1.13E+00
0.07	1.20E+00	1.20E+00	1.20E+00	1.20E+00	1.19E+00	1.18E+00	1.14E+00
0.1	1.17E+00	1.17E+00	1.17E+00	1.17E+00	1.17E+00	1.17E+00	1.14E+00
0.15	1.16E+00	1.16E+00	1.16E+00	1.16E+00	1.16E+00	1.16E+00	1.13E+00
0.2	1.11E+00	1.11E+00	1.12E+00	1.13E+00	1.14E+00	1.14E+00	1.12E+00
0.3	7.38E-01	7.52E-01	7.95E-01	8.53E-01	9.26E-01	9.91E-01	1.03E+00
0.5	3.66E-01	3.80E-01	4.25E-01	5.00E-01	6.05E-01	7.15E-01	8.15E-01
0.662	2.46E-01	2.60E-01	3.01E-01	3.73E-01	4.76E-01	5.98E-01	7.13E-01
0.7	2.29E-01	2.41E-01	2.81E-01	3.51E-01	4.52E-01	5.74E-01	6.93E-01
1	1.05E-01	1.15E-01	1.48E-01	2.15E-01	3.30E-01	4.98E-01	6.90E-01
1.25	1.00E-01	1.09E-01	1.37E-01	1.91E-01	2.81E-01	4.05E-01	5.44E-01
1.5	1.01E-01	1.08E-01	1.32E-01	1.76E-01	2.46E-01	3.35E-01	4.31E-01
2	5.15E-02	5.66E-02	7.44E-02	1.13E-01	1.87E-01	3.03E-01	4.49E-01
3	2.93E-02	3.21E-02	4.28E-02	6.76E-02	1.21E-01	2.23E-01	3.66E-01
5	1.44E-02	1.57E-02	2.05E-02	3.22E-02	6.14E-02	1.28E-01	2.43E-01
10	5.51E-03	5.93E-03	7.42E-03	1.12E-02	2.19E-02	5.26E-02	1.14E-01
15	3.16E-03	3.40E-03	4.18E-03	6.18E-03	1.23E-02	3.19E-02	7.34E-02
20	2.17E-03	2.31E-03	2.82E-03	4.12E-03	8.22E-03	2.25E-02	5.40E-02
30	1.28E-03	1.36E-03	1.65E-03	2.36E-03	4.78E-03	1.41E-02	3.54E-02
50	6.81E-04	7.18E-04	8.56E-04	1.22E-03	2.52E-03	7.99E-03	2.11E-02

Table A.4.1.3b Conversion coefficients from photon air kerma to personal absorbed dose in local skin on the rod phantom (2/2) (Otto, 2017).

	$d_{\mathrm{p\ local\ skin}}$ / (GyGy^{-1}) for a radiation incidence at α						
E_{p} / MeV	105°	120°	135°	150°	165°	180°	ROT
0.002	0.00E+00	0.00E+00	0.00E+00	0.00E+00	0.00E+00	0.00E+00	3.33E-03
0.003	6.25E-04	0.00E+00	0.00E+00	0.00E+00	0.00E+00	0.00E+00	7.32E-02
0.004	9.55E-03	0.00E+00	0.00E+00	0.00E+00	0.00E+00	0.00E+00	1.81E-01
0.005	3.52E-02	6.30E-04	0.00E+00	0.00E+00	0.00E+00	0.00E+00	2.78E-01
0.007	1.14E-01	1.10E-02	0.00E+00	0.00E+00	0.00E+00	0.00E+00	3.95E-01
0.01	2.50E-01	6.82E-02	7.49E-03	0.00E+00	0.00E+00	0.00E+00	4.86E-01
0.015	5.15E-01	3.01E-01	1.59E-01	9.31E-02	6.59E-02	5.89E-02	6.18E-01
0.02	7.36E-01	5.64E-01	4.25E-01	3.40E-01	2.95E-01	2.81E-01	7.66E-01
0.03	9.38E-01	8.34E-01	7.40E-01	6.73E-01	6.35E-01	6.22E-01	9.41E-01
0.05	1.05E+00	9.79E-01	9.14E-01	8.64E-01	8.33E-01	8.24E-01	1.05E+00
0.06	1.07E+00	1.00E+00	9.42E-01	8.97E-01	8.69E-01	8.58E-01	1.07E+00
0.07	1.09E+00	1.03E+00	9.66E-01	9.21E-01	8.93E-01	8.86E-01	1.09E+00
0.1	1.10E+00	1.05E+00	9.96E-01	9.59E-01	9.34E-01	9.26E-01	1.09E+00
0.15	1.10E+00	1.05E+00	1.01E+00	9.76E-01	9.53E-01	9.44E-01	1.09E+00
0.2	1.09E+00	1.04E+00	1.01E+00	9.79E-01	9.65E-01	9.63E-01	1.07E+00
0.3	1.04E+00	1.03E+00	1.01E+00	9.91E-01	9.76E-01	9.69E-01	9.40E-01
0.5	8.87E-01	9.25E-01	9.42E-01	9.46E-01	9.42E-01	9.42E-01	7.27E-01
0.662	8.03E-01	8.64E-01	8.97E-01	9.09E-01	9.16E-01	9.16E-01	6.39E-01
0.7	7.91E-01	8.52E-01	8.89E-01	9.04E-01	9.10E-01	9.13E-01	6.26E-01
1	8.75E-01	1.02E+00	1.11E+00	1.16E+00	1.18E+00	1.19E+00	6.65E-01
1.25	6.70E-01	7.65E-01	8.23E-01	8.57E-01	8.72E-01	8.78E-01	5.12E-01
1.5	5.16E-01	5.76E-01	6.13E-01	6.33E-01	6.43E-01	6.46E-01	3.99E-01
2	5.95E-01	7.16E-01	7.94E-01	8.38E-01	8.59E-01	8.64E-01	4.54E-01
3	5.28E-01	6.73E-01	7.75E-01	8.33E-01	8.61E-01	8.69E-01	4.14E-01
5	3.95E-01	5.54E-01	6.88E-01	7.83E-01	8.32E-01	8.46E-01	3.48E-01
10	2.04E-01	3.11E-01	4.12E-01	4.89E-01	5.39E-01	5.55E-01	2.04E-01
15	1.37E-01	2.14E-01	2.88E-01	3.45E-01	3.83E-01	3.95E-01	1.42E-01
20	1.03E-01	1.63E-01	2.23E-01	2.69E-01	2.98E-01	3.09E-01	1.09E-01
30	6.94E-02	1.12E-01	1.53E-01	1.87E-01	2.08E-01	2.16E-01	7.48E-02
50	4.21E-02	6.88E-02	9.56E-02	1.17E-01	1.30E-01	1.35E-01	4.62E-02

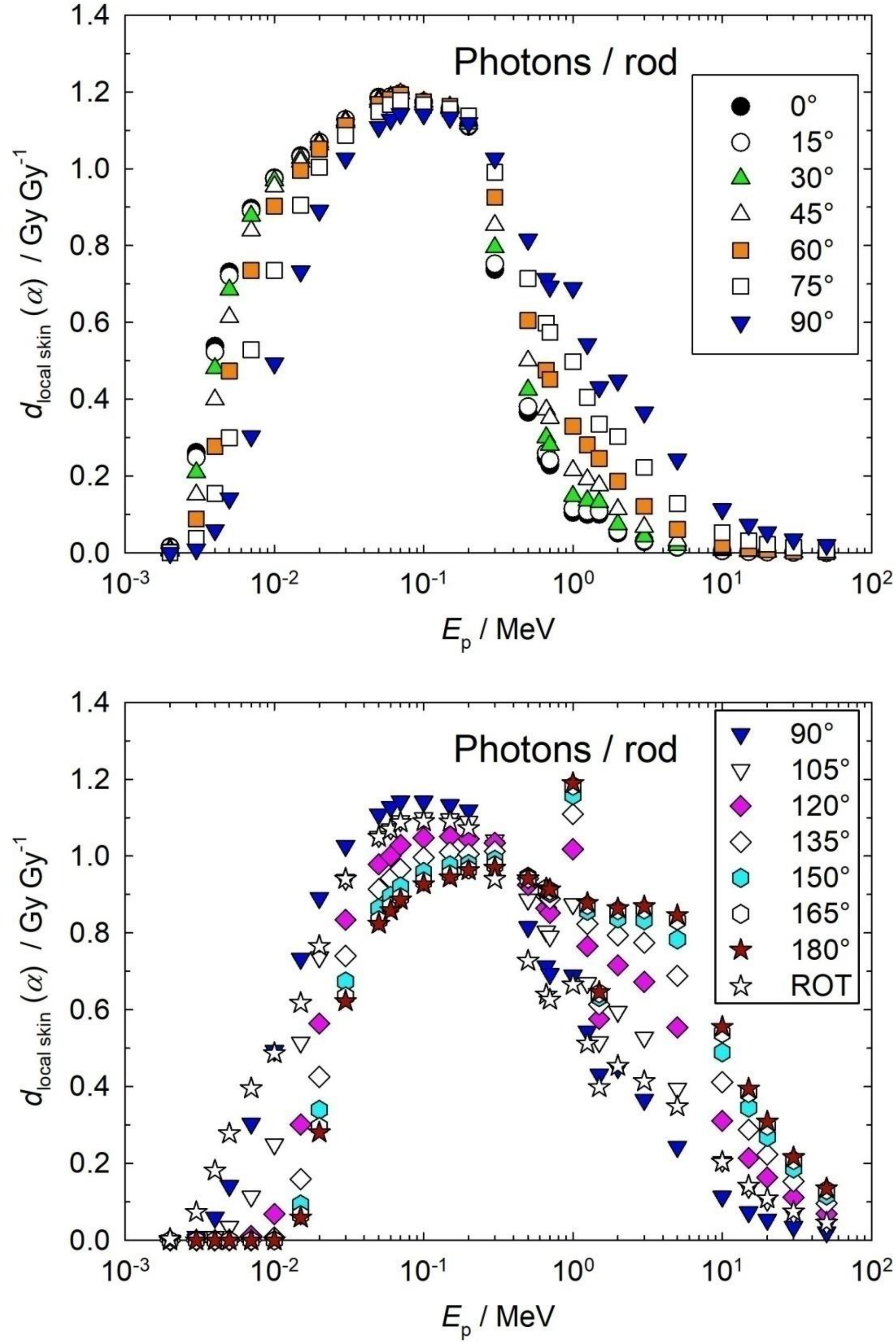

Figure A.4.1.3b Conversion coefficients from photon air kerma to personal absorbed dose in local skin on the rod phantom (Otto, 2017).

Table A.4.2.1 Conversion coefficients from neutron fluence to directional and personal absorbed dose in local skin on the slab phantom.

Figure A.4.2.1 Conversion coefficients from neutron fluence to directional and personal absorbed dose in local skin on the slab phantom.

1010 Table A.4.2.2 Conversion coefficients from neutron fluence to personal absorbed dose in local skin on
1011 the pillar phantom (1/2) (Hertel and Veinot, 2017).

	$d_{\mathrm{p\ local\ skin}}$ / (pGy cm²) for a radiation incidence at α						
E_{p} / MeV	0°	15°	30°	45°	60°	75°	90°
1.00E-09	3.14E+00	3.10E+00	2.97E+00	2.83E+00	2.52E+00	2.02E+00	7.31E-01
1.00E-08	1.77E+00	1.72E+00	1.67E+00	1.52E+00	1.34E+00	1.09E+00	5.65E-01
2.50E-08	1.44E+00	1.43E+00	1.35E+00	1.24E+00	1.12E+00	9.15E-01	5.48E-01
1.00E-07	1.18E+00	1.18E+00	1.10E+00	1.06E+00	9.44E-01	7.79E-01	5.71E-01
2.00E-07	1.09E+00	1.08E+00	1.05E+00	9.80E-01	8.91E-01	7.72E-01	6.18E-01
5.00E-07	9.87E-01	1.01E+00	9.43E-01	8.85E-01	8.62E-01	7.55E-01	6.14E-01
1.00E-06	9.36E-01	9.21E-01	8.71E-01	8.59E-01	8.10E-01	6.95E-01	6.19E-01
2.00E-06	8.41E-01	8.17E-01	8.26E-01	8.01E-01	7.45E-01	7.07E-01	5.98E-01
5.00E-06	7.95E-01	7.97E-01	7.60E-01	7.33E-01	6.88E-01	6.43E-01	1.00E-20
1.00E-05	7.34E-01	7.17E-01	7.44E-01	7.06E-01	6.69E-01	6.17E-01	5.22E-01
2.00E-05	6.98E-01	6.84E-01	6.89E-01	6.39E-01	6.05E-01	5.67E-01	5.11E-01
5.00E-05	6.31E-01	6.01E-01	6.06E-01	5.81E-01	5.70E-01	5.25E-01	4.97E-01
1.00E-04	5.65E-01	5.44E-01	5.77E-01	5.68E-01	5.20E-01	4.88E-01	4.55E-01
2.00E-04	5.35E-01	5.31E-01	5.38E-01	5.12E-01	4.93E-01	4.93E-01	4.50E-01
5.00E-04	5.25E-01	5.37E-01	5.28E-01	5.14E-01	5.04E-01	4.75E-01	4.44E-01
1.00E-03	5.50E-01	5.65E-01	5.53E-01	5.22E-01	5.14E-01	5.12E-01	4.42E-01
2.00E-03	6.08E-01	6.05E-01	6.24E-01	6.20E-01	6.08E-01	5.90E-01	5.17E-01
5.00E-03	8.93E-01	8.78E-01	8.97E-01	8.87E-01	9.02E-01	9.03E-01	7.14E-01
1.00E-02	1.35E+00	1.34E+00	1.34E+00	1.37E+00	1.40E+00	1.39E+00	1.06E+00
2.00E-02	2.23E+00	2.24E+00	2.25E+00	2.28E+00	2.33E+00	2.36E+00	1.78E+00
3.00E-02	3.04E+00	3.03E+00	3.07E+00	3.10E+00	3.20E+00	3.22E+00	2.43E+00
5.00E-02	4.46E+00	4.44E+00	4.47E+00	4.56E+00	4.67E+00	4.76E+00	3.65E+00
7.00E-02	5.65E+00	5.65E+00	5.70E+00	5.80E+00	5.94E+00	6.05E+00	4.69E+00
1.00E-01	7.18E+00	7.17E+00	7.23E+00	7.36E+00	7.56E+00	7.70E+00	6.09E+00
1.50E-01	9.27E+00	9.28E+00	9.35E+00	9.49E+00	9.74E+00	9.94E+00	8.17E+00
2.00E-01	1.10E+01	1.10E+01	1.11E+01	1.12E+01	1.15E+01	1.18E+01	9.92E+00
3.00E-01	1.40E+01	1.40E+01	1.40E+01	1.42E+01	1.45E+01	1.48E+01	1.28E+01
5.00E-01	1.74E+01	1.74E+01	1.76E+01	1.81E+01	1.87E+01	1.94E+01	1.75E+01
7.00E-01	2.06E+01	2.06E+01	2.08E+01	2.12E+01	2.18E+01	2.24E+01	2.07E+01
9.00E-01	2.41E+01	2.41E+01	2.43E+01	2.46E+01	2.52E+01	2.58E+01	2.39E+01
1.00E+00	3.05E+01	3.05E+01	3.03E+01	3.02E+01	3.04E+01	3.07E+01	2.74E+01
1.20E+00	2.77E+01	2.77E+01	2.78E+01	2.80E+01	2.85E+01	2.92E+01	2.75E+01
1.50E+00	2.96E+01	2.96E+01	2.97E+01	3.00E+01	3.07E+01	3.16E+01	3.02E+01
2.00E+00	3.29E+01	3.29E+01	3.31E+01	3.35E+01	3.42E+01	3.52E+01	3.39E+01
3.00E+00	3.83E+01	3.83E+01	3.85E+01	3.88E+01	3.96E+01	4.07E+01	3.98E+01
4.00E+00	4.45E+01	4.45E+01	4.47E+01	4.53E+01	4.63E+01	4.79E+01	4.72E+01
5.00E+00	4.63E+01	4.63E+01	4.64E+01	4.66E+01	4.72E+01	4.83E+01	4.78E+01
6.00E+00	5.10E+01	5.10E+01	5.10E+01	5.12E+01	5.18E+01	5.30E+01	1.00E-20
7.00E+00	5.00E+01	4.99E+01	5.01E+01	5.06E+01	5.12E+01	5.22E+01	5.15E+01
8.00E+00	5.27E+01	5.27E+01	5.29E+01	5.33E+01	5.41E+01	5.50E+01	5.45E+01
9.00E+00	5.56E+01	5.53E+01	5.58E+01	5.59E+01	5.65E+01	5.77E+01	5.66E+01
1.00E+01	5.82E+01	5.79E+01	5.83E+01	5.85E+01	5.91E+01	6.01E+01	5.86E+01
1.20E+01	6.37E+01	6.33E+01	6.42E+01	6.45E+01	6.58E+01	6.67E+01	6.74E+01
1.40E+01	6.59E+01	6.53E+01	6.62E+01	6.66E+01	6.75E+01	6.84E+01	6.64E+01
1.50E+01	6.86E+01	6.78E+01	6.89E+01	6.94E+01	7.06E+01	7.13E+01	7.19E+01
1.60E+01	6.87E+01	6.92E+01	6.97E+01	7.02E+01	7.09E+01	7.23E+01	7.18E+01
1.80E+01	6.80E+01	6.78E+01	6.86E+01	6.95E+01	6.99E+01	7.13E+01	7.19E+01
2.00E+01	6.99E+01	7.00E+01	7.12E+01	7.16E+01	7.22E+01	7.39E+01	7.29E+01

1012
1013

Table A.4.2 Conversion coefficients from neutron fluence to personal absorbed dose in local skin on the pillar phantom (2/2) (Hertel and Veinot, 2017).

	$d_{\mathrm{p\ local\ skin}}$ / (pGy cm^2) for a radiation incidence at α						
E_p / MeV	105°	120°	135°	150°	165°	180°	ROT
1.00E-09	2.13E-01	1.78E-01	1.52E-01	1.45E-01	1.40E-01	1.42E-01	
1.00E-08	2.47E-01	2.07E-01	1.87E-01	1.67E-01	1.72E-01	1.60E-01	
2.50E-08	2.77E-01	2.39E-01	2.11E-01	1.91E-01	1.91E-01	1.80E-01	
1.00E-07	3.75E-01	3.10E-01	2.86E-01	2.68E-01	2.54E-01	2.59E-01	
2.00E-07	4.12E-01	3.55E-01	3.24E-01	2.93E-01	2.87E-01	2.82E-01	
5.00E-07	4.77E-01	4.04E-01	3.79E-01	3.57E-01	3.45E-01	3.25E-01	
1.00E-06	4.99E-01	4.28E-01	3.91E-01	3.76E-01	3.62E-01	3.53E-01	
2.00E-06	4.98E-01	4.44E-01	3.94E-01	3.94E-01	3.77E-01	3.59E-01	
5.00E-06	5.01E-01	4.44E-01	4.25E-01	3.99E-01	3.73E-01	3.72E-01	
1.00E-05	4.88E-01	4.26E-01	4.18E-01	4.02E-01	3.78E-01	3.77E-01	
2.00E-05	4.63E-01	4.27E-01	4.00E-01	3.94E-01	3.70E-01	3.55E-01	
5.00E-05	4.28E-01	4.06E-01	3.91E-01	3.86E-01	3.47E-01	3.57E-01	
1.00E-04	4.28E-01	3.92E-01	3.67E-01	3.63E-01	3.40E-01	3.43E-01	
2.00E-04	4.07E-01	3.70E-01	3.50E-01	3.51E-01	3.30E-01	3.22E-01	
5.00E-04	3.94E-01	3.53E-01	3.43E-01	3.20E-01	3.29E-01	3.25E-01	
1.00E-03	3.69E-01	3.30E-01	3.15E-01	3.09E-01	2.98E-01	3.04E-01	
2.00E-03	3.39E-01	3.22E-01	3.05E-01	3.00E-01	2.92E-01	2.86E-01	
5.00E-03	3.81E-01	3.04E-01	2.95E-01	2.81E-01	2.64E-01	2.73E-01	
1.00E-02	4.33E-01	3.11E-01	2.90E-01	2.77E-01	2.61E-01	2.69E-01	
2.00E-02	5.80E-01	3.24E-01	2.71E-01	2.57E-01	2.62E-01	2.56E-01	
3.00E-02	7.50E-01	3.61E-01	2.83E-01	2.43E-01	2.50E-01	2.33E-01	
5.00E-02	1.11E+00	4.48E-01	3.00E-01	2.60E-01	2.54E-01	2.54E-01	
7.00E-02	1.52E+00	5.59E-01	3.49E-01	2.80E-01	2.57E-01	2.59E-01	
1.00E-01	2.12E+00	7.55E-01	4.33E-01	3.49E-01	2.90E-01	2.66E-01	
1.50E-01	3.09E+00	1.22E+00	6.34E-01	4.51E-01	3.63E-01	3.41E-01	
2.00E-01	4.09E+00	1.72E+00	9.21E-01	5.81E-01	4.90E-01	4.51E-01	
3.00E-01	5.98E+00	2.79E+00	1.54E+00	1.05E+00	8.03E-01	7.54E-01	
5.00E-01	9.36E+00	4.76E+00	2.93E+00	2.12E+00	1.71E+00	1.60E+00	
7.00E-01	1.23E+01	7.15E+00	4.94E+00	3.62E+00	3.03E+00	2.91E+00	
9.00E-01	1.51E+01	8.94E+00	6.42E+00	4.80E+00	4.12E+00	3.90E+00	
1.00E+00	1.54E+01	8.13E+00	5.11E+00	3.90E+00	3.32E+00	3.11E+00	
1.20E+00	1.84E+01	1.21E+01	9.05E+00	7.10E+00	6.05E+00	5.91E+00	
1.50E+00	2.15E+01	1.54E+01	1.18E+01	9.56E+00	8.39E+00	8.16E+00	
2.00E+00	2.59E+01	1.92E+01	1.58E+01	1.31E+01	1.21E+01	1.16E+01	
3.00E+00	3.26E+01	2.48E+01	2.20E+01	1.93E+01	1.79E+01	1.76E+01	
4.00E+00	3.90E+01	3.07E+01	2.72E+01	2.40E+01	2.24E+01	2.14E+01	
5.00E+00	4.12E+01	3.37E+01	3.07E+01	2.80E+01	2.62E+01	2.54E+01	
6.00E+00	4.53E+01	3.67E+01	3.29E+01	3.07E+01	2.90E+01	2.82E+01	
7.00E+00	4.58E+01	3.93E+01	3.61E+01	3.39E+01	3.21E+01	3.22E+01	
8.00E+00	4.81E+01	4.17E+01	3.89E+01	3.65E+01	3.43E+01	3.41E+01	
9.00E+00	5.05E+01	4.35E+01	3.99E+01	3.81E+01	3.60E+01	3.57E+01	
1.00E+01	5.19E+01	4.54E+01	4.18E+01	3.94E+01	3.82E+01	3.73E+01	
1.20E+01	5.99E+01	4.88E+01	4.60E+01	4.27E+01	4.06E+01	4.14E+01	
1.40E+01	6.14E+01	5.18E+01	4.78E+01	4.86E+01	4.67E+01	4.60E+01	
1.50E+01	6.47E+01	5.42E+01	4.87E+01	4.92E+01	4.90E+01	4.81E+01	
1.60E+01	6.60E+01	5.79E+01	5.50E+01	5.18E+01	5.06E+01	5.01E+01	
1.80E+01	6.68E+01	5.56E+01	5.39E+01	5.10E+01	5.28E+01	5.26E+01	
2.00E+01	7.00E+01	5.75E+01	5.65E+01	5.52E+01	5.55E+01	5.53E+01	

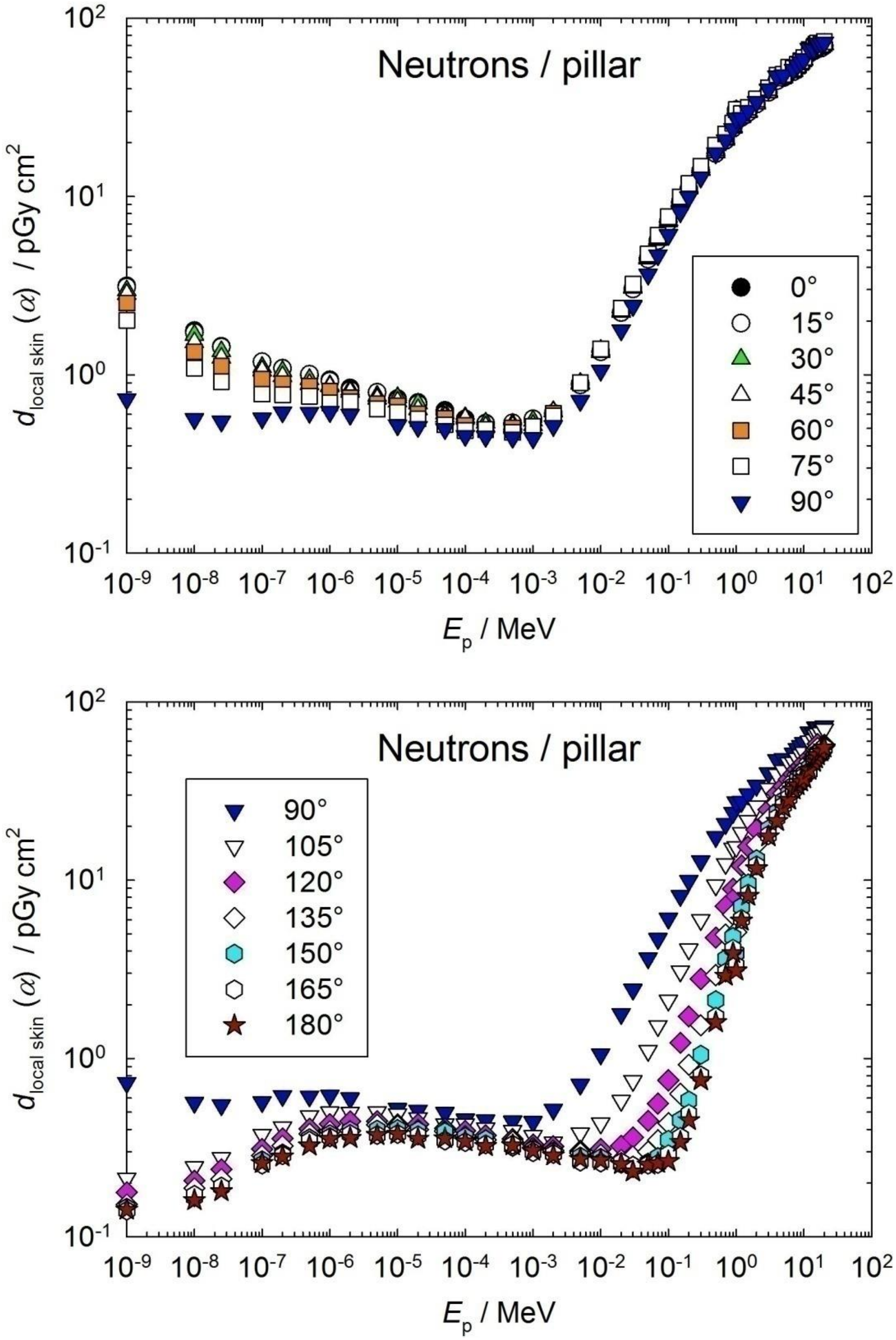

Figure A.4.2.2 Conversion coefficients from neutron fluence to personal absorbed dose in local skin on the pillar phantom (Hertel and Veinot, 2017).

Table A.4.2.3 Conversion coefficients from neutron fluence to personal absorbed dose in local skin on the rod phantom (1/2) (Hertel and Veinot, 2017).

	$d_{local\ skin}$ / pGy cm² for a radiation incidence at α						
E_p / MeV	0°	15°	30°	45°	60°	75°	90°
1.00E-09	2.66E+00	2.64E+00	2.58E+00	2.45E+00	2.12E+00	1.64E+00	1.07E+00
1.00E-08	1.22E+00	1.21E+00	1.18E+00	1.13E+00	1.05E+00	8.68E-01	6.42E-01
2.50E-08	8.56E-01	8.59E-01	8.45E-01	8.21E-01	7.51E-01	6.35E-01	5.25E-01
1.00E-07	4.95E-01	4.94E-01	4.85E-01	4.79E-01	4.61E-01	4.24E-01	3.68E-01
2.00E-07	3.80E-01	3.76E-01	3.76E-01	3.72E-01	3.68E-01	3.47E-01	3.12E-01
5.00E-07	2.55E-01	2.58E-01	2.61E-01	2.58E-01	2.58E-01	2.50E-01	2.31E-01
1.00E-06	2.05E-01	2.03E-01	2.01E-01	2.00E-01	2.04E-01	1.98E-01	1.85E-01
2.00E-06	1.44E-01	1.44E-01	1.46E-01	1.49E-01	1.50E-01	1.46E-01	1.41E-01
5.00E-06	1.03E-01	1.01E-01	1.05E-01	1.11E-01	1.16E-01	1.15E-01	1.11E-01
1.00E-05	8.05E-02	8.01E-02	8.09E-02	8.59E-02	8.89E-02	8.81E-02	8.69E-02
2.00E-05	6.64E-02	6.67E-02	6.86E-02	6.95E-02	7.06E-02	7.01E-02	6.99E-02
5.00E-05	5.28E-02	5.17E-02	5.36E-02	5.47E-02	5.74E-02	5.68E-02	5.57E-02
1.00E-04	4.71E-02	4.78E-02	4.81E-02	4.91E-02	4.95E-02	5.09E-02	4.94E-02
2.00E-04	5.03E-02	4.93E-02	5.02E-02	5.03E-02	5.34E-02	5.16E-02	4.84E-02
5.00E-04	7.24E-02	7.25E-02	7.33E-02	7.49E-02	6.85E-02	7.31E-02	6.12E-02
1.00E-03	1.22E-01	1.21E-01	1.22E-01	1.23E-01	1.19E-01	1.16E-01	1.02E-01
2.00E-03	2.20E-01	2.22E-01	2.24E-01	2.27E-01	2.23E-01	2.15E-01	1.88E-01
5.00E-03	5.21E-01	5.23E-01	5.26E-01	5.33E-01	5.31E-01	5.11E-01	4.48E-01
1.00E-02	9.99E-01	1.00E+00	1.01E+00	1.02E+00	1.02E+00	9.87E-01	8.69E-01
2.00E-02	1.89E+00	1.89E+00	1.90E+00	1.93E+00	1.93E+00	1.87E+00	1.66E+00
3.00E-02	2.69E+00	2.70E+00	2.72E+00	2.75E+00	2.76E+00	2.69E+00	2.39E+00
5.00E-02	4.11E+00	4.10E+00	4.12E+00	4.17E+00	4.19E+00	4.10E+00	3.67E+00
7.00E-02	5.30E+00	5.28E+00	5.32E+00	5.38E+00	5.42E+00	5.31E+00	4.79E+00
1.00E-01	6.77E+00	6.78E+00	6.82E+00	6.90E+00	6.96E+00	6.85E+00	6.26E+00
1.50E-01	8.80E+00	8.81E+00	8.86E+00	8.95E+00	9.06E+00	8.93E+00	8.25E+00
2.00E-01	1.06E+01	1.05E+01	1.05E+01	1.06E+01	1.07E+01	1.07E+01	9.88E+00
3.00E-01	1.33E+01	1.32E+01	1.33E+01	1.34E+01	1.34E+01	1.34E+01	1.25E+01
5.00E-01	1.66E+01	1.66E+01	1.67E+01	1.69E+01	1.72E+01	1.73E+01	1.66E+01
7.00E-01	1.96E+01	1.96E+01	1.97E+01	1.99E+01	2.01E+01	2.03E+01	1.95E+01
9.00E-01	2.26E+01	2.26E+01	2.27E+01	2.29E+01	2.31E+01	2.32E+01	2.23E+01
1.00E+00	2.77E+01	2.77E+01	2.76E+01	2.75E+01	2.74E+01	2.72E+01	2.57E+01
1.20E+00	2.59E+01	2.59E+01	2.60E+01	2.61E+01	2.61E+01	2.63E+01	2.54E+01
1.50E+00	2.79E+01	2.79E+01	2.80E+01	2.81E+01	2.81E+01	2.84E+01	2.77E+01
2.00E+00	3.12E+01	3.12E+01	3.13E+01	3.14E+01	3.14E+01	3.18E+01	3.20E+01
3.00E+00	3.64E+01	3.65E+01	3.65E+01	3.67E+01	3.68E+01	3.68E+01	3.65E+01
4.00E+00	4.23E+01	4.23E+01	4.24E+01	4.26E+01	4.28E+01	4.28E+01	4.26E+01
5.00E+00	4.40E+01	4.40E+01	4.41E+01	4.42E+01	4.42E+01	4.43E+01	4.41E+01
6.00E+00	4.79E+01	4.79E+01	4.79E+01	4.80E+01	4.79E+01	4.78E+01	4.77E+01
7.00E+00	4.79E+01	4.79E+01	4.80E+01	4.81E+01	4.78E+01	4.77E+01	4.78E+01
8.00E+00	5.08E+01	5.08E+01	5.08E+01	5.09E+01	5.08E+01	5.10E+01	5.11E+01
9.00E+00	5.33E+01	5.33E+01	5.33E+01	5.33E+01	5.34E+01	5.34E+01	5.34E+01
1.00E+01	5.56E+01	5.57E+01	5.56E+01	5.56E+01	5.44E+01	5.44E+01	5.53E+01
1.20E+01	6.12E+01	6.13E+01	6.14E+01	6.15E+01	5.82E+01	6.31E+01	6.30E+01
1.40E+01	6.36E+01	6.37E+01	6.37E+01	6.38E+01	5.93E+01	6.60E+01	6.65E+01
1.50E+01	6.60E+01	6.60E+01	6.63E+01	6.64E+01	6.13E+01	6.17E+01	6.63E+01
1.60E+01	6.70E+01	6.73E+01	6.75E+01	6.79E+01	6.22E+01	6.32E+01	6.64E+01
1.80E+01	6.63E+01	6.66E+01	6.67E+01	6.70E+01	6.24E+01	6.29E+01	6.57E+01
2.00E+01	6.86E+01	6.89E+01	6.89E+01	6.91E+01	6.32E+01	6.40E+01	6.87E+01
3.00E+01	5.81E+01	5.83E+01	5.86E+01	5.91 E+01	6.21E+01	6.27E+01	6.04E+01
5.00E+01	5.25E+01	5.27E+01	5.34 E+01	5.47 E+01	5.81E+01	--	6.12E+01

Table A.4.2.3 Conversion coefficients from neutron fluence to personal absorbed dose in local skin on the rod phantom (2/2) (Hertel and Veinot, 2017).

	$d_{\text{local skin}}$ / pGy cm² for a radiation incidence at α						
E_p / MeV	105°	120°	135°	150°	165°	180°	ROT
1.00E-09	6.44E-01	2.56E-01	1.51E-01	1.30E-01	1.30E-01	1.28E-01	
1.00E-08	4.38E-01	2.64E-01	1.80E-01	1.58E-01	1.46E-01	1.46E-01	
2.50E-08	3.78E-01	2.56E-01	1.91E-01	1.62E-01	1.53E-01	1.52E-01	
1.00E-07	2.96E-01	2.35E-01	1.94E-01	1.76E-01	1.62E-01	1.58E-01	
2.00E-07	2.65E-01	2.25E-01	1.94E-01	1.72E-01	1.66E-01	1.64E-01	
5.00E-07	2.06E-01	1.83E-01	1.62E-01	1.51E-01	1.47E-01	1.44E-01	
1.00E-06	1.71E-01	1.54E-01	1.36E-01	1.30E-01	1.27E-01	1.28E-01	
2.00E-06	1.29E-01	1.24E-01	1.17E-01	1.08E-01	1.05E-01	1.03E-01	
5.00E-06	1.06E-01	9.50E-02	9.12E-02	8.64E-02	8.57E-02	8.59E-02	
1.00E-05	8.49E-02	8.00E-02	7.61E-02	7.32E-02	7.03E-02	7.00E-02	
2.00E-05	6.78E-02	6.56E-02	6.24E-02	6.04E-02	5.85E-02	5.77E-02	
5.00E-05	5.38E-02	4.96E-02	4.70E-02	4.56E-02	4.62E-02	4.60E-02	
1.00E-04	4.65E-02	4.35E-02	3.95E-02	3.72E-02	3.74E-02	3.67E-02	
2.00E-04	4.44E-02	4.00E-02	3.50E-02	3.33E-02	3.01E-02	3.14E-02	
5.00E-04	5.79E-02	4.65E-02	3.66E-02	3.31E-02	3.00E-02	3.06E-02	
1.00E-03	8.47E-02	6.78E-02	4.65E-02	3.61E-02	3.28E-02	3.19E-02	
2.00E-03	1.54E-01	1.17E-01	8.00E-02	5.91E-02	5.16E-02	5.13E-02	
5.00E-03	3.66E-01	2.64E-01	1.88E-01	1.38E-01	1.19E-01	1.15E-01	
1.00E-02	7.10E-01	5.16E-01	3.66E-01	2.71E-01	2.35E-01	2.31E-01	
2.00E-02	1.35E+00	1.00E+00	7.20E-01	5.45E-01	4.81E-01	4.67E-01	
3.00E-02	1.98E+00	1.48E+00	1.08E+00	8.29E-01	7.33E-01	7.12E-01	
5.00E-02	3.08E+00	2.39E+00	1.74E+00	1.39E+00	1.25E+00	1.24E+00	
7.00E-02	4.09E+00	3.18E+00	2.42E+00	1.97E+00	1.80E+00	1.76E+00	
1.00E-01	5.43E+00	4.33E+00	3.38E+00	2.78E+00	2.61E+00	2.58E+00	
1.50E-01	7.16E+00	5.97E+00	4.81E+00	4.04E+00	3.84E+00	3.78E+00	
2.00E-01	8.75E+00	7.35E+00	5.99E+00	5.18E+00	4.97E+00	4.89E+00	
3.00E-01	1.13E+01	9.75E+00	8.26E+00	7.17E+00	7.03E+00	6.89E+00	
5.00E-01	1.54E+01	1.37E+01	1.20E+01	1.07E+01	1.05E+01	1.04E+01	
7.00E-01	1.82E+01	1.66E+01	1.48E+01	1.34E+01	1.33E+01	1.30E+01	
9.00E-01	2.08E+01	1.90E+01	1.71E+01	1.56E+01	1.55E+01	1.53E+01	
1.00E+00	2.34E+01	2.07E+01	1.80E+01	1.64E+01	1.57E+01	1.55E+01	
1.20E+00	2.39E+01	2.20E+01	2.02E+01	1.93E+01	1.86E+01	1.85E+01	
1.50E+00	2.63E+01	2.46E+01	2.31E+01	2.20E+01	2.16E+01	2.14E+01	
2.00E+00	2.99E+01	2.84E+01	2.69E+01	2.58E+01	2.54E+01	2.53E+01	
3.00E+00	3.53E+01	3.38E+01	3.21E+01	3.14E+01	3.12E+01	3.11E+01	
4.00E+00	4.13E+01	3.94E+01	3.73E+01	3.68E+01	3.64E+01	3.63E+01	
5.00E+00	4.30E+01	4.16E+01	4.00E+01	3.92E+01	3.91E+01	3.92E+01	
6.00E+00	4.66E+01	4.47E+01	4.30E+01	4.22E+01	4.20E+01	4.18E+01	
7.00E+00	4.69E+01	4.56E+01	4.45E+01	4.36E+01	4.36E+01	4.36E+01	
8.00E+00	4.95E+01	4.81E+01	4.65E+01	4.61E+01	4.61E+01	4.60E+01	
9.00E+00	5.17E+01	5.00E+01	4.82E+01	4.77E+01	4.78E+01	4.78E+01	
1.00E+01	5.34E+01	5.17E+01	5.02E+01	4.96E+01	4.94E+01	4.94E+01	
1.20E+01	6.31E+01	5.53E+01	5.35E+01	5.31E+01	5.28E+01	5.51E+01	
1.40E+01	6.61E+01	5.70E+01	5.53E+01	5.50E+01	5.48E+01	5.33E+01	
1.50E+01	6.74E+01	5.85E+01	5.73E+01	5.68E+01	5.67E+01	5.54E+01	
1.60E+01	6.65E+01	6.01E+01	5.85E+01	5.82E+01	5.78E+01	5.64E+01	
1.80E+01	6.62E+01	6.39E+01	5.92E+01	5.96E+01	5.95E+01	5.75E+01	
2.00E+01	6.91E+01	6.80E+01	6.02E+01	6.51E+01	6.08E+01	5.85E+01	
3.00E+01	6.04E+01	6.01E+01	5.90E+01	5.84E+01	5.81E+01	5.96E+01	
5.00E+01	6.39E+01	6.52E+01	5.43E+01	5.35E+01	5.28E+01	6.78E+01	

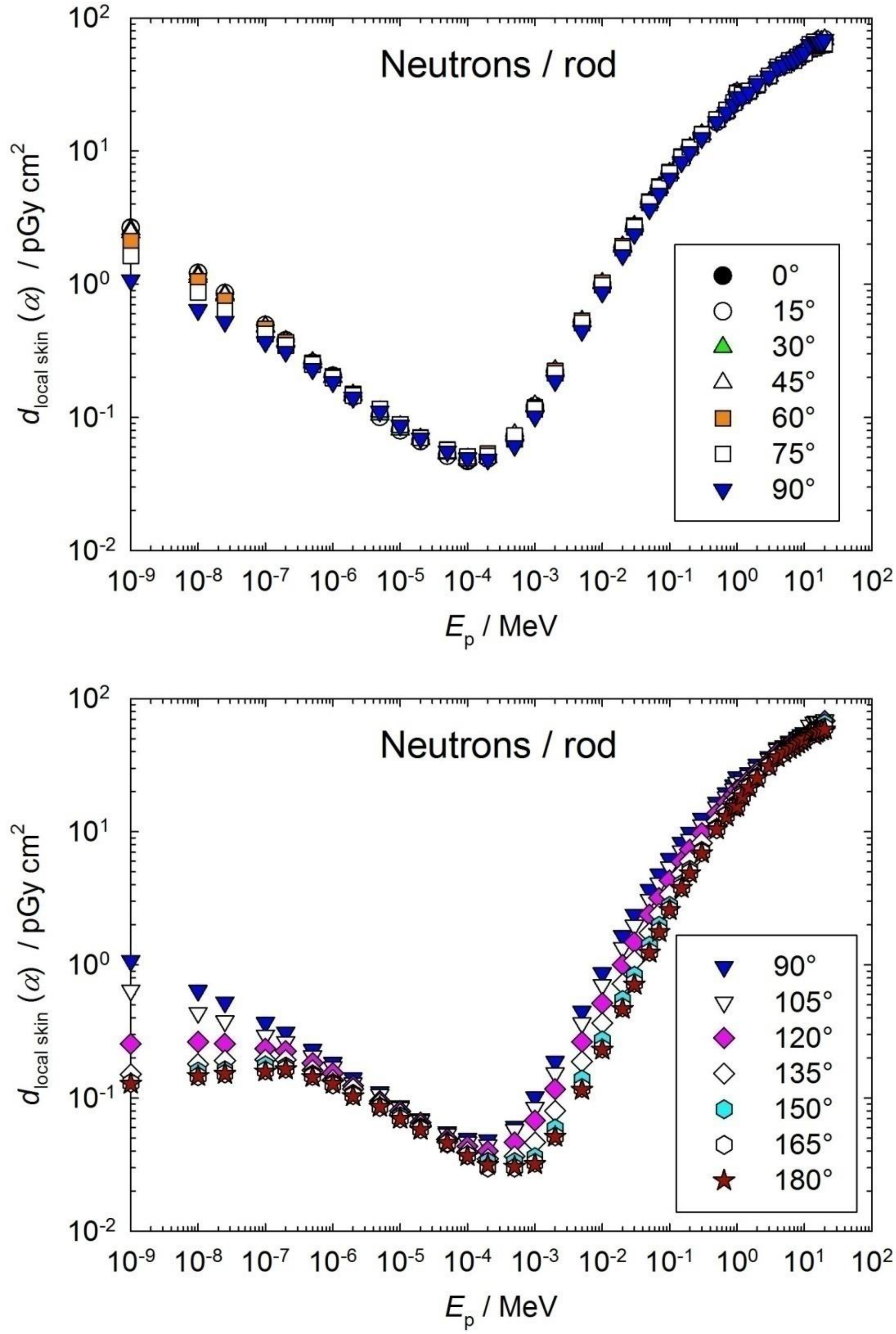

Figure A.4.2.3 Conversion coefficients from neutron fluence to personal absorbed dose in local skin on the rod phantom (Hertel and Veinot, 2017)..

Table A.4.3.1 Conversion coefficients from electron fluence to directional and personal absorbed dose in local skin on the slab phantom (Daures *et al*., 2017).

E_p / MeV	$d_{local\ skin}$ / (pGy cm^2) for a radiation incidence at α					
	0°	15°	30°	45°	60°	75°
0.01	1.18E-03	1.24E-03	1.25E-03	9.98E-04	5.93E-04	2.30E-04
0.02	4.21E-03	4.27E-03	4.39E-03	2.92E-03	2.05E-03	9.30E-04
0.05	1.62E-02	1.97E-02	1.41E-02	1.25E-02	7.51E-03	3.77E-03
0.06	1.39E+01	1.16E+01	6.29E+00	2.13E+00	5.02E-01	8.94E-02
0.07	2.22E+02	1.92E+02	1.26E+02	6.01E+01	1.93E+01	3.52E+00
0.08	6.63E+02	5.94E+02	4.23E+02	2.31E+02	8.93E+01	2.00E+01
0.09	1.10E+03	1.00E+03	7.53E+02	4.45E+02	1.96E+02	5.05E+01
0.1	1.40E+03	1.30E+03	1.03E+03	6.53E+02	3.11E+02	8.91E+01
0.11	1.51E+03	1.42E+03	1.17E+03	7.91E+02	4.07E+02	1.25E+02
0.12	1.49E+03	1.42E+03	1.22E+03	8.67E+02	4.73E+02	1.56E+02
0.15	1.21E+03	1.20E+03	1.14E+03	9.22E+02	5.67E+02	2.05E+02
0.2	8.43E+02	8.73E+02	9.29E+02	8.67E+02	6.00E+02	2.34E+02
0.3	5.44E+02	5.67E+02	6.40E+02	7.23E+02	6.20E+02	2.64E+02
0.5	3.86E+02	3.98E+02	4.38E+02	5.15E+02	5.91E+02	3.20E+02
1	3.07E+02	3.12E+02	3.34E+02	3.70E+02	4.53E+02	4.31E+02
2	2.78E+02	2.82E+02	2.94E+02	3.19E+02	3.69E+02	4.74E+02
5	2.69E+02	2.69E+02	2.75E+02	2.89E+02	3.26E+02	3.96E+02
10	2.67E+02	2.70E+02	2.73E+02	2.80E+02	3.02E+02	3.61E+02
20	2.71E+02	2.71E+02	2.74E+02	2.78E+02	2.91E+02	3.39E+02
30	2.72E+02	2.74E+02	2.76E+02	2.78E+02	2.86E+02	3.25E+02
50	2.73E+02	2.75E+02	2.77E+02	2.78E+02	2.85E+02	3.11E+02

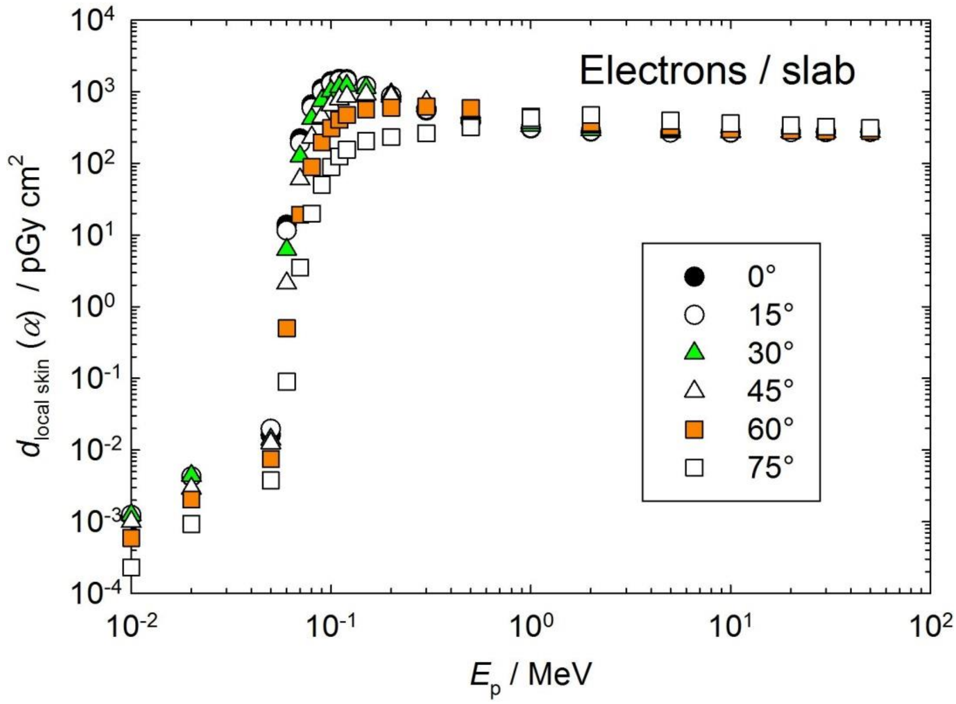

Figure A.4.3 Conversion coefficients from electron fluence to directional and personal absorbed dose in local skin on the slab phantom (Daures *et al*., 2017).

Table A.4.3.2 Conversion coefficients from electron fluence to personal absorbed dose in local skin on the pillar phantom (Otto, 2017).

	$d_{\mathrm{p\ local\ skin}}$ / (pGy cm^2) for a radiation incidence at α						
E_{p} / MeV	0°	15°	30°	45°	60°	75°	90°
0.05	2.61E-02	2.16E-02	1.70E-02	1.45E-02	8.24E-03	3.81E-03	0.00E+00
0.055	8.26E-01	6.68E-01	3.20E-01	1.09E-01	2.71E-02	5.52E-03	6.37E-04
0.06	2.26E+01	1.88E+01	1.08E+01	4.14E+00	1.04E+00	1.71E-01	8.45E-03
0.065	1.13E+02	9.77E+01	6.19E+01	2.80E+01	8.69E+00	1.68E+00	9.45E-02
0.07	2.77E+02	2.44E+02	1.65E+02	8.30E+01	2.96E+01	6.62E+00	4.05E-01
0.08	7.12E+02	6.43E+02	4.68E+02	2.66E+02	1.11E+02	3.00E+01	2.16E+00
0.09	1.14E+03	1.05E+03	8.00E+02	4.90E+02	2.27E+02	6.80E+01	5.30E+00
0.1	1.39E+03	1.30E+03	1.04E+03	6.81E+02	3.40E+02	1.11E+02	9.33E+00
0.11	1.45E+03	1.37E+03	1.14E+03	7.96E+02	4.26E+02	1.50E+02	1.33E+01
0.12	1.45E+03	1.37E+03	1.14E+03	7.96E+02	4.26E+02	1.49E+02	1.33E+01
0.15	1.13E+03	1.13E+03	1.07E+03	8.83E+02	5.62E+02	2.31E+02	2.29E+01
0.2	8.16E+02	8.35E+02	8.67E+02	8.16E+02	5.93E+02	2.67E+02	2.77E+01
0.3	5.46E+02	5.66E+02	6.28E+02	6.93E+02	6.03E+02	2.95E+02	3.11E+01
0.5	3.96E+02	4.07E+02	4.44E+02	5.16E+02	5.61E+02	3.37E+02	3.81E+01
1	3.13E+02	3.19E+02	3.38E+02	3.79E+02	4.58E+02	4.05E+02	5.83E+01
2	2.82E+02	2.85E+02	2.96E+02	3.21E+02	3.77E+02	4.53E+02	1.08E+02
5	2.71E+02	2.73E+02	2.76E+02	2.86E+02	3.14E+02	4.26E+02	2.93E+02
10	2.72E+02	2.72E+02	2.74E+02	2.78E+02	2.87E+02	3.28E+02	4.26E+02
20	2.72E+02	2.72E+02	2.74E+02	2.76E+02	2.81E+02	2.91E+02	3.40E+02
50	2.72E+02	2.73E+02	2.74E+02	2.76E+02	2.79E+02	2.85E+02	3.00E+02

	$d_{\mathrm{p\ local\ skin}}$ / (pGy cm^2) for a radiation incidence at α						
E_{p} / MeV	105°	120°	135°	150°	165°	180°	ROT
0.05	0.00E+00	0.00E+00	0.00E+00	0.00E+00	0.00E+00	0.00E+00	6.55E-03
0.055	0.00E+00	0.00E+00	0.00E+00	0.00E+00	0.00E+00	0.00E+00	1.29E-01
0.06	0.00E+00	0.00E+00	0.00E+00	0.00E+00	0.00E+00	0.00E+00	3.86E+00
0.065	0.00E+00	0.00E+00	0.00E+00	0.00E+00	0.00E+00	0.00E+00	2.12E+01
0.07	0.00E+00	0.00E+00	0.00E+00	0.00E+00	0.00E+00	0.00E+00	5.56E+01
0.08	0.00E+00	0.00E+00	0.00E+00	0.00E+00	0.00E+00	0.00E+00	1.56E+02
0.09	0.00E+00	0.00E+00	0.00E+00	0.00E+00	0.00E+00	0.00E+00	2.67E+02
0.1	0.00E+00	0.00E+00	0.00E+00	0.00E+00	0.00E+00	0.00E+00	3.48E+02
0.11	0.00E+00	0.00E+00	0.00E+00	0.00E+00	0.00E+00	0.00E+00	3.85E+02
0.12	0.00E+00	0.00E+00	0.00E+00	0.00E+00	0.00E+00	0.00E+00	3.85E+02
0.15	1.42E-04	0.00E+00	0.00E+00	0.00E+00	0.00E+00	0.00E+00	3.72E+02
0.2	2.26E-04	0.00E+00	0.00E+00	0.00E+00	0.00E+00	0.00E+00	3.18E+02
0.3	3.61E-04	3.91E-04	0.00E+00	0.00E+00	0.00E+00	0.00E+00	2.57E+02
0.5	2.10E-03	6.68E-04	0.00E+00	0.00E+00	0.00E+00	0.00E+00	2.08E+02
1	6.74E-03	5.01E-03	7.26E-03	0.00E+00	1.59E-03	1.31E-03	1.76E+02
2	2.80E-01	2.31E-02	2.88E-02	0.00E+00	2.96E-02	1.40E-02	1.65E+02
5	2.80E+01	1.32E+00	2.32E-01	2.80E-01	2.50E-01	2.10E-01	1.70E+02
10	2.17E+02	8.40E+01	1.85E+01	2.60E+00	1.02E+00	1.10E+00	1.94E+02
20	3.21E+02	3.11E+02	2.87E+02	2.53E+02	2.24E+02	2.12E+02	2.81E+02
50	3.06E+02	3.15E+02	3.23E+02	3.26E+02	3.27E+02	3.27E+02	2.99E+02

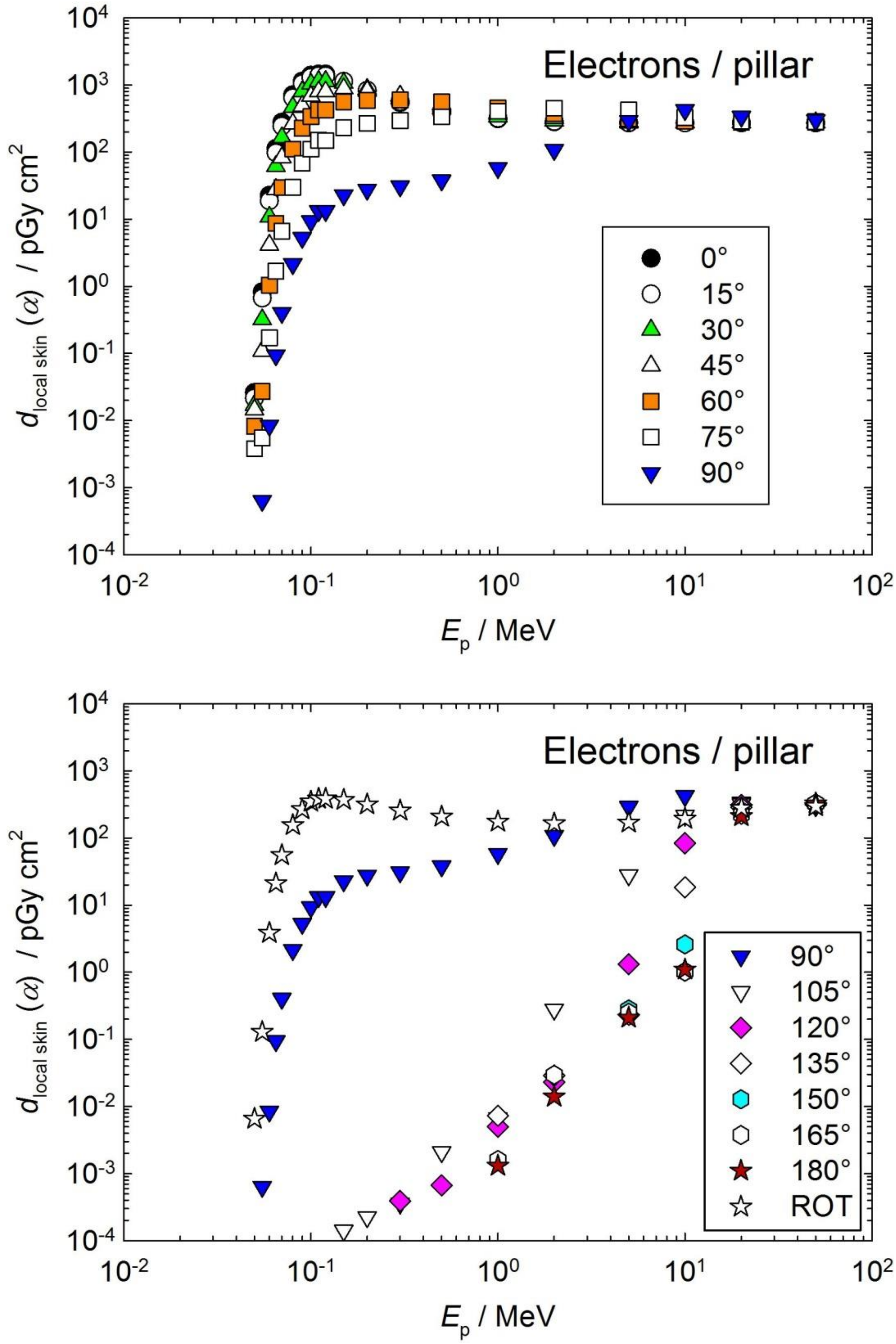

Figure A.4.3.2 Conversion coefficients from electron fluence to personal absorbed dose in local skin on the pillar phantom (Otto, 2017).

Table A.4.3.3 Conversion coefficients from electron fluence to personal absorbed dose in local skin on the rod phantom (Otto, 2017).

	$d_{\mathrm{p\ local\ skin}}$ / (pGy cm^2) for a radiation incidence at α						
E_p / MeV	0°	15°	30°	45°	60°	75°	90°
0.05	2.34E-02	2.20E-02	1.86E-02	1.41E-02	0.00E+00	0.00E+00	0.00E+00
0.055	6.44E-01	5.66E-01	3.79E-01	1.89E-01	6.86E-02	1.87E-02	0.00E+00
0.06	1.80E+01	1.60E+01	1.11E+01	5.93E+00	2.34E+00	6.59E-01	1.25E-01
0.065	9.10E+01	8.18E+01	5.92E+01	3.40E+01	1.51E+01	4.92E+00	1.09E+00
0.07	2.28E+02	2.07E+02	1.54E+02	9.34E+01	4.46E+01	1.61E+01	4.02E+00
0.08	6.22E+02	5.73E+02	4.45E+02	2.87E+02	1.51E+02	6.12E+01	1.76E+01
0.09	1.03E+03	9.61E+02	7.66E+02	5.18E+02	2.87E+02	1.25E+02	3.91E+01
0.1	1.28E+03	1.20E+03	9.86E+02	6.93E+02	4.05E+02	1.87E+02	6.20E+01
0.11	1.36E+03	1.28E+03	1.08E+03	7.88E+02	4.82E+02	2.34E+02	8.20E+01
0.12	1.33E+03	1.27E+03	1.09E+03	8.25E+02	5.23E+02	2.64E+02	9.63E+01
0.15	1.12E+03	1.10E+03	1.00E+03	8.18E+02	5.63E+02	3.08E+02	1.22E+02
0.2	8.32E+02	8.35E+02	8.17E+02	7.27E+02	5.47E+02	3.26E+02	1.39E+02
0.3	5.65E+02	5.84E+02	6.18E+02	6.08E+02	5.03E+02	3.30E+02	1.54E+02
0.5	4.06E+02	4.19E+02	4.57E+02	4.88E+02	4.42E+02	3.22E+02	1.73E+02
1	3.16E+02	3.22E+02	3.45E+02	3.90E+02	3.95E+02	3.22E+02	2.07E+02
2	2.82E+02	2.85E+02	2.95E+02	3.28E+02	3.69E+02	3.47E+02	2.69E+02
5	2.71E+02	2.71E+02	2.74E+02	2.80E+02	3.04E+02	3.29E+02	3.39E+02
10	2.71E+02	2.72E+02	2.73E+02	2.76E+02	2.84E+02	2.94E+02	3.01E+02
20	2.72E+02	2.72E+02	2.73E+02	2.75E+02	2.80E+02	2.85E+02	2.91E+02
50	2.73E+02	2.73E+02	2.74E+02	2.76E+02	2.79E+02	2.83E+02	2.88E+02

	$d_{\mathrm{p\ local\ skin}}$ / (pGy cm^2) for a radiation incidence at α						
E_p / MeV	105°	120°	135°	150°	165°	180°	ROT
0.05	0.00E+00	0.00E+00	0.00E+00	0.00E+00	0.00E+00	0.00E+00	6.97E-03
0.055	0.00E+00	1.17E-04	0.00E+00	0.00E+00	0.00E+00	0.00E+00	1.29E-01
0.06	1.36E-02	2.51E-04	0.00E+00	0.00E+00	0.00E+00	0.00E+00	3.77E+00
0.065	1.31E-01	1.40E-03	0.00E+00	0.00E+00	0.00E+00	0.00E+00	2.01E+01
0.07	5.45E-01	6.60E-03	0.00E+00	0.00E+00	0.00E+00	0.00E+00	5.28E+01
0.08	2.75E+00	3.96E-02	0.00E+00	0.00E+00	0.00E+00	0.00E+00	1.54E+02
0.09	6.76E+00	1.07E-01	0.00E+00	0.00E+00	0.00E+00	0.00E+00	2.68E+02
0.1	1.13E+01	2.03E-01	0.00E+00	0.00E+00	0.00E+00	0.00E+00	3.49E+02
0.11	1.58E+01	2.90E-01	0.00E+00	0.00E+00	0.00E+00	0.00E+00	3.87E+02
0.12	1.95E+01	3.81E-01	0.00E+00	0.00E+00	0.00E+00	0.00E+00	3.96E+02
0.15	2.66E+01	6.12E-01	0.00E+00	0.00E+00	0.00E+00	0.00E+00	3.75E+02
0.2	3.24E+01	8.99E-01	0.00E+00	0.00E+00	0.00E+00	0.00E+00	3.20E+02
0.3	3.81E+01	1.39E+00	0.00E+00	0.00E+00	0.00E+00	0.00E+00	2.60E+02
0.5	4.98E+01	2.66E+00	0.00E+00	0.00E+00	0.00E+00	0.00E+00	2.13E+02
1	8.13E+01	9.60E+00	1.56E-01	0.00E+00	0.00E+00	0.00E+00	1.86E+02
2	1.56E+02	4.83E+01	9.55E+00	1.16E+00	7.53E-02	3.14E-02	1.87E+02
5	3.30E+02	2.94E+02	2.53E+02	2.21E+02	1.99E+02	1.92E+02	2.77E+02
10	3.06E+02	3.06E+02	3.05E+02	3.04E+02	3.04E+02	3.03E+02	2.93E+02
20	2.97E+02	3.01E+02	3.05E+02	3.08E+02	3.10E+02	3.10E+02	2.91E+02
50	2.94E+02	3.00E+02	3.06E+02	3.10E+02	3.13E+02	3.14E+02	2.91E+02

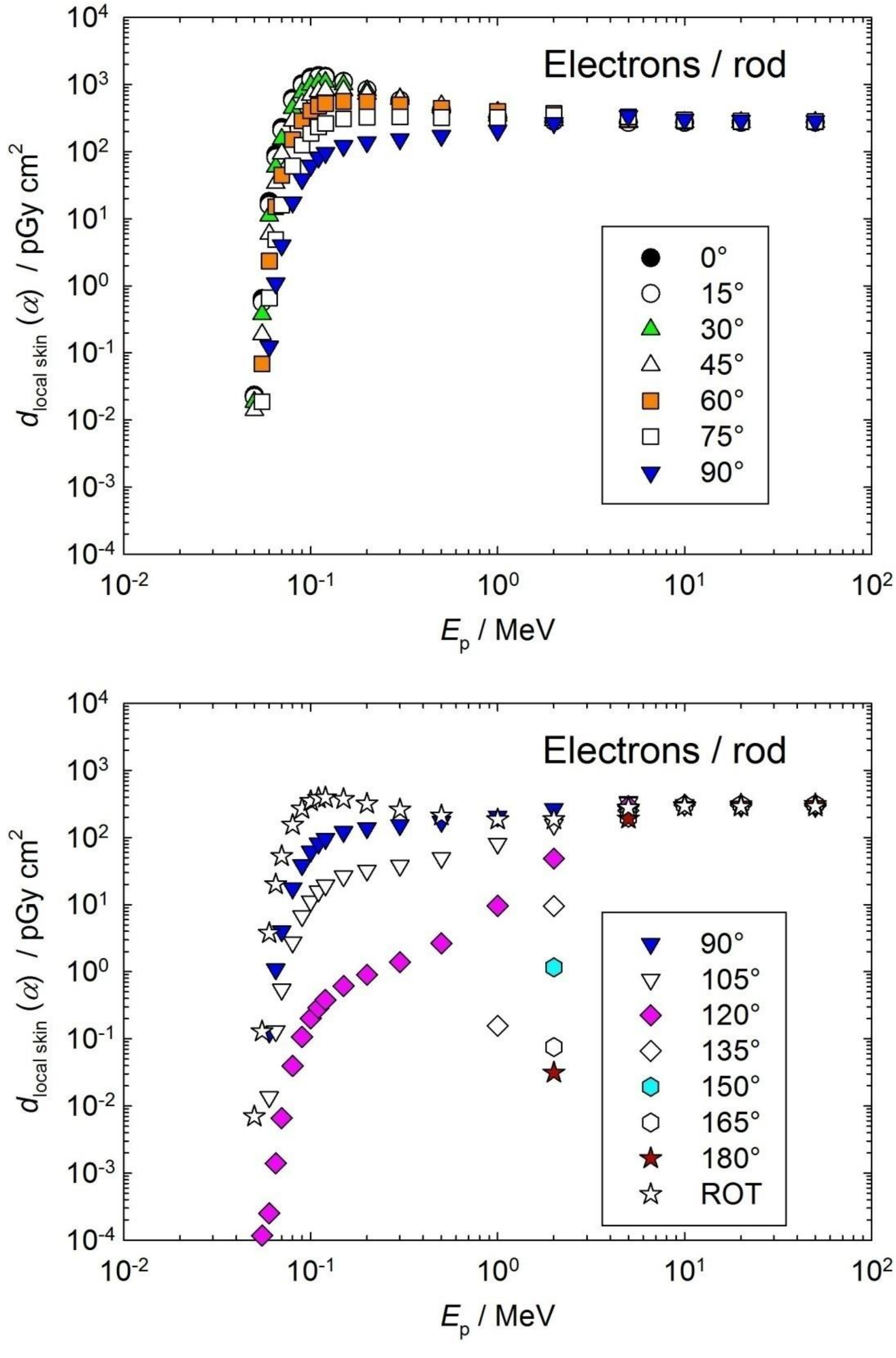

Figure A.4.3.3 Conversion coefficients from electron fluence to personal absorbed dose in local skin on the rod phantom (Otto, 2017).

1208 Table A.4.4.1 Conversion coefficients from positron fluence to directional and personal absorbed dose in
1209 local skin on the slab phantom (Daures *et al*., 2017).

E_p / MeV	$d_{\text{local skin}}$ / (pGy cm^2) for a radiation incidence at α					
	0°	15°	30°	45°	60°	75°
0.01	1.17E+01	1.11E+01	9.91E+00	7.59E+00	4.89E+00	2.02E+00
0.02	1.17E+01	1.11E+01	9.90E+00	7.55E+00	4.85E+00	2.02E+00
0.05	1.20E+01	1.11E+01	9.94E+00	7.70E+00	5.25E+00	1.91E+00
0.06	2.60E+01	2.35E+01	1.59E+01	9.71E+00	5.29E+00	2.03E+00
0.07	2.34E+02	2.04E+02	1.36E+02	6.79E+01	2.40E+01	5.53E+00
0.08	6.75E+02	6.04E+02	4.34E+02	2.39E+02	9.43E+01	2.21E+01
0.09	1.11E+03	1.01E+03	7.63E+02	4.53E+02	2.00E+02	5.24E+01
0.1	1.41E+03	1.31E+03	1.04E+03	6.60E+02	3.16E+02	9.12E+01
0.11	1.52E+03	1.43E+03	1.18E+03	7.99E+02	4.12E+02	1.28E+02
0.12	1.50E+03	1.44E+03	1.23E+03	8.75E+02	4.79E+02	1.58E+02
0.15	1.23E+03	1.22E+03	1.15E+03	9.31E+02	5.72E+02	2.08E+02
0.2	8.54E+02	8.83E+02	9.38E+02	8.73E+02	6.04E+02	2.36E+02
0.3	5.55E+02	5.77E+02	6.51E+02	7.31E+02	6.24E+02	2.66E+02
0.5	3.96E+02	4.07E+02	4.46E+02	5.20E+02	5.97E+02	3.22E+02
1	3.15E+02	3.20E+02	3.42E+02	3.77E+02	4.58E+02	4.33E+02
2	2.85E+02	2.88E+02	3.00E+02	3.23E+02	3.73E+02	4.76E+02
5	2.73E+02	2.73E+02	2.80E+02	2.93E+02	3.29E+02	3.97E+02
10	2.71E+02	2.74E+02	2.74E+02	2.82E+02	3.05E+02	3.63E+02
20	2.72E+02	2.73E+02	2.75E+02	2.80E+02	2.92E+02	3.39E+02
30	2.72E+02	2.75E+02	2.77E+02	2.78E+02	2.86E+02	3.27E+02
50	2.73E+02	2.75E+02	2.76E+02	2.78E+02	2.86E+02	3.10E+02

1210
1211

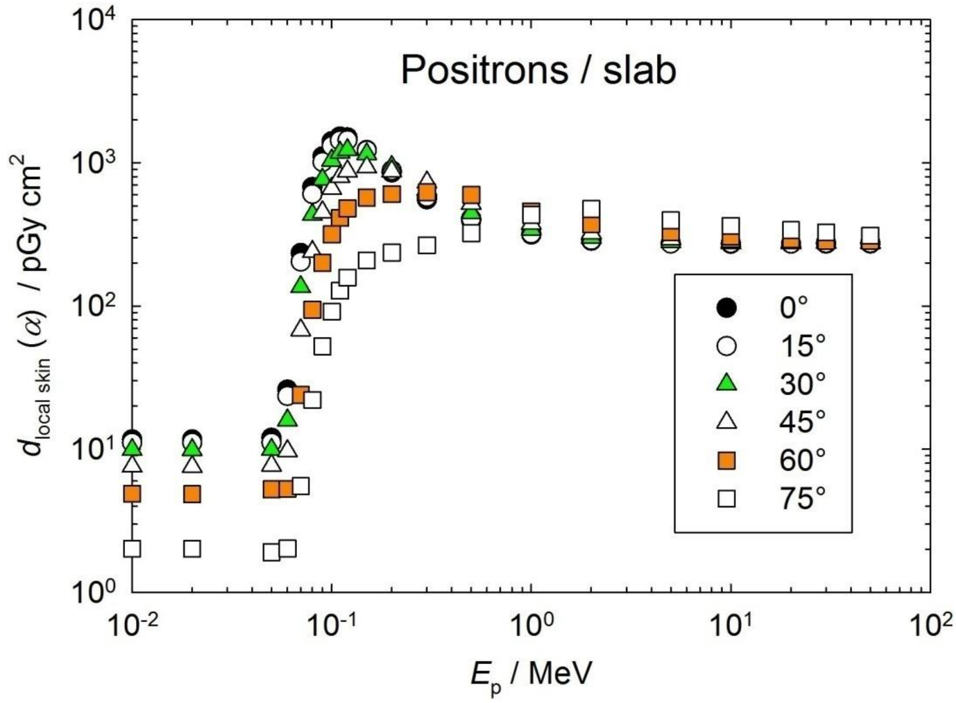

Figure A.4.4.1 Conversion coefficients from positron fluence to directional and personal absorbed dose in local skin on the slab phantom (Daures *et al*., 2017).

Table A.4.4.2 Conversion coefficients from positron fluence to personal absorbed dose in local skin on the pillar phantom (Otto, 2017).

E_p / MeV	$d_{p\text{ local skin}}$ / (pGy cm²) for a radiation incidence at α						
	0°	15°	30°	45°	60°	75°	90°
0.01	1.08E+01	1.03E+01	9.36E+00	7.64E+00	5.50E+00	3.23E+00	1.47E+00
0.02	1.07E+01	1.04E+01	9.39E+00	7.64E+00	5.46E+00	3.27E+00	1.45E+00
0.05	1.09E+01	1.05E+01	9.40E+00	7.49E+00	5.25E+00	2.97E+00	1.35E+00
0.07	2.61E+02	2.30E+02	1.56E+02	8.03E+01	3.06E+01	8.55E+00	1.69E+00
0.1	1.40E+03	1.30E+03	1.04E+03	6.73E+02	3.34E+02	1.09E+02	1.02E+01
0.11	1.47E+03	1.39E+03	1.16E+03	7.99E+02	4.25E+02	1.48E+02	1.41E+01
0.15	1.17E+03	1.16E+03	1.10E+03	9.02E+02	5.72E+02	2.34E+02	2.42E+01
0.2	8.32E+02	8.51E+02	8.82E+02	8.30E+02	6.02E+02	2.72E+02	2.92E+01
0.5	3.99E+02	4.09E+02	4.45E+02	5.14E+02	5.57E+02	3.36E+02	3.90E+01
1	3.14E+02	3.19E+02	3.38E+02	3.76E+02	4.52E+02	4.00E+02	5.86E+01
2	2.83E+02	2.86E+02	2.95E+02	3.18E+02	3.71E+02	4.47E+02	1.08E+02
5	2.73E+02	2.73E+02	2.77E+02	2.86E+02	3.11E+02	4.17E+02	2.90E+02
10	2.71E+02	2.72E+02	2.73E+02	2.77E+02	2.84E+02	3.22E+02	4.15E+02
20	2.72E+02	2.72E+02	2.73E+02	2.76E+02	2.80E+02	2.89E+02	3.33E+02
50	2.71E+02	2.72E+02	2.73E+02	2.75E+02	2.79E+02	2.84E+02	2.96E+02

E_p / MeV	$d_{p\text{ local skin}}$ / (pGy cm²) for a radiation incidence at α						
	105°	120°	135°	150°	165°	180°	ROT
0.01	9.85E-01	7.85E-01	6.93E-01	6.92E-01	6.27E-01	5.78E-01	3.92E+00
0.02	9.50E-01	7.70E-01	7.07E-01	5.99E-01	5.91E-01	6.13E-01	3.91E+00
0.05	9.58E-01	8.26E-01	6.85E-01	6.46E-01	5.73E-01	5.88E-01	3.87E+00
0.07	8.90E-01	7.53E-01	6.80E-01	6.18E-01	6.12E-01	5.52E-01	5.34E+01
0.1	9.12E-01	7.52E-01	6.72E-01	6.08E-01	5.78E-01	5.36E-01	3.47E+02
0.11	9.15E-01	6.94E-01	6.82E-01	5.76E-01	5.36E-01	5.48E-01	3.89E+02
0.15	9.04E-01	8.13E-01	6.46E-01	6.30E-01	5.64E-01	5.93E-01	3.81E+02
0.2	9.29E-01	7.22E-01	6.37E-01	5.74E-01	6.44E-01	5.85E-01	3.24E+02
0.5	1.03E+00	7.81E-01	6.87E-01	6.15E-01	6.64E-01	7.07E-01	2.09E+02
1	1.08E+00	8.44E-01	7.50E-01	7.04E-01	6.56E-01	5.82E-01	1.75E+02
2	1.44E+00	1.16E+00	9.03E-01	7.50E-01	8.34E-01	7.77E-01	1.64E+02
5	3.01E+01	2.93E+00	1.71E+00	1.64E+00	1.46E+00	1.43E+00	1.69E+02
10	2.13E+02	8.55E+01	2.19E+01	5.30E+00	3.54E+00	3.39E+00	1.92E+02
20	3.06E+02	2.91E+02	2.69E+02	2.40E+02	2.15E+02	2.05E+02	2.73E+02
50	2.99E+02	3.03E+02	3.05E+02	3.06E+02	3.05E+02	3.05E+02	2.90E+02

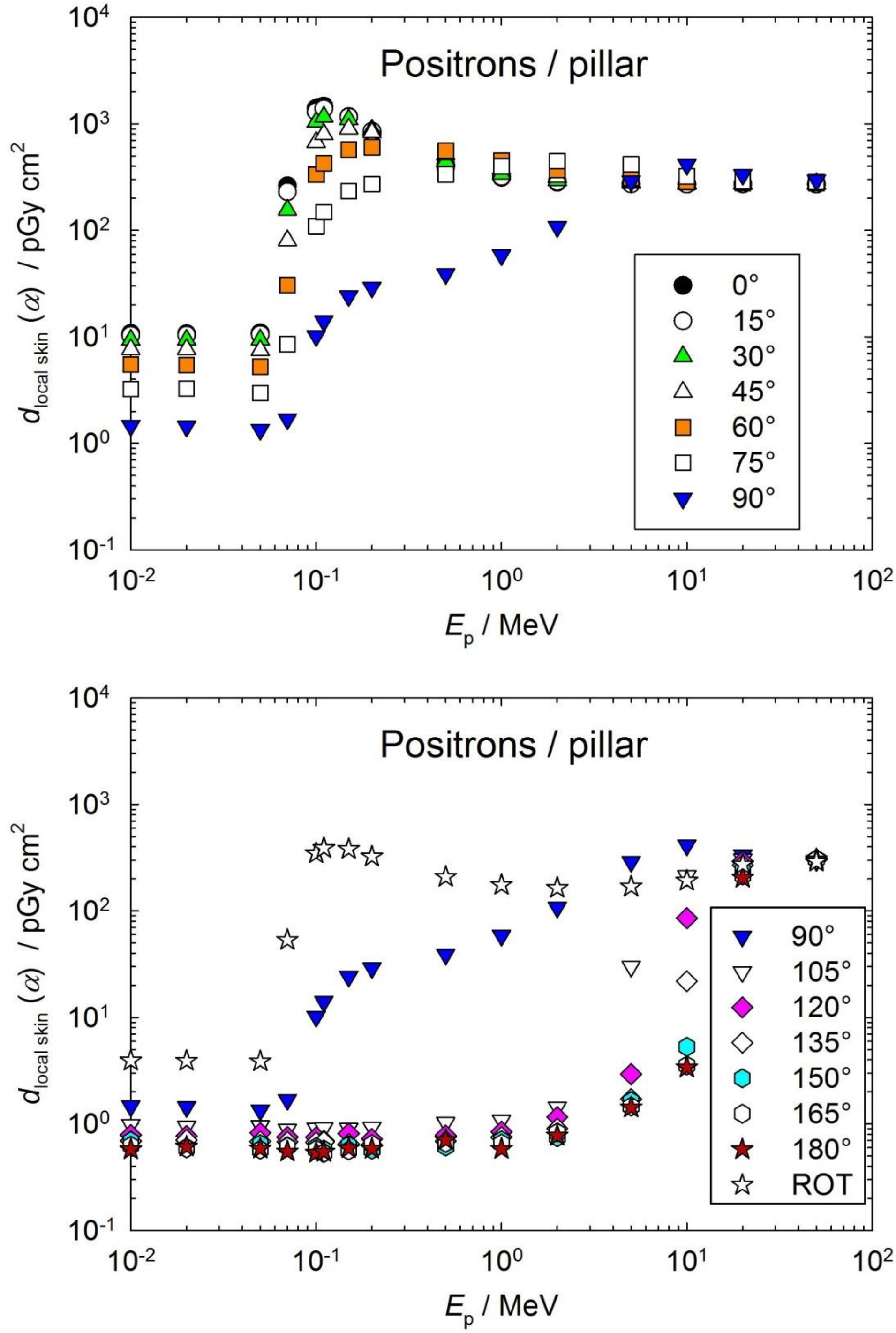

Figure A.4.4.2 Conversion coefficients from positron fluence to personal absorbed dose in local skin on the pillar phantom (Otto, 2017).

Table A.4.4.3 Conversion coefficients from positron fluence to personal absorbed dose in local skin on the rod phantom (Otto, 2017).

E_p / MeV	$d_{p\text{ local skin}}$ / (pGy cm^2) for a radiation incidence at α						
	0°	15°	30°	45°	60°	75°	90°
0.01	8.34E+00	8.08E+00	7.33E+00	6.17E+00	4.77E+00	3.38E+00	2.29E+00
0.02	8.47E+00	8.19E+00	7.43E+00	6.23E+00	4.77E+00	3.35E+00	2.24E+00
0.05	8.61E+00	8.30E+00	7.44E+00	6.15E+00	4.62E+00	3.20E+00	2.13E+00
0.07	2.25E+02	2.04E+02	1.53E+02	9.35E+01	4.59E+01	1.79E+01	5.77E+00
0.1	1.28E+03	1.20E+03	9.82E+02	6.87E+02	4.00E+02	1.84E+02	6.16E+01
0.11	1.38E+03	1.30E+03	1.09E+03	7.93E+02	4.82E+02	2.33E+02	8.19E+01
0.15	1.15E+03	1.12E+03	1.02E+03	8.34E+02	5.73E+02	3.13E+02	1.24E+02
0.2	8.48E+02	8.51E+02	8.32E+02	7.40E+02	5.56E+02	3.31E+02	1.42E+02
0.5	4.04E+02	4.16E+02	4.52E+02	4.84E+02	4.41E+02	3.23E+02	1.76E+02
1	3.15E+02	3.21E+02	3.42E+02	3.85E+02	3.91E+02	3.21E+02	2.08E+02
2	2.81E+02	2.84E+02	2.93E+02	3.23E+02	3.64E+02	3.43E+02	2.69E+02
5	2.70E+02	2.71E+02	2.73E+02	2.79E+02	3.00E+02	3.21E+02	3.30E+02
10	2.71E+02	2.71E+02	2.72E+02	2.75E+02	2.82E+02	2.90E+02	2.95E+02
20	2.72E+02	2.72E+02	2.73E+02	2.75E+02	2.79E+02	2.83E+02	2.88E+02
50	2.72E+02	2.73E+02	2.74E+02	2.76E+02	2.79E+02	2.82E+02	2.86E+02

E_p / MeV	$d_{p\text{ local skin}}$ / (pGy cm^2) for a radiation incidence at α						
	105°	120°	135°	150°	165°	180°	ROT
0.01	1.58E+00	1.22E+00	1.09E+00	1.01E+00	9.71E-01	9.76E-01	3.55E+00
0.02	1.55E+00	1.22E+00	1.09E+00	9.96E-01	9.34E-01	9.28E-01	3.56E+00
0.05	1.48E+00	1.17E+00	1.05E+00	9.89E-01	9.58E-01	9.54E-01	3.52E+00
0.07	1.98E+00	1.17E+00	1.03E+00	9.49E-01	9.13E-01	9.04E-01	5.32E+01
0.1	1.22E+01	1.37E+00	1.06E+00	9.65E-01	9.02E-01	8.70E-01	3.48E+02
0.11	1.67E+01	1.46E+00	1.05E+00	9.63E-01	9.10E-01	8.98E-01	3.91E+02
0.15	2.79E+01	1.77E+00	1.03E+00	9.65E-01	9.26E-01	9.17E-01	3.83E+02
0.2	3.41E+01	2.09E+00	1.06E+00	1.01E+00	9.76E-01	9.66E-01	3.26E+02
0.5	5.23E+01	4.14E+00	1.14E+00	1.06E+00	1.04E+00	1.03E+00	2.13E+02
1	8.42E+01	1.15E+01	1.53E+00	1.25E+00	1.18E+00	1.14E+00	1.86E+02
2	1.59E+02	5.21E+01	1.21E+01	2.91E+00	1.56E+00	1.48E+00	1.87E+02
5	3.20E+02	2.87E+02	2.50E+02	2.20E+02	2.00E+02	1.93E+02	2.74E+02
10	2.97E+02	2.94E+02	2.90E+02	2.88E+02	2.86E+02	2.86E+02	2.85E+02
20	2.91E+02	2.93E+02	2.95E+02	2.96E+02	2.97E+02	2.97E+02	2.86E+02
50	2.91E+02	2.96E+02	3.00E+02	3.03E+02	3.05E+02	3.06E+02	2.88E+02

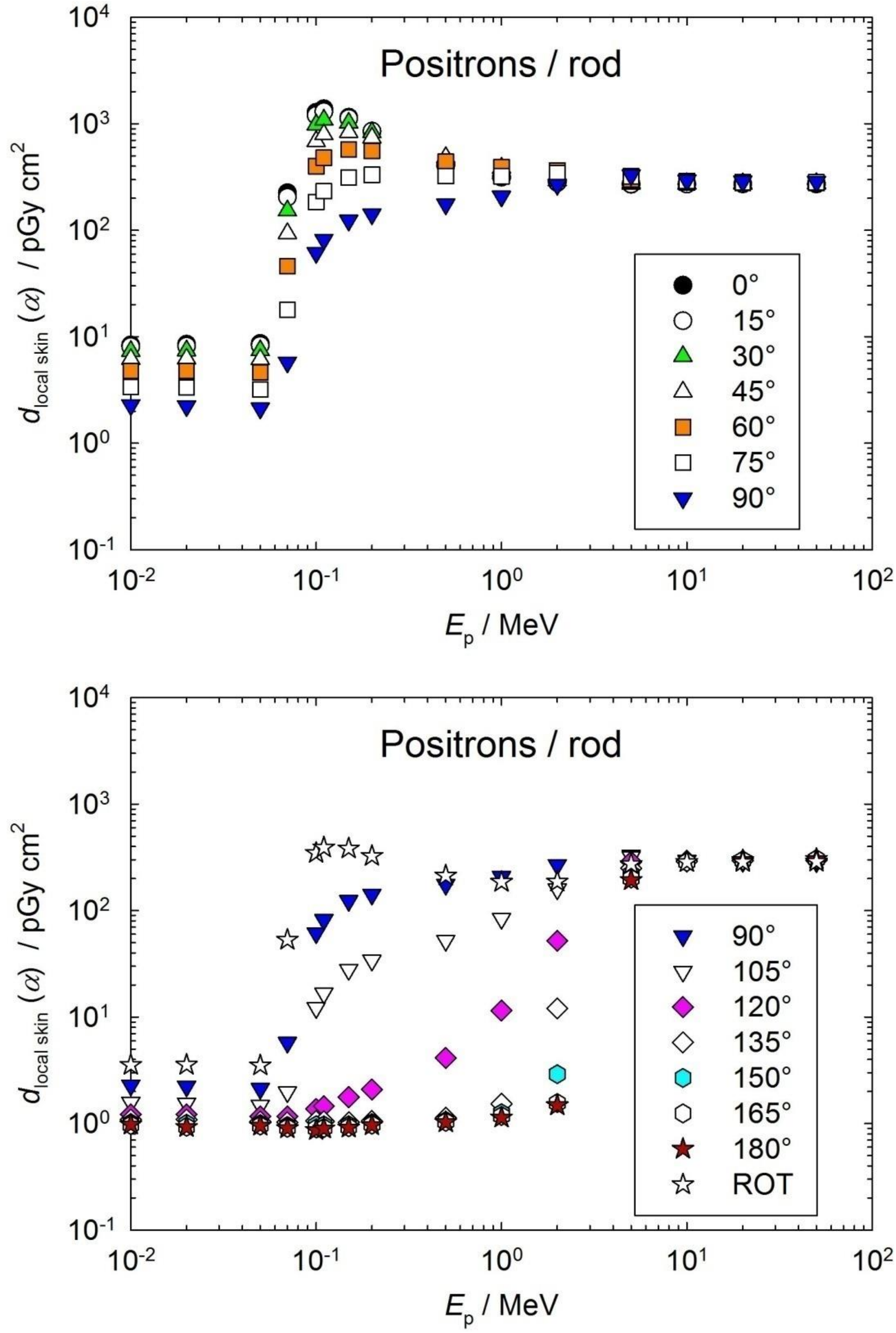

Figure A.4.4.3 Conversion coefficients from positron fluence to personal absorbed dose in local skin on the rod phantom (Otto, 2017).

Table A.4.5 Conversion coefficients from alpha particle fluence to directional and personal absorbed dose in local skin on the slab phantom (ICRP, 2010).

E_p / MeV	$d_{local\ skin}$ / (pGy cm^2) for normal incidence
6.5	1.11E+03
6.8	2.56E+04
7.0	4.20E+04
7.5	7.52E+04
8.0	1.03E+05
8.5	1.28E+05
9.0	1.50E+05
9.5	1.72E+05
10.0	1.80E+05

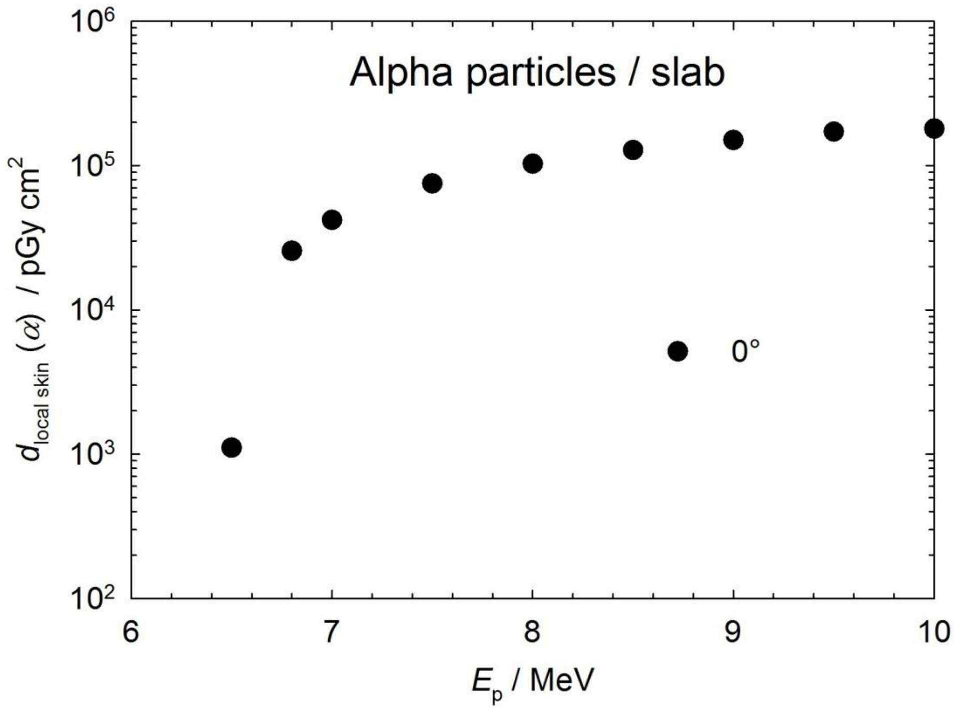

Figure A.4.5 Conversion coefficients from alpha particle fluence to directional and personal absorbed dose in local skin on the slab phantom (ICRP, 2010).

A.5 Operational Quantities for Photons for Energies up to 50 MeV Calculated with the Kerma-Approximation Method.

The calibration of area monitoring instruments and personal dosimeters to measure photons for ambient dose, personal dose, directional and personal absorbed dose in the lens of the eye and local skin, are performed routinely in air with sufficient material in front of the instrument to provide full charged-particle equilibrium. The calibration procedure is for photons and for the particles produced in air and the other material, at the point of test.

Table A.5.1a and Figure A.5.1a give values of conversion coefficients for this procedure from photon fluence to ambient dose for photon energies up to 50 MeV using the kerma-approximation to approximate charged-particle equilibrium, in Table A.5.1b and Figure A.5.1b from air kerma; Table A.5.2a and Figure A.5.2a from photon fluence to personal dose, and in Table A.5.2 b and Figure A.5.2b from air kerma; Table A.5.3a and Figure A.5.3a from photon fluence to directional and personal absorbed dose in the lens of the eye, and in Table A.5.3b and Figure A.5.3b from air kerma; Tables A.5.4.1a, A5.4.2a, A5.4.3a, and Figures A.5.4.1a, A5.4.2a, A5.4.3a from photon fluence to directional and personal absorbed dose in local skin, and in Tables A.5.4.1b, A5.4.2b, A5.4.3b and Figures A.5.4.1b, A5.4.2b, A5.4.3b from air kerma;

Table A.5.1a Conversion coefficients from photon fluence to ambient dose calculated using the kerma-approximation method (Endo, 2017).

E_p / MeV	h^*_{Emax} / (pSv cm^2)
1.00E-02	6.75E-02
1.50E-02	1.53E-01
2.00E-02	2.22E-01
3.00E-02	3.10E-01
4.00E-02	3.45E-01
5.00E-02	3.64E-01
6.00E-02	3.85E-01
7.00E-02	4.11E-01
8.00E-02	4.43E-01
1.00E-01	5.19E-01
1.50E-01	7.48E-01
2.00E-01	9.98E-01
3.00E-01	1.50E+00
4.00E-01	2.00E+00
5.00E-01	2.46E+00
6.00E-01	2.91E+00
8.00E-01	3.73E+00
1.00E+00	4.49E+00
1.50E+00	6.13E+00
2.00E+00	7.54E+00
3.00E+00	9.98E+00
4.00E+00	1.21E+01
5.00E+00	1.42E+01
6.00E+00	1.61E+01
8.00E+00	1.99E+01
1.00E+01	2.37E+01
1.50E+01	3.33E+01
2.00E+01	4.32E+01
3.00E+01	6.41E+01
4.00E+01	8.63E+01
5.00E+01	1.09E+02

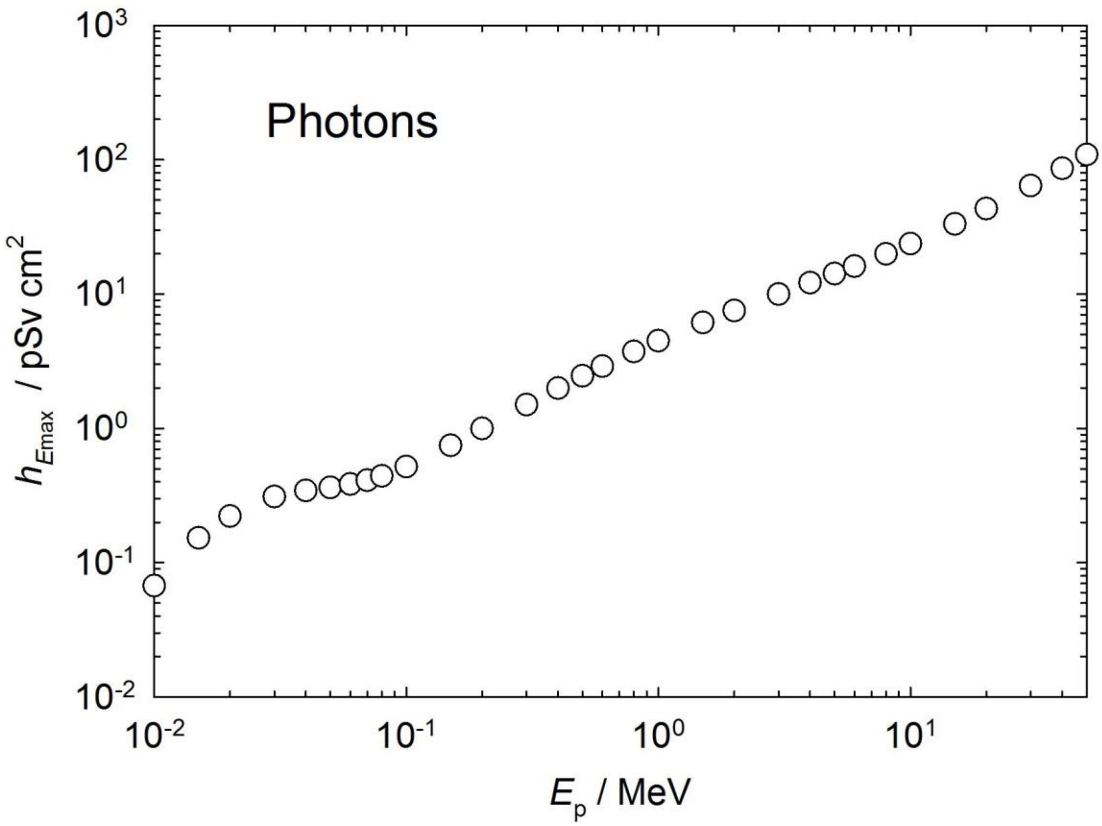

Figure A.5.1a Conversion coefficients from photon fluence to ambient dose calculated using the kerma-approximation method (Endo, 2017).

Table A.5.1b Conversion coefficients from photon air kerma to ambient dose calculated using the kerma-approximation method (Endo, 2017).

E_p / MeV	$h^*_{E\max}$ / (Sv Gy^{-1})
1.0E-02	9.12E-03
1.5E-02	4.89E-02
2.0E-02	1.32E-01
3.0E-02	4.30E-01
4.0E-02	8.05E-01
5.0E-02	1.13E+00
6.0E-02	1.33E+00
7.0E-02	1.43E+00
8.0E-02	1.44E+00
1.0E-01	1.40E+00
1.5E-01	1.25E+00
2.0E-01	1.16E+00
3.0E-01	1.09E+00
4.0E-01	1.06E+00
5.0E-01	1.04E+00
6.0E-01	1.02E+00
8.0E-01	1.01E+00
1.0E+00	1.00E+00
1.5E+00	9.98E-01
2.0E+00	9.97E-01
3.0E+00	1.00E+00
4.0E+00	1.00E+00
5.0E+00	1.00E+00
6.0E+00	9.97E-01
8.0E+00	9.89E-01
1.0E+01	9.82E-01
1.5E+01	9.65E-01
2.0E+01	9.52E-01
3.0E+01	9.34E-01
4.0E+01	9.25E-01
5.0E+01	9.17E-01

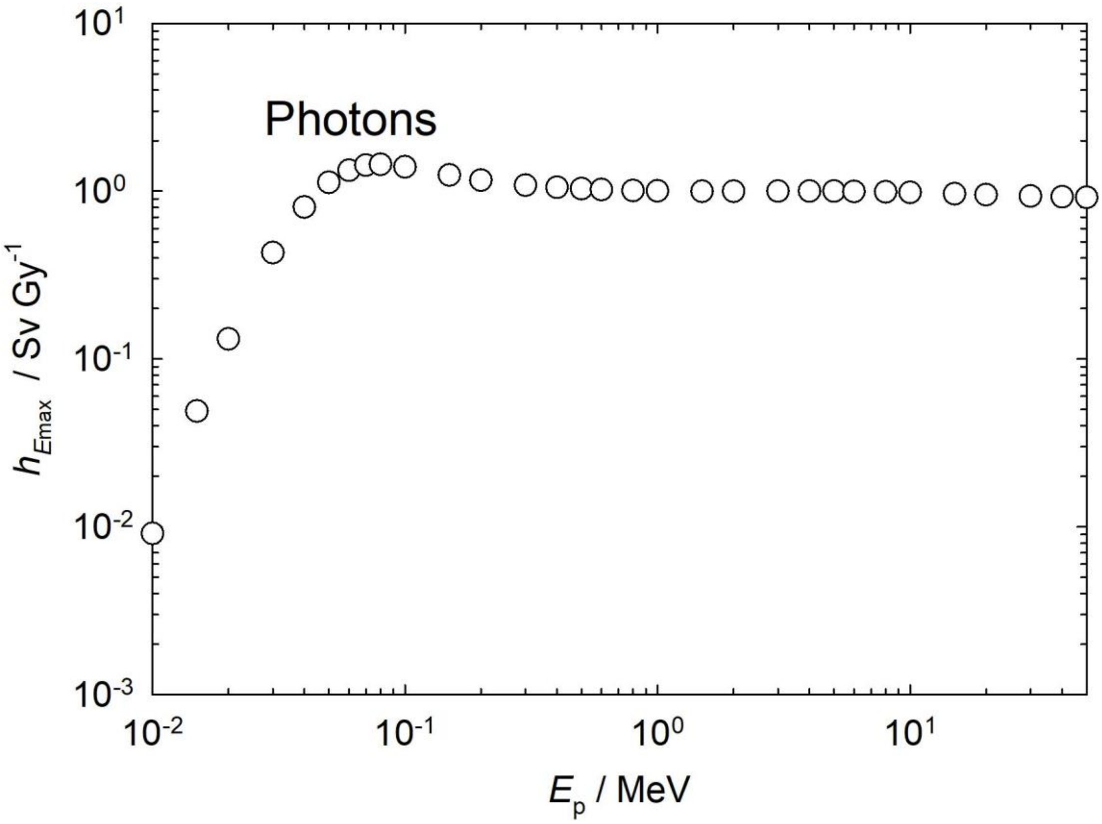

Figure A.5.1b Conversion coefficients from photon air kerma to ambient dose calculated using the kerma-approximation method (Endo, 2017).

Table A.5.2a Conversion coefficient from photon fluence to personal dose calculated using the kerma-approximation method (Endo, 2017).

E_p / MeV	$h_p(\alpha)$ / (pSv cm^2)											
	0°	max(±15°)	max(±30°)	max(±45°)	max(±60°)	max(±75°)	max(±90°)	180°	ROT	ISO	SS-ISO	IS-ISO
1.0E-02	6.75E-02	6.76E-02	6.20E-02	5.33E-02	4.27E-02	3.11E-02	1.89E-02	1.80E-02	3.31E-02	2.90E-02	2.94E-02	2.76E-02
1.5E-02	1.53E-01	1.51E-01	1.40E-01	1.19E-01	9.36E-02	6.54E-02	4.03E-02	1.53E-02	6.57E-02	5.45E-02	5.63E-02	5.33E-02
2.0E-02	2.22E-01	2.17E-01	2.04E-01	1.83E-01	1.46E-01	1.01E-01	6.25E-02	2.65E-02	9.97E-02	8.04E-02	8.00E-02	7.73E-02
3.0E-02	3.10E-01	3.07E-01	2.92E-01	2.63E-01	2.20E-01	1.63E-01	1.05E-01	9.61E-02	1.58E-01	1.24E-01	1.27E-01	1.22E-01
4.0E-02	3.45E-01	3.42E-01	3.27E-01	2.96E-01	2.52E-01	1.98E-01	1.34E-01	1.62E-01	1.97E-01	1.57E-01	1.60E-01	1.51E-01
5.0E-02	3.64E-01	3.62E-01	3.44E-01	3.15E-01	2.72E-01	2.16E-01	1.55E-01	2.07E-01	2.22E-01	1.78E-01	1.82E-01	1.72E-01
6.0E-02	3.85E-01	3.85E-01	3.66E-01	3.34E-01	2.92E-01	2.34E-01	1.70E-01	2.40E-01	2.44E-01	1.97E-01	2.01E-01	1.91E-01
7.0E-02	4.11E-01	4.08E-01	3.90E-01	3.58E-01	3.15E-01	2.55E-01	1.88E-01	2.71E-01	2.67E-01	2.16E-01	2.21E-01	2.11E-01
8.0E-02	4.43E-01	4.40E-01	4.21E-01	3.88E-01	3.41E-01	2.77E-01	2.07E-01	3.01E-01	2.95E-01	2.37E-01	2.43E-01	2.28E-01
1.0E-01	5.19E-01	5.15E-01	4.92E-01	4.59E-01	4.05E-01	3.35E-01	2.51E-01	3.61E-01	3.50E-01	2.85E-01	2.94E-01	2.76E-01
1.5E-01	7.48E-01	7.44E-01	7.18E-01	6.71E-01	5.99E-01	5.03E-01	3.85E-01	5.39E-01	5.21E-01	4.31E-01	4.44E-01	4.17E-01
2.0E-01	9.98E-01	9.93E-01	9.61E-01	9.04E-01	8.18E-01	6.95E-01	5.41E-01	7.35E-01	7.15E-01	5.94E-01	6.07E-01	5.72E-01
3.0E-01	1.50E+00	1.50E+00	1.46E+00	1.38E+00	1.27E+00	1.10E+00	8.69E-01	1.15E+00	1.11E+00	9.34E-01	9.64E-01	9.06E-01
4.0E-01	2.00E+00	1.99E+00	1.94E+00	1.85E+00	1.71E+00	1.51E+00	1.21E+00	1.57E+00	1.51E+00	1.28E+00	1.32E+00	1.25E+00
5.0E-01	2.46E+00	2.46E+00	2.40E+00	2.30E+00	2.14E+00	1.90E+00	1.55E+00	1.98E+00	1.90E+00	1.64E+00	1.68E+00	1.58E+00
6.0E-01	2.91E+00	2.90E+00	2.84E+00	2.74E+00	2.56E+00	2.30E+00	1.90E+00	2.37E+00	2.29E+00	1.98E+00	2.02E+00	1.91E+00
8.0E-01	3.73E+00	3.73E+00	3.66E+00	3.54E+00	3.34E+00	3.04E+00	2.56E+00	3.12E+00	3.01E+00	2.63E+00	2.69E+00	2.57E+00
1.0E+00	4.49E+00	4.49E+00	4.42E+00	4.28E+00	4.07E+00	3.73E+00	3.18E+00	3.82E+00	3.70E+00	3.25E+00	3.33E+00	3.18E+00
1.5E+00	6.13E+00	6.12E+00	6.05E+00	5.89E+00	5.65E+00	5.28E+00	4.62E+00	5.38E+00	5.22E+00	4.68E+00	4.77E+00	4.58E+00
2.0E+00	7.54E+00	7.53E+00	7.46E+00	7.30E+00	7.04E+00	6.63E+00	5.90E+00	6.75E+00	6.57E+00	5.95E+00	6.05E+00	5.83E+00
3.0E+00	9.98E+00	9.97E+00	9.89E+00	9.71E+00	9.43E+00	9.00E+00	8.17E+00	9.10E+00	8.90E+00	8.18E+00	8.32E+00	8.03E+00
4.0E+00	1.21E+01	1.21E+01	1.20E+01	1.19E+01	1.15E+01	1.11E+01	1.02E+01	1.12E+01	1.10E+01	1.02E+01	1.03E+01	1.00E+01
5.0E+00	1.42E+01	1.41E+01	1.40E+01	1.38E+01	1.35E+01	1.30E+01	1.21E+01	1.31E+01	1.29E+01	1.20E+01	1.22E+01	1.19E+01
6.0E+00	1.61E+01	1.61E+01	1.60E+01	1.58E+01	1.54E+01	1.49E+01	1.39E+01	1.50E+01	1.47E+01	1.38E+01	1.40E+01	1.36E+01
8.0E+00	1.99E+01	1.99E+01	1.98E+01	1.95E+01	1.91E+01	1.85E+01	1.74E+01	1.86E+01	1.83E+01	1.73E+01	1.75E+01	1.71E+01
1.0E+01	2.37E+01	2.37E+01	2.35E+01	2.32E+01	2.27E+01	2.21E+01	2.09E+01	2.22E+01	2.19E+01	2.07E+01	2.10E+01	2.05E+01
1.5E+01	3.33E+01	3.32E+01	3.30E+01	3.26E+01	3.20E+01	3.11E+01	2.96E+01	3.12E+01	3.09E+01	2.93E+01	2.96E+01	2.90E+01
2.0E+01	4.32E+01	4.31E+01	4.29E+01	4.23E+01	4.15E+01	4.04E+01	3.85E+01	4.05E+01	4.02E+01	3.82E+01	3.85E+01	3.77E+01
3.0E+01	6.41E+01	6.40E+01	6.36E+01	6.28E+01	6.16E+01	5.99E+01	5.71E+01	6.00E+01	5.96E+01	5.66E+01	5.72E+01	5.60E+01
4.0E+01	8.63E+01	8.62E+01	8.57E+01	8.45E+01	8.29E+01	8.06E+01	7.68E+01	8.08E+01	8.02E+01	7.62E+01	7.70E+01	7.54E+01
5.0E+01	1.09E+02	1.09E+02	1.09E+02	1.07E+02	1.05E+02	1.02E+02	9.73E+01	1.02E+02	1.02E+02	9.64E+01	9.75E+01	9.55E+01

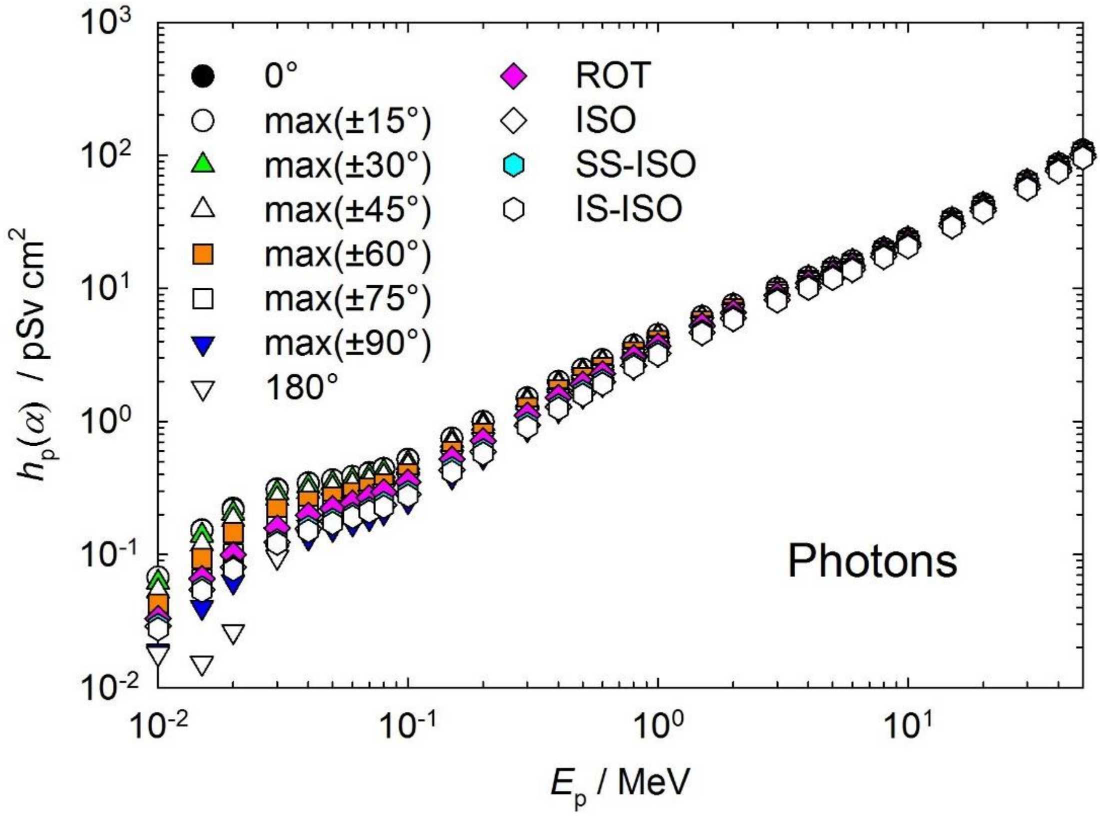

Figure A.5.2a Conversion coefficient from photon fluence to personal dose calculated using the kerma-approximation method (Endo, 2017).

Table A.5.2b Conversion coefficient from photon air kerma to personal dose calculated using the kerma-approximation method (Endo, 2017).

E_p / MeV	$h_p(\alpha)$ / (Sv Gy^{-1})											
	0°	max(±15°)	max(±30°)	max(±45°)	max(±60°)	max(±75°)	max(±90°)	180°	ROT	ISO	SS-ISO	IS-ISO
1.0E-02	9.12E-03	9.13E-03	8.38E-03	7.20E-03	5.77E-03	4.20E-03	2.55E-03	2.44E-03	4.47E-03	3.91E-03	3.98E-03	3.73E-03
1.5E-02	4.89E-02	4.84E-02	4.48E-02	3.81E-02	2.99E-02	2.09E-02	1.29E-02	4.90E-03	2.10E-02	1.74E-02	1.80E-02	1.71E-02
2.0E-02	1.32E-01	1.29E-01	1.21E-01	1.09E-01	8.68E-02	6.01E-02	3.71E-02	1.57E-02	5.92E-02	4.77E-02	4.75E-02	4.59E-02
3.0E-02	4.30E-01	4.25E-01	4.04E-01	3.64E-01	3.05E-01	2.26E-01	1.45E-01	1.33E-01	2.19E-01	1.72E-01	1.76E-01	1.69E-01
4.0E-02	8.05E-01	7.99E-01	7.63E-01	6.90E-01	5.88E-01	4.61E-01	3.12E-01	3.79E-01	4.60E-01	3.65E-01	3.74E-01	3.51E-01
5.0E-02	1.13E+00	1.12E+00	1.07E+00	9.76E-01	8.42E-01	6.68E-01	4.81E-01	6.40E-01	6.87E-01	5.52E-01	5.65E-01	5.33E-01
6.0E-02	1.33E+00	1.33E+00	1.27E+00	1.16E+00	1.01E+00	8.10E-01	5.89E-01	8.30E-01	8.44E-01	6.82E-01	6.96E-01	6.62E-01
7.0E-02	1.43E+00	1.42E+00	1.35E+00	1.24E+00	1.09E+00	8.85E-01	6.52E-01	9.41E-01	9.28E-01	7.49E-01	7.70E-01	7.32E-01
8.0E-02	1.44E+00	1.43E+00	1.37E+00	1.26E+00	1.11E+00	9.04E-01	6.76E-01	9.83E-01	9.62E-01	7.74E-01	7.93E-01	7.45E-01
1.0E-01	1.40E+00	1.39E+00	1.32E+00	1.24E+00	1.09E+00	9.02E-01	6.75E-01	9.71E-01	9.42E-01	7.67E-01	7.90E-01	7.44E-01
1.5E-01	1.25E+00	1.24E+00	1.20E+00	1.12E+00	9.99E-01	8.39E-01	6.43E-01	8.99E-01	8.69E-01	7.19E-01	7.41E-01	6.95E-01
2.0E-01	1.16E+00	1.16E+00	1.12E+00	1.06E+00	9.55E-01	8.11E-01	6.31E-01	8.58E-01	8.34E-01	6.93E-01	7.08E-01	6.68E-01
3.0E-01	1.09E+00	1.08E+00	1.06E+00	1.00E+00	9.18E-01	7.95E-01	6.28E-01	8.34E-01	8.06E-01	6.75E-01	6.97E-01	6.55E-01
4.0E-01	1.06E+00	1.05E+00	1.03E+00	9.80E-01	9.06E-01	7.97E-01	6.40E-01	8.29E-01	7.99E-01	6.79E-01	6.98E-01	6.59E-01
5.0E-01	1.04E+00	1.03E+00	1.01E+00	9.68E-01	9.00E-01	8.00E-01	6.53E-01	8.32E-01	8.01E-01	6.88E-01	7.04E-01	6.64E-01
6.0E-01	1.02E+00	1.02E+00	9.99E-01	9.62E-01	8.99E-01	8.07E-01	6.67E-01	8.35E-01	8.04E-01	6.95E-01	7.10E-01	6.72E-01
8.0E-01	1.01E+00	1.01E+00	9.90E-01	9.56E-01	9.01E-01	8.22E-01	6.90E-01	8.44E-01	8.13E-01	7.10E-01	7.25E-01	6.94E-01
1.0E+00	1.00E+00	1.00E+00	9.87E-01	9.55E-01	9.08E-01	8.32E-01	7.09E-01	8.52E-01	8.25E-01	7.25E-01	7.42E-01	7.10E-01
1.5E+00	9.98E-01	9.96E-01	9.84E-01	9.58E-01	9.19E-01	8.59E-01	7.52E-01	8.76E-01	8.50E-01	7.61E-01	7.76E-01	7.46E-01
2.0E+00	9.97E-01	9.97E-01	9.88E-01	9.66E-01	9.32E-01	8.78E-01	7.81E-01	8.93E-01	8.69E-01	7.87E-01	8.01E-01	7.71E-01
3.0E+00	1.00E+00	9.99E-01	9.91E-01	9.73E-01	9.45E-01	9.02E-01	8.19E-01	9.12E-01	8.92E-01	8.20E-01	8.34E-01	8.05E-01
4.0E+00	1.00E+00	9.99E-01	9.92E-01	9.76E-01	9.50E-01	9.12E-01	8.41E-01	9.20E-01	9.03E-01	8.39E-01	8.51E-01	8.25E-01
5.0E+00	1.00E+00	9.97E-01	9.90E-01	9.77E-01	9.53E-01	9.17E-01	8.53E-01	9.24E-01	9.08E-01	8.50E-01	8.61E-01	8.37E-01
6.0E+00	9.97E-01	9.95E-01	9.88E-01	9.75E-01	9.52E-01	9.19E-01	8.61E-01	9.26E-01	9.11E-01	8.56E-01	8.66E-01	8.43E-01
8.0E+00	9.89E-01	9.88E-01	9.82E-01	9.69E-01	9.47E-01	9.18E-01	8.65E-01	9.24E-01	9.10E-01	8.61E-01	8.70E-01	8.48E-01
1.0E+01	9.82E-01	9.81E-01	9.75E-01	9.62E-01	9.41E-01	9.15E-01	8.66E-01	9.19E-01	9.07E-01	8.59E-01	8.68E-01	8.48E-01
1.5E+01	9.65E-01	9.64E-01	9.59E-01	9.47E-01	9.28E-01	9.03E-01	8.59E-01	9.06E-01	8.96E-01	8.51E-01	8.60E-01	8.42E-01
2.0E+01	9.52E-01	9.50E-01	9.45E-01	9.33E-01	9.15E-01	8.91E-01	8.49E-01	8.93E-01	8.85E-01	8.41E-01	8.50E-01	8.32E-01
3.0E+01	9.34E-01	9.33E-01	9.28E-01	9.16E-01	8.98E-01	8.74E-01	8.33E-01	8.75E-01	8.69E-01	8.25E-01	8.34E-01	8.16E-01
4.0E+01	9.25E-01	9.24E-01	9.18E-01	9.06E-01	8.88E-01	8.64E-01	8.24E-01	8.66E-01	8.60E-01	8.16E-01	8.26E-01	8.09E-01
5.0E+01	9.17E-01	9.16E-01	9.10E-01	8.98E-01	8.81E-01	8.56E-01	8.16E-01	8.58E-01	8.52E-01	8.09E-01	8.18E-01	8.01E-01

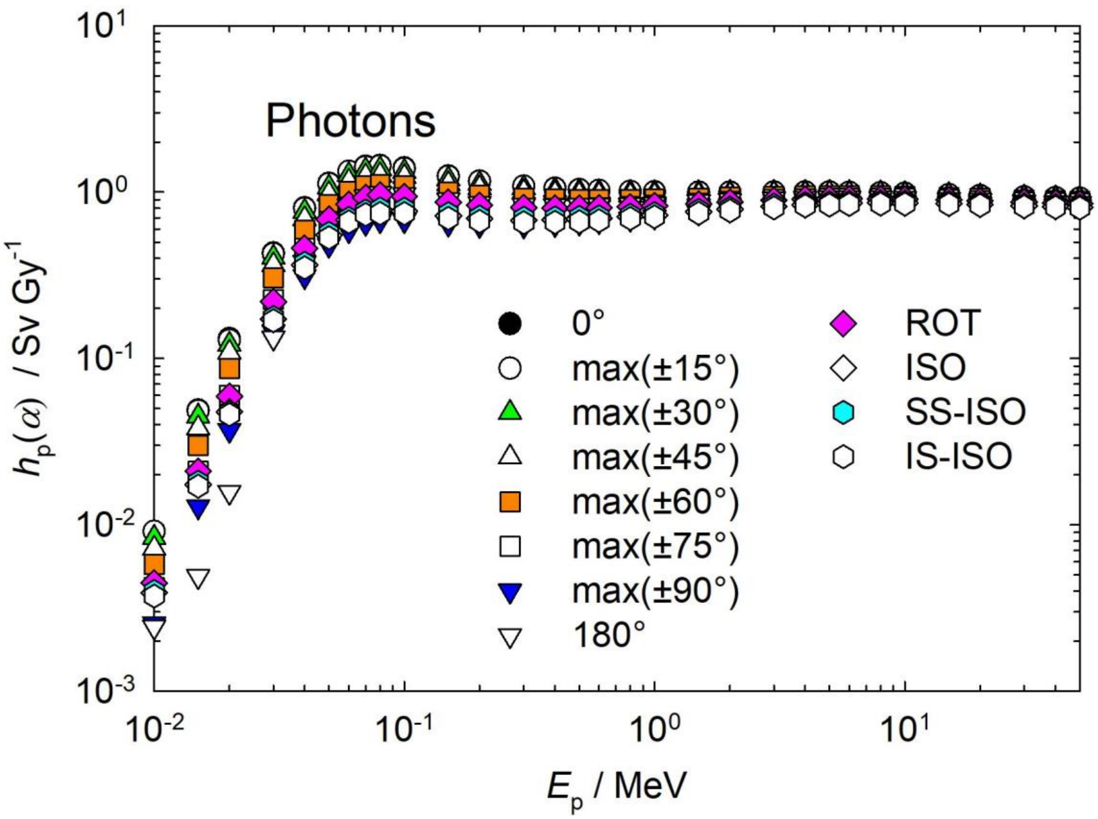

Figure A.5.2b Conversion coefficient from photon air kerma to personal dose calculated using the kerma-approximation method (Endo, 2017).

Table A.5.3a Conversion coefficients from photons fluence to the maximum absorbed dose in the complete lens for left or right irradiations calculated using the kerma-approximation method (Behrens, 2017a).

	$d_{\text{lens}}(\alpha)$/ (pGy cm²) for a radiation incidence at α							
E_p / MeV	0°	15°	30°	45°	60°	75°	90°	ROT
0.005	8.43E-06	1.56E-05	3.25E-05	3.23E-05	1.20E-05	1.59E-06	8.80E-08	6.67E-06
0.006	2.01E-03	2.34E-03	2.97E-03	2.76E-03	1.46E-03	3.83E-04	4.32E-05	8.42E-04
0.007	3.47E-02	3.55E-02	3.65E-02	3.19E-02	2.03E-02	7.95E-03	1.44E-03	1.15E-02
0.008	1.73E-01	1.72E-01	1.64E-01	1.41E-01	9.78E-02	4.72E-02	1.35E-02	5.45E-02
0.009	4.49E-01	4.40E-01	4.12E-01	3.56E-01	2.67E-01	1.51E-01	5.48E-02	1.44E-01
0.01	7.96E-01	7.78E-01	7.30E-01	6.44E-01	5.08E-01	3.22E-01	1.39E-01	2.63E-01
0.011	1.12E+00	1.10E+00	1.04E+00	9.34E-01	7.72E-01	5.36E-01	2.70E-01	3.87E-01
0.013	1.54E+00	1.52E+00	1.46E+00	1.35E+00	1.19E+00	9.34E-01	5.79E-01	5.75E-01
0.015	1.65E+00	1.63E+00	1.58E+00	1.50E+00	1.38E+00	1.16E+00	8.29E-01	6.60E-01
0.017	1.58E+00	1.57E+00	1.54E+00	1.48E+00	1.39E+00	1.23E+00	9.58E-01	6.73E-01
0.02	1.38E+00	1.38E+00	1.36E+00	1.32E+00	1.27E+00	1.17E+00	9.82E-01	6.28E-01
0.024	1.11E+00	1.12E+00	1.11E+00	1.09E+00	1.06E+00	9.99E-01	8.87E-01	5.46E-01
0.03	8.32E-01	8.36E-01	8.39E-01	8.32E-01	8.11E-01	7.78E-01	7.17E-01	4.41E-01
0.04	5.87E-01	5.95E-01	5.96E-01	5.96E-01	5.90E-01	5.71E-01	5.35E-01	3.40E-01
0.05	4.88E-01	4.90E-01	4.98E-01	4.99E-01	4.95E-01	4.79E-01	4.53E-01	2.98E-01
0.06	4.55E-01	4.56E-01	4.64E-01	4.67E-01	4.62E-01	4.46E-01	4.27E-01	2.86E-01
0.07	4.56E-01	4.62E-01	4.66E-01	4.67E-01	4.64E-01	4.52E-01	4.34E-01	2.95E-01
0.08	4.81E-01	4.87E-01	4.91E-01	4.90E-01	4.88E-01	4.78E-01	4.60E-01	3.15E-01
0.1	5.59E-01	5.62E-01	5.72E-01	5.71E-01	5.65E-01	5.59E-01	5.41E-01	3.77E-01
0.12	6.64E-01	6.67E-01	6.73E-01	6.74E-01	6.72E-01	6.66E-01	6.44E-01	4.52E-01
0.15	8.35E-01	8.39E-01	8.46E-01	8.50E-01	8.45E-01	8.39E-01	8.19E-01	5.81E-01
0.2	1.13E+00	1.14E+00	1.15E+00	1.17E+00	1.15E+00	1.15E+00	1.13E+00	8.17E-01
0.24	1.38E+00	1.39E+00	1.40E+00	1.41E+00	1.39E+00	1.38E+00	1.37E+00	1.00E+00
0.3	1.74E+00	1.74E+00	1.76E+00	1.79E+00	1.75E+00	1.75E+00	1.73E+00	1.29E+00
0.4	2.30E+00	2.34E+00	2.34E+00	2.37E+00	2.34E+00	2.32E+00	2.29E+00	1.75E+00
0.5	2.82E+00	2.85E+00	2.88E+00	2.93E+00	2.90E+00	2.84E+00	2.85E+00	2.21E+00
0.511	2.88E+00	2.90E+00	2.94E+00	2.99E+00	2.96E+00	2.90E+00	2.91E+00	2.25E+00
0.6	3.33E+00	3.35E+00	3.39E+00	3.45E+00	3.42E+00	3.35E+00	3.36E+00	2.64E+00
0.662	3.63E+00	3.65E+00	3.69E+00	3.77E+00	3.72E+00	3.65E+00	3.65E+00	2.91E+00
0.8	4.24E+00	4.28E+00	4.30E+00	4.39E+00	4.38E+00	4.28E+00	4.29E+00	3.46E+00
1	5.08E+00	5.10E+00	5.15E+00	5.25E+00	5.23E+00	5.13E+00	5.12E+00	4.21E+00
1.117	5.54E+00	5.57E+00	5.63E+00	5.69E+00	5.68E+00	5.55E+00	5.56E+00	4.63E+00
1.2	5.83E+00	5.91E+00	5.94E+00	5.99E+00	5.96E+00	5.89E+00	5.88E+00	4.92E+00
1.3	6.20E+00	6.21E+00	6.27E+00	6.37E+00	6.36E+00	6.22E+00	6.25E+00	5.24E+00
1.33	6.29E+00	6.31E+00	6.37E+00	6.46E+00	6.44E+00	6.34E+00	6.34E+00	5.36E+00
1.5	6.88E+00	6.90E+00	6.92E+00	7.04E+00	7.05E+00	6.86E+00	6.90E+00	5.86E+00
1.7	7.49E+00	7.53E+00	7.58E+00	7.67E+00	7.65E+00	7.49E+00	7.54E+00	6.48E+00
2	8.39E+00	8.39E+00	8.44E+00	8.56E+00	8.53E+00	8.41E+00	8.37E+00	7.25E+00
2.4	9.44E+00	9.49E+00	9.50E+00	9.63E+00	9.64E+00	9.48E+00	9.53E+00	8.33E+00
3	1.10E+01	1.10E+01	1.10E+01	1.11E+01	1.11E+01	1.10E+01	1.09E+01	9.77E+00
4	1.32E+01	1.32E+01	1.33E+01	1.33E+01	1.33E+01	1.32E+01	1.32E+01	1.19E+01
5	1.53E+01	1.53E+01	1.54E+01	1.54E+01	1.55E+01	1.53E+01	1.53E+01	1.39E+01
6	1.74E+01	1.74E+01	1.74E+01	1.75E+01	1.75E+01	1.74E+01	1.74E+01	1.59E+01
6.129	1.76E+01	1.77E+01	1.77E+01	1.78E+01	1.78E+01	1.76E+01	1.76E+01	1.61E+01
8	2.15E+01	2.14E+01	2.15E+01	2.15E+01	2.15E+01	2.14E+01	2.13E+01	1.94E+01
10	2.54E+01	2.54E+01	2.55E+01	2.54E+01	2.54E+01	2.53E+01	2.54E+01	2.35E+01
15	3.57E+01	3.58E+01	3.56E+01	3.56E+01	3.57E+01	3.55E+01	3.56E+01	3.28E+01
20	4.63E+01	4.66E+01	4.65E+01	4.66E+01	4.64E+01	4.63E+01	4.62E+01	4.30E+01
30	6.92E+01	6.91E+01	6.93E+01	6.91E+01	6.94E+01	6.91E+01	6.86E+01	6.39E+01
40	9.30E+01	9.35E+01	9.33E+01	9.28E+01	9.32E+01	9.32E+01	9.23E+01	8.63E+01
50	1.18E+02	1.19E+02	1.19E+02	1.18E+02	1.18E+02	1.18E+02	1.18E+02	1.09E+02

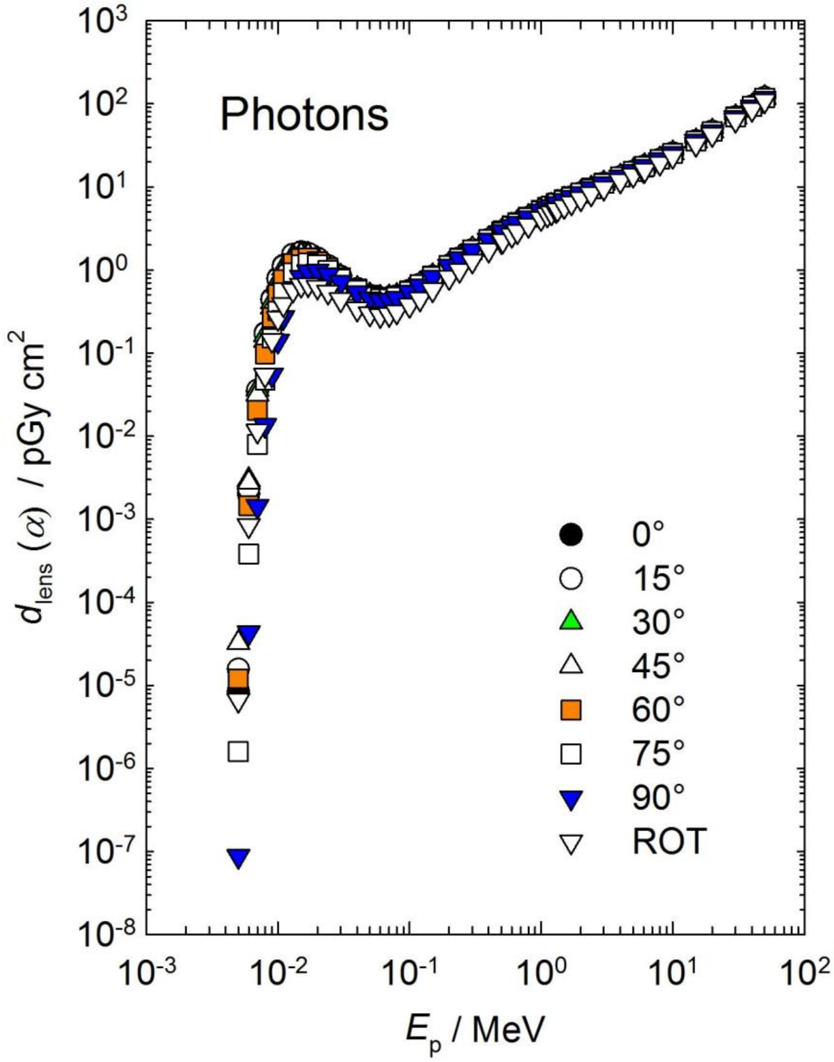

Figure A.5.3a Conversion coefficients from photons fluence to the maximum absorbed dose in the complete lens for left or right irradiations calculated using the kerma-approximation method (Behrens, 2017a).

Table A.5.3b Conversion coefficients from photon air kerma to the maximum absorbed dose in the complete lens for left or right irradiations calculated using the kerma-approximation method (Behrens, 2017a).

	$d_{\mathrm{lens}}(\alpha)/(\mathrm{Gy\ Gy^{-1}})$ for a radiation incidence at α							
E_{p} / MeV	0°	15°	30°	45°	60°	75°	90°	ROT
0.005	2.75E-07	5.10E-07	1.06E-06	1.05E-06	3.92E-07	5.20E-08	2.87E-09	2.18E-07
0.006	9.46E-05	1.10E-04	1.40E-04	1.30E-04	6.88E-05	1.80E-05	2.03E-06	3.96E-05
0.007	2.24E-03	2.29E-03	2.36E-03	2.06E-03	1.31E-03	5.13E-04	9.28E-05	7.45E-04
0.008	1.47E-02	1.46E-02	1.39E-02	1.19E-02	8.29E-03	4.00E-03	1.15E-03	4.62E-03
0.009	4.87E-02	4.77E-02	4.47E-02	3.86E-02	2.89E-02	1.64E-02	5.95E-03	1.56E-02
0.01	1.08E-01	1.05E-01	9.87E-02	8.71E-02	6.87E-02	4.35E-02	1.88E-02	3.56E-02
0.011	1.86E-01	1.83E-01	1.73E-01	1.55E-01	1.28E-01	8.87E-02	4.47E-02	6.41E-02
0.013	3.63E-01	3.58E-01	3.44E-01	3.19E-01	2.81E-01	2.20E-01	1.37E-01	1.36E-01
0.015	5.27E-01	5.21E-01	5.06E-01	4.81E-01	4.41E-01	3.72E-01	2.65E-01	2.11E-01
0.017	6.62E-01	6.57E-01	6.43E-01	6.21E-01	5.82E-01	5.13E-01	4.01E-01	2.82E-01
0.02	8.20E-01	8.17E-01	8.05E-01	7.84E-01	7.54E-01	6.92E-01	5.83E-01	3.73E-01
0.024	9.67E-01	9.70E-01	9.65E-01	9.50E-01	9.24E-01	8.69E-01	7.72E-01	4.75E-01
0.03	1.15E+00	1.16E+00	1.16E+00	1.15E+00	1.12E+00	1.08E+00	9.94E-01	6.11E-01
0.04	1.37E+00	1.39E+00	1.39E+00	1.39E+00	1.38E+00	1.33E+00	1.25E+00	7.92E-01
0.05	1.51E+00	1.52E+00	1.54E+00	1.54E+00	1.53E+00	1.48E+00	1.40E+00	9.21E-01
0.06	1.57E+00	1.58E+00	1.61E+00	1.61E+00	1.60E+00	1.54E+00	1.48E+00	9.89E-01
0.07	1.58E+00	1.61E+00	1.62E+00	1.62E+00	1.61E+00	1.57E+00	1.51E+00	1.03E+00
0.08	1.57E+00	1.59E+00	1.60E+00	1.60E+00	1.59E+00	1.56E+00	1.50E+00	1.03E+00
0.1	1.51E+00	1.51E+00	1.54E+00	1.54E+00	1.52E+00	1.50E+00	1.46E+00	1.01E+00
0.12	1.44E+00	1.45E+00	1.46E+00	1.46E+00	1.46E+00	1.45E+00	1.40E+00	9.82E-01
0.15	1.39E+00	1.40E+00	1.41E+00	1.42E+00	1.41E+00	1.40E+00	1.37E+00	9.69E-01
0.2	1.32E+00	1.33E+00	1.35E+00	1.36E+00	1.34E+00	1.34E+00	1.31E+00	9.54E-01
0.24	1.30E+00	1.31E+00	1.31E+00	1.33E+00	1.31E+00	1.30E+00	1.29E+00	9.41E-01
0.3	1.26E+00	1.26E+00	1.27E+00	1.29E+00	1.27E+00	1.26E+00	1.25E+00	9.34E-01
0.4	1.22E+00	1.23E+00	1.24E+00	1.25E+00	1.24E+00	1.23E+00	1.21E+00	9.27E-01
0.5	1.19E+00	1.20E+00	1.21E+00	1.23E+00	1.22E+00	1.19E+00	1.20E+00	9.29E-01
0.511	1.19E+00	1.19E+00	1.21E+00	1.23E+00	1.22E+00	1.19E+00	1.20E+00	9.27E-01
0.6	1.17E+00	1.18E+00	1.19E+00	1.21E+00	1.20E+00	1.18E+00	1.18E+00	9.29E-01
0.662	1.17E+00	1.17E+00	1.19E+00	1.21E+00	1.20E+00	1.17E+00	1.17E+00	9.35E-01
0.8	1.15E+00	1.16E+00	1.16E+00	1.19E+00	1.18E+00	1.16E+00	1.16E+00	9.35E-01
1	1.13E+00	1.14E+00	1.15E+00	1.17E+00	1.17E+00	1.14E+00	1.14E+00	9.39E-01
1.117	1.13E+00	1.14E+00	1.15E+00	1.16E+00	1.16E+00	1.14E+00	1.14E+00	9.47E-01
1.2	1.13E+00	1.14E+00	1.15E+00	1.16E+00	1.15E+00	1.14E+00	1.14E+00	9.52E-01
1.3	1.13E+00	1.13E+00	1.14E+00	1.16E+00	1.16E+00	1.13E+00	1.14E+00	9.53E-01
1.33	1.12E+00	1.13E+00	1.14E+00	1.15E+00	1.15E+00	1.13E+00	1.13E+00	9.57E-01
1.5	1.12E+00	1.12E+00	1.13E+00	1.15E+00	1.15E+00	1.12E+00	1.12E+00	9.54E-01
1.7	1.11E+00	1.12E+00	1.13E+00	1.14E+00	1.14E+00	1.11E+00	1.12E+00	9.63E-01
2	1.11E+00	1.11E+00	1.12E+00	1.13E+00	1.13E+00	1.11E+00	1.11E+00	9.60E-01
2.4	1.10E+00	1.11E+00	1.11E+00	1.12E+00	1.13E+00	1.11E+00	1.11E+00	9.73E-01
3	1.10E+00	1.10E+00	1.11E+00	1.11E+00	1.11E+00	1.10E+00	1.09E+00	9.79E-01
4	1.09E+00	1.09E+00	1.10E+00	1.10E+00	1.10E+00	1.08E+00	1.08E+00	9.77E-01
5	1.08E+00	1.08E+00	1.08E+00	1.09E+00	1.09E+00	1.08E+00	1.08E+00	9.80E-01
6	1.07E+00	1.08E+00	1.08E+00	1.08E+00	1.08E+00	1.07E+00	1.08E+00	9.80E-01
6.129	1.07E+00	1.08E+00	1.07E+00	1.08E+00	1.08E+00	1.07E+00	1.07E+00	9.79E-01
8	1.07E+00	1.06E+00	1.07E+00	1.07E+00	1.07E+00	1.06E+00	1.06E+00	9.66E-01
10	1.05E+00	1.05E+00	1.06E+00	1.05E+00	1.05E+00	1.05E+00	1.05E+00	9.73E-01
15	1.04E+00	1.04E+00	1.03E+00	1.03E+00	1.04E+00	1.03E+00	1.03E+00	9.52E-01
20	1.02E+00	1.03E+00	1.03E+00	1.03E+00	1.02E+00	1.02E+00	1.02E+00	9.48E-01
30	1.01E+00	1.01E+00	1.01E+00	1.01E+00	1.01E+00	1.01E+00	1.00E+00	9.32E-01
40	9.97E-01	1.00E+00	1.00E+00	9.94E-01	9.98E-01	9.99E-01	9.89E-01	9.26E-01
50	9.92E-01	9.99E-01	9.96E-01	9.93E-01	9.88E-01	9.91E-01	9.88E-01	9.18E-01

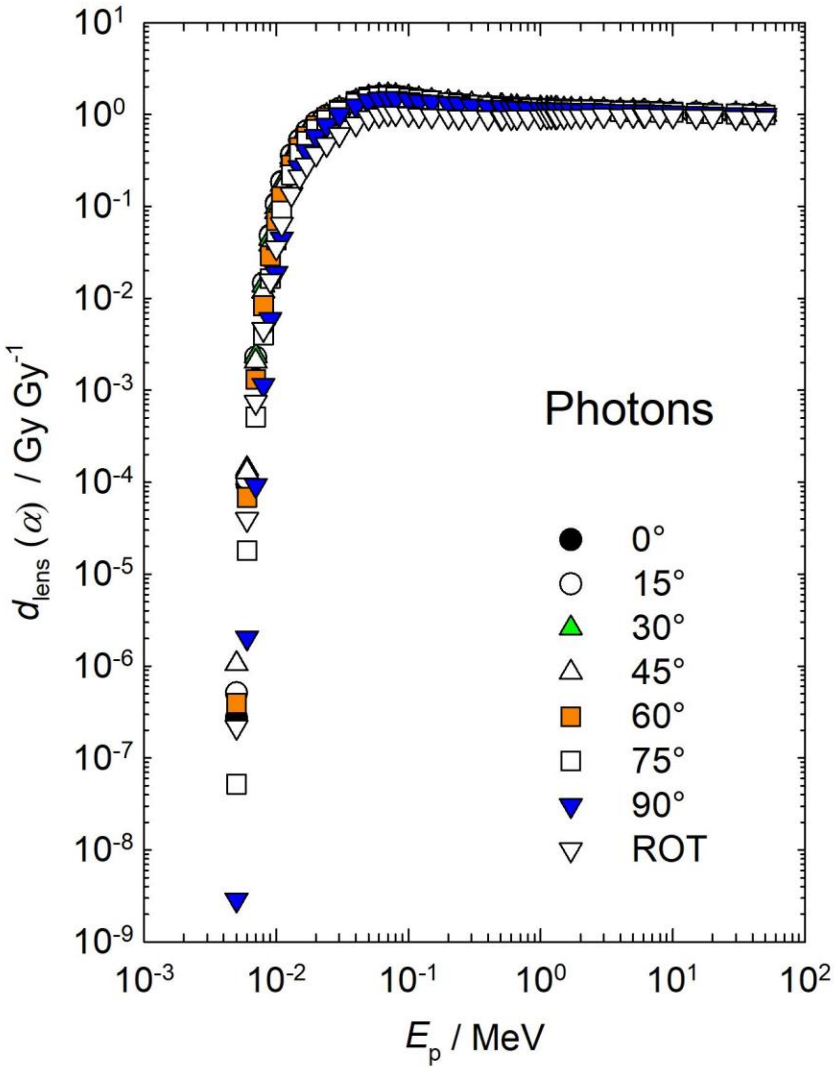

Table A.5.3b Conversion coefficients from photons air kerma to the maximum absorbed dose in the complete lens for left or right irradiations calculated using the kerma-approximation method (Behrens, 2017a).

Table A.5.4.1a Conversion coefficient from photon fluence to directional and personal absorbed dose in local skin on the slab phantom, calculated using the kerma-approximation method (Daures *et al*., 2017).

E_p / MeV	$d_{\text{local skin}}$ / (pGy cm^2) for a radiation incidence at α					
	0°	15°	30°	45°	60°	75°
0.01	7.16E+00	7.15E+00	7.13E+00	7.04E+00	6.89E+00	6.38E+00
0.015	3.20E+00	3.19E+00	3.19E+00	3.17E+00	3.14E+00	3.05E+00
0.02	1.84E+00	1.83E+00	1.83E+00	1.82E+00	1.80E+00	1.75E+00
0.03	9.28E-01	9.26E-01	9.21E-01	9.08E-01	8.83E-01	8.34E-01
0.04	6.47E-01	6.45E-01	6.40E-01	5.21E-01	6.01E-01	5.52E-01
0.05	5.43E-01	5.40E-01	5.35E-01	5.21E-01	4.97E-01	4.52E-01
0.06	5.10E-01	5.08E-01	5.02E-01	4.90E-01	4.67E-01	4.24E-01
0.07	5.15E-01	5.12E-01	5.07E-01	4.95E-01	4.72E-01	4.33E-01
0.08	5.40E-01	5.38E-01	5.33E-01	5.22E-01	5.01E-01	4.62E-01
0.1	6.25E-01	6.24E-01	6.21E-01	6.11E-01	5.92E-01	5.54E-01
0.15	9.14E-01	9.13E-01	9.15E-01	9.09E-01	8.97E-01	8.61E-01
0.2	1.23E+00	1.23E+00	1.23E+00	1.23E+00	1.23E+00	1.20E+00
0.3	1.84E+00	1.84E+00	1.86E+00	1.87E+00	1.89E+00	1.87E+00
0.4	2.42E+00	2.42E+00	2.44E+00	2.46E+00	2.50E+00	2.51E+00
0.5	2.96E+00	2.96E+00	2.99E+00	3.02E+00	3.07E+00	3.11E+00
0.6	3.47E+00	3.47E+00	3.50E+00	3.54E+00	3.61E+00	3.66E+00
0.662	3.77E+00	3.78E+00	3.81E+00	3.84E+00	3.92E+00	4.00E+00
0.8	4.40E+00	4.41E+00	4.44E+00	4.49E+00	4.58E+00	4.69E+00
1	5.24E+00	5.25E+00	5.29E+00	5.34E+00	5.45E+00	5.58E+00
1.25	6.18E+00	6.19E+00	6.23E+00	6.28E+00	6.40E+00	6.57E+00
1.5	7.03E+00	7.03E+00	7.08E+00	7.13E+00	7.26E+00	7.46E+00
2	8.55E+00	8.54E+00	8.59E+00	8.64E+00	8.79E+00	9.01E+00
3	1.11E+01	1.11E+01	1.12E+01	1.12E+01	1.13E+01	1.16E+01
5	1.55E+01	1.55E+01	1.56E+01	1.56E+01	1.57E+01	1.60E+01
10	2.57E+01	2.57E+01	2.57E+01	2.57E+01	2.58E+01	2.60E+01
15	3.60E+01	3.59E+01	3.60E+01	3.60E+01	3.61E+01	3.62E+01
20	4.67E+01	4.67E+01	4.68E+01	4.67E+01	4.69E+01	4.70E+01
30	6.96E+01	6.95E+01	6.97E+01	6.96E+01	6.97E+01	6.97E+01
50	1.19E+02	1.19E+02	1.19E+02	1.19E+02	1.19E+02	1.19E+02

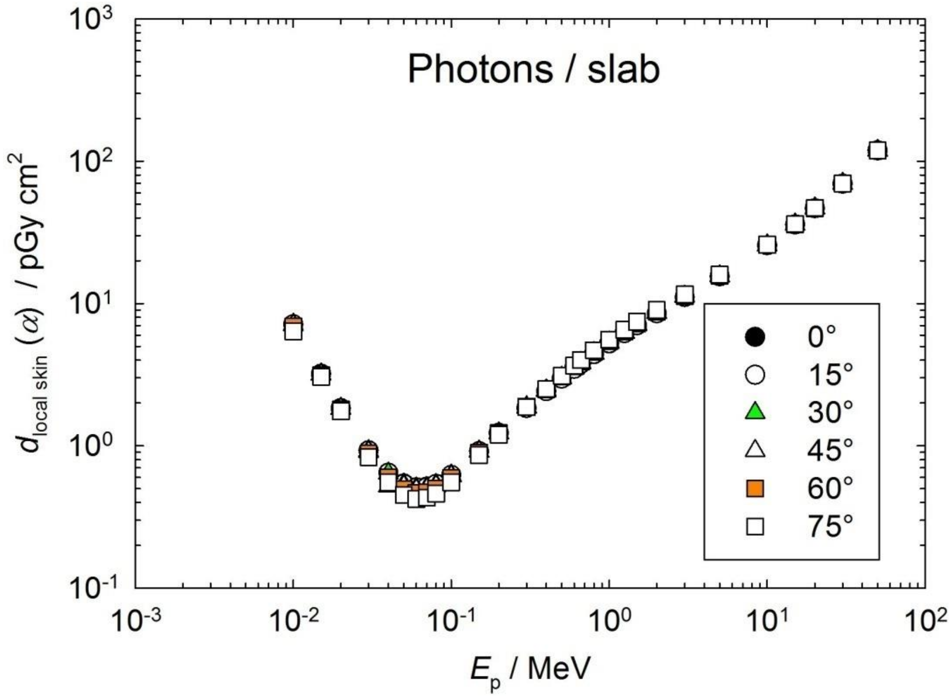

Figure A.5.4.1a Conversion coefficient from photon fluence to directional and personal absorbed dose in local skin on the slab phantom calculated using the kerma-approximation method (Daures *et al*., 2017).

Table A.5.4.1b Conversion coefficient from photon air kerma to directional and personal absorbed dose in local skin on the slab phantom calculated using the kerma-approximation method (Daures *et al*. 2017).

E_p / MeV	$d_{\mathrm{local\ skin}}$ / (GyGy^{-1}) for a radiation incidence at α					
	0°	15°	30°	45°	60°	75°
0.01	9.68E-01	9.66E-01	9.64E-01	9.51E-01	9.31E-01	8.62E-01
0.015	1.02E+00	1.02E+00	1.02E+00	1.01E+00	1.00E+00	9.76E-01
0.02	1.09E+00	1.09E+00	1.09E+00	1.08E+00	1.07E+00	1.04E+00
0.03	1.29E+00	1.28E+00	1.28E+00	1.26E+00	1.22E+00	1.16E+00
0.04	1.51E+00	1.50E+00	1.49E+00	1.21E+00	1.40E+00	1.29E+00
0.05	1.68E+00	1.67E+00	1.66E+00	1.61E+00	1.54E+00	1.40E+00
0.06	1.77E+00	1.76E+00	1.74E+00	1.70E+00	1.62E+00	1.47E+00
0.07	1.79E+00	1.78E+00	1.76E+00	1.72E+00	1.64E+00	1.50E+00
0.08	1.76E+00	1.75E+00	1.74E+00	1.70E+00	1.63E+00	1.51E+00
0.1	1.68E+00	1.68E+00	1.67E+00	1.65E+00	1.59E+00	1.49E+00
0.15	1.52E+00	1.52E+00	1.53E+00	1.52E+00	1.50E+00	1.44E+00
0.2	1.44E+00	1.44E+00	1.44E+00	1.44E+00	1.44E+00	1.40E+00
0.3	1.33E+00	1.33E+00	1.34E+00	1.35E+00	1.37E+00	1.35E+00
0.4	1.28E+00	1.28E+00	1.29E+00	1.30E+00	1.32E+00	1.33E+00
0.5	1.24E+00	1.24E+00	1.26E+00	1.27E+00	1.29E+00	1.31E+00
0.6	1.22E+00	1.22E+00	1.23E+00	1.24E+00	1.27E+00	1.29E+00
0.662	1.21E+00	1.21E+00	1.22E+00	1.23E+00	1.26E+00	1.29E+00
0.8	1.19E+00	1.19E+00	1.20E+00	1.21E+00	1.24E+00	1.27E+00
1	1.17E+00	1.17E+00	1.18E+00	1.19E+00	1.22E+00	1.25E+00
1.25	1.16E+00	1.16E+00	1.17E+00	1.18E+00	1.20E+00	1.23E+00
1.5	1.14E+00	1.14E+00	1.15E+00	1.16E+00	1.18E+00	1.21E+00
2	1.13E+00	1.13E+00	1.14E+00	1.14E+00	1.16E+00	1.19E+00
3	1.11E+00	1.11E+00	1.12E+00	1.12E+00	1.13E+00	1.16E+00
5	1.09E+00	1.09E+00	1.10E+00	1.10E+00	1.11E+00	1.13E+00
10	1.07E+00	1.07E+00	1.07E+00	1.07E+00	1.07E+00	1.08E+00
15	1.04E+00	1.04E+00	1.04E+00	1.04E+00	1.05E+00	1.05E+00
20	1.03E+00	1.03E+00	1.03E+00	1.03E+00	1.03E+00	1.04E+00
30	1.01E+00	1.01E+00	1.02E+00	1.01E+00	1.02E+00	1.02E+00
50	9.98E-01	9.98E-01	9.98E-01	9.98E-01	9.98E-01	9.98E-01

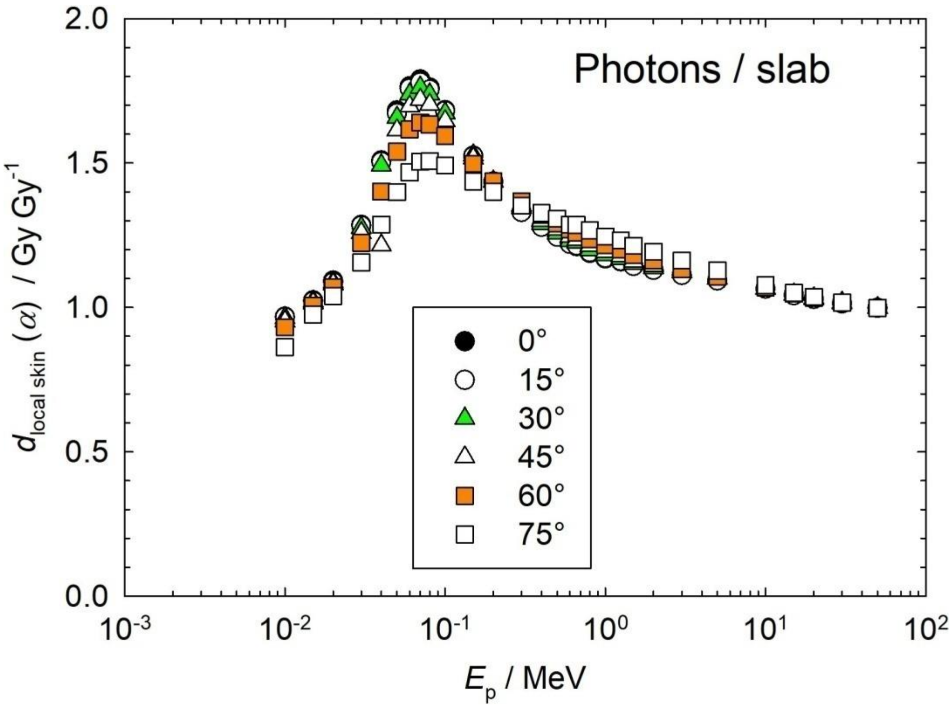

Figure A.5.4.1b Conversion coefficient from photon air kerma to directional and personal absorbed dose in local skin on the slab phantom calculated using the kerma-approximation method (Daures *et al*., 2017).

Table A.5.4.2a Conversion coefficient from photon fluence to personal absorbed dose in local skin on the pillar phantom calculated using the kerma-approximation method (1/2) (Otto, 2017).

E_p / MeV	$d_{p\ \text{local skin}}$ / (pGy cm^2) for a radiation incidence at α						
	0°	15°	30°	45°	60°	75°	90°
0.002	2.95E+00	2.58E+00	1.67E+00	6.77E-01	1.09E-01	2.16E-03	2.33E-05
0.003	2.08E+01	1.99E+01	1.69E+01	1.20E+01	5.71E+00	8.70E-01	2.59E-03
0.004	2.62E+01	2.57E+01	2.39E+01	2.04E+01	1.43E+01	5.19E+00	9.66E-02
0.005	2.26E+01	2.24E+01	2.16E+01	1.98E+01	1.64E+01	9.14E+00	5.54E-01
0.007	1.40E+01	1.39E+01	1.38E+01	1.34E+01	1.24E+01	9.83E+00	1.84E+00
0.01	7.23E+00	7.20E+00	7.20E+00	7.12E+00	6.93E+00	6.37E+00	2.44E+00
0.015	3.22E+00	3.23E+00	3.22E+00	3.19E+00	3.17E+00	3.09E+00	1.99E+00
0.02	1.84E+00	1.85E+00	1.84E+00	1.84E+00	1.82E+00	1.78E+00	1.41E+00
0.03	9.07E-01	9.04E-01	8.99E-01	8.93E-01	8.79E-01	8.67E-01	7.70E-01
0.05	4.64E-01	4.71E-01	4.59E-01	4.68E-01	4.59E-01	4.59E-01	4.28E-01
0.07	4.22E-01	4.18E-01	4.19E-01	4.12E-01	4.13E-01	4.13E-01	3.89E-01
0.1	5.19E-01	5.14E-01	5.18E-01	5.14E-01	5.07E-01	5.12E-01	4.89E-01
0.15	7.87E-01	7.87E-01	7.86E-01	7.89E-01	7.89E-01	7.95E-01	7.69E-01
0.2	1.08E+00	1.09E+00	1.09E+00	1.09E+00	1.09E+00	1.11E+00	1.07E+00
0.3	1.68E+00	1.67E+00	1.67E+00	1.68E+00	1.70E+00	1.72E+00	1.69E+00
0.5	2.78E+00	2.78E+00	2.77E+00	2.80E+00	2.82E+00	2.85E+00	2.85E+00
0.662	3.62E+00	3.57E+00	3.55E+00	3.61E+00	3.66E+00	3.65E+00	3.66E+00
0.7	3.77E+00	3.77E+00	3.75E+00	3.78E+00	3.85E+00	3.83E+00	3.85E+00
1	5.13E+00	5.03E+00	5.02E+00	5.06E+00	5.15E+00	5.21E+00	5.20E+00
1.25	6.00E+00	5.99E+00	5.97E+00	6.00E+00	6.07E+00	6.18E+00	6.14E+00
1.5	6.96E+00	6.86E+00	6.83E+00	6.92E+00	6.97E+00	6.98E+00	6.94E+00
2	8.38E+00	8.30E+00	8.31E+00	8.24E+00	8.36E+00	8.79E+00	8.34E+00
3	1.10E+01	1.11E+01	1.11E+01	1.09E+01	1.12E+01	1.12E+01	1.08E+01
5	1.58E+01	1.53E+01	1.51E+01	1.54E+01	1.56E+01	1.50E+01	1.55E+01
7	1.96E+01	1.94E+01	1.95E+01	1.96E+01	1.95E+01	1.93E+01	1.94E+01
10	2.56E+01	2.56E+01	2.58E+01	2.55E+01	2.51E+01	2.52E+01	2.54E+01
15	3.71E+01	3.55E+01	3.53E+01	3.65E+01	3.61E+01	3.65E+01	3.61E+01
20	4.85E+01	4.53E+01	4.67E+01	4.73E+01	4.64E+01	4.71E+01	4.71E+01
30	7.16E+01	6.92E+01	6.95E+01	7.08E+01	6.98E+01	6.95E+01	6.91E+01
50	1.20E+02	1.19E+02	1.19E+02	1.22E+02	1.20E+02	1.19E+02	1.20E+02

Table A.5.4.2a Conversion coefficient from photon fluence to personal absorbed dose in local skin on the pillar phantom calculated using the kerma-approximation method (2/2) (Otto, 2017).

	$d_{\mathrm{p\ local\ skin}}$ / (pGy cm²) for a radiation incidence at α						
E_{p} / MeV	105°	120°	135°	150°	165°	180°	ROT
0.002	0.00E+00	0.00E+00	0.00E+00	0.00E+00	0.00E+00	0.00E+00	5.43E-01
0.003	0.00E+00	0.00E+00	0.00E+00	0.00E+00	0.00E+00	0.00E+00	5.48E+00
0.004	0.00E+00	0.00E+00	0.00E+00	0.00E+00	0.00E+00	0.00E+00	8.56E+00
0.005	0.00E+00	0.00E+00	0.00E+00	0.00E+00	0.00E+00	0.00E+00	8.44E+00
0.007	0.00E+00	0.00E+00	0.00E+00	0.00E+00	0.00E+00	0.00E+00	6.01E+00
0.01	4.60E-03	0.00E+00	0.00E+00	0.00E+00	0.00E+00	0.00E+00	3.41E+00
0.015	1.94E-01	1.17E-02	8.12E-04	1.39E-04	2.81E-05	3.28E-05	1.64E+00
0.02	4.40E-01	1.17E-01	3.79E-02	1.71E-02	1.02E-02	7.85E-03	1.01E+00
0.03	4.61E-01	2.68E-01	1.67E-01	1.25E-01	1.02E-01	9.23E-02	5.70E-01
0.05	3.23E-01	2.35E-01	1.85E-01	1.49E-01	1.35E-01	1.41E-01	3.39E-01
0.07	3.11E-01	2.39E-01	1.96E-01	1.70E-01	1.52E-01	1.52E-01	3.18E-01
0.1	4.01E-01	3.20E-01	2.63E-01	2.35E-01	2.13E-01	2.12E-01	4.04E-01
0.15	6.47E-01	5.27E-01	4.51E-01	3.94E-01	3.67E-01	3.53E-01	6.39E-01
0.2	9.14E-01	7.48E-01	6.49E-01	5.83E-01	5.41E-01	5.37E-01	8.98E-01
0.3	1.46E+00	1.26E+00	1.12E+00	9.94E-01	9.48E-01	9.45E-01	1.43E+00
0.5	2.54E+00	2.23E+00	2.00E+00	1.88E+00	1.81E+00	1.74E+00	2.47E+00
0.662	3.33E+00	2.93E+00	2.68E+00	2.52E+00	2.45E+00	2.35E+00	3.22E+00
0.7	3.49E+00	3.11E+00	2.84E+00	2.67E+00	2.56E+00	2.51E+00	3.39E+00
1	4.72E+00	4.38E+00	3.93E+00	3.79E+00	3.74E+00	3.67E+00	4.64E+00
1.25	5.65E+00	5.29E+00	4.93E+00	4.71E+00	4.50E+00	4.45E+00	5.56E+00
1.5	6.53E+00	6.07E+00	5.71E+00	5.58E+00	5.36E+00	5.41E+00	6.41E+00
2	8.09E+00	7.43E+00	7.14E+00	6.83E+00	6.80E+00	6.66E+00	7.85E+00
3	1.07E+01	1.02E+01	9.51E+00	9.51E+00	9.05E+00	9.23E+00	1.04E+01
5	1.52E+01	1.46E+01	1.38E+01	1.34E+01	1.34E+01	1.34E+01	1.48E+01
7	1.87E+01	1.81E+01	1.74E+01	1.79E+01	1.70E+01	1.71E+01	1.87E+01
10	2.47E+01	2.44E+01	2.38E+01	2.28E+01	2.29E+01	2.27E+01	2.46E+01
15	3.49E+01	3.42E+01	3.32E+01	3.15E+01	3.27E+01	3.18E+01	3.48E+01
20	4.54E+01	4.47E+01	4.28E+01	4.26E+01	4.15E+01	4.19E+01	4.51E+01
30	6.64E+01	6.49E+01	6.50E+01	6.40E+01	6.41E+01	6.14E+01	6.73E+01
50	1.14E+02	1.12E+02	1.10E+02	1.06E+02	1.03E+02	1.03E+02	1.15E+02

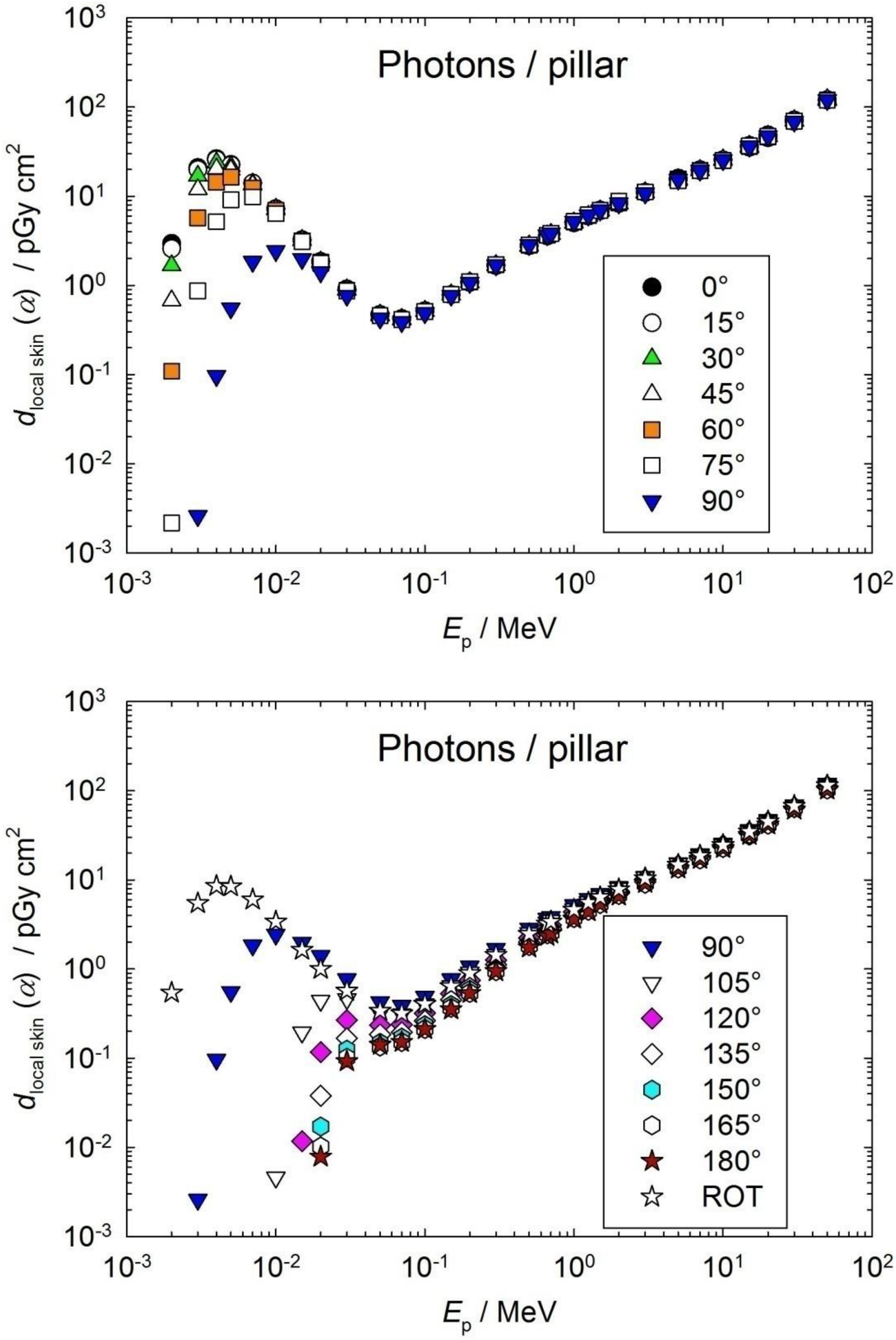

Figure A.5.4.2a Conversion coefficient from photon fluence to personal absorbed dose in local skin on the pillar phantom calculated using the kerma-approximation method (Otto, 2017).

Table A.5.4.2b Conversion coefficient from photon air kerma to personal absorbed dose in local skin on the pillar phantom calculated using the kerma-approximation method (1/2) (Otto, 2017).

	$d_{\mathrm{p\ local\ skin}}$ / (GyGy^{-1}) for a radiation incidence at α						
E_{p} / MeV	0°	15°	30°	45°	60°	75°	90°
0.002	1.80E-02	1.58E-02	1.02E-02	4.13E-03	6.67E-04	1.32E-05	1.42E-07
0.003	2.77E-01	2.64E-01	2.25E-01	1.59E-01	7.58E-02	1.15E-02	3.44E-05
0.004	5.51E-01	5.39E-01	5.01E-01	4.28E-01	3.01E-01	1.09E-01	2.03E-03
0.005	7.39E-01	7.31E-01	7.04E-01	6.47E-01	5.37E-01	2.98E-01	1.81E-02
0.007	9.02E-01	8.99E-01	8.88E-01	8.61E-01	8.02E-01	6.34E-01	1.19E-01
0.01	9.76E-01	9.73E-01	9.73E-01	9.62E-01	9.37E-01	8.61E-01	3.30E-01
0.015	1.03E+00	1.03E+00	1.03E+00	1.02E+00	1.01E+00	9.90E-01	6.36E-01
0.02	1.09E+00	1.10E+00	1.09E+00	1.09E+00	1.08E+00	1.06E+00	8.37E-01
0.03	1.26E+00	1.25E+00	1.25E+00	1.24E+00	1.22E+00	1.20E+00	1.07E+00
0.05	1.44E+00	1.46E+00	1.42E+00	1.45E+00	1.42E+00	1.42E+00	1.32E+00
0.07	1.47E+00	1.45E+00	1.45E+00	1.43E+00	1.43E+00	1.44E+00	1.35E+00
0.1	1.40E+00	1.38E+00	1.40E+00	1.38E+00	1.37E+00	1.38E+00	1.32E+00
0.15	1.31E+00	1.31E+00	1.31E+00	1.32E+00	1.32E+00	1.33E+00	1.28E+00
0.2	1.26E+00	1.27E+00	1.27E+00	1.27E+00	1.27E+00	1.29E+00	1.25E+00
0.3	1.21E+00	1.21E+00	1.21E+00	1.21E+00	1.23E+00	1.24E+00	1.22E+00
0.5	1.17E+00	1.17E+00	1.16E+00	1.18E+00	1.19E+00	1.20E+00	1.20E+00
0.662	1.16E+00	1.15E+00	1.14E+00	1.16E+00	1.17E+00	1.17E+00	1.18E+00
0.7	1.15E+00	1.15E+00	1.15E+00	1.16E+00	1.18E+00	1.17E+00	1.18E+00
1	1.14E+00	1.12E+00	1.12E+00	1.13E+00	1.15E+00	1.16E+00	1.16E+00
1.25	1.13E+00	1.12E+00	1.12E+00	1.13E+00	1.14E+00	1.16E+00	1.15E+00
1.5	1.13E+00	1.12E+00	1.11E+00	1.13E+00	1.13E+00	1.14E+00	1.13E+00
2	1.11E+00	1.10E+00	1.10E+00	1.09E+00	1.11E+00	1.16E+00	1.10E+00
3	1.10E+00	1.11E+00	1.11E+00	1.10E+00	1.12E+00	1.12E+00	1.08E+00
5	1.12E+00	1.08E+00	1.07E+00	1.09E+00	1.10E+00	1.06E+00	1.09E+00
7	1.08E+00	1.06E+00	1.07E+00	1.08E+00	1.07E+00	1.06E+00	1.07E+00
10	1.06E+00	1.06E+00	1.07E+00	1.06E+00	1.04E+00	1.04E+00	1.05E+00
15	1.08E+00	1.03E+00	1.03E+00	1.06E+00	1.05E+00	1.06E+00	1.05E+00
20	1.07E+00	9.99E-01	1.03E+00	1.04E+00	1.02E+00	1.04E+00	1.04E+00
30	1.04E+00	1.01E+00	1.01E+00	1.03E+00	1.02E+00	1.01E+00	1.01E+00
50	1.01E+00	1.00E+00	9.98E-01	1.03E+00	1.00E+00	9.95E-01	1.01E+00

Table A.5.4.2b Conversion coefficient from photon air kerma to personal absorbed dose in local skin on the pillar phantom calculated using the kerma-approximation method (2/2) (Otto, 2017).

	$d_{\mathrm{p\ local\ skin}}$ / (GyGy^{-1}) for a radiation incidence at α						
E_{p} / MeV	105°	120°	135°	150°	165°	180°	ROT
0.002	0.00E+00	0.00E+00	0.00E+00	0.00E+00	0.00E+00	0.00E+00	3.32E-03
0.003	0.00E+00	0.00E+00	0.00E+00	0.00E+00	0.00E+00	0.00E+00	7.28E-02
0.004	0.00E+00	0.00E+00	0.00E+00	0.00E+00	0.00E+00	0.00E+00	1.80E-01
0.005	0.00E+00	0.00E+00	0.00E+00	0.00E+00	0.00E+00	0.00E+00	2.75E-01
0.007	0.00E+00	0.00E+00	0.00E+00	0.00E+00	0.00E+00	0.00E+00	3.88E-01
0.01	6.21E-04	0.00E+00	0.00E+00	0.00E+00	0.00E+00	0.00E+00	4.60E-01
0.015	6.21E-02	3.75E-03	2.60E-04	4.45E-05	8.99E-06	1.05E-05	5.25E-01
0.02	2.61E-01	6.97E-02	2.25E-02	1.02E-02	6.08E-03	4.66E-03	5.97E-01
0.03	6.39E-01	3.71E-01	2.32E-01	1.73E-01	1.41E-01	1.28E-01	7.89E-01
0.05	1.00E+00	7.27E-01	5.73E-01	4.60E-01	4.19E-01	4.37E-01	1.05E+00
0.07	1.08E+00	8.31E-01	6.82E-01	5.92E-01	5.28E-01	5.28E-01	1.11E+00
0.1	1.08E+00	8.63E-01	7.07E-01	6.32E-01	5.73E-01	5.71E-01	1.09E+00
0.15	1.08E+00	8.80E-01	7.53E-01	6.57E-01	6.12E-01	5.89E-01	1.07E+00
0.2	1.07E+00	8.73E-01	7.58E-01	6.81E-01	6.32E-01	6.27E-01	1.05E+00
0.3	1.05E+00	9.11E-01	8.11E-01	7.19E-01	6.86E-01	6.83E-01	1.04E+00
0.5	1.07E+00	9.38E-01	8.42E-01	7.89E-01	7.63E-01	7.33E-01	1.04E+00
0.662	1.07E+00	9.41E-01	8.62E-01	8.09E-01	7.89E-01	7.55E-01	1.03E+00
0.7	1.07E+00	9.49E-01	8.68E-01	8.16E-01	7.83E-01	7.67E-01	1.03E+00
1	1.05E+00	9.78E-01	8.78E-01	8.45E-01	8.35E-01	8.18E-01	1.03E+00
1.25	1.06E+00	9.92E-01	9.25E-01	8.83E-01	8.44E-01	8.35E-01	1.04E+00
1.5	1.06E+00	9.87E-01	9.29E-01	9.08E-01	8.72E-01	8.80E-01	1.04E+00
2	1.07E+00	9.83E-01	9.45E-01	9.03E-01	8.99E-01	8.81E-01	1.04E+00
3	1.07E+00	1.02E+00	9.53E-01	9.53E-01	9.07E-01	9.25E-01	1.05E+00
5	1.07E+00	1.03E+00	9.76E-01	9.48E-01	9.46E-01	9.46E-01	1.04E+00
7	1.03E+00	9.96E-01	9.57E-01	9.81E-01	9.33E-01	9.42E-01	1.03E+00
10	1.02E+00	1.01E+00	9.85E-01	9.46E-01	9.47E-01	9.41E-01	1.02E+00
15	1.01E+00	9.94E-01	9.65E-01	9.13E-01	9.50E-01	9.24E-01	1.01E+00
20	1.00E+00	9.85E-01	9.44E-01	9.40E-01	9.15E-01	9.23E-01	9.95E-01
30	9.68E-01	9.46E-01	9.48E-01	9.33E-01	9.34E-01	8.95E-01	9.82E-01
50	9.58E-01	9.43E-01	9.19E-01	8.86E-01	8.65E-01	8.65E-01	9.62E-01

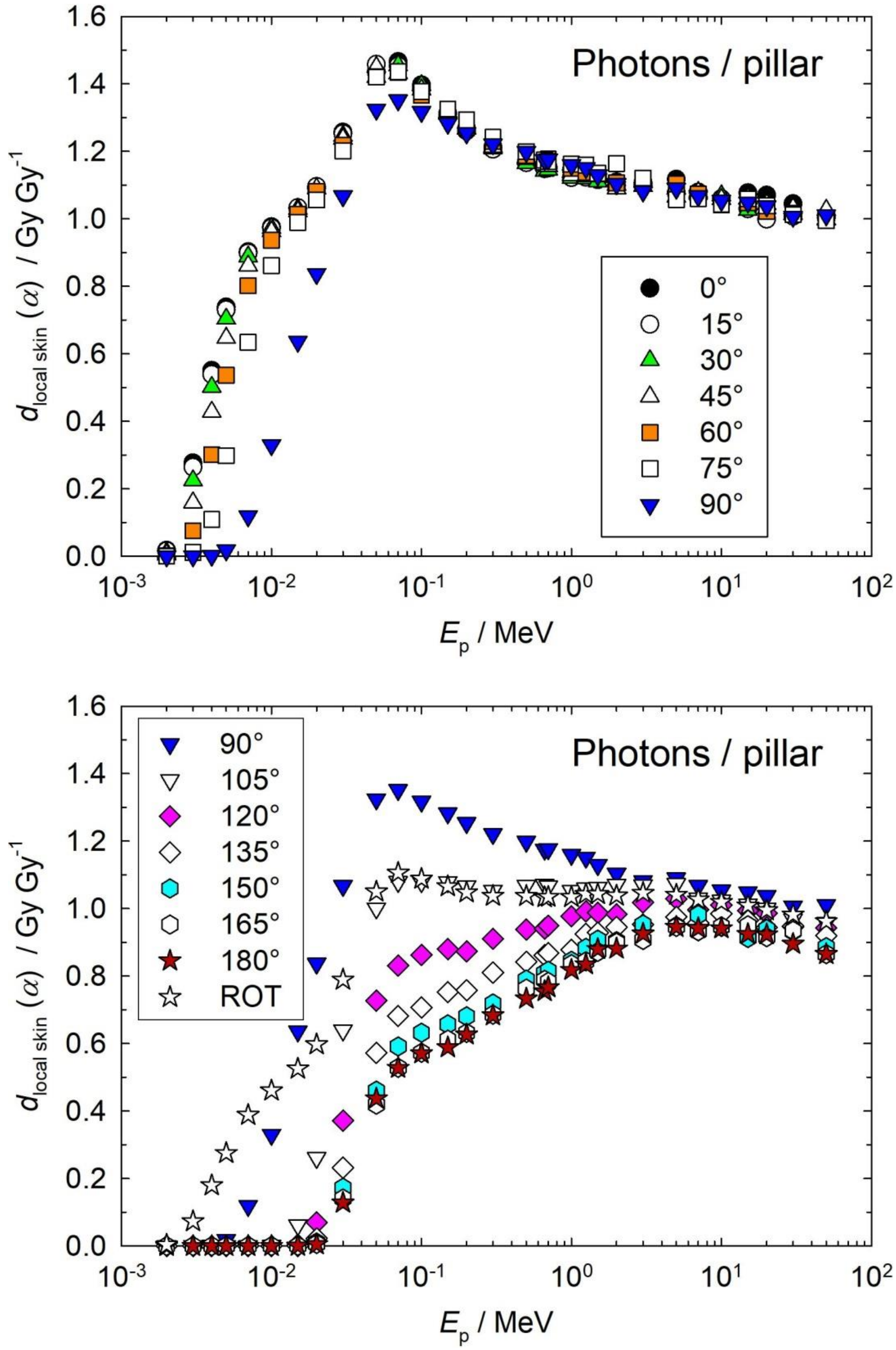

Figure A.5.4.2b Conversion coefficient from photon air kerma to personal absorbed dose in local skin on the pillar phantom calculated using the kerma-approximation method (Otto, 2017).

Table A.5.4.3a Conversion coefficient from photon fluence to personal absorbed dose in local skin on the rod phantom calculated using the kerma-approximation method (1/2) (Otto, 2017).

E_p / MeV	$d_{p\ \mathrm{local\ skin}}$ / (pGy cm^2) for a radiation incidence at α						
	0°	15°	30°	45°	60°	75°	90°
0.002	2.54E+00	2.28E+00	1.63E+00	9.08E-01	3.63E-01	8.56E-02	0.00E+00
0.003	1.97E+01	1.87E+01	1.58E+01	1.14E+01	6.66E+00	2.91E+00	7.39E-01
0.004	2.56E+01	2.49E+01	2.29E+01	1.90E+01	1.32E+01	7.35E+00	2.84E+00
0.005	2.24E+01	2.21E+01	2.10E+01	1.88E+01	1.45E+01	9.19E+00	4.36E+00
0.007	1.39E+01	1.39E+01	1.36E+01	1.30E+01	1.14E+01	8.19E+00	4.71E+00
0.01	7.21E+00	7.20E+00	7.15E+00	7.04E+00	6.64E+00	5.39E+00	3.62E+00
0.015	3.21E+00	3.21E+00	3.20E+00	3.18E+00	3.12E+00	2.84E+00	2.30E+00
0.02	1.81E+00	1.81E+00	1.80E+00	1.79E+00	1.77E+00	1.69E+00	1.50E+00
0.03	8.16E-01	8.15E-01	8.13E-01	8.10E-01	8.04E-01	7.84E-01	7.42E-01
0.05	3.79E-01	3.80E-01	3.80E-01	3.81E-01	3.80E-01	3.74E-01	3.59E-01
0.06	3.42E-01	3.42E-01	3.42E-01	3.41E-01	3.40E-01	3.36E-01	3.25E-01
0.07	3.46E-01	3.44E-01	3.43E-01	3.42E-01	3.40E-01	3.37E-01	3.28E-01
0.1	4.43E-01	4.43E-01	4.43E-01	4.43E-01	4.42E-01	4.38E-01	4.26E-01
0.15	6.98E-01	6.98E-01	6.98E-01	6.99E-01	7.00E-01	6.98E-01	6.86E-01
0.2	9.90E-01	9.87E-01	9.87E-01	9.87E-01	9.88E-01	9.87E-01	9.71E-01
0.5	2.67E+00	2.67E+00	2.67E+00	2.67E+00	2.68E+00	2.68E+00	2.65E+00
0.662	3.49E+00	3.49E+00	3.49E+00	3.49E+00	3.49E+00	3.49E+00	3.46E+00
1	4.98E+00	4.97E+00	4.97E+00	4.98E+00	4.98E+00	4.98E+00	4.95E+00
1.25	5.93E+00	5.93E+00	5.94E+00	5.95E+00	5.96E+00	5.95E+00	5.92E+00
1.5	6.78E+00	6.79E+00	6.79E+00	6.80E+00	6.81E+00	6.80E+00	6.77E+00
2	8.31E+00	8.32E+00	8.32E+00	8.32E+00	8.34E+00	8.33E+00	8.30E+00
3	1.09E+01	1.09E+01	1.09E+01	1.09E+01	1.10E+01	1.09E+01	1.09E+01
5	1.53E+01	1.54E+01	1.54E+01	1.54E+01	1.54E+01	1.53E+01	1.53E+01
10	2.56E+01	2.56E+01	2.55E+01	2.55E+01	2.55E+01	2.55E+01	2.54E+01
20	4.68E+01	4.68E+01	4.68E+01	4.66E+01	4.65E+01	4.65E+01	4.65E+01
30	6.91E+01	6.92E+01	6.91E+01	6.91E+01	6.91E+01	6.90E+01	6.87E+01
50	1.19E+02	1.19E+02	1.19E+02	1.19E+02	1.19E+02	1.19E+02	1.18E+02

Table A.5.4.3a Conversion coefficient from photon fluence to personal absorbed dose in local skin on the rod phantom calculated using the kerma-approximation method (2/2) (Otto, 2017).

	$d_{\mathrm{p\ local\ skin}}$ / (pGy cm^2) for a radiation incidence at α						
E_{p} / MeV	105°	120°	135°	150°	165°	180°	ROT
0.002	0.00E+00	0.00E+00	0.00E+00	0.00E+00	0.00E+00	0.00E+00	5.45E-01
0.003	4.70E-02	0.00E+00	0.00E+00	0.00E+00	0.00E+00	0.00E+00	5.51E+00
0.004	4.54E-01	0.00E+00	0.00E+00	0.00E+00	0.00E+00	0.00E+00	8.62E+00
0.005	1.09E+00	1.93E-02	0.00E+00	0.00E+00	0.00E+00	0.00E+00	8.52E+00
0.007	1.77E+00	1.72E-01	0.00E+00	0.00E+00	0.00E+00	0.00E+00	6.14E+00
0.01	1.83E+00	4.98E-01	5.45E-02	0.00E+00	0.00E+00	0.00E+00	3.59E+00
0.015	1.61E+00	9.40E-01	5.00E-01	2.93E-01	2.05E-01	1.80E-01	1.92E+00
0.02	1.24E+00	9.51E-01	7.19E-01	5.79E-01	5.05E-01	4.81E-01	1.29E+00
0.03	6.77E-01	6.02E-01	5.35E-01	4.87E-01	4.59E-01	4.50E-01	6.80E-01
0.05	3.38E-01	3.14E-01	2.93E-01	2.78E-01	2.70E-01	2.67E-01	3.39E-01
0.06	3.09E-01	2.90E-01	2.72E-01	2.60E-01	2.52E-01	2.50E-01	3.09E-01
0.07	3.14E-01	2.95E-01	2.78E-01	2.65E-01	2.57E-01	2.55E-01	3.12E-01
0.1	4.09E-01	3.88E-01	3.69E-01	3.54E-01	3.46E-01	3.43E-01	4.08E-01
0.15	6.66E-01	6.37E-01	6.08E-01	5.86E-01	5.73E-01	5.69E-01	6.57E-01
0.2	9.43E-01	9.06E-01	8.70E-01	8.45E-01	8.28E-01	8.23E-01	9.34E-01
0.5	2.60E+00	2.53E+00	2.47E+00	2.42E+00	2.39E+00	2.38E+00	2.58E+00
0.662	3.41E+00	3.33E+00	3.26E+00	3.20E+00	3.17E+00	3.16E+00	3.38E+00
1	4.88E+00	4.80E+00	4.72E+00	4.65E+00	4.59E+00	4.58E+00	4.85E+00
1.25	5.84E+00	5.75E+00	5.66E+00	5.59E+00	5.55E+00	5.54E+00	5.82E+00
1.5	6.70E+00	6.61E+00	6.52E+00	6.44E+00	6.39E+00	6.37E+00	6.67E+00
2	8.23E+00	8.12E+00	8.02E+00	7.95E+00	7.92E+00	7.92E+00	8.19E+00
3	1.08E+01	1.07E+01	1.06E+01	1.05E+01	1.05E+01	1.05E+01	1.08E+01
5	1.52E+01	1.51E+01	1.50E+01	1.49E+01	1.48E+01	1.48E+01	1.52E+01
10	2.53E+01	2.52E+01	2.50E+01	2.49E+01	2.48E+01	2.47E+01	2.53E+01
20	4.64E+01	4.61E+01	4.58E+01	4.56E+01	4.55E+01	4.54E+01	4.63E+01
30	6.85E+01	6.80E+01	6.76E+01	6.75E+01	6.74E+01	6.75E+01	6.85E+01
50	1.17E+02	1.16E+02	1.16E+02	1.15E+02	1.14E+02	1.15E+02	1.17E+02

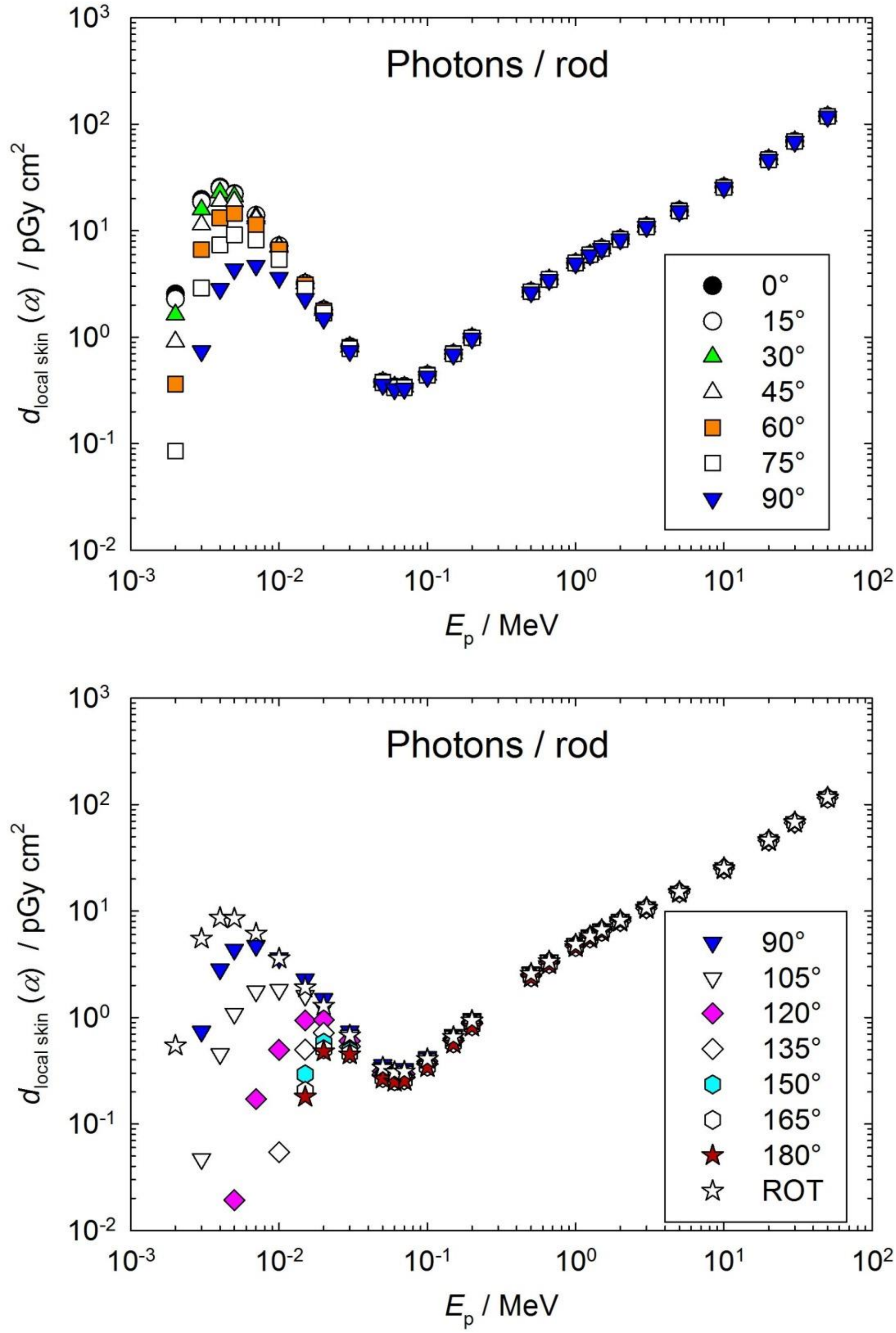

Figure A.5.4.3a Conversion coefficient from photon fluence to personal absorbed dose in local skin on the rod phantom calculated using the kerma-approximation method (Otto, 2017).

Table A.5.4.3b Conversion coefficients from photon air kerma to personal absorbed dose in local skin on the rod phantom calculated using the kerma-approximation method (1/2) (Otto, 2017).

E_p / MeV	$d_{p\,\text{local skin}}$ / (GyGy^{-1}) for a radiation incidence at α						
	0°	15°	30°	45°	60°	75°	90°
0.002	1.55E-02	1.39E-02	9.96E-03	5.55E-03	2.22E-03	5.23E-04	0.00E+00
0.003	2.62E-01	2.48E-01	2.10E-01	1.51E-01	8.84E-02	3.86E-02	9.81E-03
0.004	5.38E-01	5.23E-01	4.81E-01	3.99E-01	2.77E-01	1.54E-01	5.96E-02
0.005	7.31E-01	7.21E-01	6.85E-01	6.13E-01	4.73E-01	3.00E-01	1.42E-01
0.007	8.97E-01	8.97E-01	8.77E-01	8.39E-01	7.35E-01	5.28E-01	3.04E-01
0.01	9.74E-01	9.73E-01	9.66E-01	9.51E-01	8.97E-01	7.28E-01	4.89E-01
0.015	1.03E+00	1.03E+00	1.02E+00	1.02E+00	9.98E-01	9.09E-01	7.36E-01
0.02	1.07E+00	1.07E+00	1.07E+00	1.06E+00	1.05E+00	1.00E+00	8.91E-01
0.03	1.13E+00	1.13E+00	1.13E+00	1.12E+00	1.11E+00	1.09E+00	1.03E+00
0.05	1.17E+00	1.18E+00	1.18E+00	1.18E+00	1.18E+00	1.16E+00	1.11E+00
0.06	1.18E+00	1.18E+00	1.18E+00	1.18E+00	1.18E+00	1.16E+00	1.12E+00
0.07	1.20E+00	1.20E+00	1.19E+00	1.19E+00	1.18E+00	1.17E+00	1.14E+00
0.1	1.19E+00	1.19E+00	1.19E+00	1.19E+00	1.19E+00	1.18E+00	1.15E+00
0.15	1.16E+00	1.16E+00	1.16E+00	1.17E+00	1.17E+00	1.16E+00	1.14E+00
0.2	1.16E+00	1.15E+00	1.15E+00	1.15E+00	1.15E+00	1.15E+00	1.13E+00
0.5	1.12E+00	1.12E+00	1.12E+00	1.12E+00	1.13E+00	1.13E+00	1.11E+00
0.662	1.12E+00	1.12E+00	1.12E+00	1.12E+00	1.12E+00	1.12E+00	1.11E+00
1	1.11E+00	1.11E+00	1.11E+00	1.11E+00	1.11E+00	1.11E+00	1.10E+00
1.25	1.11E+00	1.11E+00	1.11E+00	1.12E+00	1.12E+00	1.12E+00	1.11E+00
1.5	1.10E+00	1.10E+00	1.10E+00	1.11E+00	1.11E+00	1.11E+00	1.10E+00
2	1.10E+00	1.10E+00	1.10E+00	1.10E+00	1.10E+00	1.10E+00	1.10E+00
3	1.09E+00	1.09E+00	1.09E+00	1.09E+00	1.10E+00	1.09E+00	1.09E+00
5	1.08E+00	1.09E+00	1.09E+00	1.09E+00	1.09E+00	1.08E+00	1.08E+00
10	1.06E+00	1.06E+00	1.06E+00	1.06E+00	1.06E+00	1.06E+00	1.05E+00
20	1.03E+00	1.03E+00	1.03E+00	1.03E+00	1.03E+00	1.03E+00	1.03E+00
30	1.01E+00	1.01E+00	1.01E+00	1.01E+00	1.01E+00	1.01E+00	1.00E+00
50	9.98E-01	9.98E-01	9.98E-01	9.98E-01	9.98E-01	9.98E-01	9.90E-01

1805 Table A.5.4.3b Conversion coefficient from photon air kerma to personal absorbed dose in local skin on
1806 the rod phantom calculated using the kerma-approximation method (2/2) (Otto, 2017).

	$d_{\mathrm{p\ local\ skin}}$ / (GyGy^{-1}) for a radiation incidence at α						
E_{p} / MeV	105°	120°	135°	150°	165°	180°	ROT
0.002	0.00E+00	0.00E+00	0.00E+00	0.00E+00	0.00E+00	0.00E+00	3.33E-03
0.003	6.24E-04	0.00E+00	0.00E+00	0.00E+00	0.00E+00	0.00E+00	7.32E-02
0.004	9.53E-03	0.00E+00	0.00E+00	0.00E+00	0.00E+00	0.00E+00	1.81E-01
0.005	3.56E-02	6.30E-04	0.00E+00	0.00E+00	0.00E+00	0.00E+00	2.78E-01
0.007	1.14E-01	1.11E-02	0.00E+00	0.00E+00	0.00E+00	0.00E+00	3.96E-01
0.01	2.47E-01	6.73E-02	7.36E-03	0.00E+00	0.00E+00	0.00E+00	4.85E-01
0.015	5.15E-01	3.01E-01	1.60E-01	9.38E-02	6.56E-02	5.76E-02	6.14E-01
0.02	7.36E-01	5.65E-01	4.27E-01	3.44E-01	3.00E-01	2.86E-01	7.66E-01
0.03	9.38E-01	8.34E-01	7.41E-01	6.75E-01	6.36E-01	6.24E-01	9.42E-01
0.05	1.05E+00	9.72E-01	9.07E-01	8.61E-01	8.36E-01	8.27E-01	1.05E+00
0.06	1.07E+00	1.00E+00	9.42E-01	9.00E-01	8.72E-01	8.65E-01	1.07E+00
0.07	1.09E+00	1.03E+00	9.66E-01	9.21E-01	8.93E-01	8.86E-01	1.08E+00
0.1	1.10E+00	1.04E+00	9.94E-01	9.53E-01	9.32E-01	9.24E-01	1.10E+00
0.15	1.11E+00	1.06E+00	1.01E+00	9.78E-01	9.56E-01	9.49E-01	1.10E+00
0.2	1.10E+00	1.06E+00	1.02E+00	9.86E-01	9.66E-01	9.61E-01	1.09E+00
0.5	1.09E+00	1.06E+00	1.04E+00	1.02E+00	1.00E+00	1.00E+00	1.08E+00
0.662	1.10E+00	1.07E+00	1.05E+00	1.03E+00	1.02E+00	1.02E+00	1.09E+00
1	1.09E+00	1.07E+00	1.05E+00	1.04E+00	1.02E+00	1.02E+00	1.08E+00
1.25	1.10E+00	1.08E+00	1.06E+00	1.05E+00	1.04E+00	1.04E+00	1.09E+00
1.5	1.09E+00	1.08E+00	1.06E+00	1.05E+00	1.04E+00	1.04E+00	1.09E+00
2	1.09E+00	1.07E+00	1.06E+00	1.05E+00	1.05E+00	1.05E+00	1.08E+00
3	1.08E+00	1.07E+00	1.06E+00	1.05E+00	1.05E+00	1.05E+00	1.08E+00
5	1.07E+00	1.06E+00	1.06E+00	1.05E+00	1.04E+00	1.04E+00	1.07E+00
10	1.05E+00	1.04E+00	1.04E+00	1.03E+00	1.03E+00	1.02E+00	1.05E+00
20	1.02E+00	1.02E+00	1.01E+00	1.01E+00	1.00E+00	1.00E+00	1.02E+00
30	9.99E-01	9.91E-01	9.86E-01	9.84E-01	9.83E-01	9.84E-01	9.99E-01
50	9.82E-01	9.73E-01	9.73E-01	9.65E-01	9.56E-01	9.65E-01	9.82E-01

1807

1808

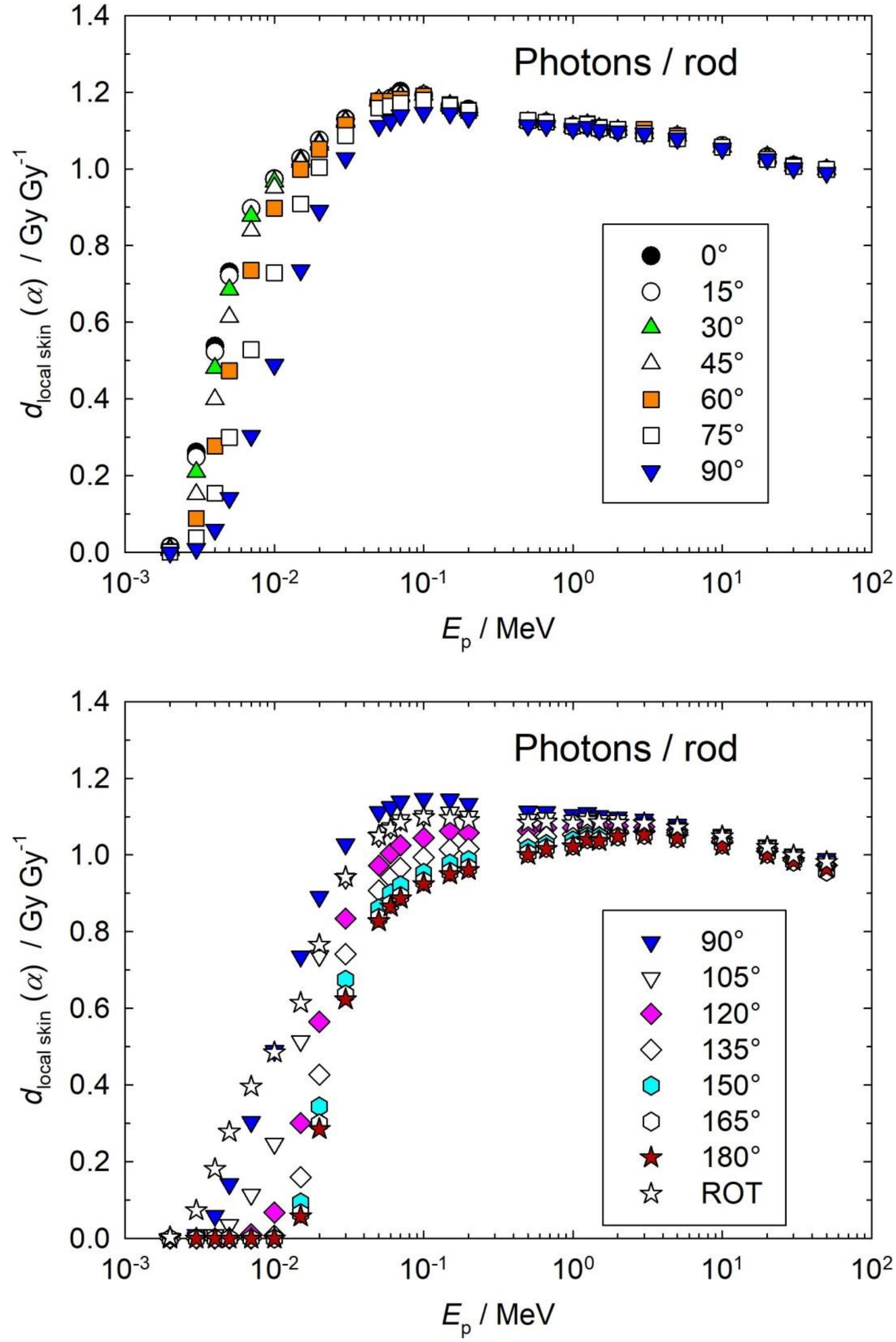

Figure A.5.4.3b Conversion coefficient from photon air kerma to personal absorbed dose in local skin on the rod phantom calculated using the kerma-approximation method (Otto, 2017).

A.6 Air Kerma

The Table gives values of conversion coefficients from photon fluence to air kerma for energies from 2keV to 50 MeV. Air kerma coefficients, $K_{\mathrm{air}}/\Phi = (\mu_{\mathrm{en}}/\rho)\, E\, (1-g)^{-1}$ are used for the conversion from dose per fluence to dose per air kerma. The values for (μ_{en}/ρ) are from the calculations of Seltzer (1993) and Hubbell and Seltzer (1995) with renormalized Scofield photoeffect cross sections (ICRU, 2014). The values for g are from Seltzer (2017). The values written in ***bold italics*** are obtained by interpolation as no values for (μ_{en}/ρ) are available[a)].

Table A.6 Conversion coefficients from photon fluence to air kerma.

Photon energy E (MeV)	Air kerma coefficient (pGy cm²)	Photon energy E (MeV)	Air kerma coefficient (pGy cm²)
0.002	163.7	0.500	2.379
0.003	75.32	***0.511***	***2.431***
0.004	47.62	0.600	2.844
0.005	30.65	***0.662***	***3.112***
0.006	21.25	***0.700***	***3.275***
0.007	***15.50***	0.800	3.702
0.008	11.79	1.000	4.481
0.009	***9.221***	***1.117***	***4.884***
0.010	7.400	***1.200***	***5.165***
0.011	6.043	***1.250***	***5.332***
0.012	***5.022***	***1.300***	***5.498***
0.013	***4.236***	***1.330***	***5.596***
0.015	3.125	1.500	6.147
0.017	***2.388***	***1.700***	***6.725***
0.020	1.684	2.000	7.557
0.024	***1.150***	***2.400***	***8.563***
0.025	***1.056***	3.000	9.977
0.030	0.7217	4.000	12.14
0.040	0.4289	5.000	14.18
0.050	0.3229	6.000	16.17
0.060	0.2889	***6.129***	***16.44***
0.070	***0.2878***	***7.000***	***18.19***
0.080	0.3067	8.000	20.13
0.100	0.3714	10.000	24.13
0.120	***0.4606***	15.000	34.46
0.150	0.5994	20.000	45.36
0.200	0.8567	30.000	68.59
0.240	***1.062***	40.000	93.29
0.300	1.383	50.000	119.2
0.400	1.892		

[a] A log-log-interpolation was used except for 70 keV: At this energy, the values take a minimum resulting in a curved energy dependence. Therefore, a natural cubic spline was used for this energy.

Appendix B

Descriptions of codes

B.1 PHITS

The PHITS (Particle and Heavy Ion Transport Code System) code is a multipurpose Monte Carlo code that simulates the transport and interaction of hadrons, leptons, and heavy ions in arbitrary three-dimensional geometries (Sato et al., 2013). PHITS 2.82 was used in this report.

In the PHITS code, neutron transport below 20 MeV down to 10^{-5} eV is simulated in a manner similar to that employed in the MCNP4C code (Briesmeister, 2000), and is based on evaluated nuclear data libraries. For neutrons above 20 MeV and for protons, mesons, and other hadrons up to 200 GeV, the intra-nuclear cascade models INCL4.6 (Boudard et al., 2013) and JAM (Nara et al., 1999) are employed for simulating the dynamic stage of hadron-induced nuclear reactions in the intermediate and high energy regions, respectively. Nucleus-induced reactions are simulated by the JQMD model (Niita et al, 1995) for energies from 10 MeV/u up to 100 GeV/u. The evaporation and fission model GEM (Furihata, 2000) is adopted for simulating the static stage for both hadron- and nucleus-induced reactions. The energy losses of charged particles, except for electrons, are calculated using the SPAR (Armstrong and Chandler, 1973) or ATIMA (Geissel et al., 2013) codes with the continuous slowing down approximation.

Transport of photons and electrons are simulated in a similar way as in the EGS5 (Hirayama et al., 2005) code. Photo-nuclear reactions can be treated up to 1 GeV using JQMD and GEM.

The PHITS code is capable of: (1) providing good estimations of generated particle spectra produced from nucleon–nucleus and nucleus–nucleus collisions using the INCL4.6, JAM and JQMD models; (2) determining the energy of charged particles emitted from low-energy neutron-induced nuclear reactions using the event generator mode, instead of the kerma approximation; and (3) estimating the probability density of absorbed dose in terms of LET and lineal energy.

B.2 FLUKA

FLUKA is a general-purpose Monte Carlo program for calculations of particle and photon transport (Böhlen et al., 2014; Ferrari et al., 2005) that can simulate the interactions and propagation of approximately 60 different particles in matter, including heavy ions. Photonuclear interactions can be simulated. FLUKA 2011 was used in this report.

Depending on the energies of the primary particles, hadronic interactions are simulated by different physical models (Ballarini et al., 2004). For higher energies, the Dual Parton model is used. Below 3–5 GeV c-1, the PEANUT (Cascade–Pre-equilibrium model) package includes a very detailed generalized intra-nuclear cascade (GINC) and a pre-equilibrium stage, while at high energies, the Gribov-Glauber multiple collision mechanism is included in a less-refined GINC. Nuclear interactions generated by ions are treated through interfaces to external event generators, except for the low-energy (<150 MeV/u) range for which a model based on the Boltzmann master equation has been implemented. The relativistic quantum molecular dynamics generator is invoked from 100 MeV/u to 5 GeV/u, and the DPMJET code is used for energies over 5 GeV/u.

The transport of charged particles is described by applying a multiple scattering algorithm based on Moliere's theory of Coulomb scattering. The algorithm includes an accurate treatment of curved trajectories in magnetic fields. The energy loss is determined according to the Bethe–Bloch theory and from bremsstrahlung and pair production. Ionization fluctuations are accounted for.

For neutrons with energies lower than 20 MeV, FLUKA employs a multigroup transport algorithm that uses a subdivision of the neutron energy range in 260 groups and is based on neutron cross section libraries containing more than 200 different materials, selected for their use in physics, dosimetry, and accelerator engineering. Energy depositions for nuclei other than hydrogen are calculated by kerma coefficients.

B.3 MCNP6

The particle radiation transport code Monte Carlo N-Particle (MCNP)is a general purpose three-dimensional simulation tool that transports 37 different particle types. It can be applied in many applications including radiation protection and dosimetry, radiation shielding, radiography, medical physics, nuclear criticality safety, detector design and analysis, accelerator target design, fission and fusion reactor design, decontamination and decommissioning. The specific release of the code used in this report was version 6.1. (Pelowitz et al. 2013)The code covers the following ranges:10^{-11} MeV to 20 MeV for neutrons with data up to 150 MeV for some nuclides, 1 keV to 1 GeV for electrons (and positrons), and 1 keV to 100 GeV for photons.

Neutron, proton, electron and photon are transported using tabulated data below an upper energy table limit. That upper energy limit varies with nuclide and cross section data requested. Above that upper energy limit, a combination of models can be used to describe the transport and reactions. The reader is referred to (Goorley et al. 2013) for more details on the models available for use it.

The neutron calculations in the report performed with MCNP6, version 1.0, used pointwise cross-section. In the present calculations, the S(α,β) thermal neutron scattering model for water was used in the computations of neutron skin doses and lens of the eye doses. If available, nuclide cross section tables extending to 150 MeV were used for the computations at 30 MeV and 50 MeV. The code mix and matches tabulated cross section library data and physics models as needed to cover the energy ranges of the computation. The neutron library data used in the present computations is shown in Table B.1; the tabulated cross section with the latest evaluation was selected for this work.

For photons, the code accounts for incoherent and coherent scattering, the possibility of fluorescent emission after photoelectric absorption, absorption in pair production with local emission of annihilation radiation, and bremsstrahlung. A continuous-slowing-down model is used for electron transport that includes positrons, k x-rays, and bremsstrahlung. Photonuclear physics is available for a subset of umber of nuclides

MCNP contains numerous flexible tallies: surface current & flux (surface crossing), volume flux (track length), point or ring detectors, particle heating, fission heating, pulse height tally for energy or charge deposition, mesh tallies, and radiography tallies.

Neutron Cross Sections Used in MCNP6 Computations. (J. L. Conlin et al. 2005)

Nuclide	MCNP Identifier	Source (Upper Energy Limit of Data Tables)
H-1	1001.62c	ENDF/B-VI.8 (150 MeV)
H-2	1002.80c	ENDF/B-VII.1 (150 MeV)
Natural Carbon	6000.80c	ENDF/B-VII.1 (150 MeV)
N-14	7014.80c	ENDF/B-VII.1 (150 MeV)
N-15	7015.80c	ENDF/B-VII.1 (20 MeV)
O-16	8016.80c	ENDF/B-VII.1 (150 MeV)
O-17	8017.80c	ENDF/B-VII.1 (150 MeV)
Na-23	11023.80c	ENDF/B-VII.1 (20 MeV)
P-31	15031.80c	ENDF/B-VII.1 (150 MeV)
S-32	16032.80c	ENDF/B-VII.1 (20 MeV)
S-33	16033.80c	ENDF/B-VII.1 (20 MeV)
S-35	16035.80c	ENDF/B-VII.1 (20 MeV)
S-36	16036.80c	ENDF/B-VII.1 (20 MeV)
Cl-35	17035.80c	ENDF/B-VII.1 (20 MeV)
Cl-37	17037.80c	ENDF/B-VII.1 (20 MeV)
K-39	19039.80c	ENDF/B-VII.1 (20 MeV)
K-40	19040.80c	ENDF/B-VII.1 (20 MeV)
K-41	19041.80c	ENDF/B-VII.1 (20 MeV)

B.4 EGSnrc

For the calculations presented in this report, the electron-gamma-shower code system EGSnrc Version v4-r2-4-0 (Kawrakow et al., 2013) has been used. This code is an extended and improved version of EGS4 (Nelson et al., 1985), maintained by the National Research Council of Canada (NRC). The transport of photons, electrons, and positrons can be simulated for particle kinetic energies from a few keV up to several hundred GeV. Some enhancements to the physics, however, can only be enabled below 1 GeV.

For photon transport, bound Compton scattering and photo-electrons fromK, L, and M shells are considered for all energies. In both cases, resulting fluorescence or Auger and Coster-Kronig electrons are followed. Photon–nuclear reactions are not taken into consideration as their contribution to organ dose was shown to be much less than 1%. In this report, photon transport is terminated when the photon energy falls below 10keV.Exceptions are used for primary particles with an initial kinetic energy below 510 keV, whose histories are followed down to 1keV.

Electron and positron transport calculations are performed by a Class II condensed history technique (Berger, 1963), which transports generated particles produced above a certain chosen energy. Bremsstrahlung cross sections are those from Bethe-Heitler, i.e. as in EGS4 (Nelson et al., 1985). Bremsstrahlung angular sampling following Koch and Motz (1959) is used. Electron impact ionization is modeled using default cross sections (Kawrakow, 2002). When the sampling does not lead to ionization, the classical Møller or Bhabha cross sections are applied. For elastic scattering, spin effects are taken into account. Pair production is simulated as in EGS4 (Nelson et al., 1985). Triplet-production processes are neglected for all particles. In this report, the transport history of electrons is generally terminated when their kinetic energy falls below 10keV. Exceptions are used for primary particles with an initial kinetic energy below 110keV, whose histories are followed down to 1keV. For external irradiation, electrons with kinetic energies below 500 keV rarely reach internal organs. The dose to those organs is low and mainly caused by bremsstrahlung production within the first few millimetres of the phantoms.

B.5 Revised Stopping Powers

The ICRU Report 90 *Key Data for Ionizing-Radiation Dosimetry: Measurement Standards and Applications*, (ICRU, 2017) has changed slightly the charged-particle stopping powers in water. This is not expected to make a noticeable difference to the Monte Carlo calculations used in this Report.

Appendix C

Informative: Alternative Conversion Coefficients to Absorbed Dose to the Lens of the Eye

C.1 Directional and Personal Absorbed Dose to the Lens of the Eye, Maximum Absorbed Dose to the Sensitive cells or the Complete Lens

The numerical values of conversion coefficients from particle fluence to directional absorbed dose in the lens of the eye $d'_{\text{lens max}}$ and from fluence to personal absorbed dose in the lens of the eye $d_{\text{plens max}}$ are the same and the symbol $d_{\text{lens max}}$, is used in the following Tables. The conversion coefficients given here are to the maximum value of the absorbed dose in the radiation sensitive cells or the complete lens of the eye, calculated for whole-body exposure of the stylized eye model (Behrens and Dietze, 2011) for broad parallel beams incident for angles from 0° (A-P) to 90° in 15° steps, the maximum value of right or left irradiations is taken; and for a rotational field (ROT).

Tables C.1.1a to C.1.4, and Figures C.1.1a to C.1.4 give the numerical values of the conversion coefficients from particle fluence for photons, neutrons, electrons, and positrons for energies up to 50 MeV; Table C.1.1b and Figure C.1.1b from air kerma.

Table C.1.1a Conversion coefficients from photon fluence to the maximum absorbed dose in the sensitive cells or the complete lens for left or right irradiations (Behrens, 2017a).

	$d_{\text{lens, max}}(\alpha)$/ (pGy cm^2) for a radiation incidence at α							
E_p / MeV	0°	15°	30°	45°	60°	75°	90°	ROT
0.005	4.17E-05	7.65E-05	1.54E-04	1.52E-04	6.90E-05	8.41E-06	3.34E-07	4.34E-05
0.006	7.75E-03	9.30E-03	1.06E-02	1.05E-02	5.87E-03	1.73E-03	1.70E-04	3.28E-03
0.007	1.13E-01	1.07E-01	1.05E-01	9.55E-02	6.16E-02	2.48E-02	5.50E-03	3.64E-02
0.008	4.46E-01	4.12E-01	3.77E-01	3.37E-01	2.37E-01	1.22E-01	3.95E-02	1.37E-01
0.009	9.37E-01	8.79E-01	8.00E-01	7.04E-01	5.20E-01	3.18E-01	1.30E-01	2.94E-01
0.01	1.42E+00	1.34E+00	1.23E+00	1.09E+00	8.49E-01	5.74E-01	2.82E-01	4.63E-01
0.011	1.75E+00	1.68E+00	1.57E+00	1.41E+00	1.15E+00	8.45E-01	4.68E-01	6.03E-01
0.013	2.01E+00	1.99E+00	1.89E+00	1.73E+00	1.54E+00	1.23E+00	8.09E-01	7.58E-01
0.015	1.94E+00	1.96E+00	1.89E+00	1.75E+00	1.62E+00	1.41E+00	1.01E+00	7.91E-01
0.017	1.76E+00	1.79E+00	1.74E+00	1.64E+00	1.55E+00	1.40E+00	1.09E+00	7.62E-01
0.02	1.45E+00	1.49E+00	1.48E+00	1.39E+00	1.36E+00	1.26E+00	1.03E+00	6.74E-01
0.024	1.14E+00	1.16E+00	1.16E+00	1.12E+00	1.10E+00	1.04E+00	9.07E-01	5.61E-01
0.03	8.26E-01	8.54E-01	8.45E-01	8.17E-01	8.27E-01	8.02E-01	7.08E-01	4.48E-01
0.04	5.80E-01	5.96E-01	6.03E-01	5.89E-01	5.92E-01	5.74E-01	5.30E-01	3.39E-01
0.05	4.83E-01	4.94E-01	5.04E-01	4.96E-01	4.95E-01	4.78E-01	4.47E-01	2.95E-01
0.06	4.50E-01	4.63E-01	4.69E-01	4.64E-01	4.61E-01	4.50E-01	4.28E-01	2.85E-01
0.07	4.55E-01	4.63E-01	4.67E-01	4.63E-01	4.61E-01	4.53E-01	4.33E-01	2.94E-01
0.08	4.82E-01	4.83E-01	4.89E-01	4.85E-01	4.90E-01	4.80E-01	4.58E-01	3.15E-01
0.1	5.59E-01	5.62E-01	5.69E-01	5.72E-01	5.70E-01	5.57E-01	5.41E-01	3.77E-01
0.12	6.66E-01	6.70E-01	6.72E-01	6.79E-01	6.71E-01	6.63E-01	6.43E-01	4.52E-01
0.15	8.38E-01	8.42E-01	8.46E-01	8.45E-01	8.48E-01	8.38E-01	8.11E-01	5.80E-01
0.2	1.13E+00	1.15E+00	1.17E+00	1.17E+00	1.15E+00	1.14E+00	1.13E+00	8.10E-01
0.24	1.39E+00	1.40E+00	1.41E+00	1.42E+00	1.40E+00	1.38E+00	1.39E+00	1.01E+00
0.3	1.74E+00	1.75E+00	1.77E+00	1.83E+00	1.79E+00	1.75E+00	1.75E+00	1.28E+00
0.4	2.29E+00	2.32E+00	2.34E+00	2.38E+00	2.36E+00	2.32E+00	2.36E+00	1.75E+00
0.5	2.83E+00	2.84E+00	2.89E+00	2.93E+00	2.96E+00	2.84E+00	2.85E+00	2.22E+00
0.511	2.88E+00	2.90E+00	2.97E+00	3.02E+00	3.02E+00	2.89E+00	2.89E+00	2.26E+00
0.6	3.34E+00	3.36E+00	3.40E+00	3.46E+00	3.47E+00	3.36E+00	3.35E+00	2.64E+00
0.662	3.63E+00	3.65E+00	3.66E+00	3.77E+00	3.73E+00	3.65E+00	3.66E+00	2.90E+00
0.8	4.26E+00	4.28E+00	4.33E+00	4.39E+00	4.44E+00	4.28E+00	4.33E+00	3.48E+00
1	5.06E+00	5.09E+00	5.14E+00	5.27E+00	5.24E+00	5.14E+00	5.12E+00	4.20E+00
1.117	5.50E+00	5.55E+00	5.56E+00	5.65E+00	5.64E+00	5.58E+00	5.57E+00	4.63E+00
1.2	5.83E+00	5.84E+00	5.86E+00	5.98E+00	5.95E+00	5.82E+00	5.92E+00	4.87E+00
1.3	6.07E+00	6.14E+00	6.16E+00	6.35E+00	6.31E+00	6.15E+00	6.26E+00	5.18E+00
1.33	6.16E+00	6.26E+00	6.26E+00	6.40E+00	6.45E+00	6.29E+00	6.38E+00	5.25E+00
1.5	6.59E+00	6.63E+00	6.71E+00	6.88E+00	6.91E+00	6.74E+00	6.83E+00	5.76E+00
1.7	6.92E+00	6.93E+00	7.08E+00	7.25E+00	7.40E+00	7.23E+00	7.37E+00	6.20E+00
2	7.04E+00	7.16E+00	7.29E+00	7.66E+00	7.92E+00	7.88E+00	8.05E+00	6.75E+00
2.4	6.84E+00	6.93E+00	7.24E+00	7.84E+00	8.47E+00	8.64E+00	8.74E+00	7.32E+00
3	6.35E+00	6.49E+00	6.92E+00	7.87E+00	8.99E+00	9.61E+00	9.32E+00	7.86E+00
4	5.62E+00	5.85E+00	6.43E+00	7.67E+00	9.64E+00	1.09E+01	1.10E+01	8.63E+00
5	5.13E+00	5.35E+00	6.08E+00	7.68E+00	1.01E+01	1.22E+01	1.26E+01	9.35E+00
6	4.82E+00	5.05E+00	5.87E+00	7.60E+00	1.07E+01	1.34E+01	1.40E+01	9.99E+00
6.129	4.79E+00	5.06E+00	5.76E+00	7.62E+00	1.08E+01	1.34E+01	1.43E+01	1.01E+01
8	4.42E+00	4.67E+00	5.52E+00	7.47E+00	1.16E+01	1.56E+01	1.71E+01	1.14E+01
10	4.17E+00	4.38E+00	5.19E+00	7.16E+00	1.22E+01	1.76E+01	1.95E+01	1.27E+01
15	3.97E+00	4.16E+00	4.78E+00	6.58E+00	1.25E+01	2.08E+01	2.57E+01	1.58E+01
20	3.94E+00	4.08E+00	4.60E+00	6.15E+00	1.24E+01	2.29E+01	3.09E+01	1.89E+01
30	4.01E+00	4.12E+00	4.58E+00	5.84E+00	1.19E+01	2.46E+01	3.79E+01	2.45E+01
40	4.09E+00	4.18E+00	4.68E+00	5.69E+00	1.17E+01	2.55E+01	4.22E+01	2.95E+01
50	4.16E+00	4.32E+00	4.71E+00	5.70E+00	1.16E+01	2.64E+01	4.53E+01	3.36E+01

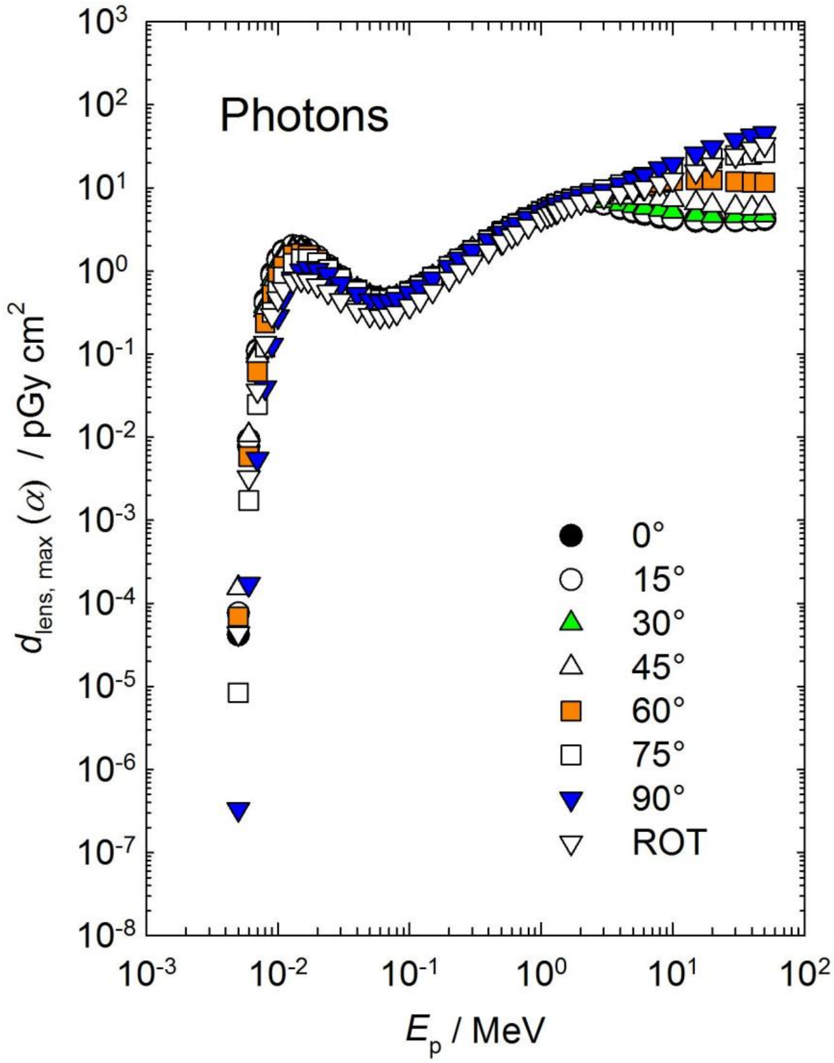

Figure C.1.1a Conversion coefficients from photon fluence to the maximum absorbed dose in the sensitive cells or the complete lens, for left or right irradiations (Behrens, 2017a).

2011 Table C.1.1b Conversion coefficients from photon air kerma to the maximum absorbed dose to the
2012 sensitive cells or the complete lens, for left or right irradiations (Behrens, 2017a).

E_p / MeV	$d_{lens, max}(\alpha)$/ (Gy Gy^{-1}) for a radiation incidence at α							ROT
	0°	15°	30°	45°	60°	75°	90°	
0.005	1.36E-06	2.50E-06	5.01E-06	4.95E-06	2.25E-06	2.74E-07	1.09E-08	1.42E-06
0.006	3.64E-04	4.38E-04	4.98E-04	4.95E-04	2.76E-04	8.16E-05	7.99E-06	1.54E-04
0.007	7.27E-03	6.90E-03	6.78E-03	6.16E-03	3.97E-03	1.60E-03	3.55E-04	2.35E-03
0.008	3.78E-02	3.49E-02	3.20E-02	2.86E-02	2.01E-02	1.03E-02	3.35E-03	1.16E-02
0.009	1.02E-01	9.53E-02	8.68E-02	7.63E-02	5.63E-02	3.45E-02	1.41E-02	3.19E-02
0.01	1.91E-01	1.80E-01	1.66E-01	1.48E-01	1.15E-01	7.75E-02	3.82E-02	6.25E-02
0.011	2.89E-01	2.78E-01	2.59E-01	2.34E-01	1.90E-01	1.40E-01	7.74E-02	9.97E-02
0.013	4.74E-01	4.71E-01	4.47E-01	4.07E-01	3.62E-01	2.91E-01	1.91E-01	1.79E-01
0.015	6.21E-01	6.26E-01	6.04E-01	5.60E-01	5.19E-01	4.51E-01	3.24E-01	2.53E-01
0.017	7.36E-01	7.48E-01	7.30E-01	6.85E-01	6.51E-01	5.86E-01	4.56E-01	3.19E-01
0.02	8.63E-01	8.82E-01	8.78E-01	8.24E-01	8.09E-01	7.51E-01	6.15E-01	4.00E-01
0.024	9.94E-01	1.01E+00	1.01E+00	9.70E-01	9.59E-01	9.05E-01	7.89E-01	4.87E-01
0.03	1.14E+00	1.18E+00	1.17E+00	1.13E+00	1.15E+00	1.11E+00	9.81E-01	6.21E-01
0.04	1.35E+00	1.39E+00	1.41E+00	1.37E+00	1.38E+00	1.34E+00	1.24E+00	7.91E-01
0.05	1.50E+00	1.53E+00	1.56E+00	1.54E+00	1.53E+00	1.48E+00	1.38E+00	9.15E-01
0.06	1.56E+00	1.60E+00	1.62E+00	1.61E+00	1.60E+00	1.56E+00	1.48E+00	9.86E-01
0.07	1.58E+00	1.61E+00	1.62E+00	1.61E+00	1.60E+00	1.58E+00	1.51E+00	1.02E+00
0.08	1.57E+00	1.58E+00	1.59E+00	1.58E+00	1.60E+00	1.57E+00	1.49E+00	1.03E+00
0.1	1.51E+00	1.51E+00	1.53E+00	1.54E+00	1.54E+00	1.50E+00	1.46E+00	1.01E+00
0.12	1.44E+00	1.46E+00	1.46E+00	1.47E+00	1.46E+00	1.44E+00	1.40E+00	9.82E-01
0.15	1.40E+00	1.40E+00	1.41E+00	1.41E+00	1.41E+00	1.40E+00	1.35E+00	9.67E-01
0.2	1.32E+00	1.34E+00	1.36E+00	1.37E+00	1.34E+00	1.33E+00	1.32E+00	9.46E-01
0.24	1.31E+00	1.32E+00	1.32E+00	1.33E+00	1.32E+00	1.30E+00	1.31E+00	9.55E-01
0.3	1.26E+00	1.27E+00	1.28E+00	1.33E+00	1.29E+00	1.26E+00	1.26E+00	9.28E-01
0.4	1.21E+00	1.23E+00	1.24E+00	1.26E+00	1.25E+00	1.22E+00	1.25E+00	9.27E-01
0.5	1.19E+00	1.19E+00	1.21E+00	1.23E+00	1.24E+00	1.19E+00	1.20E+00	9.31E-01
0.511	1.18E+00	1.19E+00	1.22E+00	1.24E+00	1.24E+00	1.19E+00	1.19E+00	9.28E-01
0.6	1.18E+00	1.18E+00	1.20E+00	1.22E+00	1.22E+00	1.18E+00	1.18E+00	9.28E-01
0.662	1.17E+00	1.17E+00	1.18E+00	1.21E+00	1.20E+00	1.17E+00	1.18E+00	9.31E-01
0.8	1.15E+00	1.16E+00	1.17E+00	1.19E+00	1.20E+00	1.15E+00	1.17E+00	9.41E-01
1	1.13E+00	1.13E+00	1.15E+00	1.18E+00	1.17E+00	1.15E+00	1.14E+00	9.36E-01
1.117	1.13E+00	1.14E+00	1.14E+00	1.16E+00	1.15E+00	1.14E+00	1.14E+00	9.48E-01
1.2	1.13E+00	1.13E+00	1.14E+00	1.16E+00	1.15E+00	1.13E+00	1.15E+00	9.42E-01
1.3	1.10E+00	1.12E+00	1.12E+00	1.16E+00	1.15E+00	1.12E+00	1.14E+00	9.43E-01
1.33	1.10E+00	1.12E+00	1.12E+00	1.14E+00	1.15E+00	1.12E+00	1.14E+00	9.39E-01
1.5	1.07E+00	1.08E+00	1.09E+00	1.12E+00	1.12E+00	1.10E+00	1.11E+00	9.37E-01
1.7	1.03E+00	1.03E+00	1.05E+00	1.08E+00	1.10E+00	1.08E+00	1.10E+00	9.22E-01
2	9.32E-01	9.48E-01	9.64E-01	1.01E+00	1.05E+00	1.04E+00	1.07E+00	8.93E-01
2.4	7.99E-01	8.10E-01	8.46E-01	9.16E-01	9.89E-01	1.01E+00	1.02E+00	8.54E-01
3	6.36E-01	6.51E-01	6.93E-01	7.89E-01	9.02E-01	9.63E-01	9.35E-01	7.88E-01
4	4.63E-01	4.82E-01	5.29E-01	6.32E-01	7.94E-01	9.01E-01	9.04E-01	7.11E-01
5	3.62E-01	3.77E-01	4.29E-01	5.41E-01	7.15E-01	8.61E-01	8.89E-01	6.60E-01
6	2.98E-01	3.12E-01	3.63E-01	4.70E-01	6.62E-01	8.30E-01	8.68E-01	6.18E-01
6.129	2.92E-01	3.08E-01	3.50E-01	4.63E-01	6.55E-01	8.13E-01	8.69E-01	6.15E-01
8	2.20E-01	2.32E-01	2.74E-01	3.71E-01	5.74E-01	7.73E-01	8.47E-01	5.67E-01
10	1.73E-01	1.81E-01	2.15E-01	2.97E-01	5.06E-01	7.28E-01	8.07E-01	5.26E-01
15	1.15E-01	1.21E-01	1.39E-01	1.91E-01	3.62E-01	6.04E-01	7.47E-01	4.59E-01
20	8.69E-02	9.00E-02	1.01E-01	1.35E-01	2.74E-01	5.04E-01	6.81E-01	4.17E-01
30	5.84E-02	6.00E-02	6.68E-02	8.51E-02	1.74E-01	3.59E-01	5.53E-01	3.57E-01
40	4.39E-02	4.48E-02	5.01E-02	6.10E-02	1.26E-01	2.73E-01	4.52E-01	3.16E-01
50	3.49E-02	3.62E-02	3.95E-02	4.79E-02	9.77E-02	2.21E-01	3.80E-01	2.82E-01

2013

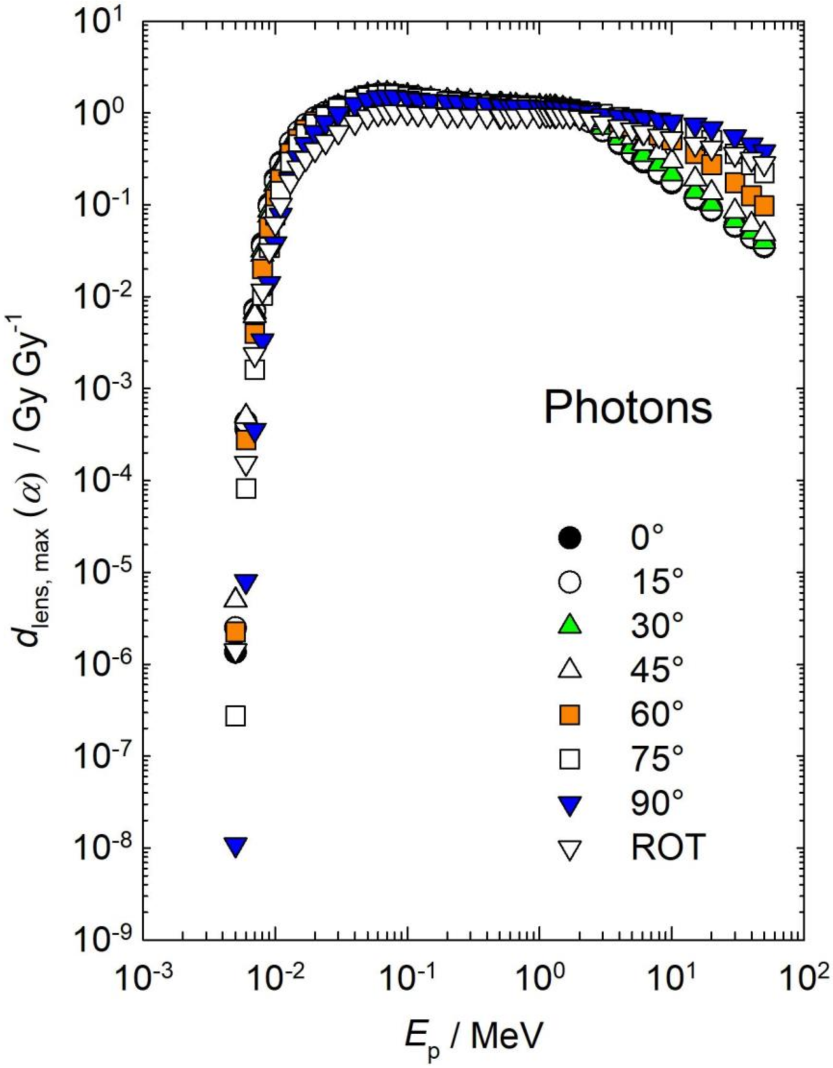

Figure C.1.1b Conversion coefficients from photon air kerma to the maximum absorbed dose in the sensitive cells or the complete lens, for left or right irradiations (Behrens, 2017a).

Table C.1.2 Neutrons

Figure C.1.2 Neutrons

Table C.1.3 Conversion coefficients from electron fluence to the maximum absorbed dose in the sensitive cells or the complete lens, for left or right irradiations (Behrens,2017a).

	$d_{\text{lens, max}}(\alpha)$/ (pGy cm^2) for a radiation incidence at α							
E_p / MeV	0°	15°	30°	45°	60°	75°	90°	ROT
0.01	1.68E-06	1.81E-06	1.43E-06	1.16E-06	7.55E-07	7.04E-07	3.74E-07	3.32E-07
0.015	2.26E-05	3.34E-05	2.34E-05	2.22E-05	1.96E-05	1.66E-05	6.43E-06	4.60E-06
0.02	8.15E-05	7.79E-05	7.25E-05	5.81E-05	4.99E-05	3.24E-05	2.73E-05	3.40E-05
0.03	2.23E-04	2.30E-04	2.25E-04	1.89E-04	1.26E-04	1.12E-04	6.60E-05	7.02E-05
0.04	4.16E-04	3.40E-04	4.04E-04	3.49E-04	2.71E-04	2.00E-04	1.02E-04	1.13E-04
0.05	6.07E-04	6.75E-04	6.16E-04	5.09E-04	4.08E-04	3.06E-04	1.86E-04	1.72E-04
0.06	8.47E-04	8.68E-04	7.80E-04	6.15E-04	5.57E-04	3.87E-04	2.24E-04	2.83E-04
0.08	1.31E-03	1.33E-03	1.23E-03	1.08E-03	8.32E-04	6.11E-04	4.21E-04	4.60E-04
0.1	1.92E-03	1.80E-03	1.66E-03	1.57E-03	1.20E-03	7.97E-04	5.48E-04	5.86E-04
0.15	3.24E-03	3.36E-03	3.11E-03	2.47E-03	2.23E-03	1.65E-03	1.02E-03	1.20E-03
0.2	5.04E-03	5.21E-03	4.60E-03	4.07E-03	3.47E-03	2.59E-03	1.64E-03	1.77E-03
0.3	9.58E-03	9.08E-03	7.91E-03	7.83E-03	6.02E-03	4.52E-03	3.11E-03	3.20E-03
0.4	1.41E-02	1.47E-02	1.29E-02	1.25E-02	1.00E-02	7.88E-03	5.09E-03	4.83E-03
0.5	2.06E-02	2.06E-02	1.91E-02	1.76E-02	1.41E-02	1.13E-02	7.66E-03	7.78E-03
0.6	1.75E-01	2.32E-01	3.17E-01	2.97E-01	1.86E-01	7.49E-02	2.32E-02	9.44E-02
0.7	7.56E+00	8.46E+00	9.60E+00	8.88E+00	6.08E+00	2.89E+00	8.98E-01	3.08E+00
0.8	4.62E+01	4.66E+01	4.57E+01	3.93E+01	2.77E+01	1.50E+01	5.51E+00	1.54E+01
1	2.29E+02	2.18E+02	1.89E+02	1.50E+02	1.04E+02	6.11E+01	2.66E+01	6.64E+01
1.25	3.87E+02	3.73E+02	3.29E+02	2.69E+02	1.92E+02	1.19E+02	5.77E+01	1.17E+02
1.5	4.42E+02	4.30E+02	3.94E+02	3.39E+02	2.57E+02	1.69E+02	8.67E+01	1.44E+02
1.75	4.45E+02	4.41E+02	4.17E+02	3.80E+02	3.06E+02	2.12E+02	1.16E+02	1.57E+02
2	4.30E+02	4.29E+02	4.19E+02	4.01E+02	3.39E+02	2.52E+02	1.46E+02	1.62E+02
2.5	4.08E+02	4.12E+02	4.13E+02	4.09E+02	3.75E+02	3.13E+02	2.02E+02	1.65E+02
3	3.78E+02	3.87E+02	3.99E+02	4.11E+02	3.85E+02	3.49E+02	2.46E+02	1.64E+02
3.5	3.54E+02	3.66E+02	3.82E+02	4.05E+02	3.91E+02	3.70E+02	2.85E+02	1.64E+02
4	3.39E+02	3.51E+02	3.69E+02	3.99E+02	3.87E+02	3.80E+02	3.14E+02	1.64E+02
5	3.23E+02	3.35E+02	3.54E+02	3.92E+02	3.68E+02	3.82E+02	3.50E+02	1.65E+02
6	3.15E+02	3.28E+02	3.49E+02	3.94E+02	3.49E+02	3.76E+02	3.69E+02	1.68E+02
7	3.10E+02	3.22E+02	3.46E+02	4.01E+02	3.37E+02	3.64E+02	3.75E+02	1.72E+02
8	3.07E+02	3.18E+02	3.41E+02	4.06E+02	3.56E+02	3.53E+02	3.76E+02	1.77E+02
10	3.04E+02	3.12E+02	3.30E+02	4.03E+02	4.20E+02	3.36E+02	3.61E+02	1.85E+02
15	3.01E+02	3.06E+02	3.09E+02	3.53E+02	4.60E+02	3.15E+02	3.29E+02	2.01E+02
20	3.01E+02	3.03E+02	3.05E+02	3.23E+02	4.28E+02	3.76E+02	3.15E+02	2.12E+02
30	3.03E+02	3.04E+02	3.06E+02	3.12E+02	3.71E+02	3.67E+02	3.20E+02	2.36E+02
40	3.03E+02	3.07E+02	3.03E+02	3.13E+02	3.47E+02	3.46E+02	3.20E+02	2.64E+02
50	3.00E+02	3.01E+02	3.06E+02	3.10E+02	3.41E+02	3.32E+02	3.21E+02	2.90E+02

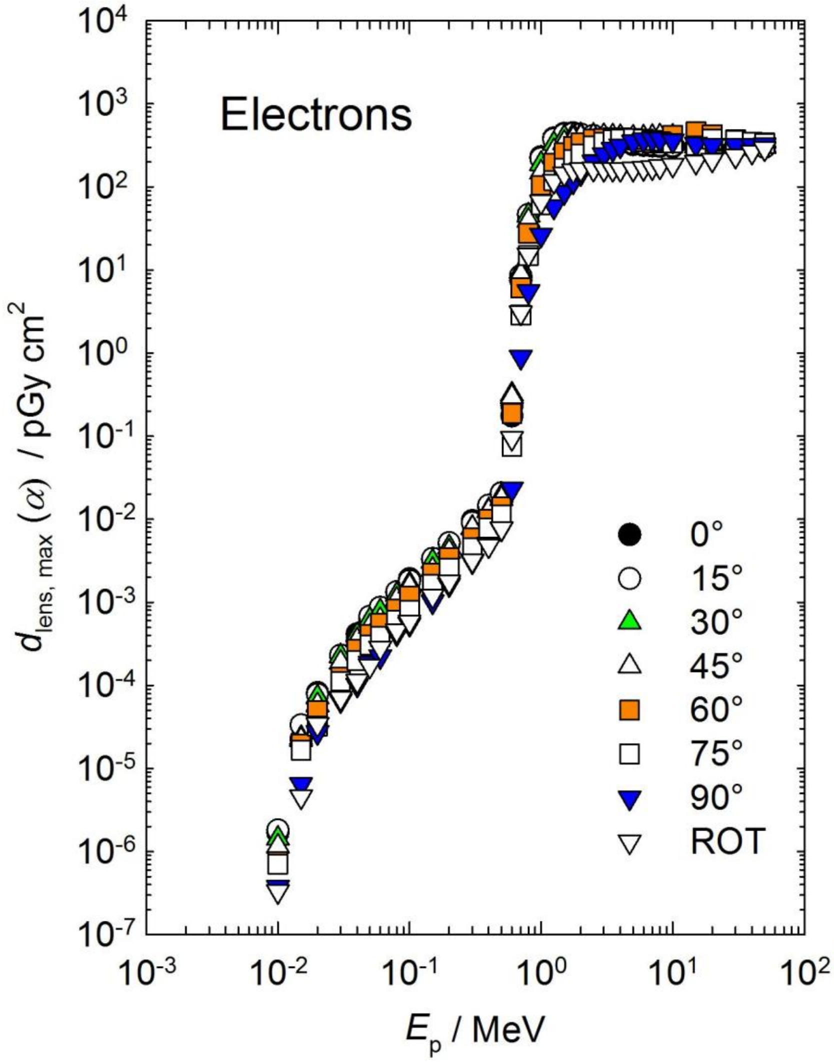

Figure C.1.3 Conversion coefficients from electron fluence to the maximum absorbed dose in the sensitive cells or the complete lens, for left or right irradiations (Behrens, 2017a).

2063 Table C.1.4 Conversion coefficients from positron fluence to the maximum absorbed dose in the
2064 sensitive cells or the complete lens, for left or right irradiations (Behrens, 2017a).

E_p / MeV	$d_{lens, max}$ (α)/ (pGy cm^2) for a radiation incidence at α							
	0°	15°	30°	45°	60°	75°	90°	ROT
0.001	7.43E+00	7.94E+00	7.89E+00	7.35E+00	6.13E+00	4.91E+00	3.47E+00	3.06E+00
0.002	7.17E+00	7.47E+00	7.43E+00	6.98E+00	5.88E+00	4.58E+00	3.21E+00	2.87E+00
0.003	6.99E+00	7.26E+00	7.39E+00	6.71E+00	5.61E+00	4.43E+00	3.05E+00	2.76E+00
0.004	6.88E+00	7.34E+00	7.28E+00	6.64E+00	5.70E+00	4.36E+00	3.01E+00	2.72E+00
0.005	7.02E+00	7.17E+00	7.29E+00	6.72E+00	5.67E+00	4.24E+00	3.07E+00	2.74E+00
0.006	6.97E+00	7.18E+00	7.33E+00	6.59E+00	5.54E+00	4.33E+00	2.91E+00	2.70E+00
0.007	6.85E+00	7.31E+00	7.22E+00	6.65E+00	5.58E+00	4.33E+00	2.98E+00	2.69E+00
0.008	6.92E+00	7.31E+00	7.21E+00	6.65E+00	5.51E+00	4.27E+00	2.95E+00	2.77E+00
0.009	6.84E+00	7.30E+00	7.14E+00	6.60E+00	5.57E+00	4.30E+00	2.94E+00	2.73E+00
0.01	6.87E+00	7.26E+00	7.18E+00	6.61E+00	5.52E+00	4.31E+00	2.94E+00	2.67E+00
0.013	6.78E+00	7.32E+00	7.20E+00	6.62E+00	5.53E+00	4.23E+00	2.98E+00	2.65E+00
0.015	6.88E+00	7.29E+00	7.08E+00	6.55E+00	5.65E+00	4.38E+00	2.92E+00	2.69E+00
0.017	6.96E+00	7.19E+00	7.23E+00	6.56E+00	5.55E+00	4.30E+00	2.94E+00	2.63E+00
0.02	6.79E+00	7.13E+00	7.17E+00	6.59E+00	5.49E+00	4.24E+00	3.01E+00	2.72E+00
0.024	6.93E+00	7.22E+00	7.28E+00	6.57E+00	5.59E+00	4.30E+00	2.92E+00	2.67E+00
0.03	6.95E+00	7.18E+00	7.27E+00	6.49E+00	5.59E+00	4.31E+00	2.94E+00	2.68E+00
0.04	6.94E+00	7.15E+00	7.26E+00	6.69E+00	5.62E+00	4.39E+00	2.91E+00	2.67E+00
0.05	6.87E+00	7.20E+00	7.20E+00	6.76E+00	5.55E+00	4.29E+00	2.92E+00	2.77E+00
0.06	6.91E+00	7.04E+00	7.28E+00	6.74E+00	5.61E+00	4.31E+00	3.00E+00	2.71E+00
0.07	6.99E+00	7.17E+00	7.35E+00	6.48E+00	5.52E+00	4.33E+00	2.96E+00	2.68E+00
0.08	6.96E+00	7.20E+00	7.21E+00	6.80E+00	5.61E+00	4.38E+00	3.01E+00	2.71E+00
0.1	6.97E+00	7.43E+00	7.26E+00	6.71E+00	5.57E+00	4.25E+00	3.00E+00	2.73E+00
0.15	6.94E+00	7.30E+00	7.30E+00	6.68E+00	5.63E+00	4.23E+00	2.98E+00	2.79E+00
0.2	7.13E+00	7.42E+00	7.60E+00	6.93E+00	5.76E+00	4.43E+00	2.99E+00	2.75E+00
0.3	7.29E+00	7.61E+00	7.66E+00	6.97E+00	5.80E+00	4.50E+00	3.12E+00	2.90E+00
0.4	7.60E+00	7.97E+00	7.71E+00	7.12E+00	5.88E+00	4.70E+00	3.16E+00	2.96E+00
0.5	7.91E+00	8.35E+00	8.11E+00	7.36E+00	6.23E+00	4.70E+00	3.24E+00	3.02E+00
0.6	8.44E+00	8.70E+00	8.86E+00	8.11E+00	6.67E+00	4.98E+00	3.39E+00	3.26E+00
0.7	1.71E+01	1.84E+01	1.95E+01	1.80E+01	1.34E+01	8.33E+00	4.46E+00	6.91E+00
0.8	5.95E+01	5.97E+01	5.86E+01	5.03E+01	3.65E+01	2.15E+01	9.54E+00	2.02E+01
1	2.48E+02	2.37E+02	2.06E+02	1.64E+02	1.15E+02	6.88E+01	3.18E+01	7.28E+01
1.25	3.94E+02	3.79E+02	3.35E+02	2.77E+02	2.03E+02	1.27E+02	6.18E+01	1.21E+02
1.5	4.34E+02	4.24E+02	3.90E+02	3.41E+02	2.61E+02	1.72E+02	9.22E+01	1.45E+02
1.75	4.32E+02	4.24E+02	4.10E+02	3.72E+02	3.06E+02	2.13E+02	1.20E+02	1.54E+02
2	4.13E+02	4.13E+02	4.05E+02	3.87E+02	3.35E+02	2.50E+02	1.46E+02	1.58E+02
2.5	3.88E+02	3.94E+02	3.97E+02	3.92E+02	3.68E+02	3.04E+02	2.03E+02	1.59E+02
3	3.59E+02	3.69E+02	3.78E+02	3.96E+02	3.69E+02	3.37E+02	2.47E+02	1.61E+02
3.5	3.38E+02	3.47E+02	3.65E+02	3.85E+02	3.73E+02	3.53E+02	2.76E+02	1.59E+02
4	3.22E+02	3.36E+02	3.53E+02	3.81E+02	3.68E+02	3.69E+02	3.03E+02	1.58E+02
5	3.10E+02	3.22E+02	3.42E+02	3.74E+02	3.49E+02	3.70E+02	3.40E+02	1.60E+02
6	3.05E+02	3.17E+02	3.38E+02	3.80E+02	3.36E+02	3.60E+02	3.52E+02	1.63E+02
7	3.00E+02	3.12E+02	3.34E+02	3.84E+02	3.25E+02	3.46E+02	3.64E+02	1.69E+02
8	2.99E+02	3.06E+02	3.32E+02	3.91E+02	3.46E+02	3.38E+02	3.61E+02	1.71E+02
10	2.96E+02	3.02E+02	3.23E+02	3.88E+02	4.08E+02	3.23E+02	3.44E+02	1.80E+02
15	2.97E+02	3.01E+02	3.06E+02	3.40E+02	4.39E+02	3.10E+02	3.23E+02	1.94E+02
20	2.98E+02	2.99E+02	3.01E+02	3.16E+02	4.12E+02	3.58E+02	3.11E+02	2.07E+02
30	2.99E+02	2.99E+02	3.00E+02	3.07E+02	3.59E+02	3.47E+02	3.09E+02	2.31E+02
40	2.99E+02	3.03E+02	3.03E+02	3.03E+02	3.40E+02	3.30E+02	3.06E+02	2.60E+02
50	3.02E+02	3.00E+02	3.03E+02	3.02E+02	3.31E+02	3.23E+02	3.10E+02	2.83E+02

2065

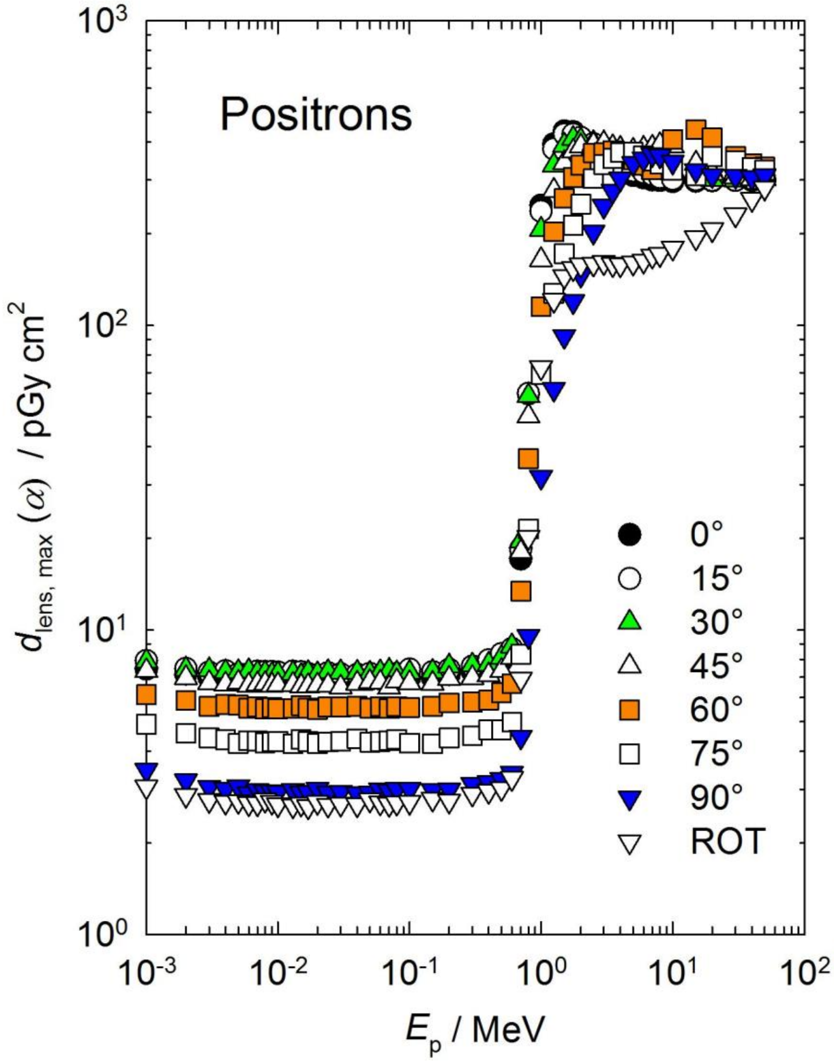

Figure C.1.4 Conversion coefficients from positron fluence to the maximum absorbed dose in the sensitive cells or the complete lens, for left or right irradiations (Behrens, 2017a).

C.2 Photons for Energies up to 50MeV in Fields with Charged-Particle Equilibrium.

The calibration of are monitoring instruments and personal dosimeters to measure photons for ambient dose, directional and personal absorbed dose in the lens of the eye and local skin, and personal dose, are performed routinely in air with sufficient material in front of the instrument to provide full charged-particle equilibrium. The calibration procedure is for photons and for the particles produced in air and the other material at the point of test.

Table C.2.1a and Figure C.2.1a give values of conversion coefficients for this procedure for photon energies up to 50 MeV using the kerma-approximation method to give charged-particle equilibrium, from photon fluence to directional and personal absorbed dose in the lens of the eye, and in Table C.2.1b and Figure C.2.1b from air kerma. The conversion coefficients are to the value of the absorbed dose to the lens of the eye, the maximum value of that to the radiation sensitive cells or the complete lens, calculated for whole-body exposure of the stylized eye model (Behrens and Dietze, 2011) for broad parallel beams incident for angles from 0° (A-P) to 90° in 15° steps, the maximum value of the absorbed dose of the right or left irradiations is taken; and for a rotational field.

Table C.2.1a Conversion coefficients from photon fluence to the maximum absorbed dose in the sensitive cells or the complete lens, for left or right irradiations, calculated using the kerma-approximation method (Behrens, 2017a).

	$d_{\text{lens, max}}(\alpha)$ / (pGy cm^2) for a radiation incidence at α							
E_p / MeV	0°	15°	30°	45°	60°	75°	90°	ROT
0.005	4.10E-05	6.91E-05	1.48E-04	1.56E-04	5.95E-05	7.94E-06	4.11E-07	3.06E-05
0.006	7.94E-03	8.87E-03	1.06E-02	1.02E-02	5.73E-03	1.56E-03	1.74E-04	3.13E-03
0.007	1.07E-01	1.06E-01	1.05E-01	9.16E-02	6.22E-02	2.67E-02	4.67E-03	3.39E-02
0.008	4.25E-01	4.12E-01	3.79E-01	3.24E-01	2.35E-01	1.23E-01	3.65E-02	1.29E-01
0.009	9.03E-01	8.76E-01	7.97E-01	6.77E-01	5.21E-01	3.20E-01	1.22E-01	2.85E-01
0.01	1.38E+00	1.34E+00	1.23E+00	1.06E+00	8.58E-01	5.79E-01	2.63E-01	4.52E-01
0.011	1.73E+00	1.69E+00	1.57E+00	1.39E+00	1.15E+00	8.45E-01	4.43E-01	5.92E-01
0.013	2.02E+00	2.00E+00	1.90E+00	1.74E+00	1.53E+00	1.25E+00	7.87E-01	7.59E-01
0.015	1.98E+00	1.96E+00	1.89E+00	1.77E+00	1.63E+00	1.41E+00	1.02E+00	7.97E-01
0.017	1.80E+00	1.79E+00	1.74E+00	1.67E+00	1.55E+00	1.40E+00	1.11E+00	7.72E-01
0.02	1.49E+00	1.49E+00	1.47E+00	1.43E+00	1.35E+00	1.26E+00	1.07E+00	6.87E-01
0.024	1.16E+00	1.17E+00	1.15E+00	1.14E+00	1.11E+00	1.05E+00	9.27E-01	5.79E-01
0.03	8.53E-01	8.48E-01	8.50E-01	8.50E-01	8.24E-01	7.93E-01	7.28E-01	4.59E-01
0.04	5.89E-01	5.95E-01	5.97E-01	5.96E-01	5.90E-01	5.77E-01	5.35E-01	3.43E-01
0.05	4.89E-01	4.90E-01	4.98E-01	5.00E-01	4.97E-01	4.80E-01	4.53E-01	2.99E-01
0.06	4.55E-01	4.56E-01	4.64E-01	4.67E-01	4.62E-01	4.46E-01	4.28E-01	2.86E-01
0.07	4.56E-01	4.63E-01	4.66E-01	4.67E-01	4.64E-01	4.52E-01	4.34E-01	2.95E-01
0.08	4.81E-01	4.87E-01	4.91E-01	4.90E-01	4.88E-01	4.78E-01	4.60E-01	3.15E-01
0.1	5.59E-01	5.62E-01	5.72E-01	5.71E-01	5.65E-01	5.59E-01	5.42E-01	3.77E-01
0.12	6.64E-01	6.70E-01	6.73E-01	6.74E-01	6.72E-01	6.66E-01	6.44E-01	4.56E-01
0.15	8.35E-01	8.39E-01	8.48E-01	8.50E-01	8.45E-01	8.39E-01	8.19E-01	5.81E-01
0.2	1.14E+00	1.14E+00	1.16E+00	1.17E+00	1.15E+00	1.15E+00	1.13E+00	8.17E-01
0.24	1.38E+00	1.40E+00	1.40E+00	1.41E+00	1.42E+00	1.40E+00	1.38E+00	1.00E+00
0.3	1.75E+00	1.76E+00	1.76E+00	1.79E+00	1.80E+00	1.76E+00	1.73E+00	1.30E+00
0.4	2.30E+00	2.37E+00	2.34E+00	2.37E+00	2.39E+00	2.34E+00	2.29E+00	1.75E+00
0.5	2.82E+00	2.85E+00	2.88E+00	2.93E+00	3.01E+00	2.86E+00	2.85E+00	2.23E+00
0.511	2.91E+00	2.91E+00	2.95E+00	3.00E+00	2.98E+00	2.90E+00	2.92E+00	2.26E+00
0.6	3.35E+00	3.37E+00	3.42E+00	3.48E+00	3.49E+00	3.39E+00	3.38E+00	2.64E+00
0.662	3.64E+00	3.65E+00	3.69E+00	3.78E+00	3.78E+00	3.66E+00	3.65E+00	2.92E+00
0.8	4.24E+00	4.33E+00	4.31E+00	4.39E+00	4.41E+00	4.32E+00	4.31E+00	3.46E+00
1	5.09E+00	5.10E+00	5.15E+00	5.25E+00	5.31E+00	5.13E+00	5.12E+00	4.24E+00
1.117	5.58E+00	5.57E+00	5.71E+00	5.69E+00	5.74E+00	5.57E+00	5.56E+00	4.63E+00
1.2	5.83E+00	5.93E+00	5.94E+00	5.99E+00	6.03E+00	5.90E+00	5.88E+00	4.92E+00
1.3	6.23E+00	6.27E+00	6.29E+00	6.41E+00	6.43E+00	6.25E+00	6.26E+00	5.25E+00
1.33	6.32E+00	6.36E+00	6.37E+00	6.46E+00	6.51E+00	6.37E+00	6.35E+00	5.39E+00
1.5	6.89E+00	6.98E+00	6.92E+00	7.04E+00	7.10E+00	6.90E+00	6.90E+00	5.98E+00
1.7	7.49E+00	7.58E+00	7.59E+00	7.68E+00	7.78E+00	7.55E+00	7.54E+00	6.49E+00
2	8.39E+00	8.44E+00	8.47E+00	8.56E+00	8.62E+00	8.42E+00	8.37E+00	7.25E+00
2.4	9.44E+00	9.53E+00	9.52E+00	9.71E+00	9.72E+00	9.48E+00	9.60E+00	8.33E+00
3	1.10E+01	1.10E+01	1.11E+01	1.11E+01	1.12E+01	1.10E+01	1.09E+01	9.82E+00
4	1.32E+01	1.33E+01	1.34E+01	1.33E+01	1.34E+01	1.32E+01	1.32E+01	1.19E+01
5	1.54E+01	1.54E+01	1.55E+01	1.57E+01	1.56E+01	1.53E+01	1.55E+01	1.39E+01
6	1.74E+01	1.74E+01	1.75E+01	1.76E+01	1.75E+01	1.74E+01	1.75E+01	1.59E+01
6.129	1.76E+01	1.77E+01	1.77E+01	1.80E+01	1.81E+01	1.76E+01	1.76E+01	1.61E+01
8	2.15E+01	2.17E+01	2.15E+01	2.15E+01	2.16E+01	2.15E+01	2.16E+01	1.94E+01
10	2.54E+01	2.55E+01	2.57E+01	2.55E+01	2.55E+01	2.56E+01	2.56E+01	2.36E+01
15	3.59E+01	3.61E+01	3.57E+01	3.57E+01	3.59E+01	3.55E+01	3.56E+01	3.32E+01
20	4.63E+01	4.66E+01	4.69E+01	4.66E+01	4.67E+01	4.65E+01	4.64E+01	4.35E+01
30	6.96E+01	6.97E+01	6.96E+01	6.93E+01	6.94E+01	7.00E+01	6.86E+01	6.45E+01
40	9.40E+01	9.35E+01	9.35E+01	9.40E+01	9.49E+01	9.33E+01	9.23E+01	8.72E+01
50	1.19E+02	1.19E+02	1.20E+02	1.19E+02	1.19E+02	1.18E+02	1.18E+02	1.09E+02

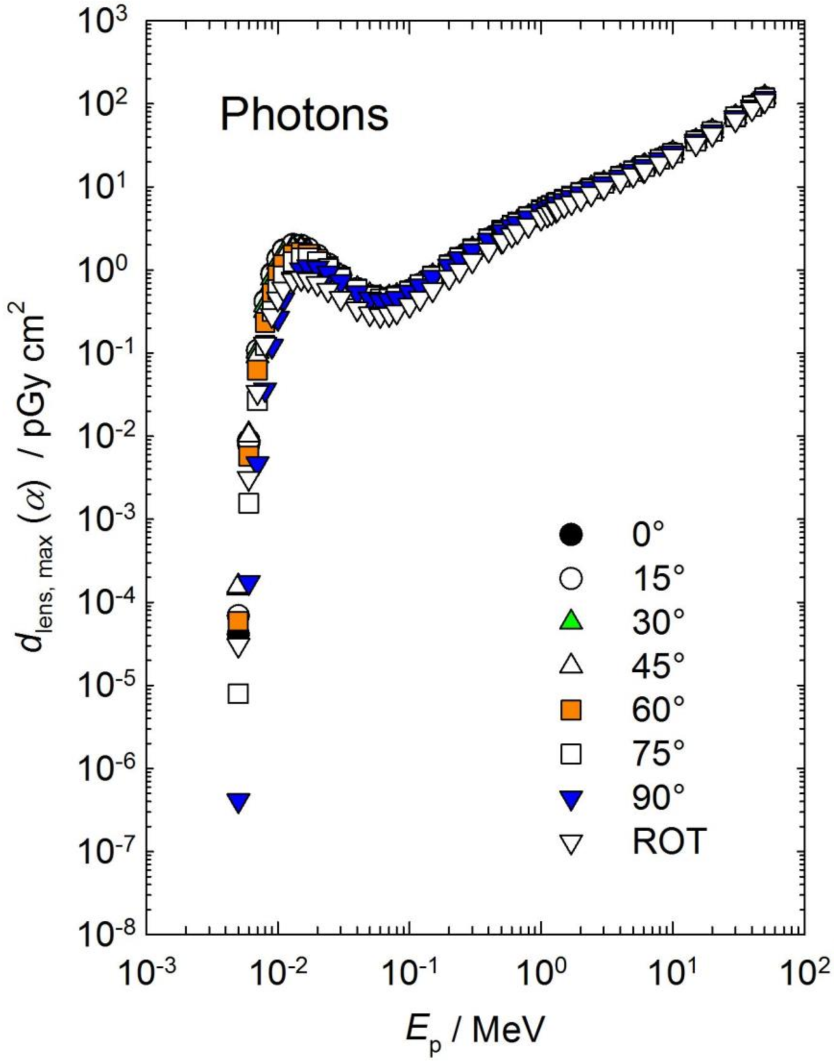

Figure C.2.1a Conversion coefficients from photon fluence to the maximum absorbed dose in the sensitive cells or the complete lens, for left or right irradiations, calculated using the kerma-approximation method (Behrens, 2017a).

Table C.2.1b Conversion coefficients from photon air kerma to the maximum absorbed dose in the sensitive cells or the complete lens, for left or right irradiations, calculated using the kerma-approximation method (Behrens, 2017a).

	$d_{\text{lens, max}}(\alpha)/(\text{Gy Gy}^{-1})$ for a radiation incidence at α							
E_p / MeV	0°	15°	30°	45°	60°	75°	90°	ROT
0.005	1.34E-06	2.25E-06	4.84E-06	5.10E-06	1.94E-06	2.59E-07	1.34E-08	9.99E-07
0.006	3.74E-04	4.17E-04	4.99E-04	4.79E-04	2.69E-04	7.33E-05	8.20E-06	1.47E-04
0.007	6.88E-03	6.86E-03	6.75E-03	5.91E-03	4.01E-03	1.72E-03	3.01E-04	2.19E-03
0.008	3.61E-02	3.50E-02	3.21E-02	2.75E-02	1.99E-02	1.05E-02	3.09E-03	1.10E-02
0.009	9.80E-02	9.50E-02	8.65E-02	7.35E-02	5.65E-02	3.47E-02	1.33E-02	3.09E-02
0.01	1.86E-01	1.81E-01	1.66E-01	1.44E-01	1.16E-01	7.82E-02	3.55E-02	6.11E-02
0.011	2.86E-01	2.79E-01	2.59E-01	2.29E-01	1.90E-01	1.40E-01	7.32E-02	9.80E-02
0.013	4.78E-01	4.71E-01	4.48E-01	4.11E-01	3.61E-01	2.96E-01	1.86E-01	1.79E-01
0.015	6.33E-01	6.26E-01	6.03E-01	5.68E-01	5.22E-01	4.51E-01	3.25E-01	2.55E-01
0.017	7.56E-01	7.49E-01	7.29E-01	7.01E-01	6.49E-01	5.86E-01	4.63E-01	3.23E-01
0.02	8.87E-01	8.83E-01	8.74E-01	8.47E-01	8.03E-01	7.51E-01	6.36E-01	4.08E-01
0.024	1.01E+00	1.02E+00	1.00E+00	9.90E-01	9.62E-01	9.13E-01	8.07E-01	5.04E-01
0.03	1.18E+00	1.18E+00	1.18E+00	1.18E+00	1.14E+00	1.10E+00	1.01E+00	6.35E-01
0.04	1.37E+00	1.39E+00	1.39E+00	1.39E+00	1.38E+00	1.34E+00	1.25E+00	7.99E-01
0.05	1.52E+00	1.52E+00	1.54E+00	1.55E+00	1.54E+00	1.49E+00	1.40E+00	9.27E-01
0.06	1.57E+00	1.58E+00	1.61E+00	1.61E+00	1.60E+00	1.54E+00	1.48E+00	9.89E-01
0.07	1.58E+00	1.61E+00	1.62E+00	1.62E+00	1.61E+00	1.57E+00	1.51E+00	1.03E+00
0.08	1.57E+00	1.59E+00	1.60E+00	1.60E+00	1.59E+00	1.56E+00	1.50E+00	1.03E+00
0.1	1.51E+00	1.51E+00	1.54E+00	1.54E+00	1.52E+00	1.50E+00	1.46E+00	1.01E+00
0.12	1.44E+00	1.45E+00	1.46E+00	1.46E+00	1.46E+00	1.45E+00	1.40E+00	9.90E-01
0.15	1.39E+00	1.40E+00	1.42E+00	1.42E+00	1.41E+00	1.40E+00	1.37E+00	9.69E-01
0.2	1.33E+00	1.34E+00	1.35E+00	1.36E+00	1.34E+00	1.34E+00	1.31E+00	9.54E-01
0.24	1.30E+00	1.32E+00	1.32E+00	1.33E+00	1.34E+00	1.32E+00	1.30E+00	9.41E-01
0.3	1.27E+00	1.27E+00	1.27E+00	1.29E+00	1.30E+00	1.27E+00	1.25E+00	9.38E-01
0.4	1.22E+00	1.25E+00	1.24E+00	1.25E+00	1.26E+00	1.24E+00	1.21E+00	9.27E-01
0.5	1.19E+00	1.20E+00	1.21E+00	1.23E+00	1.26E+00	1.20E+00	1.20E+00	9.37E-01
0.511	1.20E+00	1.20E+00	1.21E+00	1.23E+00	1.22E+00	1.19E+00	1.20E+00	9.29E-01
0.6	1.18E+00	1.18E+00	1.20E+00	1.22E+00	1.23E+00	1.19E+00	1.19E+00	9.30E-01
0.662	1.17E+00	1.17E+00	1.19E+00	1.21E+00	1.22E+00	1.18E+00	1.17E+00	9.37E-01
0.8	1.15E+00	1.17E+00	1.16E+00	1.19E+00	1.19E+00	1.17E+00	1.16E+00	9.35E-01
1	1.14E+00	1.14E+00	1.15E+00	1.17E+00	1.18E+00	1.14E+00	1.14E+00	9.45E-01
1.117	1.14E+00	1.14E+00	1.17E+00	1.16E+00	1.18E+00	1.14E+00	1.14E+00	9.48E-01
1.2	1.13E+00	1.15E+00	1.15E+00	1.16E+00	1.17E+00	1.14E+00	1.14E+00	9.52E-01
1.3	1.13E+00	1.14E+00	1.14E+00	1.17E+00	1.17E+00	1.14E+00	1.14E+00	9.55E-01
1.33	1.13E+00	1.14E+00	1.14E+00	1.15E+00	1.16E+00	1.14E+00	1.13E+00	9.62E-01
1.5	1.12E+00	1.13E+00	1.13E+00	1.15E+00	1.15E+00	1.12E+00	1.12E+00	9.72E-01
1.7	1.11E+00	1.13E+00	1.13E+00	1.14E+00	1.16E+00	1.12E+00	1.12E+00	9.65E-01
2	1.11E+00	1.12E+00	1.12E+00	1.13E+00	1.14E+00	1.11E+00	1.11E+00	9.60E-01
2.4	1.10E+00	1.11E+00	1.11E+00	1.13E+00	1.14E+00	1.11E+00	1.12E+00	9.73E-01
3	1.10E+00	1.11E+00	1.11E+00	1.11E+00	1.13E+00	1.10E+00	1.09E+00	9.84E-01
4	1.09E+00	1.10E+00	1.11E+00	1.10E+00	1.10E+00	1.09E+00	1.09E+00	9.77E-01
5	1.09E+00	1.08E+00	1.09E+00	1.11E+00	1.10E+00	1.08E+00	1.09E+00	9.80E-01
6	1.08E+00	1.08E+00	1.08E+00	1.09E+00	1.08E+00	1.08E+00	1.08E+00	9.80E-01
6.129	1.07E+00	1.08E+00	1.07E+00	1.09E+00	1.10E+00	1.07E+00	1.07E+00	9.79E-01
8	1.07E+00	1.08E+00	1.07E+00	1.07E+00	1.07E+00	1.07E+00	1.07E+00	9.66E-01
10	1.05E+00	1.05E+00	1.07E+00	1.06E+00	1.06E+00	1.06E+00	1.06E+00	9.78E-01
15	1.04E+00	1.05E+00	1.03E+00	1.04E+00	1.04E+00	1.03E+00	1.03E+00	9.62E-01
20	1.02E+00	1.03E+00	1.03E+00	1.03E+00	1.03E+00	1.03E+00	1.02E+00	9.58E-01
30	1.01E+00	1.02E+00	1.01E+00	1.01E+00	1.01E+00	1.02E+00	1.00E+00	9.41E-01
40	1.01E+00	1.00E+00	1.00E+00	1.01E+00	1.02E+00	1.00E+00	9.89E-01	9.35E-01
50	9.95E-01	1.00E+00	1.01E+00	9.97E-01	9.95E-01	9.91E-01	9.88E-01	9.18E-01

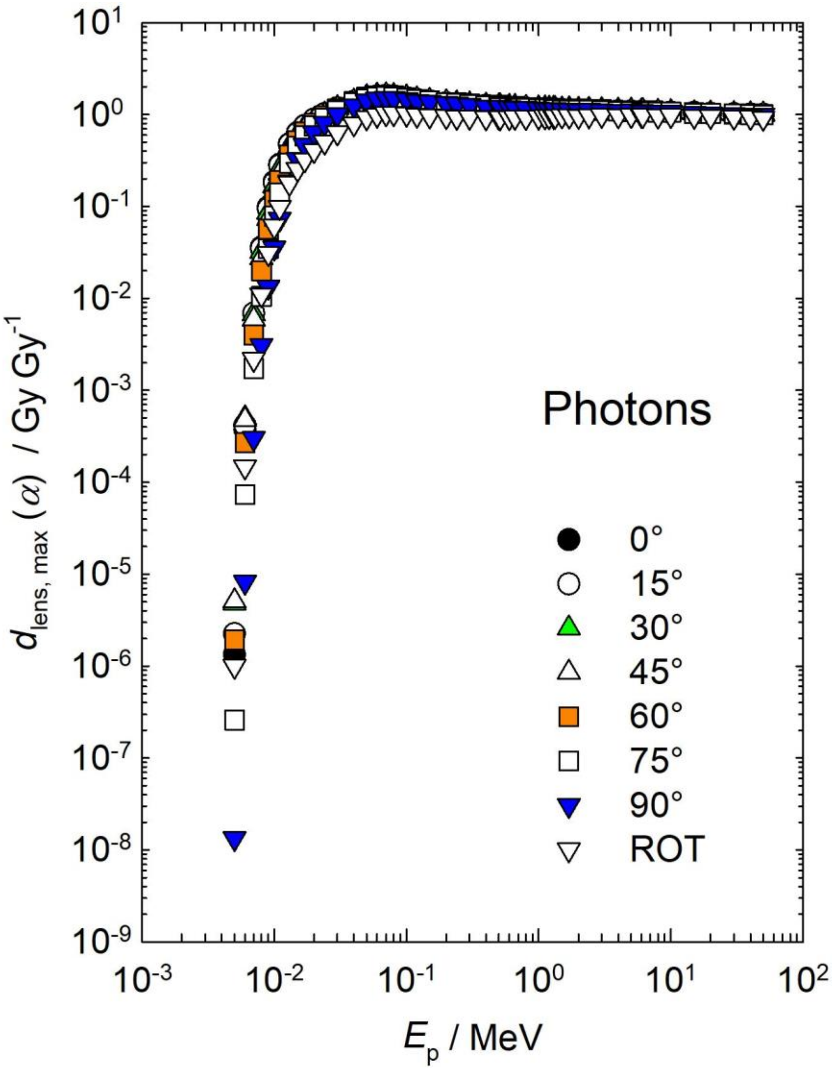

Figure C.2.1b Conversion coefficients from photon air kerma to the maximum absorbed dose in the sensitive cells or the complete lens, for left or right irradiations, calculated using the kerma-approximation method (Behrens, 2017a).

References

ARMSTRONG, T.W., AND CHANDLER, K.C. *SPAR, a FORTRAN Program for Computing Stopping Powers and Ranges for Muons, Charged Pions, Protons and Heavy Ions*. ORNL-4869 (Oak Ridge National Laboratory, Tennessee, TN) (1973).

Attix, F. H. (1979a). "The partition of kerma to account for bremsstrahlung," Health Phys. **36**, 347-354.

Attix, F. H. (1979b). "Addendum to 'The partition of kerma to account for bremsstrahlung'," Health Phys. **36**, 536.

Ballarini, F., Battistoni, G., Cerutti, F., Empl, A., Fassò, A., Ferrari, A., Gadioli, E., Garzelli, M.V. Ottolenghi, A., Pinsky, L.S., Ranft, J., Roesler, S., Sala, P.R. and Smirnov, G. *Nuclear Models in FLUKA: Present Capabilities, Open Problems and Future Improvements*. SLAC-PUB-10813. (SLAC, Stanford, CA.). (2004).

Bartlett, D.T. and Dietze, G. *ICRU Operational Quantities*. Radiat. Prot. Dosim. **139**(4), 425-426 (2010).

Bartlett, D.T., Dietze, G., Hertel, N., Bordy, J-M., Endo, A., Gualdrini, G., Pelliccioni, M., Ambrosi, P., Siebert, B. and Veinot, K. *Operational Quantities for External Radiation Exposure: Deficiencies and Options*. In: the Fifth International MELODI Workshop, Brussels, 7-10 October 2013.

Behrens and Dietze *Dose conversion coefficients for photon exposure of the human eye lens*. Phys. Med. Biol.**56**, 415-437 (2011).

Behrens, R. *On the operational quantity $H_p(3)$ for eye lens dosimetry.* J. Radiol. Prot. **32**, 455-464 (2012).

Behrens, R. *Compilation of conversion coefficients for the dose to the lens of the eye*. Radiat.Prot. Dosim. **174**, 348-370 (2017a).

Behrens, R. *Conversion coefficients for $H'(3;\Omega)$ for photons*. J. Radiol. Prot. **37** 354–378 (2017b)

Berger, M.J. Monte Carlo calculation of the penetration and diffusion of fast charged particles. In: Alder, B., Fernbach, S., Rotenberg, M. (Eds.), Methods in Computational Physics. Academic Press, New York, pp. 135–215 (1963).

Böhlen, T.T., Cerutti, F., Chin, M.P.W., A. Fassò, A., Ferrari, A., Ortega, P.G., Mairani, A., Sala, P.R., Smirnov, G., and Vlachoudis, V. *The FLUKA code: Developments and challenges for high energy and medical applications*, Nucl. Data Sheets 120, 211-214 (2014).

Boudard, A., Cugnon, J., David, J.C., Leray, S., and Mancusi, D. *New potentialities of the Liege intranuclear cascade model for reactions induced by nucleons and light charged particles*, Phys. Rev. **C87**, 014606 (2013).

Briesmeister, J.F. *MCNP – A General Monte Carlo N-Particle Transport Code, Version 4C*. Report LA-13709-M (Los Alamos National Laboratory, Los Alamos, NM) (2000).

Burlin, T.E. and Wheatley, B.M., *A unified Approach to Dosimetry in Radiological Protection,* Phys. Med. Biol. **16**, 47-56 (1971).

Burlin, T.E., Davies, M.L. and Wheatley, B.M., *Cavity Ionisation Theory applied to the Design of a Maximum Permissible Fluence Instrument,* Phys. Med. Biol. **24 (1)** 44-56 (1979).

Burlin, T E, *The Relevance of Fluence Data to Radiation Protection* IN Proc. European Seminar on Radiation Protection Quantities for External Exposure, Braunschweig, 1980. (Harwood/CEC: Brussels and Luxembourg) (1981).

Commission of the European Communities *Operational quantities for use in external radiation protection measurements. An investigation of concepts and principles.* Radiological Protection-27, Report Eur 8346 EN (European Communities:Luxembourg) (1983).

J. L. Conlin et al., Listing of Available ACE Data Tables,Los Alamos National Laboratory, Los Alamos, New Mexico, LA-UR-13-21822, Issued June 5, 2005.(Rev.1)

Daures, J. Gouriou, J. and Bordy, J-M. *Monte carlo determination of the conversion coefficients $H_p(3)/K_a$ in a right cylinder phantom with penelope code. comparison with "mcnp" simulations*“ Radiat. Prot. Dosim. **144**(1-4):37-42 (2011).

Daures, J., Gouriou, J. and .Bordy, J-M. Personal Communication (2017).

Dimbylow, P.J. and Francis, T.M. *The effect of photon scatter and consequent electron build-up in air on the calculation of dose equivalent quantities in the ICRU sphere for photon energies from 0.662 to 10 MeV,* Phys. Med. Biol. **28**, 817-828, (1983).

Dimbylow, P.J. and Francis, T.M. T*he calculation of dose equivalent quantities in the ICRU sphere for photon energies from 0.01 to 10 MeV,* Radiat. Prot. Dosim. **9**, 49-53, (1984).

Endo, A. *Operational quantities and new approach by ICRU*. Proceedings of the Third International Symposium on the System of Radiological Protection, Ann. ICRP 45(1S), 178-187 (2016a).

Endo, A. Personal Communication (2016b).

Endo, A. *Calculation of Fluence-to-Effective Dose Conversion Coefficients for the Operational Quantity Proposed by ICRU RC26*. Radiat. Prot. Dosim. **175**, 378-387 (2017).

Ferrari, A. and Pelliccioni, M., *On the conversion coefficients from fluence to ambient dose equivalent,* Radiat. Prot. Dosim. **51**, 251-255, (1994).

Ferrari, F and Gualdrini, G. *Eye Lens Dosimetry for Electrons. Hp(3) per unit fluence conversion coefficients for electrons from800 keV to 10 MeV based on MCNPX simulations on a cylindrical phantom* ENEA - Radiation Protection Institute Report RT/2012/6/ENEA (2012).

Ferrari, A., Sala, P.R., Fassò, A., and Ranft, J. *FLUKA: A Multi-particle Transport Code,* CERN-2005-10, INFN/TC_05/11, SLAC-R-773 (2005).

Furihata, S. *Statistical analysis of light fragment production from medium energy proton-induced reactions*, Nucl. Instrum. Meth. **B171**, 251–258 (2000).

Geissel, H., Scheidenberger, C., Malzacher, P., Kunzendorf, J., and Weick, H. ATIMA. Germany: GSI [cited 2013 Mar 4]. Available from: http://web-docs.gsi.de/˜weick/atima/

Goorley J.T. et al., Initial MCNP6 Release Overview - MCNP6 version 1.0, LA-UR-13-22934, April 2013

Goorley J.T. et al., Initial MCNP6 Release Overview, Nuclear Technology 180, 298-315 (2013).

Grosswendt, B and Chartier, J-L. *Fluence-to-Absorbed-Dose Conversion Coefficients and Angular-Dependence Factors for 4-Element ICRU Tissue, Water and PMMA Slab Phantoms Irradiated by Broad Electron Beams* Physikalisch-Technische Bundesanstalt Report PTB-Bericht Dos—24 (1994).

Gualdrini, G., Mariotti, F., Wach, S., Bilski, P.,Denoziere, M., Daures, J., Bordy, J.-M., Ferrari, P.,Monteventi, F., Fantuzzi, E. andVanhavere, F. *A New Cylindrical Phantom for Eye Lens Dosimetry Development.* Rad. Meas. **46**, 1231-1234 (2011).

Harrison, J.D., Balonov, M., Martin, C.J., Ortiz Lopez, P., Menzel, H-G., Simmonds, J.R., Smith-Bindman, R. and Wakeford, R. *Use of Effective Dose*. Proceedings of the Third International Symposium on the System of Radiological Protection, Ann. ICRP 45(1S), 215-224 (2016).

Hertel, N.E. and Veinot, K.V. Personal Communication, (2017)

Hirayama, H., Namito, Y., Bielajew, A.F., Wilderman, S.J. and Nelson, W.R. *TheEGS5 code system*. SLAC-R-730 and KEK Report 2005–8, SLAC NationalAccelerator Laboratory and High Energy Accelerator Research Organization (2005).

Hubbell, J. H. and Seltzer, S. M. *Tables of x-ray mass attenuation coefficients and mass energy-absorption coefficients 1 keV to 20 MeV for elements Z = 1 to 92 and 48 additional substances of dosimetric interest* Report NISTIR 5632 (1995)

International Commission on Radiation Units and Measurements, ICRU Report 19, *Radiation Quantities and Units*, (ICRU: Bethesda) (1971a).

International Commission on Radiation Units and Measurements, ICRU Report 20, *Radiation Protection Instrumentation and Its Application*, (ICRU: Bethesda) (1971b).

International Commission on Radiation Units and Measurements, ICRU Report 33, *Radiation Quantities and Units*, (ICRU: Bethesda) (1980).

International Commission on Radiation Units and Measurements. ICRU Report 39 *Determination of Dose Equivalents Resulting from External Radiation Sources*, (ICRU: Bethesda) (1985).

International Commission on Radiation Units and Measurements. ICRU Report 43 *Determination of Dose Equivalents from External Radiation Sources- part 2*, (ICRU: Bethesda) (1988).

International Commission on Radiation Units and Measurements. ICRU Report 47 *Measurements of Dose Equivalents from External Photon and Electron Radiations*, (ICRU: Bethesda) (1992).

International Commission on Radiation Units and Measurements, ICRU Report 51, *Quantities and Units in Radiation Protection Dosimetry*, (ICRU: Bethesda) (1993).

International Commission on Radiation Units and Measurements. Gamma-ray Spectrometry in the Environment. ICRU Report 53 (International Commission on Radiation Units and Measurements, Bethesda, Maryland) (1994).

International Commission on Radiation Units and Measurements, ICRU Report 57, *Conversion Coefficients for Use in Radiological Protection against External Radiation*, (ICRU: Bethesda) (1998).

International Commission on Radiation Units and Measurements, ICRU Report 66, *Determination of Operational Dose Equivalent Quantities for Neutrons*, Journal of ICRU **1**(3) (Oxford University Press:Oxford) (2001).

International Commission on Radiation Units and Measurements, ICRU Report 84, *Reference Data for the Validation of Doses from Cosmic-Radiation Exposure of Aircraft Crew*, Journal of ICRU **10** (2) (Oxford University Press:Oxford) (2010).

International Commission on Radiation Units and Measurements, ICRU Report 85a, *Fundamental Quantities and Units for Ionizing Radiation*, Journal of ICRU **11** (11) (Oxford University Press:Oxford) (2011).

International Commission on Radiation Units and Measurements, Report 90, *Key Data for Ionizing-Radiation Dosimetry: Measurement Standards and Applications*, Journal of ICRU **14** (1) (Oxford University Press:Oxford) (2014).

International Commission on Radiological Protection, ICRP Publication 15 *Protection against Ionizing Radiation from External Sources.* (Pergamon Press: Oxford) (1969).

International Commission on Radiological Protection, ICRP Publication 21 *Protection against Ionizing Radiation from External Sources: Supplement to ICRP Publication 15*. (Pergamon Press: Oxford) (1971).

International Commission on Radiological Protection. ICRP Publication 26. *Recommendations of the International Commission on Radiological Protection*, (Pergamon Press: Oxford) (1977a).

International Commission on Radiological Protection, ICRP Publication 60, *1990 Recommendations of the International Commission on Radiological Protection*, (Pergamon Press: Oxford) (1991).

International Commission on Radiological Protection, ICRP Publication 74, *Conversion Coefficients for Use in Radiological Protection against External Radiation*, Ann. ICRP **26**(3/4). (Elsevier Science: Oxford) (1996).

International Commission on Radiological Protection, ICRP Publication 89, *Basic Anatomical and Physiological Data for use in Radiological Protection*, Ann. ICRP **32** (3/4). (Elsevier Science: Oxford) (2002).

International Commission on Radiological Protection,ICRP Publication 103, *The 2007 Recommendations of the International Commission on Radiological Protection*.. Ann, ICRP (Elsevier Science: Oxford) (2007).

International Commission on Radiological Protection *Adult Reference Computational Phantoms*, ICRP Publication 110. Ann. ICRP (Elsevier Science: Oxford) (2009).

International Commission on Radiological Protection *Conversion Coefficients for Radiological Protection for External Radiation Exposures*, ICRP Publication 116. Ann. ICRP (Elsevier Science: Oxford) (2010).

International Commission on Radiological Protection *Statement on Tissue Reactions / Early and Late Effects of Radiation in Normal Tissues and Organs – Threshold Doses for Tissue Reactions in a Radiation Protection Context,* ICRP Publication 118. Ann. ICRP 41 (1/2) (Elsevier Science: Oxford) (2012).

International Commission on Radiological Protection *Assessment of Radiation Exposure of Astronauts in Space*, ICRP Publication 123. Ann. ICRP **42** (4) (Elsevier Science: Oxford) (2013).

International Commission on Radiological Protection *Radiological Protection from Cosmic Radiation in Aviation*, ICRP Publication 132. Ann. ICRP **45** (1) (Elsevier Science: Oxford) (2016).

International Organization for Standardization, ISO 8529-3:1998, *Reference neutron radiations -- Part 3: Calibration of area and personal dosemeters and the measurement of their response as a function of energy and angle of incidence*. (ISO Geneva, Switzerland) (1998).

International Organization for Standardization, ISO 4037-3:1999, *X and gamma reference radiation for calibrating dosemeters and doserate meters and for determining their response as a function of photon energy — Part 3: Calibration of area and personal dosemeters and the measurement of their response as a function of energy and angle of incidence*. (ISO Geneva, Switzerland) (1999).

International Organization for Standardization, ISO 6980-3:2006, *Nuclear energy -- Reference beta-particle radiation -- Part 3: Calibration of area and personal dosemeters and the determination of their response as a function of beta radiation energy and angle of incidence*, (ISO Geneva, Switzerland) (2006).

International Organization for Standardization, ISO 29661:2012,*Reference radiation fields for radiation protection — Definitions and fundamental concepts*, (ISO Geneva, Switzerland) (2012).

Jahr, R. Hollnagel, R.A., and Siebert, B.R.L., *A conceptual physical basis for monitoring external radiation*, Radiat. Prot. Dosim. **1**, 299-304, (1981).

Kawrakow, I., Mainegra-Hing, E., Rogers, D.W.O., Tessier, F. and Walters, B.R.B., *The EGSnrc Code System: Monte Carlo Simulation of Electron and Photon Transport*. PIRS Report 701. National Research Council of Canada, Ottawa. (2013).

Kawrakow, I. *Electron impact ionization cross sections for EGSnrc.* Med. Phys. **29**, 1230 (2002).

Kim, J. O. and Kim, J. K. *Dose equivalent per unit fluence near the surface of the ICRU phantom by including the secondary electron transport for photons.* Radiat. Prot. Dosim. **83**(3), 211–219 (1999).

Koch, H.W., Motz, J.W., 1959. Bremsstahlung cross-section formulas and related data. Rev. Mod. Phys.**31**, 920–955.

Nara, Y., Otuka, H., Ohnishi, A., Niita, K., and Chiba, S. *Relativistic nuclear collisions at 10 A GeV energies from p+Be to Au+Au with the hadronic cascade model*, Phys. Rev. C61, 024901 (1999).

National Council on Radiation Protection and Measurements NCRP Report 38 *Protection against neutron radiation*, (NCRP:Washington) (1971).

Nelson, W.R., Hirayama, H., Rogers, D.W.O. The EGS4 Code System. SLAC Report 265. Stanford Linear Accelerator Center, Stanford, CA (1985).

Niita. K., Chiba, S., Maruyama, T., Maruyama, T., Takada, H., Fukahori, T., Nakahara, Y., and Iwamoto, A. *Analysis of the (N,Xn') reactions by quantum molecular dynamics plus statistical decay model*, Phys. Rev. **C52**, 2620–2635 (1995).

Nuclear Regulatory Authority. Report on the Investigation for Distributions of Radioactive Substances Released from the TEPCO Fukushima Daiichi NuclearPower Plant Accident. Available from: http://radioactivity.nsr.go.jp/ja/list/338/list-1.html. (Japanese) (2012).

Otto, T. Personal Communication (2017).

Pelliccioni, M. *Fluence to dose equivalent conversion data and Radiation Weighting Factors for High Energy Radiation.* Radiat. Prot. Dosim. **77**, 159 - 170 (1998).

Pelliccioni, M. *Overview of Fluence-to-Effective Dose and Fluence-to-Ambient Dose Equivalent Conversion Coefficients for High Energy Radiation Calculated using the FLUKA Code* Radiat. Prot. Dosim. **88**, 279-297 (2000).

Pelowitz D.B. (ed.), MCNP6 USER'S MANUAL Version 1.0, Manual Rev. 0, Los Alamos National Laboratory, Los Alamos, New Mexico, LA-CP-13-00634, Rev. 0, May 2013.

Petoussi-Henss, N., Schlattl, H., Zankl, M., Endo, A. and Saito, K. *Organ Doses from Environmental Exposures Calculated using Voxel Phantoms of Adults and Children*, Phys. Med. Biol. **57**, 5679-5713 (2012).

Saito, K., Ishigure. N., Petoussi-Henss, N. and Schlattl, H. *Effective Dose Conversion Coefficients for Radionuclides Exponentially Distributed in the Ground*, Radiat. Environ. Biophys. **51**, 411-423 (2012).

Saito, K. and Petoussi-Henss, N. *Ambient Dose Equivalent Conversion Coefficients for Radionuclides Exponentially Distributed in the Ground*, J. Nucl. Sci. Technol. **51**, 1274-1287 (2014).

Sato, T., Niita, K., Matsuda, N., Hashimoto, S., Iwamoto, Y., Noda, S., Ogawa, T., Iwase, H., Nakashima, H., Fukahori, T., Okumura, K., Kai, T., Chiba, S., Furuta, T., and Sihver, L. P*article and heavy ion transport code system PHITS, Version 2.52,*J. Nucl. Sci. Technol. **50**, 913-923 (2013).

Sidwell, J.M., Burlin, T.E. and Wheatley, B.M.*Calculations of the absorbed dose in a phantom from photon fluence and some applications to radiological protection.* Br. J. Radiol. **42**, 522-529 (1969).

Seltzer, S.M. *Calculation of Photon Mass Energy-Transfer and Mass Energy-Absorption Coefficients.* Radiation Research **136** 147-170 (1993).

Seltzer, S.M. Personal Communication. (2017).

Siebert, B.R.L. and Bartlett, D.T., *Proposal of an operational quantity based directly on protection quantities,* Presented at 8th Symp. Neutron Dosimetry, Paris, November 1995 (1995).

Vanhavere, F. et al. Carinou, E., Gualdrini, G., Clairand, I., Sans Merce, M., Ginjaume, M., Nikodemova, D., Jankowski, J., Bordy, J.-M., Rimpler, A., Wach, S., Martin, P., Struelens, L., Krim, S., Koukorava, C., Ferrari, P., Mariotti, F., Fantuzzi, E., Donadille, L., Itié, C., Ruiz, N., Carnicer, A., Fulop, M., Domienik, J., Brodecki, M., Daures, J., Barth, I., Bilski, P. *ORAMED: Optimization of Radiation Protection of Medical Staff.* EURADOS Report 2012-02. ISBN 978-3-943701-01-2 (2012).

Veinot,K. and Hertel, N. E. *Personal Dose Equivalent Conversion coefficients for photons to 1 GeV*. Radiat Prot Dosim. **145**(1) 28-35 (2011).

Weinberg, A.V. and Wigner, E.P. The Physical Theory of Neutron Chain Reactors. University of Chicago Press, (1958).